

Fall 2006

Evaluation of characterization techniques for beneficial use of underutilized slag materials

Thomas Sandy Weymouth
University of New Hampshire, Durham

Follow this and additional works at: <https://scholars.unh.edu/thesis>

Recommended Citation

Weymouth, Thomas Sandy, "Evaluation of characterization techniques for beneficial use of underutilized slag materials" (2006).
Master's Theses and Capstones. 214.
<https://scholars.unh.edu/thesis/214>

This Thesis is brought to you for free and open access by the Student Scholarship at University of New Hampshire Scholars' Repository. It has been accepted for inclusion in Master's Theses and Capstones by an authorized administrator of University of New Hampshire Scholars' Repository. For more information, please contact nicole.hentz@unh.edu.

EVALUATION OF CHARACTERIZATION TECHNIQUES FOR
BENEFICIAL USE OF UNDERUTILIZED SLAG MATERIALS

By

Thomas Sandy Weymouth

B.S., Bates College, 1998

THESIS

Submitted to the University of New Hampshire
in Partial Fulfillment of
the Requirements for the Degree of

Master of Science

in

Civil Engineering

September, 2006

UMI Number: 1437647

INFORMATION TO USERS

The quality of this reproduction is dependent upon the quality of the copy submitted. Broken or indistinct print, colored or poor quality illustrations and photographs, print bleed-through, substandard margins, and improper alignment can adversely affect reproduction.

In the unlikely event that the author did not send a complete manuscript and there are missing pages, these will be noted. Also, if unauthorized copyright material had to be removed, a note will indicate the deletion.

UMI[®]

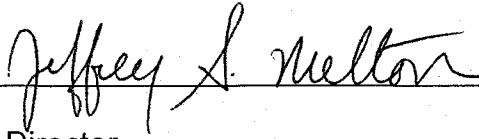
UMI Microform 1437647

Copyright 2006 by ProQuest Information and Learning Company.

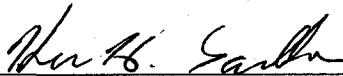
All rights reserved. This microform edition is protected against unauthorized copying under Title 17, United States Code.

ProQuest Information and Learning Company
300 North Zeeb Road
P.O. Box 1346
Ann Arbor, MI 48106-1346

This thesis has been examined and approved.



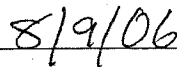
Thesis Director
Dr. Jeffrey S. Melton
Research Assistant Professor of Civil
Engineering



Dr. Kevin H. Gardner
Research Associate Professor of Civil
Engineering



Dr. Jenna R. Jambeck
Research Assistant Professor of Civil
Engineering



Date

ACKNOWLEDGEMENTS

I would like to express my thanks to my advisor Dr. Jeffrey Melton for his belief in me and the support he provided throughout my time here at the University of New Hampshire. Many times in this process I questioned my ability to successfully carry out my research and complete the Masters program and Jeff was always there to convince me otherwise. I also would like to thank the other members of my advising committee, Dr. Kevin Gardner and Dr. Jenna Jambeck, as well as the other professors and students here in the Environmental Research Group who answered my questions when I needed help.

I would like to thank the Federal Highways Administration for providing funding for this research. In addition, I would like to thank SMC, Inc. for providing the test materials used in this research and Lincoln Electric for providing materials as well as funding. Without this support this important work would not have been possible.

I would especially like to thank my family members and my wife Jenny for all of their support and especially the patience they showed towards the many late nights I spent in Gregg Hall. I would not have been able to make it this far without them.

TABLE OF CONTENTS

ACKNOWLEDGEMENTS	iii
LIST OF TABLES	vii
LIST OF FIGURES	x
ABSTRACT	xv
1. INTRODUCTION	1
2. LITERATURE REVIEW	11
2.1 Steel and Iron Slag	11
2.2 Submerged Arc Welding Slag	23
2.3 Leaching Overview	26
2.3.1 Physical Factors Affecting Leaching	27
2.3.2 Chemical Factors Affecting Leaching	31
2.3.3 Release Mechanisms	35
2.3.4 Fate and Transport	38
2.3.5 Mismanagement Scenarios	39
2.3.6 Background Concentrations	42
3. MATERIALS AND METHODS	52
3.1 Material Characterization	52
3.1.1 Grain Size Distribution	54
3.1.2 Moisture Content	54
3.1.3 Surface Area Analysis	55
3.1.4 SEM Analysis	56
3.1.5 X-ray Powder Diffraction (XRPD)	56
3.2 Total Composition	58
3.3 Availability Test	59
3.4 TCLP/SPLP Test	61

3.5 Natural pH Test	62
3.6 Kosson Framework	64
3.6.1 LS Ratio Leaching Test	65
3.6.2 pH-Dependent Leaching Test	66
3.6.3 Compacted Granular Leaching Test	70
3.6.4 Regulatory Standards	76
3.7 Particle Size Reduction	77
3.8 MINTEQA2 Modeling	78
3.9 IWEM Modeling	80
3.10 Laboratory Analysis	82
3.10.1 UNH Laboratory Analysis	82
3.10.2 Additional Laboratory Analysis	84
4. RESULTS AND DISCUSSION	95
4.1 Physical Characteristics	95
4.1.1 Grain Size Distribution	95
4.1.2 Moisture Content	96
4.1.3 Surface Area	97
4.1.4 SEM Analysis	98
4.1.5 XRPD	100
4.2 Total Leachable Composition	102
4.3 Availability Test	103
4.3.1 SSFF Slag	104
4.3.2 SSFW Slag	104
4.3.3 BOF Slag	105
4.3.4 SAW Slag	105
4.3.5 BF Slag	106
4.4 TCLP/SPLP Test	106
4.5 Natural pH Test	108
4.6 LS Ratio Leaching Test	110
4.6.1 BOF Slag	112

4.6.2 SSFF Slag	114
4.6.3 SSFW Slag	115
4.6.4 BF Slag	116
4.6.5 SAW Slag	117
4.6.6 LS Ratio Calculations	119
4.7 pH-Dependent Leaching	121
4.7.1 Acid Neutralization Capacity (ANC)	122
4.7.2 SSFF Slag	124
4.7.3 SSFW Slag	125
4.7.4 BOF Slag	126
4.7.5 BF Slag	127
4.7.6 SAW Slag	128
4.7.7 pH Calculations	129
4.8 Compacted Granular Leaching Test	129
4.8.2 CGLT Diffusion Modeling	134
4.9 MINTEQA2 Modeling	135
4.10 IWEM Modeling	137
4.11 Laboratory Validation	139
5. CONCLUSIONS	210
5.1 Laboratory Test Conclusions	210
5.2 Recommendations for Material Use	216
6. RECOMMENDATIONS FOR FUTURE RESEARCH	219
LIST OF REFERENCES	221
APPENDIX	228

LIST OF TABLES

Table 1.1. USGS slag production/consumption data	10
Table 2.1. Physical properties of steel and iron slags.	44
Table 2.2. Physical properties of aged oxidized and reduced slags	45
Table 2.3. Slag surface area measurements	46
Table 2.4. Slag surface area measurements	46
Table 2.5. Steel and iron slag compositional data from the literature.	47
Table 2.6. Compositional data of oxidized and reduced steel slag	47
Table 2.7. Physical properties of Lincolnweld 995N flux from Lincoln Electric Product Certificate	48
Table 2.8. Compositional analysis of Lincolnweld 995N flux from Lincoln Electric Product Certificate.	48
Table 2.9. TCLP data for SAW slags provided by Lincoln Electric.	49
Table 2.10. BOF slag mass transfer values calculated with tank leaching tests	50
Table 2.11. Contaminants and their local sources found on Australian highways	51
Table 3.1. Sample weights of slags supplied to the RMRC by SMC, Inc	86
Table 3.2. EPA MCL Primary Drinking Water Standards.	94
Table 3.3. Average IDL concentrations calculated for the ICP-AES	94
Table 4.1. Percent moisture content of received slags.	142
Table 4.2. Effective surface area analysis of different particle	

sized slags.	142
Table 4.3. BOF Slag XRPD mineral list with FOMs.	149
Table 4.4. SSFF Slag XRPD mineral list with FOMs.	150
Table 4.5. SSFW Slag XRPD mineral list with FOMs	151
Table 4.6. BF Slag XRPD mineral list with FOMs.	152
Table 4.7. SAW Slag XRPD mineral list with FOMs.	153
Table 4.8. TCLP and SPLP analytical results from Resource Laboratories.	158
Table 4.9. Final pHs of LS ratio leachates prior to sampling	171
Table 4.10. LS ratio conversion to time for three hypothetical scenarios.	172
Table 4.11. Two different hypothetical scenarios showing an As MCL exceedance.	173
Table 4.12. R2 pH dependent leaching acid addition schedule	175
Table 4.13. BOF Slag CGLT results for the cumulative constituent release in mg/m ² .	194
Table 4.14. BOF Slag CGLT graphed interval slopes identifying intervals with diffusional release.	195
Table 4.15. BOF Slag CGLT observed diffusivity (Dobs) and pDe calculations for intervals with diffusional release.	196
Table 4.16. SSFF Slag CGLT results for the cumulative constituent release in mg/m ² .	197
Table 4.17. SSFF Slag CGLT graphed interval slopes identifying intervals with diffusional release.	197
Table 4.18. SSFF Slag CGLT observed diffusivity (Dobs) and pDe calculations for intervals with diffusional release.	198
Table 4.19. SSFW Slag CGLT results for the cumulative constituent release in mg/m ² .	199

Table 4.20. SSFW Slag CGLT graphed interval slopes identifying intervals with diffusional release.	199
Table 4.21. SSFW Slag CGLT observed diffusivity (Dobs) and pDe calculations for intervals with diffusional release.	200
Table 4.22. SAW Slag CGLT results for the cumulative constituent release in mg/m ² .	200
Table 4.23. SAW Slag CGLT graphed interval slopes identifying intervals with diffusional release.	201
Table 4.24. SAW Slag CGLT observed diffusivity (Dobs) and pDe calculations for intervals with diffusional release.	201
Table 4.25. Compiled CGLT pDe, Tortuosity, and Retention Factor values.	202
Table 4.26. Compiled CGLT pDe and Tortuosity values from the literature.	203
Table 4.27. LS ratio availability results and re-calculated pDe values.	204
Table 4.28. Re-calculated tortuosity and R values using LS ratio availability results.	205
Table 4.29. Predicted long-term Ba and Cr diffusional release from BOF and SFFF slags	205
Table 4.30. BOF slag MINTEQA2 modeling results showing minerals controlling constituent solubility over the indicated pH range..	206
Table 4.31. SAW slag MINTEQA2 modeling results showing minerals controlling constituent solubility over the indicated pH range.	206
Table 4.32. BF slag MINTEQA2 modeling results showing minerals controlling constituent solubility over the indicated pH range.	207
Table 4.33. Laboratory validation split samples sent to EA, Inc.	209

LIST OF FIGURES

Figure 2.1. Steel and iron slag grain size distribution	45
Figure 3.1. BOF slag received from SMC, Inc.	87
Figure 3.2. BF slag received from SMC, Inc.	87
Figure 3.3. SSFF slag received from SMC, Inc.	88
Figure 3.4. SSFW slag received from SMC, Inc.	88
Figure 3.5. SAW slag received from Lincoln Electric.	89
Figure 3.6. Tristar 3000 BET analyzer.	89
Figure 3.7. Leaching framework presented by Kosson, et al. 2002.	90
Figure 3.8. Continuous sample tumbler used for equilibrium leaching tests.	91
Figure 3.9. Schott Autotitrator used for tests requiring acid/base addition.	91
Figure 3.10. Schott Autotitrator used for tests requiring acid/base addition.	92
Figure 3.11. Ceramic hammer used for CGLT mold compaction.	92
Figure 3.12. United Nuclear 12lb ball mill with neoprene bladder.	93
Figure 3.13. Varian ICP-AES used for inorganic analysis of leachates .	93
Figure 4.1. Grain size distribution from sieve analysis.	141
Figures 4.2-4.4: SEM images of SSFF slag in 17.3x, 1,000x, and 10,000x resolution	143
Figures 4.5-4.7: SEM images of SSFW slag in 25.4x, 1,000x, and 10,000x resolution	144
Figures 4.8-4.10: SEM images of BOF slag in 25x, 1,000x,	

and 10,000x resolution	145
Figures 4.11-4.13: SEM images of BF slag in 30.4x, 1,000x, and 10,000x resolution	146
Figures 4.14-4.16: SEM images of SAW slag in 19.1x, 1,000x, and 10,000x resolution	147
Figures 4.17-4.19: SEM images of flat and spherical BOF slag particles and SAW flux fused in the slag surface	148
Figure 4.20. BOF slag total leachable composition results graphed with the corresponding EPA MCLs.	154
Figure 4.21. SSFF slag total leachable composition results graphed with the corresponding EPA MCLs.	154
Figure 4.22. SSFW slag total leachable composition results graphed with the corresponding EPA MCLs.	155
Figure 4.23. SAW slag total leachable composition results graphed with the corresponding EPA MCLs.	155
Figure 4.24. SSFF slag availability test results graphed with the corresponding EPA MCLs and IDLs.	156
Figure 4.25. SSFW slag availability test results graphed with the corresponding EPA MCLs and IDLs.	156
Figure 4.26. BOF slag availability test results graphed with the corresponding EPA MCLs and IDLs.	157
Figure 4.27. SAW slag availability test results graphed with the corresponding EPA MCLs and IDLs.	157
Figure 4.28. BF slag availability test results graphed with the corresponding EPA MCLs and IDLs.	158
Figure 4.29. Slag natural pH over 24 hours in open containers.	159
Figure 4.30. Slag natural pH over range of LS ratios in closed containers.	159
Figures 4.31-4.36. BOF slag <i>Al</i> , <i>As</i> , <i>Ba</i> , <i>Ca</i> , <i>Cd</i> , and <i>Cr</i> LS ratio leaching test results	160

Figures 4.37-4.42. BOF slag <i>Cu, Mg, Pb, Sb, Se,</i> and <i>TI</i> LS ratio leaching test results	161
Figures 4.43-4.48. SSFF slag <i>Al, As, Ba, Be, Ca,</i> and <i>Cd</i> LS ratio leaching test results	162
Figures 4.49-4.55. SSFF slag <i>Cr, Cu, Mg, Pb, Sb, Se,</i> and <i>TI</i> LS ratio leaching test results	163
Figures 4.56-4.61. SSFW slag <i>Al, As, Ba, Ca, Cr,</i> and <i>Cu</i> LS ratio leaching test results	164
Figures 4.62-4.67. SSFW slag <i>Fe, Mg, Pb, Sb, Se,</i> and <i>TI</i> LS ratio leaching test results	165
Figures 4.68-4.73. BF slag <i>Al, As, Ba, Ca, Cu,</i> and <i>Fe</i> LS ratio leaching test results	166
Figures 4.74-4.77. BF slag <i>Mn, Mg, Se,</i> and <i>TI</i> LS ratio leaching test results	167
Figures 4.78-4.83. SAW slag <i>Al, As, Ba, Be, Ca,</i> and <i>Cd</i> LS ratio leaching test results	168
Figures 4.84-4.89. SAW slag <i>Cr, Cu, Fe, Mn, Mg,</i> and <i>Se</i> LS ratio leaching test results	169
Figures 4.90-4.92. SAW slag <i>Sb, Pb,</i> and <i>TI</i> LS ratio leaching test results	170
Figure 4.93. Steel slag LS ratio example with 1 cubic meter section of slag.	172
Figure 4.94. Initial ANC curves using continuous acid addition.	173
Figure 4.95. ANC curves using 15 minute equalization time between acid additions.	174
Figure 4.96. Test used to determine the change in pH over 48 hours during the LS ratio leaching test	174
Figures 4.97-4.102. Individual pH dependent leaching final pH measurements (ANC) and combined values for comparison.	176
Figures 4.103-4.108. SSFF <i>Al, As, Ba, Be, Ca,</i> and <i>Cd</i>	

pH dependent leaching curves.	177
Figures 4.109-4.114. SSFF <i>Cr, Cu, Fe, Mg, Mn, and Pb</i> pH dependent leaching curves.	178
Figures 4.115-4.117. SSFF <i>Sb, Se, and Tl</i> pH dependent leaching curves.	179
Figures 4.118-4.123. SSFW <i>Al, As, Ba, Be, Ca, and Cd</i> pH dependent leaching curves.	180
Figures 4.124-4.129. SSFW <i>Cr, Cu, Fe, Mg, Mn, and Pb</i> pH dependent leaching curves.	181
Figures 4.130-4.132. SSFW <i>Sb, Se, and Tl</i> pH dependent leaching curves	182
Figures 4.133-4.138. BOF <i>Al, As, Ba, Be, Ca, and Cd</i> pH dependent leaching curves.	183
Figures 4.139-4.144. BOF <i>Cr, Cu, Fe, Mg, Mn, and Pb</i> pH dependent leaching curves.	184
Figures 4.145-4.147. SSFW <i>Sb, Se, and Tl</i> pH dependent leaching curves	185
Figures 4.148-4.153. BF <i>Al, As, Ba, Be, Ca, and Cd</i> pH dependent leaching curves.	186
Figures 4.154-4.161. BF <i>Cr, Cu, Fe, Mg, Mn, Pb, Se, and Tl</i> pH dependent leaching curves.	187
Figures 4.162-4.167. SAW <i>Al, As, Ba, Be, Ca, and Cd</i> pH dependent leaching curves.	188
Figures 4.168-4.173. SAW <i>Cr, Cu, Fe, Mg, Mn, and Pb</i> pH dependent leaching curves.	189
Figures 4.174-4.176. SAW <i>Sb, Se, and Tl</i> pH dependent leaching curves	190
Figures 4.177-4.181. ANC curves with acid rain neutralization time predictions.	191
Figure 4.182. BOF slag CGLT cumulative release plot.	192

Figure 4.183. SSFF slag CGLT cumulative release plot.	192
Figure 4.184. SSFW slag CGLT cumulative release plot.	193
Figure 4.185. SAW slag CGLT cumulative release plot	193
Figure 4.186. IWEM modeling for Sb concentrations in a monitoring well located 20 m from the source over 100 years.	208

ABSTRACT

EVALUATION OF CHARACTERIZATION TECHNIQUES FOR BENEFICIAL USE OF UNDERUTILIZED SLAG MATERIALS

By

Thomas Sandy Weymouth

University of New Hampshire, September, 2006

Wisely using byproduct materials in beneficial use applications such as highway construction is becoming more important in the United States as virgin materials are depleted and landfill capacity declines. Slags are byproducts of the steel and iron industries found in the Midwestern United States. Historically, many of these materials have historically been used in construction applications, but methods for characterizing their environmental risk are limited. This research considers a series of steps used to identify whether a particular slag poses an environmental or human health risk. The first step involves identifying the appropriate use of the material. The second step involves identifying the site-specific parameters such as precipitation rates and expected pH conditions. The third step involves characterizing the material with a set of leaching procedures that test the material under the range of expected site-specific conditions. The

majority of this research focused on this characterization step. The final step involves fate and transport modeling of the appropriate leaching data to identify the ultimate constituent concentrations expected at a receptor.

Three steelmaking slags, an ironmaking slag, and one submerged arc welding slag were obtained to identify and verify testing methods that could be utilized to characterize these and other similar byproduct materials. The laboratory methodology involved both simplified and complex procedures used to identify the environmental properties of the materials under a range of conditions. A total composition test was conducted to identify the total amount of constituents in the material by digesting the slags in acid. Due to the high silica content of the samples, full digestion was not possible and instead the total leachable concentration was determined. An availability test was used as a screening tool to determine the maximum amount of constituents that could leach from the samples under more realistic conditions expected in actual field use (neutral to slightly acidic pHs). This test was considered successful at identifying leachable constituents but may not be appropriate for highly alkaline materials such as steel and iron slags that will most likely not reach neutral pHs in a realistic timeframe. Two commonly used regulatory tests, the Toxicity Characteristic Leaching Procedure and the Synthetic Precipitate Leaching Procedure, were used to compare results with other more complex leaching tests. These tests have

historically been used to characterize byproduct materials but have recently come under criticism for this type of use.

Since constituent solubility is often a function of pH, a set of tests was used to identify the natural pH of the materials over a range of conditions and timeframes. The pH tests classified the slags as alkaline materials with high buffering capacities capable of controlling the local pH environment for a long time period. An equilibrium-based liquid-to-solid ratio leaching test was conducted to identify short and long term leaching potentials and the release mechanisms involved. This test was simple to conduct and is recommended for the slags since the leachate pH is controlled by the material's own buffering capacity. If site specific precipitation rates and material geometries are known, liquid-to-solid ratios can be translated to timescales and constituent release predictions can be calculated from the leaching test results. A second equilibrium-based test was used to identify the pH-dependent leaching behavior of constituents over a range of pHs (2-12). Due to the high buffering capacity of the slags, this test was time consuming and it is recommended that a shortened more realistic pH range be used. pH conditions expected in field applications are either controlled by the material's own buffering capacity or the environmental conditions surrounding the material. If these pH conditions can be identified from knowledge of the material's natural pH or from site-specific conditions, the pH-dependent leaching data can be used to predict release.

A mass transfer-based compacted granular leaching test was used to characterize the diffusional release of constituents from the materials. When a granular material is placed in the base layer of a road and compacted it may act more like a monolith with percolating water flowing around it rather than through it. This may lead to mass transfer limited release rather than solubility limited release. Data from this test can be used to calculate material specific properties such as diffusion coefficients, tortuosity values, and chemical retention factors. The majority of constituents tested in this research were not released in large enough quantities to use in the mass transfer calculations.

A critical step in characterizing beneficial use materials such as slag is the interpretation of analytical data from leaching tests. One approach is to compare the data directly to appropriate regulatory standards such as EPA Maximum Contaminant Level drinking water standards. This could be considered overly conservative unless groundwater drinking wells were located directly adjacent to the material. A second approach used in this research is the use of fate and transport models to predict future contaminant concentrations at receptors. The EPA's Industrial Waste Management Evaluation Model was designed to help decision makers decide on the most appropriate waste management unit for a particular waste. The software program was used in this research to model antimony

concentrations over 100 years in a monitoring well located downgradient from a hypothetical slag layer in a highway application. Using the model's conservative parameters and antimony leaching results from the liquid-to-solid ratio leaching test, antimony was predicted to exceed the EPA regulatory level in 14 years for the welding slag and 75 years for one of the steel slags. Using a less conservative approach, a user defined soil-water partitioning coefficient from the literature was entered into the model. Using this method the antimony concentrations in the monitoring well were all non-detect after 100 years. This modeling exercise points out the importance of using a fate and transport model to interpret leaching results and identifies how using site specific information, such as known partitioning coefficients, can change the model outcome.

CHAPTER 1

INTRODUCTION

The beneficial use of recycled and secondary materials in engineering applications is an important step in moving towards a more sustainable society. Materials that normally are either stockpiled indefinitely or disposed of in landfills can be used in combination or in place of natural aggregates in applications such as highway construction. Some materials, such as blast furnace slag, have reached commodity status and are widely used while other materials, such as submerged arc welding slag, are new to the market and are not widely used. One barrier that prevents the use of some materials is the lack of information regarding their physical and environmental properties. In 1998 and 1999 the Association of State and Territorial Solid Waste Management Officials (ASTSWMO) conducted a Beneficial Use Survey to determine the issues states faced when using a variety of secondary materials. The data from the 40 States that completed the survey was presented in an April 2000 report (ASTSWMO, 2000). Among a list of barriers States face when dealing with secondary materials, the report identified the largest barrier as the lack of good information to use

in evaluating the risks to human health and the environment. The physical properties of a material may be well documented but information on whether a material will leach contaminants after placement, for example, is not known. Testing protocols involving appropriate laboratory leaching methods for recycled and secondary materials are not well established or used widely. There is a lack of laboratory and field data but also a lack of guidelines that material producers and contractors can use to determine whether a material is safe to use or not. Many of these secondary materials have specific properties that make them unique from natural aggregates. Therefore the guidelines that are used for natural aggregates are not always appropriate for these materials. This research addresses these issues with regard to the beneficial use of underutilized steel and iron slags and a welding slag.

Steel and iron slags are generated during the steel and iron production process. According to the National Slag Association (NSA), slag from an iron mill, called blast furnace slag (BF slag) is produced when a fluxing agent (either limestone or dolomite) is combined with iron ore or pellets and coke ash in a blast furnace. The lime in the fluxing agent combines with aluminates and silicates in the ore and coke to form a non-metallic molten slag. This slag is cooled in several different ways to produce different types of blast furnace slag: air cooled, expanded, pelletized, and granulated. Steel slag is formed in either a basic oxygen furnace (BOF) containing

scrap or molten iron, or an electric arc furnace (EAF) containing scrap and/or metallized ore. In both types, lime or dolomitic lime is used as a fluxing agent to remove impurities in the molten steel. In the BOF process, oxygen is injected into the molten steel to remove carbon. The EAF process uses an AC or DC electric arc to melt the ore (NSA, 2006).

According to a 2006 USGS mineral commodity summary, about 21 million tons of domestic steel and iron slag was consumed in 2005 at a value of \$326 million (USGS, 2006). Of this total, blast furnace slag accounted for 60% of the tonnage and of this amount 80% was granulated. There were 29 slag processing companies servicing iron and steel companies or reprocessing old slag piles at 130 locations. This includes 40 sites in 14 states for blast furnace slag and 90 sites in 32 states for steel slag. According to the report, the majority of imported slag was unground granulated blast furnace slag. Additional USGS slag data is listed in Table 1.1. The average slag production between 1991 and 2005 was 19.5 million tons with recent production above that average. Limited slag use data shows the majority of BF slag was used as either road base material or in asphalt/concrete applications while the majority of steel slag use varied between road base, asphalt/concrete applications, and fill material. It appears that the number of companies processing slag in the US has increased annually since 2001. In 2001, Illinois, Indiana, Michigan, and Ohio accounted for 58% of blast furnace slag sold or used while Maryland,

New York, Pennsylvania, and West Virginia accounted for 30% of the sales. The USGS did not provide more recent BF state usage data or state steel slag usage data.

In general, specifications for steel and iron slag are limited and can vary between states. A search on the Ohio Department of Transportation (ODOT) website for “slag” produced supplemental specifications for ACBF slag, GGBF slag, and steel slag. Only the ACBF slag specification addressed the leaching characteristics of the slag whereas the other guidelines addressed the physical properties of the materials. Supplemental 907 and 1027 titled “Sulphur Leachate Test for Air Cooled Blast Furnace Slag” is a method designed to test slag stockpiles for sulfur content. The test involves soaking a sample of slag in a 5-gallon bucket half-filled with water for 15 days and periodically checking the color of the water. If the water is darker or equal to hue 10Y on a rock color chart then the sample and stockpile it originated from are rejected. Additionally, the specification requires that the pH stay between 6.5 and 9, the conductivity stay below 2400 mho/cm, and the total dissolved solids stay below 1500 mg/l. An additional search result was a short study titled “pH of Air Cooled Blast-Furnace Slag Leachate Over a Six Month Period”. The study identified the leaching of sulphur compounds, specifically CaS, as an issue for ACBF slag and that high pH is an indicator of this type of contamination. The study did not specify what was considered a high pH value. A search on the Indiana

DOT (InDOT) website found a similar test for ACBF slag as the ODOT leaching test except that conductivity and TDS are not measured and the acceptable pH range is 6.5 to 10.5. The overall length of the InDOT test is 7 days instead of 15 days. A search of Illinois' DOT (IDOT) website found a 2003 "Policy Memorandum" describing several physical test methods required for blast furnace and steel slag. These differences in specifications from state-to-state identify the need for harmonization. For instance, a slag in Ohio with a pH of 10 would not be accepted as a beneficial use material in that state but would pass inspection in neighboring Indiana. Therefore, Indiana slag producers may have a better opportunity to market their slag in their state than Ohio slag producers do in theirs, regardless of whether the materials are the same.

A search on the Ohio EPA's website found policy DSW-0400.007 titled "Beneficial Use of Nontoxic Bottom Ash, Fly Ash and Spent Foundry Sand, and Other Exempt Waste" which facilitates the beneficial use of these materials to assure that water contamination does not occur (OEPA, 1994). The policy states that steel and ironmaking slags are covered by a separate policy which had not yet been identified by the completion of this research. For the included materials, Policy 0400.007 recommends leaching the materials with either the Toxicity Characterization Leaching Procedure (TCLP) or the ASTM D-3987 leach test, but states that the leaching solution should be chosen to best represent the end use of the site. The leachates

should be analyzed for 13 inorganic constituents. The policy only provides regulatory criteria for seven of these constituents however, and the purpose of analyzing for the other six is unclear. For the seven constituents, the leachates must not exceed 30 times the EPA Primary Maximum Contaminant Level (MCL) drinking water standards. It is unclear in the policy how this multiplier was calculated but it is possibly a dilution factor for leachate concentrations once they enter a hydrogeologic system. The TCLP test specified in this policy is discussed in Section 3.4 and has more recently been criticized (see Section 2.3) as a characterization tool for beneficial use applications since it was designed for municipal solid waste landfills. The ASTM D-3987 test titled "Standard Test Method for Shake Extraction of Solid Waste with Water" is used by several states including AR, IL, IA, and OH to classify waste streams (SAIC, 2003) but was not used in this research. This test uses an LS ratio of 20 and reagent grade water as an extraction solution with the solution pH determined by the material.

In addition to steel and iron slags, this research studied the environmental properties of a submerged arc welding (SAW) slag. SAW slag is created during the submerged arc welding of two pieces of steel. According to the Lincoln Electric (LE) website, the process involves forming an electric current, or arc, with either an AC or DC power source between the metal being welded (workpiece) and a welding electrode wire. The intense heat (6500°F) created by the arc melts the wire and the edges of the workpiece

to form a molten metal pool which cools and hardens into a weld. Metals at high temperatures can react with oxygen and nitrogen in the air which can weaken the strength of the weld. One way to shield the welding reaction from the atmosphere is to submerge the arc beneath a pile of granular flux, which also partially melts into the molten metal pool. According to a schematic of the SAW process found on the website for flux supplier Bavaria Schweisstechnik, as the electrode wire is guided along a seam, it leaves behind a hardened weld, a layer of hardened slag, and un-melted granular flux (Bavaria Schweisstechnik, 2006). LE is a worldwide distributor of arc welding products including the granular flux and electrode wires used in the SAW process. They provide a variety of fluxes and wires that can be used depending on the application. According to a feasibility study by The Welding Institute (TWI), LE provides between 60,000 and 80,000 tons of SAW flux worldwide and approximately 36,000 tons in North America (in 1996) (Routley, 2004) . The descriptions of the wires on the LE website differentiate between products with such characteristics as containing amounts of manganese, silicon, nickel, and molybdenum. It is unclear what effect this electrode wire composition has on the final SAW slag product. Currently there is no established market for the beneficial use of SAW slag. Although not extensively searched, there do not appear to be any specifications concerning the use of SAW slag in any application. LE contacted the Recycled Materials Resource Center (RMRC) with an interest in characterizing the environmental properties of SAW slag produced with

their flux and wire products. LE would like to provide their clients with the option to beneficially use their SAW slag rather than opt for disposal or costly reprocessing.

Lack of material specifications and environmental data are just some of the barriers that prevent the more widespread beneficial use of secondary and recycled materials. Economically, it may be cheaper to use natural aggregates than recycled materials due to higher transportation or processing costs. For example, a contractor in a rural setting may be more likely to use gravel from a source near the construction site rather than transport a material from another region. A recycled material may also require an extra step of aging or grading that makes using a natural aggregate more cost effective. Recycled and secondary materials have unique technical properties as well as environmental properties that may prevent their use. For example, a material may fail technically in colder regions of the country where freeze/thaw cycles occur regularly. The technical properties of steel and iron slag are well established and therefore testing methods were not included in this research. Technical properties of the SAW slag were not investigated as well since currently LE contacted the RMRC to only look at the environmental properties. The ideal beneficial use of the SAW slag has not been determined and therefore technical data is limited for this type of material. An additional barrier that prevents beneficial use of these materials is the belief by both the public and the regulators and

end-users that recycled and secondary materials are not safe to use. Mostly this is a result of historical mismanagement scenarios where a material failed physically or environmentally. End-users may rather use a historically safe natural aggregate to avoid the supposed risk of replacing a recycled material that fails technically or paying for costly cleanup from environmental damage. The public may also outwardly support the use of a recycled material until it is discovered that the application is near their neighborhood. To help remove this barrier the end-users and the public need access to more information regarding these materials to show them which ones are safe to use. This research was conducted to determine the proper steps slag producers and users should take to prevent environmental mismanagement scenarios and change the attitude towards beneficial use of these materials.

Table 1.1. USGS slag production/consumption data from 1991 to 1995 (U.S. only).

Slag Statistics	1996	1997	1998	1999	2000	2001	2002	2003	2004	2005 ¹
Production-marketable	20,500	18,900	18,400	19,000	16,300	16,900	19,100	19,700	21,200	21,000
Imports for consumption	346	663	700	920	1,200	2,600	1,100	1,100	1,000	1,700
Exports	3	9	10	12	20	<0.5 ²	100	100	100	<0.5 ²
Consumption-reported	20,800	19,600	19,000	19,900	20,200	19,500	19,100	19,700	21,100	21,000
BF Slag Production (% total)	65	65	60	65	57	69	65	60	60	60
Slag Producing Companies	16	16	15	15	15	15	18	23	25	29
Major Slag Uses-BF Slag (%)										
road base	40	43	35	40	29	37	33	---	---	---
asphalt/concrete products	38	40	40	33	37	35	45	---	---	---
fill	10	11	15	15	9	9	7	---	---	---
Major Slag Uses-Steel Slag (%)										
road base	39	40	25	23	30	33	37	---	---	---
asphalt/concrete products	15	16	30	30	27	18	22	---	---	---
fill	19	20	30	28	13	20	22	---	---	---

Notes:

--- not available

¹ Estimated values

CHAPTER 2

LITERATURE REVIEW

This chapter identifies and briefly describes previous research that is relevant to the work performed in this research. This includes physical, chemical, and beneficial use information on the slag materials as well as appropriate characterization and analytical methods performed on materials similar to the slags. An overview of the mechanisms that affect the release of constituents from a material is also given.

2.1 Steel and Iron Slag

Steel and iron slags have been used in engineering applications for over 150 years (NSA, 2006). Slag uses include natural aggregate substitution in bound and unbound applications, fill material, railroad ballast, Portland cement replacement, and soil amendment. Table 2.1 lists some physical properties from slag studies of both steel and iron slag. The studies used a range of slag types and aging extents so the results provide a general overview of slag properties. With the exception of two studies, the slag densities are lower than the granite and flint values shown in the table. The

higher slag densities represent samples qualified for hydraulic engineering purposes such as bank erosion prevention (Motz and Geiseler, 2001).

Steel and iron slags vary physically depending on the process in which they were produced. With blast furnace slag, the cooling method used during production controls the final slag product. Allowing the material to cool slowly produces air-cooled slag which can be processed into a variety of sizes and used as a construction aggregate. Quickly cooling the slag with water or steam produces a lightweight material called pelletized or expanded blast furnace slag. Cooling the material with large quantities of water produces a finer slag called ground granulated blast furnace slag which can be ground and used as cement (NSA, 2006; van Oss, 2002). Figure 2.1 shows the particle size distribution of a blast furnace slag and two steel slags (Proctor et al., 2000). The maximum slag particle size produced during the steel and iron-making processes is unclear; however the literature gives an example of 250 mm slag fractions used as riprap (Proctor et al., 2000). Blast furnace slag is desirable in construction applications because of its hydraulic binding properties. This reaction occurs slowly compared to cement but produces less heat. The cementing behavior is more effective when the particles are finer (Makela and Hoynala, 2000; van Oss, 2002) Ground granulated blast furnace slag can be mixed with cement to make Portland-slag cement. This is favorable because calcium hydroxide released by Portland cement hydration acts as a catalyst

to activate the cementing properties of the slag (Makela and Hoynala, 2000; van Oss, 2002). Slag cementation can also occur without the Portland cement lime hydration, possibly from calcium hydroxide release from calcium sulfide hydration (Makikyro, 2004). This is beneficial for blast furnace use in roadbases as the self-cementing properties allow for flexible pavement depths to be reduced (Lemass, 1992). The physical properties of air-cooled blast furnace slag with respect to road construction are comparable if not better than natural aggregates (Arm et al., 2001). Blast furnace slag is also desirable to use in construction applications because generally it does not have the same risk of expansion that steel slags have due to a lower expandable oxides content (Wang and Emery, 2004). However, Juckes (2003) references the British Standards Institution (EN1744-1:1998) which states that volume instability can occur in blast furnace slag through hydration of sulfide phases if the concentrations are high enough. Mathur et al. (1999) looked at the physical properties of blast furnace slag and steel slag and concluded that both materials were suitable to replace natural stone aggregates in base and subbase road layers, as long as the steel slag was adequately weathered. The study also mixed various slags together and determined that a mixture of ACBF slag (50%), steel slag (20%), granulated blast furnace slag (20%), fly ash (6%), and lime (4%) would self-stabilize over time and form an adequate bound base or subbase road layer.

Steel slag is not as widely used as aggregate in bound applications due to expansion issues during free lime reactions with water that lead to material deterioration and instability (Rohde et al., 2003; Nomura and Enokido, 1981; Dippenaar, 2005). In addition, if the magnesium oxide content is high the slag may contain free MgO which is also subject to expansion. The majority of the free lime and magnesium are remnants of the slag production process. In addition to remnants of the production process, free lime can also be a result of the disassociation of tricalcium silicate described in the following equation (Viklund-White and Ye, 1999):



Free lime can be observed in nodules several mm in diameter within the slag particles (Juckes, 2003). The free lime and magnesium reactions are presented as follows (Makikyro, 2004):



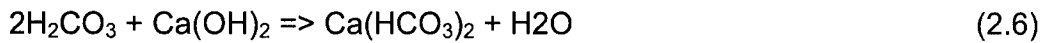
The reaction and subsequent production of calcium and magnesium hydroxides results in an increase in sample volume. The free magnesium oxide hydrates slower than the free lime creating a more long-term expansion issue. (Viklund-White and Ye, 1999; Motz and Geiseler, 2001).

Due to this expansion issue, steel slag is often used in unbound applications such as unpaved parking lots and roads (Motz and Geiseler, 2001) The extent of expansion during material use can be lessened through an aging process where the slag is stockpiled and hydrated over a period of time to allow the free lime and/or free MgO to transform into hydroxides (Rohde et al., 2003; Motz and Geisler, 2001). This process does not decrease the amount of expansion but rather allows the material to expand in the stockpile rather than in an engineering application (Makikyro, 2004). For steel slag produced in Ohio, ODOT Supplemental Specification 905 requires periodic mixing and watering of the stockpile for at least 6 months followed by expansion testing equivalent to Pennsylvania DOT PTM No. 130. The maximum total expansion for the test should not exceed 0.5 percent. Stockpiles that fail this test are aged for a minimum of 2 more months. One issue with common aging processes is that often the free lime is located within the slag particles and not readily hydrated compared to the free lime located on or near the surface. This free lime can be released later in the slag's life cycle as particles break down leading to later periods of expansion (Juckes, 2003). Aging the slag with steam decreases the aging time because the reaction is accelerated with the increased temperatures and because the small steam particles intrude the slag particles faster than the larger water molecules to reach included free oxides (Morishita et al., 1997).

Rohde et al. (2003) studied the physical properties of EAF slags and in particular their expansive properties. A fresh slag and a slag aged for four months were tested with ASTM D4792 (Potential Expansion of Aggregates from Hydration Reactions). ASTM D2940 titled "Graded Aggregate Material for Bases or Subbases for Highways or Airports" requires that the expansion from this test should not exceed 0.5% after 168h of testing. After 168h the aged sample was below 0.3% while the fresh sample was 0.9% suggesting that 4 months of curing time is adequate for that particular EAF slag. Resilient modulus testing with slags with various ages showed that aging time does not affect the modulus of elasticity of the EAF samples. Additional physical properties of aged slag samples from this study are shown in Table 2.2. Rohde et al. (2003) concluded that the high California bearing ratio (close to 200%) and resilient moduli (almost 500 MPa for a confining stress of 100 kPa) of the EAF slag supports its use as a base material in low volume roads.

Studies have found that a second reaction can occur with steel slag that is disadvantageous for its use in unbound applications. Carbonic acid formed from the reaction of carbon dioxide (atmospheric and from auto exhaust) with water can react with the calcium hydroxide formed from the free lime hydration. The reaction forms a highly soluble calcium bicarbonate solution which can evaporate with atmospheric contact to re-release CO₂ and precipitate calcium carbonate, also known as tufa. The deposition of tufa is

more prevalent in warmer climates where evaporation occurs readily, whereas in colder climates the CO₂ often remains in solution (Gupta et al., 1994).



Because tufa precipitation relies on evaporation, it is most often deposited at the mouths of drainage pipes or around embankment seeps. Boyer (1994) identified a similar scenario in which leachate within a base layer becomes saturated with Ca(OH)₂ in the absence of CO₂. Once the leachate leaves the base layer it reacts with atmospheric CO₂ to form H₂CO₃ which disassociates to form (CO₃)²⁺ which then reacts with Ca²⁺ to form CaCO₃. This scenario differs slightly from Gupta et al.'s (1994) interpretation in that the Ca(OH)₂ solution reacts directly with atmospheric CO₂ rather than precipitation containing dissolved CO₂ (carbonic acid). This is important since Boyer's (1994) interpretation does not require leachate evaporation to form tufa and therefore could occur in colder climates.

Gupta et al. (1994) identifies the slag reactivity, surface area, particle size, pore size distribution, effective porosity, and degree of weathering as

factors that control the tufa precipitation. It appears the most important factor regarding tufa precipitation, as well as slag expansion, is the amount of free lime in the slag. Therefore slags containing low or no amounts of free lime, such as blast furnace slag, have a lower risk of forming tufa (Gupta et al., 1994). The aging process previously mentioned is an attempt to hydrate the free lime prior to placement to reduce slag expansion and tufa precipitation. Gupta et al. (1994) took samples of stockpiled aging steel slag from depths ranging 0-7 feet and analyzed for free lime content using an anhydrous ethylene glycol test. The results showed that the percent free lime in the slag increased with depth but that even at the surface of an aged pile the slag still contained some free lime. In addition, tufa was produced in the laboratory using aged and un-aged samples indicating extended stockpiling is not completely effective at halting tufa formation after placement. This was also suggested by Boyer (1994) who found extensive tufa precipitation from slag that was supposedly aged for decades prior to placement in a highway base layer. This study is further discussed later in this literature review.

Only two studies involving slag surface area were uncovered in this literature search. Gupta, et al. (1994) looked at the surface area of a blast furnace slag and two steel slags a study regarding tufa deposition from highway base layers. The slag samples were analyzed with a Micromeritics Gemini 2360 Analyzer using the Brunauer, Emmett, and Teller (BET)

methods. The results from this test are shown in Table 2.3. In general, the aged open hearth (OH) and basic oxygen furnace (BOF) slags showed higher surface areas than the un-aged samples. The one aged blast furnace slag had a lower surface area than most of the aged steel slag samples. Gupta et al. (1994) hypothesized that slags with higher surface areas should be more reactive than the samples with lower surface areas. Additional surface area data of four steel slag samples is presented by Tossavainen et al. (2005) and is shown in Table 2.4.

The most extensive steel slag work has been performed by Ann-Marie Fallman of the Swedish Geotechnical Institute. Fallman and Rosen (2001) studied the leaching from blast furnace and EAF steel slags in lysimeters and laboratory experiments. The goal of the study was to determine what the controlling factors were in the field lysimeters and compare them to the controlling factors in the laboratory experiments. An additional goal of the study was to determine if leaching from a material after placement in the field could be predicted from laboratory experiments. Laboratory testing involved a column test (NT ENVIR 002), an availability test under natural and oxidized conditions, and a pH static test at pH 4, 6, 8, 10, and 12. The availability and pH static results were presented in Fallman and Hartlen (1994). The results from these tests were compared to samples collected from lysimeters containing the same slags. Direct comparisons were made based on the liquid to solid ratios reached in the laboratory and field tests.

The lysimeters were loosely packed and therefore had low water retention which led to an increase in atmospheric exposure and a decrease in pH. With the steel slag, constituent concentrations were greater in the lysimeters than in the column tests with the exception of aluminum, barium, and lead. The barium decrease in the lysimeter is explained as result of barium precipitation after barium sulfide oxidation. For the blast furnace slag, all constituents detected were greater in the lysimeter than in the column test. Variability in constituent release was found between the normal and oxidized availability tests. Metals commonly bound to sulfides such as cadmium, copper, nickel, and lead were more readily released under the oxidizing conditions. Additionally, barium and vanadium release increased with oxidation while iron release decreased greatly due to precipitation. Fallman and Hartlen (1994) concluded that pH influences the solubility of the slags more than oxidation, but that oxidation makes the constituents more available for pH influence. Additionally, pH and redox conditions in the lysimeters varied significantly from the laboratory tests after one year leading to large differences in the leachability of some constituents. This highlights the problem with comparing laboratory results to field conditions. Fallman and Hartlen (1994) concluded that it is possible to predict field behavior with laboratory analysis but recommend that pH and redox conditions be closely controlled in the tests.

Due to its high alkalinity, steel slag is often used to passively control acid mine drainage (AMD) emanating from tailing piles. As mining tailings are brought to the ground surface, oxygen and water oxidize sulfide minerals within the waste to form sulfate-rich acidic drainage (Simmons and Ziemkiewicz, 2003). Left untreated, AMD can flow into nearby waterways destroying plant and animal habitat. This scenario is often found in coal-producing states such as West Virginia and Pennsylvania. Limestone is commonly used as a neutralizing amendment due to its cost; however, the amount of alkalinity produced from limestone is not as great as the concentration produced by steel slag (Ziemkiewicz et al., 1997). The slag can be placed in a retention pond or channel to neutralize the pH of flowing AMD or mixed into the tailings as an alkaline amendment (Ziemkiewicz et al., 2002; Skousan et al., 1998). An additional option is to pump a slurry containing steel slag into the mine for in-situ treatment of the exposed cave walls (NSA). The high amounts of calcium, magnesium, and manganese within the material mainly contribute to the acid neutralization capacity of the slag (Yan et al., 2000; Ziemkiewicz 1998). Although highly effective at neutralizing acidic wastes, there is concern with hazardous metals leaching from slag as it comes in contact with AMD (Skousan et al., 1998).

Many studies have published chemical composition data for steel and iron slags. Some of this composition data is presented in Table 2.5 as weight percent. For the steel slags (BOF and EAF), regardless of aging extent, the

chemical composition consists of the following oxides in descending order: CaO, SiO₂, MgO. Both Al₂O₃ and MnO followed MgO in composition depending on the study and some studies identified small percentages of P₂O₅ as well. The steel slags that were tested for total iron contained percentages ranging 14 to 30. Only one of the iron slags was tested for total iron and showed a very low percentage of 0.49. The two iron slags in Table 2.5 show high CaO percentages similar to the steel slags but show higher SiO₂ content. Iron slags generally contain high concentrations of silica and alumina from the ore used in the iron-making process as well as calcium and magnesium from the fluxing agents (Proctor et al., 2000). Rohde et al. (2003) presents oxide composition data from Geyer (2000) of slags taken from two separate stages of the EAF process: an oxidized slag from the electric arc furnace and a reduced slag from the subsequent reducing furnace. These slags are normally mixed in the industrial process (Rohde et al., 2003). The oxide composition of these two slags is shown in Table 2.6. In comparison, the oxidized slag shows a decrease in CaO, SiO₂, and SO₃ and an increase in FeO. MgO and Al₂SO₃ were the same for both slags.

Gupta et al. (1994) analyzed slag samples with x-ray diffraction to determine the dominating mineralogy. The results showed that the dominating minerals in the ACBF slag were calcium magnesium silicate (Ca₂MgSi₂O₇) and an unknown phase (Fe-Mg-Al-SiO), and in the BOF slags, dicalcium silicate (Ca₂SiO₄) and dicalcium ferrite (Ca₂Fe₂O₅)

dominated. The tufa reaction minerals CaCO_3 , MgO , and Ca(OH)_2 were found in the majority of the BOF slag samples with an absence of these minerals explained as differences in atmospheric weathering (Gupta et al., 1994). None of these three minerals were found in the ACBF slag validating the previous findings that blast furnace slag should not produce tufa (Gupta et al., 1994). Geiseler and Motz (2001) identify the dominating minerals of BOF and EAF slags as Ca_2SiO_4 , $\text{Ca}_2\text{Fe}_2\text{O}_5$, and FeO , and Vicklund-White and Ye (1999) present the same minerals for BOF slag. Tossavainen and Lind (2005) identified the major crystal phase of BOF slag as Ca_2SiO_4 , and for EAF slag, Ca_2SiO_4 and merwinite ($\text{Ca}_3\text{Mg}(\text{SiO}_4)_2$). Vicklund-White and Ye (1999) identify the main mineral phases in BOF slag as Ca_2SiO_4 , $\text{Ca}_2\text{Fe}_2\text{O}_5$, and FeO .

2.2 Submerged Arc Welding Slag

Very little literature was found for the submerged arc welding slag, mostly because it is produced in limited quantities compared to the iron and steel slags and is a more underutilized slag. Limited physical and chemical data was provided by Lincoln Electric in a Product Certificate for Lincolnweld 995N Flux, a specific SAW flux that gives an indication of the SAW slag properties. The physical data is presented in Table 2.7 and the compositional data is presented in Table 2.8. Additionally included in the Product Certificate is a Basicity Index number of 1.29 calculated using the Boniszewski formula shown below:

$$BI = \frac{0.5(FeO + MnO) + CaO + MgO + Na_2O + K_2O + CaF_2}{SiO_2 + 0.5(TiO_2 + ZrO_2 + Al_2O_3)} \quad (2.8)$$

According to the website for Bavaria Schweisstechnik, a German company that supplies SAW fluxes, the basicity index is the ratio of the basic and acid oxides of the flux (Bavaria Schweisstechnik, 2006). The higher the B.I., the lower the O₂ content in the weld metal which is not desirable in the submerged arc welding process. According to the website, this particular flux is classified as Semibasic/Basic because its B.I. is between 1.2 and 2. The compositional data listed in Table 2.8 show high percentages of Al₂O₃, SiO₂, MgO, CaF₂, and Mn_xO_y in descending order. The only leaching data found in the literature review are the TCLP results shown in Table 2.9 for Lincoln Electric fluxes. Barium was detected in every flux sample and chromium was detected in more than half of the samples. The only other detections are a lead concentration for L60 & H560 and arsenic, lead, and selenium concentrations for 995N & L61. None of the TCLP concentrations were detected above the USEPA Toxicity Characteristics list standards. MSDS sheets provided on the Lincoln Electric website list compositional data by weight percent of individual fluxes and electrodes used in the SAW process. Even though both the flux and the electrode are used in the creation of the slag, the compositional data cannot be directly used for the slag. Lincoln Electric contracted The Welding Institute (TWI) to perform a feasibility report on global SAW slag utilization. The TWI report quoted

Lincoln Electric as saying that manganese and iron concentrations are most likely to change from the flux compositions. The iron usually increases and the manganese can increase or decrease by over 300%. Most of the other elements can increase or decrease by 5 to 40%. The MSDS sheets therefore provide only an estimate of what elements are expected in the slag rather than actual percentages.

The TWI report identified two companies that recycle SAW slag, Harbert's Products Inc. and Titus Steel Co., by reprocessing the slag back into usable flux and returning it to the slag supplier. According to a Harbert's technical brochure, approximately 25% of the slag by weight is lost during the recycling process and magnetic impurities are separated from the slag and disposed of as waste (Harberts, 2006). The report concluded that the regions investigated were interested in using the SAW slag in beneficial use applications and that the most feasible applications were those currently associated with steel slag beneficial use (aggregate, road building, and construction applications). TWI acknowledged that the composition of SAW slag is more complex than that of steel slags. The volume of SAW slag generated worldwide is also much less than the steel and iron slag volumes. Additionally, steel and iron slag production is centralized to steel and iron mills, making collection and transport easier than for SAW slag, which is produced in more fragmented locations. TWI concluded that specific SAW slag analysis should be used for specific beneficial use applications.

2.3 Leaching Overview

One of the largest barriers towards the beneficial use of secondary materials is the risk of hazardous contaminants leaching from the material after placement. This threat often leads to the use of materials considered safe based on historical use such as natural aggregates. Therefore, an important step in promoting the use a material is to characterize its leaching properties under a range of environmental conditions. Historically, decision makers have attempted to characterize materials based on a single test, such as the EPA Toxicity Characterization Leaching Procedure (TCLP). The TCLP test was established to replace the formally used Extraction Procedure (EP). The goal of the TCLP test is to classify whether a material is safe for co-disposal with solid waste in a municipal solid waste landfill. It is this assumption of co-disposal that has fueled criticism of the TCLP test considering the recent push to keep secondary and recycled materials out of landfills and involve them in beneficial use applications. A 1999 Scientific Advisory Board review (SAB, 1999) identified issues with the TCLP test and recommended that the EPA “improve leach test procedures, validate them in the field, and then implement them.” The review identified the need for testing that, if needed, could be waste specific and site specific and could cover a range of expected parameters. The committee admitted that this would not be possible with one test so multiple tests and possibly a tiered testing scheme would be required. The recommendations did not include

which parameters the testing protocol should include but the report did mention particle size, liquid-to-solid (LS) ratio, pH, leaching kinetics, and aging extent, among others, as factors that can affect leachability.

2.3.1 Physical Factors Affecting Leaching

Of the physical factors that affect leaching, particle size is important to consider. In larger particle sizes, the release of constituents from within the particle is controlled by diffusion. Since diffusion-controlled release is often slower, leaching tests with larger particle sizes are more time consuming. Therefore, in equilibrium based tests, particle size reduction will allow for a faster and more practical test (van der Sloot and Mulder, 2002; Lehmann et al., 2000). van der Sloot and Mulder (2002) proposed the following equation relating particle size with constituent equilibrium, assuming all other properties remain constant:

$$r = \sqrt{(2 \times De \times t)} \quad (2.9)$$

where r is the particle size (m), De is the effective diffusion coefficient (m^2/s), and t is the time to equilibrium (s). Size reduction increases particle surface area and exposes fresh surfaces to the atmosphere and leachant used in a leaching test. This change can affect the leaching characteristics of a material, especially one that has undergone surficial weathering where the surface chemistry varies greatly from the chemistry within the particles.

Particle size can also affect the surface wash-off leaching mechanism. A weathered material containing fines will have a higher surface area than a coarser material, and may therefore have more soluble surface deposition available for wash-off. Particle size is most important for non-porous materials such as slag, where low porosity prohibits leachant contact with the internal particle matrix. It is important to fully understand how particle size affects leaching when evaluating leaching data since the particle size used in a laboratory test may differ from the particle size used in the field application. Particle size can also change during and after field placement due to compaction, vehicular loading, and weathering (SAIC, 2003). Particle size reduction may have a strong effect on pH and redox conditions as well, which can strongly alter leaching conditions. For example, the idea that reducing particle size will increase constituent release may not always be true if the increased surface area raises the pH to a level of minimum solubility for a particular constituent. (van der Sloot and Mulder, 2002).

An additional physical factor affecting leaching characteristics is sample size. Samples of heterogeneous materials will require either homogenization through particle size reduction or a larger sample aliquot used in the leaching test (Kosson et al., 2002). Temperature is normally not controlled in leaching tests but is known to affect leaching mechanisms (Lehmann et al., 2000). The majority of the leaching tests discussed in this research are performed at room temperature. During equilibrium testing it is

important to completely mix the sample container to ensure equal contact between the leachant and the material. This is either accomplished by end-over-end rotation of closed sample containers or constant stirring with magnetic stir bars or overhead mixers. It is important that latter method does not stir the sample enough to cause CO₂ uptake of a high pH leachate which may change pH conditions (Lehmann et al., 2000).

The main mode of transport of constituents from a material is through contact with water. This contact is normally a result of water percolating down through the material or from contact with groundwater if the material is placed below the water table. An additional source of water is moisture released from the actual material after placement and compaction (Kosson et al., 1996). Depending on the beneficial use scenario and the regional weather conditions, a material will come into contact with varying amounts of water over its life use. Materials placed in bound applications or below impermeable surfaces will encounter less water than materials used in an embankment for example. Infiltration rates vary depending on the geographical location and time of year. Water contact is also dependent on the extent of compaction. Water may flow through a loosely compacted material leading to an equilibrium based leaching mechanism, or around heavily compacted materials leading to a mass transfer controlled release mechanism (Kosson et al., 2002). Specific leaching tests are designed to

address both of these infiltration scenarios and will be discussed in a later section.

The amount of liquid a material comes in contact with is explained with a liquid-to-solid (LS) ratio, which is the ratio of the amount of leachant to the amount of material for a particular test. The LS ratio is calculated according to (Kosson et al., 1996):

$$LS_{site} = 10 \times \frac{inf \times t_{year}}{\rho \times H_{fill}} \quad (2.10)$$

where LS_{site} is the site-specific liquid to solid ratio (L/kg), inf is the anticipated annual infiltration rate (cm/year), t is the estimated time period (year), ρ is the material fill density (kg/m²), H_{fill} is the fill depth (m), and 10 is a conversion factor. Kosson et al. (2002) recommends a hypothetical estimated time frame of 100 years for assessing constituent release from a material. Lower concentrations of less soluble species and higher concentrations of more soluble species may be present in low LS ratios (SAIC, 2003). SAIC (2003) references Lowenbach (1978) explaining that smaller LS ratios may limit the amount of leaching because of the common ion effect. Additionally, high LS ratios may result in higher concentrations of some constituents as well as a larger number of constituents leaching. Constituent concentrations in higher LS ratios may asymptotically approach the total leachable, or available, amount of that constituent (SAIC, 2003).

High LS ratios, however, are often not applicable to certain applications, such as a road base layer under an impermeable surface, because the LS ratio is unachievable in a realistic time-frame. LS ratios will be discussed in more detail in the section on leaching mechanism scenarios.

2.3.2 Chemical Factors Affecting Leaching

Chemical factors also affect constituent leaching from recycled materials. pH is known to control the solubility of many inorganic species (Lehmann et al., 2000; Kosson et al., 2002; SAIC 2003) so characterizing leaching behavior as a function of pH covers a range of relevant conditions and is helpful in determining environmental impact (van der Sloot, 2000). Additionally, pH affects the formation of complexes and sorbing conditions after constituents are released from a material (Lehmann et al., 2000). In terms of general leaching behavior, van der Sloot (2000) states that metals have a minimum solubility at neutral pH, oxyanions show a minimum solubility at neutral to slightly alkaline pH, and salt solubility shows no relation to pH. In the field, pH is influenced either by the properties of the material used or the environment surrounding the waste. Generally lower pH values are encountered in some applications, such as acid mine drainage remediation, but they are not ideal for beneficial use of recycled or secondary materials (van der Sloot, 1991). If a material is highly buffering, as slags and many waste materials are known to be, it may control the local pH depending on its acid neutralization capacity (ANC). The ANC of a

material determines how much the pH will change as acid is added to the leaching process (Yan et al., 1998). It also identifies how long a material can impose its pH conditions on a leachate (Kosson and van der Sloot, 1997).

pH conditions may be different for different types of materials due to differences in chemical composition, mineralogy, morphology, and chemical properties (Yan et al., 1998). Yan et al. (1998) studied the acid neutralization capacity of MSWI bottom ash and steel slag with acid titration and determined that pH-dependent leaching from waste materials occurs in one direction (the solid cannot be reformed), but that depending on their equilibria with the aqueous solution, solids can precipitate and re-dissolve. All of these reactions define the solution pH. Yan et al. (1998) also studied the rate at which the neutralization reactions occurred and determined that if acid is added quickly, the reactions do not have enough time to react with the protons at the rate they are added. If the acid is added slowly the reaction occurs at the same rate as the acid addition. Therefore, the two scenarios may give different pHs for the same amount of acid added. Through geochemical simulation, it was determined that the major elements controlling the ANC were in the two materials were calcium, magnesium, and silica and calcium provided the largest neutralization capacity. Yan et al. (1998) also determined that the role of silica was complicated because most of the secondary minerals precipitated in the neutralization reaction

are silicate minerals. The neutralization capacity of the steel slag was highest above pH 8.5 and lower in the weakly alkaline or neutral pH range. Yan et al. (1998) also determined that the long term ANC of steel slag below pH 9 should be analyzed for more than 500 hours and that a 24-hour test provides less than 60% of the full ANC, even with particle sizes under 160 microns (Yan et al., 2000).

Similar to pH, the reduction and oxidation (redox) properties of a material can influence the leaching of particular constituents (Kosson et al., 2002; SAIC 2003). Comans et al. (1991) studied the chemical behavior of BOF steel slag with respect to oxidation/reduction environments in both laboratory and pilot scale experiments. Redox conditions can influence the leaching of particular constituents such as chromium, arsenic, selenium (Kosson et al., 2002). Angus and Glasser (1986) observed reducing conditions when slag is in contact with water as sulfide species leach from the material. Tossavainen and Lind (2005) found a high sulfur content (1.4%) in blast furnace slag. Samples identified as “more porous” and “more dense” were used in the experiments as well as a sample analyzed under inert nitrogen conditions. The laboratory testing included a total composition analysis, an availability test, and a tank leaching test. The total composition analysis was conducted to calculate the concentrations of sodium, potassium, calcium, magnesium, barium, fluoride, sulfate, chloride, and vanadium in each slag sample. The availability test involved leaching the

samples at a constant pH of 4 and a liquid to solid ratio of 100. In the tank leaching test, the sample is immersed in water which is sampled and refreshed periodically. From this test the cumulative flux of constituents can be calculated as well as the effective diffusion coefficient. These methods are discussed in more detail in the Methods and Materials section.

The results from the Comans et al. (1991) laboratory testing are shown in Table 2.10. The study concluded the high calcium leaching from the tank leaching test for #2 was a remnant from the calcium (fluxing agent) used in the BOF process. Slag deterioration, which can occur with the hydration of calcium (free lime), was observed in this sample after 30 days of tank leaching. Comans et al. (1991) also proposed that the low vanadium and high barium releases for the #2 sample were consistent with reducing environments. Barium is released from BaSO_4 if the redox potential is low enough to reduce the SO_4^{2-} whereas vanadium release decreases under reducing conditions (Comans et al., 1991). For the pilot scale experiment conducted in this study, 1350 kg of slag was placed in a 1 m^3 container which was then filled with tap water. Water was pumped horizontally across the top of the layer via inflow and outflow pipes. Five sampling ports located vertically on the container were used to sample interstitial water from different depths in the slag bed. After a few days of the experiment, a sharp redox/pH interface formed where above 15-35 cm the system was oxidized with a lower pH (8 to 9.5) whereas below this depth the conditions were

reducing with a more alkaline pH (12.5-13.5). Above the interface calcium precipitated from the water as CaCO_3 while in the reduced zone calcium stayed in solution. This difference is explained by the presence and absence of CO_2 in the oxidized and reduced zones, respectively (Comans et al., 1991). Additionally, magnesium, sodium, potassium, and chloride did not leach from the slag in significant amounts. Barium showed increased release below the interface while sulfate showed a decreased release below the interface. Vanadium release showed an initial release throughout the slag bed attributed to surface wash-off followed by continued release only in the oxidized zone.

2.3.3 Release Mechanisms

An important part of laboratory leaching test is identifying the expected waste management scenario for a material. This includes identifying a site-specific LS ratio, the expected field pH, a time frame for assessment, and the major release mechanisms involved (Kosson et al., 2002). The mechanisms considered in this research are solubility (equilibrium) and mass-transfer controlled release. Solubility control occurs when a solution in contact with a waste is saturated with a constituent of concern. This most often occurs at low LS ratios found in percolation scenarios (Kosson et al., 1996) where water is in contact with the material long enough for constituent equilibrium to occur. Percolation scenarios include precipitation flowing through and uncapped embankment or precipitation seeping

through cracks in a road surface and trickling down through the base layers. The material in the embankment scenario may have a higher LS ratio than the base layer scenario because more water can seep through the uncapped application than the paved application. In addition, pH and redox conditions may vary between the uncapped and capped scenarios if atmospheric exposure differs. These are important considerations since both pH and LS ratio can affect constituent solubility (Kosson et al., 2002; Sanchez and Kosson, 2005). Equilibrium based leaching tests therefore measure contaminant release as a function of these parameters. Solubility can increase in the presence of complexing agents such as chloride or reduced in the presence of co-precipitating species such as sulfate and sulfide (Kosson et al., 1996). Equilibrium based leaching test data can be used to predict long-term constituent release by calculating the cumulative mass of constituent released per unit mass of material. First the expected field LS ratio is calculated from Equation 2. The leaching time frame, infiltration rate, fill density, and fill height are required for this. The calculated LS ratio is then used along with solubility data as a function of pH for a particular constituent to calculate the cumulative mass released at time t_{year} (Kosson et al., 1996, 2002):

$$M_{\Sigma} = (LS_{\text{site}}) \times (S) \quad (2.11)$$

where M_{Σ} is the cumulative constituent mass released per unit mass (mg/kg) and S is the constituent solubility at the expected field pH (mg/L). The cumulative mass released per underlying unit area of a layer of material is also calculated (Kosson et al., 1996, 2002):

$$M_t = \rho \times H_{fill} \times M_{\Sigma} \quad (2.12)$$

where M_t is the cumulative constituent mass released per underlying unit area (mg/m²). Equilibrium based leaching mechanisms are further discussed in the Methods and Materials section.

Mass transfer controlled release occurs when the limiting step is the rate at which constituents leach from a material. This release is usually controlled by diffusion (Kosson et al., 1996). This mechanism can occur when water predominantly flows around a monolithic or compacted granular material rather than percolates through it, as is described in the equilibrium based release scenario (Kosson et al., 1996, 2002). Release is therefore limited by the rate at which constituents diffuse from inside the monolith or compacted layer to the material-leachant interface. This mechanism is significant for this research because it can be applied to granular materials that act as a monolith due to compaction during field placement. The compaction may lower the permeability of the layer causing percolating water to flow around the layer rather than through it. It is assumed in this scenario that equilibrium conditions are not reached (Kosson et al., 1996). Ogunro and

Inyang (2003) explain the diffusion process as starting when a leachant (normally water) permeates into a material particle (or monolith) and dissolves constituents releasing them into solution within the particle. As more constituent dissolves, a concentration gradient is formed causing the constituent to diffuse to the particle/leachant interface where the concentration is lower. Some constituent is lost during this process to sorption, ion exchange, and precipitation. Diffusion continues until the concentration gradient is removed and equilibrium occurs between the particle and the leachant. Reactions such as precipitation and sorption can occur subsequent to this but they occur at a constant rate of exchange to maintain equilibrium conditions. Constituent diffusion is considered to continue until the cumulative release reaches the constituent availability (Kosson et al., 1996). Mass transfer based leaching mechanisms are further discussed in the Methods and Materials section.

2.3.4 Fate and Transport

Leaching tests provide data for constituent concentrations located at or near the source, either in the pore-water or at the material-leachant interface. In a field application, as leachate leaves a material and moves through the unsaturated zone into the groundwater, constituent concentrations are decreased by adsorption, degradation, and dilution (SAIC, 2003). This highlights the importance of fate and transport modeling of leach test data to fully determine the environmental risk of a material. One example of a

program is the Environmental Protection Agency Composite Model for Leachate Migration with Transformation Products (EPACMTP) which can simulate the fate and transport of constituents released from waste management units (WMUs) into the unsaturated and saturated zones. The model accounts for sorption, degradation, and dilution to produce a maximum predicted groundwater exposure concentration at a receptor. The EPA's Industrial Waste Management Evaluation Model (IWEM) is a more user-friendly program that utilizes the EPACMTP model to calculate contaminant concentrations. Both the EPACMTP and IWEM programs were designed to model contaminant fate and transport from industrial waste applications such as landfills, waste piles, and surface impoundments. However, work is currently underway to apply the user-friendly IWEM program to beneficial use applications such as road construction so that it can be used by producers and end users of recycled materials. The IWEM program will be discussed in further detail.

2.3.5 Mismanagement Scenarios

Problematic barriers affecting the beneficial use of steel and iron slag are historical mismanagement scenarios. When given the opportunity to use a recycled material over a natural aggregate, a user might choose the natural aggregate to avoid any environmental or structural issues that have been documented in past recycled material use. Only two mismanagement scenarios regarding slags were identified in this literature search. The first

involves a runway construction project at Cleveland Hopkins International Airport that used crushed slag as a fill material. According to an article in Recyclingtoday.com, after slag placement in the runway, a “milky white, sulfuric runoff” was found seeping into a nearby creek. An EPA spokesperson was quoted in the article as saying that slag is considered safe for construction use if “it has been aged and treated to remove pollutants” (Recycling Today, 2001). Several articles identify the slag as steel slag; however it seems more plausible that a leachate with high sulfur content would emanate from blast furnace slag. A report by the Rocky River Watershed Council identifies the first discovery of the leachate in Abram Creek as occurring in the summer of 2001. It states that 600,000 cubic yards of “improperly aged” steel slag was placed as a base material for a new taxiway and runway at the airport (Rocky River Watershed Council, 2002). Discharge from the slag layer contaminated a storm water basin before entering and contaminating Abram Creek and the Rocky River. In response to the contamination the Ohio EPA ordered the removal of the slag. A July 2002 report archived on Cleveland.com states that a contractor removed 100,000 tons of slag from the runway and replaced it with crushed stone. It was unclear from the article what the total cleanup cost was but it did say that the City of Cleveland had agreed to pay \$2.1 million to the contractor (Cleveland.com, 2002).

The second mismanagement scenario involves the deposition of tufa along highways in which steel slag was used as a construction material. One tufa scenario described by Feldmann et al. (1982) occurred along highways in northeastern Ohio. Calcareous tufa was discovered clogging drain outlets and catch basins, and covering embankment slopes at over one hundred locations. This was identified as a problem because clogged drainage systems could prevent proper drainage of the highway pavement and subbase and lead to structural failure. The deposits were also considered an eyesore and interfered with highway maintenance operations. Feldmann et al. (1982) found that the tufa deposition was directly related to the use of slag as a subbase and underdrain backfill aggregate. The study concluded that as long as slag was used extensively as subbase or backfill material, tufa deposition would occur. Additional work on the tufa deposits of northeastern Ohio was conducted by Gupta et al. (1994).

A second tufa scenario was identified by Boyer (1994) as occurring along a highway embankment in Maryland. In April 1986, a white solid was discovered on an embankment along I-695 and categorized as a suspected chemical spill. The solid was removed but was discovered again in October 1987. The source of the material was identified as a spring in the side of the embankment with an effluent pH exceeding 12.5. This was considered hazardous waste by the Maryland Department of Environment prompting the construction of a lined containment pond that required periodic pumping

and treatment. The source of the leachate was identified as an unidentified slag material used in the embankment construction. Tufa production is known to occur in fresh steel slag samples with high free lime contents. However, as previously mentioned, the slags studied by Boyer were supposedly aged for decades prior to placement in the embankment. As of 1994 the total remediation cost of the tufa had reached \$1 million and a hydrochloric acid neutralization treatment plant was scheduled to treat the effluent.

2.3.6 Background Concentrations

An important consideration in the beneficial use of recycled materials in a highway application is the determination of contaminant background levels in surrounding soils, groundwater, and surface water. Background concentrations of contaminants are referred to here as concentrations that would exist in the soil, groundwater, and surface water surrounding a highway prior to the placement of a particular recycled material. This data is important because these concentrations may be higher than concentrations of the same constituent leaching out of a recycled material. A decision maker should be aware of these background concentrations when making a beneficial use determination based on leachate data.

One source of these background concentrations is the degradation and deposition of natural parent materials containing these constituents

indicated by consistent levels throughout the soil column (Pils et al., 2004). Another source is the deposition of these constituents via runoff and air pollution indicated by an increase in contaminants in the top section of the soil column (Turer et al., 2001). Local sources of contaminants in a highway environment are identified by Ball et al. (1998) and shown in Table 2.11. Since this study was conducted in Australia, the list may vary in the United States depending on differences in highway engineering and maintenance (pavement roughness, pesticide use, etc.). The list does however show the variety of sources for EPA regulated constituents such as *Cu*.

The implications of high background levels in soils, groundwater, and surface water are unclear. If the background levels are higher than those predicted to leach from the recycled material, a regulator could approve the material since it poses less of a threat than the surrounding environment. Alternatively, a regulator could reject the beneficial use of a material because any addition of constituents to a hydrogeologic system already containing elevated concentrations could increase the risk of exceeding regulatory standards. A third possibility is that any change in pH in the saturated/unsaturated zone resulting from highly buffered or acidic leachate could release background constituents sorbed to organic matter in the soil.

Table 2.1. Physical properties of steel and iron slags from the literature.

Property	Lemass (1992)		FHWA		Nomura and Enokido (1981)		Motz and Geiseler (2001)	Geisler (1994)	Rohde, et al. (2003)	Mathur et al. (1999)	
	BF Slag	Steel Slag	BF Slag	Steel Slag	BF Slag	Steel Slag	Steel Slag	Steel Slag	Steel Slag	Steel Slag	BF Slag
Specific Gravity			2-2.5	3.2-3.6	2.47-2.67	2.94-3.6			3.41-3.52	3220	2650
Bulk Density (kg/m ³) (loose)	1200-1300	1650-175	1120-1360	1600-1920	1580	1830-2330	3300-3500	3100-3800		2100	1800
Water Adsorption %			6-Jan	<3	3.19-3.62	1.85-2.56	0.7-1.0	0.2-1	1.8-2.9	1-1.4	1.5-2.5

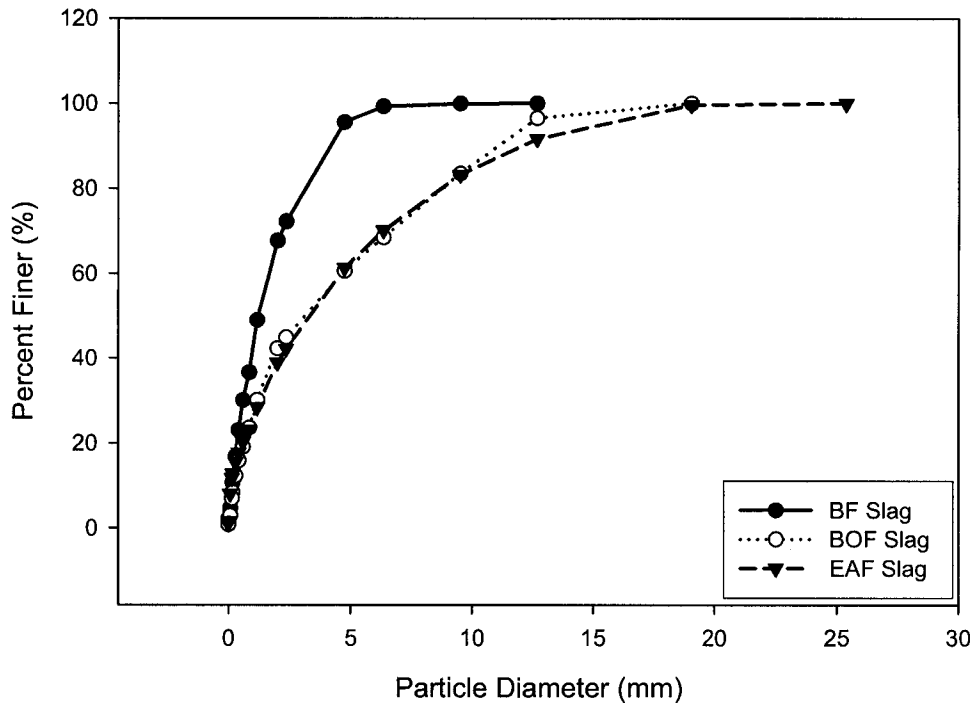


Figure 2.1. Steel and iron slag grain size distribution from Proctor, et al. (2002).

Table 2.2. Physical properties of aged oxidized and reduced slags from Rhode et al. (2003).

Property	Oxidizing Slag		Reducing Slag	
	Aged-2 months	Aged-4 months	Aged-2 months	Aged-4 months
Soundness (%)	0.1	0	0.1	0
Specific Gravity	3.45	3.41	3.44	3.52
Water Absorption (%)	2.9	2.4	2.4	1.8
Los Angeles value (%)	40.9	37.8	36.5	37.9

Table 2.3. Slag surface area measurements from Gupta et al. (1994).

Slag Type	BET Single Point Sa (m ² /gram)	BET Multi-point SA (m ² /gram)
Bf Slag	4.41	4.64
Open Hearth #1 (aged)	2.84	3.05
Open Hearth #2 (aged)	20.59	21.15
Open Hearth #3 (aged)	23.84	14.61
BOF #1 (aged)	10.88	11.2
BOF #2 (un-aged)	3.53	3.67
BOF #3 (aged)	17.62	17.96
BOF #4 (un-aged)	11	11.44

Table 2.4. Slag surface area measurements from Tossavainen et al., (2005).

Sample	BET Surface Area (m ² /g)
Ladle Slag	0.75
BOF Slag	2.35
EAF Slag-1	2.23
EAF Slag-2	1.23

Table 2.5. Steel and iron slag compositional data from the literature.

Component	Viklund -White (1999)	Geiseler (1994)				Piret, et al. (1980)	Nomura and Enokido (1981)			Gupta, et al. (1994)			Yan et al. (1998)	Tossavainen and Lind (2006)	Tossavainen et al. (2005)
	BOF	BOF- low MgO	BOF- high MgO	EAF- low MgO	EAF- high MgO	BOF aged 9 months	Fresh Steel Slag	Aged Steel Slag*	ACBF Slag	BOF Fresh	BOF aged	BF Slag	EAF Slag	ACBF	BOF
CaO	30-55	45-55	42-50	30-40	25-35	41.6	41.6	36.9	42.9	35.27	38.49	40.09	31.1	30.4	45
SiO ₂	10-20	12-18	12-15	12-17	10-15	15.3	13.9	14	32.56	12.77	12.41	38.09	12.6	33.7	11.1
Al ₂ O ₃	1-5	<3	<3	4-7	4-7	1	1.5	3	15.55	3.75	4.46	8.52	4.16	12.5	1.9
MgO	1-10	<3	5-8	4-8	8-15	5.3	7.7	10.6	6.61	10.52	8.35	10.8	7.46	16.9	9.6
MnO	2-8	<5	<5	<6	<6	5.6	4.5	5.2	0.36	2.81	4.48	0.71	6.17	na	3.1
P ₂ O ₅	1-2	<2	<2	<1.5	<1.5	1.4	1.71	1.41	nd	0.29	0.13	0.02	1.05	na	na
Fetotal	15-30	14-20	15-20	18-29	20-29	20.7	20.61	19.27	0.49	na	na	na	na	na	23.9
CaO free		<10	<10	<3	<3	na	4.72	3.82	nd	na	na	na	na	na	

47

Table 2.6. Compositional data of oxidized and reduced steel slag from Geyer (2000).

Sample	CaO	MgO	SiO ₂	Al ₂ O ₃	FeO	MnO	SO ₃
Oxidizing Slag	30-35	8-12	15-20	3-9	24-35	3-6	---
Reducing Slag	45-55	8-12	20-25	3-9	0.5-3.5	0.5-3.5	0.5

Table 2.7. Physical properties of Lincolnweld 995N flux from Lincoln Electric Product Certificate.

Flux Sizing Distribution	
Mesh Size	Diameter Percentage
+ 12 Mesh	10% maximum
- 12 + 60 Mesh	88% Maximum
- 60 Mesh	2% Maximum
Density (g/cm ³)	1
Water Content (@1800F)	0.05% max

Table 2.8. Compositional analysis of Lincolnweld 995N flux from Lincoln Electric Product Certificate.

Component	Composition Percentage
Al ₂ O ₃	25-30
SiO ₂	16-21
MgO	14-19
CaF ₂	10-15
Mn _x O _y	7-12
ZrO ₂	1-6
CaO	1-6
Na ₂ O	1-5
K ₂ O	1-5

Table 2.9. TCLP data for SAW slags provided by Lincoln Electric. The product is listed as flux and electrode combination.

Product	Sample	As	Ba	Cd	Cr	Pb	Hg	Se	Ag	Date
ST100	Slag	<0.10	0.65		<0.04	<0.10	<0.002	<0.10	<0.04	2/14/1990
L61 & 780	Slag	<0.10	0.69	<0.10	<0.02	<0.05	<0.002	<0.10	<0.02	3/11/1991
L61 & 860	Slag	<0.10	0.33	<0.10	<0.03	<0.05	<0.002	<0.10	<0.02	3/11/1991
A96S	Slag	<0.10	0.25	<0.10	0.4	<0.05	<0.002	<0.10	<0.02	5/31/1991
L60 & H560	Slag	ND	0.27	ND	0.36	0.06	ND	ND	ND	6/23/1993
L61 & 960	Slag	<0.05	0.68	<0.05	<0.05	<0.05	<0.002	<0.05	<0.05	3/22/1995
L60 & 781	Slag	<0.05	1.3	<0.05	0.08	<0.05	<0.002	<0.05	<0.05	3/22/1995
L60 & 761	Slag	<0.05	0.94	<0.05	0.15	<0.05	<0.002	<0.05	<0.05	3/22/1995
802	Slag				0.39					8/5/1998
Lincore 420 & 880	Slag	<0.05	0.57	<0.05	0.15	<0.05	<0.002	<0.05	<0.05	4/26/1995
995N & L61	Slag	0.07	0.08	<0.01	<0.02	0.07	<0.002	0.14	<0.01	9/26/2002
Maximum limit per USA EPA		5	100	1	5	5	0.2	1	5	

Table 2.10. BOF slag mass transfer values calculated with tank leaching tests from Comans et al. (1991).

Element	Sample #	Total Concentration (mg/kg)	Availability (mg/kg)	Effective Diffusion Coefficient (-log(De)) (m ² /s)	Cumulative Flux 64 days (mg/m ²)
Ca	1 (dense)	285600	51400	14.1	20600
	2 (porous)	345700	82600	14.7	11300
	3 (dense)	246200	80900	12.7	142700
	4 (porous)	241600	53670	13.7	34500
	5 (nitrogen)	279800	67200	14.2	25200
V	1 (dense)	2045	3.1	9.7	193
	2 (porous)	2878	14.8	10.9	180
	3 (dense)	2570	67	13.5	24
	4 (porous)	3980	4	10.6	100
	5 (nitrogen)	2870	22	12.2	63
Ba	1 (dense)	45	1.2	12.9	3
	2 (porous)	156	15	14.5	3
	3 (dense)	96	3.1	11.6	9
	4 (porous)	148	7.8	13.7	5
	5 (nitrogen)	133	6.9	13.4	6
F	1 (dense)	196	2.8	12.2	10
	2 (porous)	356	7.2	12.3	17
	3 (dense)	285	6.7	12.4	17
	4 (porous)	95	3.3	12.6	7
	5 (nitrogen)	280	5	11.8	31
SO4	1 (dense)	7200	224	13.5	171
	2 (porous)	5780	174	12.8	232
	3 (dense)	4700	163	12.7	100
	4 (porous)	2790	173	13.5	123
	5 (nitrogen)	5900	183	12.6	440
K	1 (dense)	4700	87	13.9	42
	2 (porous)	3400	68	13.2	80
	3 (dense)	2600	52	13.4	70
	4 (porous)	3000	137	13.7	45
	5 (nitrogen)	3000	86	12.8	170
Na	1 (dense)	2900	47	12	200
	2 (porous)	6700	64	12.2	150
	3 (dense)	7000	67	12	270
	4 (porous)	6000	40	12.3	180
	5 (nitrogen)	6600	55	12.2	200

Table 2.11. Contaminants and their local sources found on Australian highways from Ball et al. (1998).

Constituent	Primary Sources
Nitrogen/Phosphorous	Atmosphere, roadside fertilizer application
Lead	Auto exhaust, tire wear, lubricating oil and grease, bearing wear
Zinc	Tire wear, motor oil, grease
Iron	Auto rust, steel highway structures, moving engine parts
Copper	Metal plating, bearing and brushing wear, moving engine parts, break lining wear, fungicides/insecticides
Cadmium	Tire wear, insecticide application
Chromium	Metal plating, moving parts, break lining wear
Nickel	Diesel fuel and petrol exhaust, lubricating oil, metal plating, brushing wear, brake lining wear, asphalt paving
Manganese	Moving engine parts
Sodium/Calcium/Chloride	Deicing salts
Cyanide	Deicing compounds
Sulfate	Roadway beds, fuels, deicing salts

Chapter 3

METHODS AND MATERIALS

This chapter discusses the methods and laboratory procedures utilized in this research to characterize the slag materials. The methods include physical characterization techniques, leaching tests to identify constituents of concern, laboratory analyzation techniques, and modeling methods used to interpret the results. Although five materials were studied in this research, only four of them were subjected to the complete suite of tests. From the literature review it was determined that iron slag (BF slag) has been involved in a large number of studies and has been fully physically and environmentally classified. It was therefore not subjected to as much laboratory testing as the other slags involved in this research.

3.1 Material Characterization

Steel and iron slag samples were supplied to the RMRC by Dan Daily of Scrap Metal Consulting, Inc. (SMC) in Cincinnati, OH in Spring 2004. The materials arrived in clear plastic bags in the amounts indicated in Table 3.1 and consisted of a blast furnace slag, a BOF slag, and fresh and weathered steel slag fines samples. A larger quantity of BF and BOF slag was received

than the fines samples. According to Dan Daily (email), with the exception of the weathered sample, the slags were less than 6 months old. Mr. Daily explained that since the samples were sampled by hand from slag piles, the deeper and therefore older slags would not be accessible without the help of machinery. The weathered sample was collected from a pile that had accumulated for years but was probably not older than 1 year for the same reason that deeper and therefore older samples were not accessible. Mr. Daily did not identify which type of steel slag process (BOF or EAF) produced the fines samples from but stated that they had the most market potential if they were considered safe to use. Mr. Daily concluded that more information requests on the samples would be difficult since the producer had already supplied a lot of information. Figures 3.1 through 3.4 show photos of the samples received from Mr. Daily. Upon arrival at the RMRC, the samples were placed into new sealed plastic bags and stored in 2-gallon plastic buckets in a temperature controlled cold room. The samples were stored in this way to prevent atmospheric contact and possible subsequent aging. The slag was sub-sampled into sealed 60 ml and 250 ml containers, depending on the particle size, for use in the laboratory leaching tests.

The RMRC received a 5-gallon plastic bucket of SAW slag from LE in July 2004. The bucket contained elongated pieces of slag ranging in size from fine particles settled to the bottom of the bucket up to 9 mm. The SAW slag is shown in Figure 3.5.

3.1.1 Grain Size Distribution

A grain size analysis was conducted to compare the slag materials with slags from other studies as well as the grain size distribution of natural aggregates. The samples were sieved through U.S. Standard Sieves in sizes 0.125, 0.3, 0.425, 0.833, 2, 4.76, 6.3, 9.5, and 12.5 mm. The sieves were shaken on a Humboldt H-4325 shaker for 15 minutes and sample fractions retained on each sieve were weighed. The results were plotted as percent retained by weight against the sieve size opening in mm.

3.1.2 Moisture Content

Slag moisture content was calculated by first weighing 15 grams of fresh sample from the as-received sample container and placing it into a 60 ml poly container. The container with the sample was weighed again and then placed into a vacuum tube for 24 hours of freeze drying. Finally, the container and sample is weighed again and moisture content is determined with the following equation:

$$MC = \left(1 - \frac{W_{dry}}{W_{as-received}}\right) * 100 \quad (3.1)$$

where MC is the material moisture content (%), W_{dry} is the material weight after drying (g), and $W_{as-received}$ is the original weight (g).

3.1.3 Surface Area Analysis

Surface area analysis was conducted with a Micromeritics Tristar 3000 Gas Adsorption Analyzer (Figure 3.6). Prior to surface area analysis, the sample was degassed in a SmartPrep Degasser to remove contaminants that could be adsorbed to the particle surface. In the degassing process, the samples were heated and flooded with nitrogen until the sample weights stabilized. Once this occurred, the sample weight was measured and entered into the Tristar 3000 software. At the beginning of the surface area analysis, the analysis tube containing the sample is lowered into a liquid nitrogen bath and is evacuated of gas. The analysis gas (helium) is then introduced into the tube at different pressures causing the gas to adsorb to the sample particle surface. As the pressure is increased, more gas molecules adsorb to the surface which is measured along with the ratio of equilibrated gas pressure to saturated pressure. The progression of adsorption begins with the micropores filling with adsorbed gas molecules, followed by the particle free surface, and finally the larger macropores. Once bulk saturation of the gas has occurred the process is reversed and the desorption process is monitored for change in gas pressure and the quantity of gas desorbed. The data from the adsorption and desorption processes is used to create sorption isotherms which in turn can be used to determine particle surface area.

3.1.4 SEM Analysis

An Amray 3300FE scanning electron microscope (SEM) located at UNH was used to provide a three-dimensional large visual interpretation of the surface of the slag samples. In an SEM analysis, electrons emitted from a tungsten or lanthanum source are aimed at the sample surface. The electrons react with free electrons within the sample causing a secondary electron emission. These electrons are detected by the instrument producing an image of the sample surface containing black and white areas relating to weak and strong secondary electron emission, respectively. Sample preparation involved securing a small aliquot of dried sample with particle size less than 8 mm to a ¾" aluminum disk with conductive carbon paste as an adhesive. The sample was then sprayed with a 200 Angstrom gold-palladium film using a Hummer V sputter coater to increase image resolution and sharpness. The disks were individually placed into the SEM chamber and analyzed with an accelerating voltage of 7 kV. The instrument was equipped with a micrograph camera which took scaled screenshots of the sample surface. For each sample, a low and high magnification micrograph was recorded.

3.1.5 X-ray Powder Diffraction (XRPD)

XRPD is a non-destructive method used to identify mineral phases within the sample matrix. According to the USGS (USGS website), the XRPD process involves heating a filament which emits electrons that hit a copper

(or molybdenum) target. This emits x-rays that are directed at the sample which is ground to a powder. The x-rays are emitted toward the sample over a range of angles. As the x-rays hit the sample and the mineral lattices within the sample they are diffracted at patterns unique to individual minerals. These diffraction patterns are detected and compared to standard reference patterns to identify the minerals present in the sample. The XRPD analyzer used in this research was a Rigaku-Geigerflex goniometer with Cu-K α radiation (45 kV, 35 mA), a 1° scattering slit, a 1° divergence slit, a 0.3° crystal receiving slit, and a 0.6° monochromator receiving slit. The instrument used an angle range of 4 to 90 degrees 2 θ with a step size of 0.1 and dwell time of 2.4 degrees/min. A quartz calibration standard was used prior to sample analysis as well as a tungsten internal calibration check placed within the sample. The samples were ground to a particle size under 125 microns and placed on a glass XRD slide. The XRPD results were collected with the Datascan 3.1 software and analyzed with the Jade 5 software, both by Materials Data, Inc. The Jade 5 software matches the diffractogram peaks and assigns each with a Figure of Merit (FOM) based on how well they compare to the peaks of pure mineral phases found in the International Centre for Diffraction Data (ICDD) database, which Jade 5 accesses. The software can identify major, minor, and trace mineral phases with this method and assigns a lower FOM for phases with confident identification. Due to the large amount of minerals detected in each sample, only minerals with FOMs below ten were considered for this research. Each

of the slag samples was analyzed by the XRPD analyzer three times to improve on mineral identification accuracy.

3.2 Total Composition

Total composition analysis was attempted using a modified EPA Method 3051 titled "Microwave Assisted Acid Digestion of Sediments, Sludges, Soils, and Oils" located in the SW-846 manual. The method involves microwave assisted digestion of 0.5 g of sample in 10 ml of nitric acid. The instrument used was a CEM Mars 5 microwave digester ramped to 180 °C for ten minutes and then held at 180 °C for another 10 minutes. The samples were ground to particle size below 125 microns and were placed in inert polymeric vessels. An additional 3ml of HCL was added to the 10ml of acid to aid in sample digestions. After the digester chamber had cooled to below 50 °C the samples were removed, filtered, and diluted for ICP analysis. This method however was unsuccessful in completely digesting the samples, most likely due to high silica content which is identified in the literature review as a major component of the slags. In response to the incomplete digestion, EPA Method 3052 titled "Microwave Assisted Acid Digestion of Siliceous and Organically Based Matrices" was attempted which uses 9 ml of nitric acid and 3 ml of hydrofluoric acid to assist silica digestion. Hydrofluoric acid is a hazardous chemical that is highly reactive with glass and therefore requires a special ICP configuration to prevent glass corrosion within the instrument. Method 3052 however was unsuccessful in digesting a recognizable amount of additional material and

therefore the previously digested samples (Method 3051) were used for analysis. The results therefore are characterized as Total Leachable Concentration (TLC) rather than Total Composition since the amount of constituent bound in the undigested silica is unknown. One future recommendation from this research is to analyze the slag samples by an alternative method such as X-ray Fluorescence or Atomic Absorption Spectroscopy.

3.3 Availability Test

Kosson et al. (2002) identifies two approaches for determining the available leachable content, or availability, of a material. The first is identified as AV001.1 and involves leaching a sample first at a pH of 8 and then at a pH of 4. The leachates from the two pHs are combined and analyzed. A second approach identified as AV002.1 involves using ethylenediamine-tetraacetic acid (EDTA) to chelate constituents in solution using a single extraction. Kosson et al. (2002) notes two difficulties with this method are that a pretitration is necessary and pH control is difficult. Kosson et al. (2002) only provides method details for AV002.1, which was not chosen for this research. Instead, Method EA NEN 7341:2004 titled "The Maximum Availability Leaching Test", was used. This method is similar to AV001.1 but uses target pHs of 7 and 4 instead of 8 and 4. The test uses a particle size under 125 microns to minimize diffusion controlled release and an LS ratio of 50 ml/g. According to the method, samples with natural pHs above 10 are considered alkaline reactive and 1 M HNO₃ should be used in the test to

lower the pH to the target values. If the pH is between 7 and 10 it is considered neutral reactive and 0.2 M HNO₃ should be used. The slags in this research were identified from the pH-dependent leaching tests as having high buffering capacities, so 2 M and 4 M HNO₃ was used to decrease the amount of liquid added to the sample to maintain the target pHs. The acid was added to the samples using the Schott Autotitrators which can be set to maintain a pH value by automatically adding small amounts of acid. The test involves maintaining a pH of 7 for three hours followed by 15 minutes of settling and filtration of all of the leachate in which the original sample volume is maintained in the sampling beaker. Any sample that remains in the filter paper is washed back into the beaker. After filtration, DI water is added to the sample bringing the LS ratio back to 50 and the pH is then maintained at 4 for three hours. Following settling, the filtered leachate from this step is combined with the leachate from the pH 7 step and the homogenized leachate is sampled and preserved for ICP analysis. ICP results in ug/l are converted to ug/kg by multiplying by the LS ratio (ml of DI and acid added/grams sample).

For the steel and iron slags, as the acid was titrating there was a noticeable irregularity in the pH measurements indicated by a sharp decrease in pH followed by a slower rise in pH over a short interval. This behavior was identical to the reactions observed in the ANC tests but was not as evident in the SAW slag availability titrations. The test criteria were satisfied since the pH stayed within +/-0.5 of the target. However, since the pH did not

stabilize throughout the test, reactions were possibly still occurring between the matrix and the acid indicating a possible underestimation of release. Although not referred to by Kosson et al. (2002) as an equilibrium-based test (as in Tier 2), it could be argued that the test is more accurate and repeatable if equilibrium is reached at some point during the three hour titration.

3.4 TCLP/SPLP Test

The Toxicity Characteristic Leaching Procedure (TCLP) is Method 1311 in the EPA SW-846 publication titled "Test Methods for Evaluating Solid Waste, Physical/Chemical Methods". SW-846 contains methods that have been approved for use in complying with the Resource Conservation and Recovery Act (RCRA) guidelines (EPA.gov). According to the method, the test is designed to determine the mobility of organic and inorganic constituents in liquid, solid, and multiphase wastes. The test was designed to replace the EP test and simulate a mismanagement scenario in which waste is combined with actively decomposing MSW in a landfill (SAIC, 2003). Therefore, the TCLP leaching (extraction) fluid consists of an acetic acid solution with pH 4.93 +/- 0.05 designed to simulate a typical low pH organic solution found in MSW landfills. If the material is highly alkaline, a second acetic acid extraction fluid is also used with pH 2.88 +/- 0.05. One stipulation identified on the EPA TCLP Frequently Asked Questions page is that a material's total composition concentrations can be used instead of the TCLP test. If the waste is 100% solid then the total composition result can

be divided by 20 to convert the result to maximum leachable concentration (EPA, 2006). This number is from the LS ratio of 20 used in the TCLP method. The results from the TCLP method and the total composition method are compared to the Toxicity Characteristic (TC) list (40 CFR 261.24) to determine whether the material is considered hazardous or non-hazardous. If at least one regulated constituent exceeds the concentration identified in the TC list then the material is considered hazardous. Samples were sent to Resource Laboratories (RL) in Portsmouth, NH for TCLP analysis.

The Synthetic Precipitation Leaching Procedure (SPLP) test is Method 1312 in the EPA SW-846 publication. The test is designed to determine the leaching potential of a material exposed to precipitation. According to the method, the SPLP test uses an LS ratio of 20 and an acidic extraction solution of a mixture of sulfuric and nitric acids designed to simulate acid rain. Since precipitation pH varies regionally, two extraction fluids are included in the test. If the planned material application is east of the Mississippi River the extraction fluid has a pH of 4.2 +/- 0.05 and if the application is west of the Mississippi the extraction fluid has a pH of 5.00 +/- 0.05. Samples were sent to Resource Laboratories (RL) in Portsmouth, NH for SPLP analysis.

3.5 Natural pH Test

Materials will have different affects on leachate pH depending on their acid buffering capacity. Because leaching of many constituents is dependent on pH and because the pH of an environment such as a base layer of a road is often dependent on the material in situ, it is important to determine the natural pH of a material in water. For each slag, the natural pH was determined using two methods. The first involved continuously stirring and measuring the pH of each material in an open container with an LS ratio of 20 for 24 hours. The second method involved placing the sample in closed containers over a range of LS ratios (1 to 500) and continuously tumbling the sample for 24 hours followed by pH measurement. The two tests were conducted to identify the effect of atmosphere and LS ratio on the natural pH of the materials.

Since the reduction and oxidation (redox) properties of a material have been shown to influence leaching (Kosson et al., 2002; SAIC, 2003), attempts were made in this research to characterize the redox potentials of the materials both in their natural state and during the leaching tests. Issues were encountered during almost all of these attempts however, and accurate redox measurements were not possible. Despite using several different redox probes, redox measurements rarely stabilized and often produced different successive measurements for the same sample. Therefore, redox cannot very accurately be used to explain the leaching behavior of the slags since accurate measurements were not recorded. It could be assumed from the literature that reducing conditions were present

during the leaching tests with the exception of those tests that involved the addition of HNO₃ (nitric acid), an oxidizing agent.

3.6 Kosson Framework

Kosson et al. (2002) presents a framework for evaluating the leaching of inorganic constituents from wastes and secondary materials. The framework identifies 4 steps in this evaluation: 1) define management scenarios for the material and the mechanisms in these scenarios that control constituent leaching, 2) determine the leaching parameters of the material under a range of conditions, 3) use release models with the leaching results to estimate fluxes and long-term cumulative release under the identified management scenarios, and 4) compare the release estimates to accepted criteria. The framework is incorporated into a three-tiered testing program (Figure 3.7) with each tier producing data more specific to the material. The tiers are employed after a material has been identified and the management scenario(s) has been determined. The tiers include a screening-based assessment, an equilibrium-based assessment, and a mass-transfer based assessment for Tiers 1, 2, and 3, respectively. Moving from Tier 1 to Tier 3 progresses from a more conservative estimate to a more realistic estimate of constituent release. Within Tiers 2 and 3, three levels of testing are presented (A, B, and C). According to Kosson et al. (2002), characterization testing (Level A) gives a detailed baseline description of the leaching parameters of a class of materials. Compliance

testing (Level B) is either used to determine if a material is the same as a class previously characterized, used if data from a similar material is available, or used if a limited sample amount is available for testing. Quality control testing (Level C) is used if a material changes from batch to batch, if prior characterization and compliance testing data is available, or is used to manage the ongoing production of a large amount of material. Detailed examples of these levels of testing are presented in Kosson et al. (2002). The screening, equilibrium, and mass transfer rate leaching tests included in this framework are discussed further in this section.

3.6.1 LS Ratio Leaching Test

Method SR003.1 identified in Kosson et al. (2002) was used to determine constituent solubility and release as a function of LS ratio. This method involves leaching a material over a range of LS ratios from 0.5 ml/g to 10 ml/g with continuous rotation for 48 hours on a sample tumbler (Figure 3.8). For this research an additional LS ratio of 100 ml/g was added to look at long term release and the total leachable amount for more soluble constituents. As previously mentioned, LS ratio can be related to time if local infiltration rates can be estimated. A high LS ratio can also limit complete saturation of the leachate therefore allowing the maximum allowable amount to leach from the material into solution. The LS ratios and sample amounts used in this method are shown below.

LS ratio	0.5	1	2	5	10	100
Sample Amount (g)	200	100	100	20	20	2
DI water (ml)	100	100	200	100	200	200

The leachates from each test were vacuum filtered, sampled, and preserved for ICP analysis. The method recommends a minimum sample volume of 40 grams, however, due to material volume constraints some sample amounts were less than this recommendation. All of the equilibrium based tests were performed in two rounds. During the first round of testing, the samples were removed from the tumbler after 48 hours and allowed to settle for 15 minutes prior to vacuum filtration. During the second round of testing, the samples were centrifuged for 10 minutes at 1000 rpm to improve liquid-particle separation prior to filtration. pH measurements prior to sampling were recorded for both rounds of testing and ORP measurements were taken during the second round of testing.

3.6.2 pH-Dependent Leaching Test

Method SR002.1 identified in Kosson et al. (2002) was used to determine constituent solubility and release as a function of pH. This method involves leaching a sample over a range of pH values to determine what affect pH has on constituent release. The pore water pH within a layer of material may change over time depending on depending on local environmental conditions (CO₂, precipitation pH, etc.) and the buffering capacity of the material. Prior to conducting Method SR002.1, a material-specific pH titration curve is generated following Method pH001.0. In this method, the pH of a material in DI water with an LS ratio of 100 ml/g is measured as small aliquots of acid or base are added to the sample. Acid (NH₄) or base (NaOH) is added depending on the starting natural pH of the material and

the desired direction on the pH scale. The slags in this research were mostly alkaline (pHs above 9) so nitric acid was used to reach neutral and low pH values. After initial natural pH stabilization, Method pH001.0 recommends adding 0.1 to 0.5 ml aliquots of acid or base to the sample and stirring continuously for 20 to 30 minutes followed by 5 minutes of settling and finally pH measurement. The recommended pH range is 3 to 12. In this research, pH titration curve generation was first attempted using a Schott Autotitrator (Figure 3.9) that simultaneously adds predetermined amounts of acid or base and measures and graphs pH change. The sample addition was set at a slow rate (0.1 ml/min) in order to allow for pH stabilization and a pH range was set from 2 to 12. Separate acid and base titrators were used. It was determined that this method of continuously adding small amounts of acid/base did not allow enough time for pH stabilization so the titrator was programmed to add a small amount of acid/base and then stop the addition for 15 minutes (the maximum allowed) to allow for stabilization. Despite the longer equalization time a seismic pattern was observed in which the pH dropped and then increased after each acid addition. Subsequent to this method of adding acid in intervals, similar ANC curves were found in research by Lehmann et al. (2000) in NORDTEST Report TR 466. In this report the influence of test conditions such as LS ratio, time, particle size, and mixing speed on pH-dependent leaching tests of MSWI ash were studied. ANC curves in the report showed a similar seismic pattern as the pH dropped and then increased after each acid addition. The report however does not identify this pattern in the graphs or discuss why it

occurs. One recommendation in the report was that acid titrations of certain materials should be performed very slowly to obtain equilibrium at any point on the titration curve. One possibility was to decrease the acid aliquot until the equilibrium time of 15 minutes was sufficient. However, this would greatly increase the length of the test since the total amount of acid needed to reach the target pHs would not change. It was determined that this method also did not provide enough time for pH stabilization so a trial and error test was conducted in which acid/base amounts were estimated from the previously described titration curves and then were added to samples with an LS ratio of 100 in closed 250 ml poly containers. The samples were rotated for 48 hours and measured for pH. This method proved most accurate for determining a titration curve that could be used for Method SR002.1 since that method also leaches samples in closed containers. An acid/base addition schedule was calculated from the titration curves according to the method. SR002.1 uses an LS ratio of 10 ml/g, a particle size under 2 mm, and recommends a sample size of 40 grams. Due to material volume constraints a sample amount of 15 grams was used. After the sample was weighed and placed into a 250 ml container, the required volume of DI was added followed by the volume of acid or base, depending on the addition schedule. The DI was added first to prevent any aggressive reactions that might have occurred from direct contact between concentrated acid and the sample. The samples were rotated for 48 hours, filtered, and preserved for ICP analysis. pH measurements were recorded prior to sample filtration. Achieving the target pH values after 48 hours was

difficult due to the complexity and buffering capacity of the slag samples. More importantly than reaching the exact target values was achieving full coverage of the pH range.

In discussing pH-dependent leaching, the NORDTEST Report TR 466 (Lehmann et al., 2000) stated that as the leaching test approaches equilibrium the transfer of mass from the solid phase to the solution phase slows. Therefore, if the pH is still changing at the end of the test, constituents are possibly still exchanging between the solid and liquid phase. A test was designed to determine if 48 hours was sufficient time for the pH within a sample container to reach equilibrium. In the test, 6 identical samples were prepared with the same LS ratio (100) and particle diameter (<2 mm) used in the pHD test. SSFF slag was used since it would be the most conservative due to its high buffering capacity. An aliquot of 8ml of 2N nitric acid was added to each of the samples which were then closed and rotated. A sample was taken off at time 0, 0.5, 1, 6, 24, and 48 hours and measured for pH to identify changes over time.

Once pH-dependent solubility curves have been identified for a material, pH modeling can be used to estimate when constituents could possibly leach from the material in hazardous levels. For example, if *Ba* has been shown to leach above regulatory levels once the pore-water pH drops below 7, knowing when this will occur is beneficial for a decision maker. One way that a material's buffering capacity can decrease is from contact with acid

rain. If a precipitation rate can be estimated, and the material's ANC is known, time predictions can be made. A synthetic acid rain solution was created in the laboratory to determine how much nitric acid was required to drop the pH of a liter of water to 4.5. Using the precipitation rate for Columbus, OH, the volume of acid in an annual volume of rainfall was calculated. This was then applied to the ANC curve to determine how much precipitation (containing acid) was required to drop the pH to a particular target value.

3.6.3 Compacted Granular Leaching Test

This test is used to determine the mass transfer properties of constituents in a sample such as the effective diffusion coefficient and the tortuosity factor. The method used in this research was method MT002.1 as identified in Kosson et al. (2002). The method consists of compacting a sample with particle size <1 cm into a 10 cm diameter mold (Figure 3.10) to a depth of 10 cm. The mold consisted of a MA Industries standard compaction mold with modifications as shown in the figure. The sample is compacted in three lifts using a modified Proctor test. The method did not identify the specifics of the Proctor Test equipment so a hammer was created using a 2lb 9" long ceramic cylinder and a PVC pipe (Figure 3.11). The ceramic hammer was used to reduce the risk of metal contamination that could occur using a metallic hammer. The method states that the sample should be compacted at its optimum moisture content to achieve the optimum packing density. The method recommends using ASTM Method D 1557 titled "Standard Test

Methods for Laboratory Compaction Characteristics of Soil Using Modified Effort” to determine this number. This step was not performed in this research because it required additional sample amounts, which were overall limited, and because the validity of optimum moisture content for granular materials such as these was questioned. Instead, a small amount of water (approximately 200 ml) was added to each sample to increase the sample compaction. Prior to starting the first lift the empty mold was weighed. Each sample lift was compacted by placing the wetted sample into the mold and dropping the ceramic hammer 25 times with an 18” drop. The length of the hammer drop was regulated with a marked piece of cord. The hammer was moved around the compacted surface to ensure even compaction. After compaction of the third lift the sample depth was approximately 10 cm and was just below a line of drainage holes that were evenly spaced around the mold. The mold containing the sample was weighed again and then was placed into a Cole-Parmer extraction vessel (#AP-06083-15) (white container in Figure 3.10) containing DI water with an LS ratio of 10 ml for every cm² of exposed compacted surface. For a 10 cm diameter mold this was 785 ml of DI water for 78.5 cm² exposed surface. The mold was slowly placed into the extraction vessel to minimize sample disturbance and covered with a lid which came with the identified Cole-Parmer extraction vessel model. The lid prevents atmospheric exposure and subsequent reactions with carbon dioxide. The method identifies a recommended sampling schedule of 2, 5, and 8 hours, and 1, 2, 4, and 8 days. It also states that the schedule can be extended and recommends sampling times

of 14, 21, 28, and every 4 weeks thereafter. At each sampling time, the mold was carefully lifted from the extraction vessel and the surface was allowed to drain through the drainage holes. Following drainage the mold was weighed to determine moisture uptake that occurred both in the pore spaces and within the particles. A second empty extraction vessel was filled with DI to the same LS ratio and the mold was then carefully placed back into the vessel until the next scheduled sample time. The extraction vessel containing the current sample was then filtered through a vacuum filter and sampled and preserved for ICP analysis. Following the method instructions, pH and conductivity measurement for the leachate were recorded. In this method, the refreshing of the DI water ensures a constant concentration gradient between the inner particle and the particle-leachant surface which is required for diffusion to continue. This assumes that equilibrium is not reached which may or may not be valid with highly mobile constituents. In this research, the BOF slag CGL test was conducted before the other slag materials. The BOF sampling schedule is consistent with the other material tests for the first recommended schedule but varied slightly with the extended schedule. The extended schedule for all of the samples did not exactly follow the recommended schedule in the method due to scheduling conflicts.

The leachate samples from each sampling interval are analyzed with ICP-AES. Constituents with detectable concentrations are applied to the

following equation to determine the mass of constituent released during that time interval (Kosson et al., 2002):

$$M_{ti} = \frac{C_i V_i}{A} \quad (3.2)$$

where M_{ti} is the mass of constituent released during the leaching interval (mg/m^2), C_i is the constituent concentration for the interval (mg/l), V_i is the leachant volume during the interval (L), and A is the specimen surface area (m^2). The specimen surface area is area of exposed material exposed to the leachant. For a given surface area, such as the bottom surface of a layer of slag in an embankment, the calculated M_{ti} value is the amount of the constituent that will leach from that surface for a given time interval. The logarithm of the cumulative M_{ti} values are calculated for each interval and graphed against the logarithm of time for that interval. Constituent release for intervals with plot line slopes of 0.5 ± 0.15 are considered diffusion controlled. Intervals with slopes below this range are considered washoff controlled and slopes above this range are considered dissolution controlled. For the diffusion controlled intervals the following equation is applied to calculate the observed diffusivity (D_{obs}) for that interval (Kosson et al., 2002):

$$D_{\text{obs},i} = \pi \left(\frac{M_{ti}}{2\rho C_o(\sqrt{t_i} - \sqrt{t_i - 1})} \right)^2 \quad (3.3)$$

where $D_{obs,i}$ is the observed diffusion coefficient for interval i (m^2/s), C_o is the initial leachable content from the availability test (mg/kg), t_i is the leaching interval (s), and t_{i-1} is the previous leaching interval (s). Kosson et al. (2002) recommends using results from the availability test for the initial leachable content (C_o). For each constituent the D_{obs} values for each interval are averaged to determine the overall observed diffusivity, or effective diffusion coefficient, D_e . The negative log of this average, pDe , can be used to identify constituent mobility according to the following parameters found in the tank leaching test (NEN 7375) as shown in the following equation:

$$-\log De = pDe \quad (3.4)$$

where pD_e values above 12.5 are considered low mobility, values between 11 and 12.5 are considered average mobility, and values below 11 are considered high mobility. Once the D_{obs} (or D_e) has been calculated for a constituent, the value can be used to predict the cumulative constituent release (diffusional transport) for a given mass of material at time t using the following equation:

$$Mt, mass = 2 \times Co \times \frac{S}{V} \times \left(\frac{Dobs \times t}{\pi} \right)^{0.5} \quad (3.5)$$

where $M_{t, \text{mass}}$ is the cumulative release at time t (mg/kg), S is the fill surface area (m^2), and V is the fill volume (m^3). The D_e value can also be used to calculate the tortuosity and retardation factors. Tortuosity is a dimensionless physical retardation factor that describes the path an ion must take as it diffuses from a particle into a leachant. Sodium is used to calculate the tortuosity of the sample since it is generally non-reactive as it travels through the sample matrix. Tortuosity (τ) is calculated using the following equation (de Groot and van der Sloot, 1992):

$$\tau = \frac{D_{na}}{D_{e, na}} \quad (3.6)$$

where τ is the tortuosity of the matrix (dimensionless), D_{na} is the diffusion coefficient of sodium in water (m^2/s), and $D_{e, na}$ is the effective diffusion coefficient of sodium in the matrix (m^2/s). Once τ has been calculated for the matrix it can be used to calculate the chemical retardation factor for each constituent with the following equation (de Groot and van der Sloot, 1992):

$$R = \frac{D_x}{D_{e, x} \times \tau} \quad (3.7)$$

where R is the chemical retardation factor (dimensionless), D_x is the diffusion coefficient of component x in water (m^2/s), and $D_{e, x}$ is the effective diffusion coefficient of component x in the matrix (m^2/s). The chemical retardation factor describes the retardation of a diffusing ion due to chemical

reactions within the matrix compared to the release of a non-reactive ion such as sodium. A constituent that does not react with the material matrix has a R factor equal to 1 (van der Sloot et al., 2003). The chemical retention factor is influenced by pore-water pH and redox conditions (de Groot and van der Sloot, 1992). Both τ and R are important values when looking at the release of constituents from a material. Since these factors cannot be calculated in the field it is important to perform these calculations as part of a laboratory test such as the Compacted Granular Leaching test.

3.6.4 Regulatory Standards

Kosson et al. (2002) does not specify in the framework how to interpret leaching results from the tests with regard to regulatory criteria. This is expected since regulatory standards change from country to country and can also differ among local governments in the United States. Unlike the TCLP test which has its own set of standards, it is ultimately up to the regulators to decide what criteria to compare to the leaching result. In this research, the decision was made to compare the leaching results to EPA MCL Primary Drinking Water Standards which includes the following inorganic constituents: antimony, arsenic, barium, beryllium, cadmium, chromium (total), copper, lead, selenium, and thallium. The MCLs for these constituents are shown in Table 3.2.

3.7 Particle Size Reduction

Particle size reduction is necessary for equilibrium-based tests to decrease the possibility of diffusion controlled constituent release from a material. This research used particle sizes ranging from under 125 microns to 1 cm, depending on the test method. The LS ratio and pH-dependent leaching tests required a particle size below 2 mm (Kosson et al., 2002). For the first of two rounds of testing for the BOF, SSFF, and SSFW slags, a No. 10 (2 mm) sieve was used to remove particles larger than 2 mm. After the first round of sampling for these samples was conducted it was determined that the excluded larger particles may contain different mineralogy (harder minerals) than the smaller particles and therefore should not be excluded to prevent sample heterogeneity between test methods. For the second round of LS ratio and pH-dependent testing for these three materials the entire range of particles sizes was sampled and size reduced to below 2 mm. For these tests the SAW slag was size reduced from the entire range of particle sizes for both rounds of testing and the BF slag was as well for the single test round. The CGL Test required particle sizes under 1 cm which was achieved for the BOF, SSFF, and SSFW slags with a 3/8 " (9.5 mm) sieve. Due to the elongated shape of the SAW slag, the material particle size was reduced to obtain enough sample required for the test. Particle size reduction was attempted with two methods. The first method used a United Nuclear 12 lb capacity ball mill with ceramic media (Figure 3.12). The slag was placed into a 7.5" diameter neoprene barrel along with 3/4" long pieces of ceramic grinding media and continuously rotated. After several test runs it

was concluded that the high hardness of the slags prevented size reduction of the samples. After running a sample for several days the larger slag particles would become rounded rather than size reduced resulting in slightly smaller rounded particles and a fine dust comprised of the originally smaller particle sizes that had effectively been size reduced. It was concluded that a more efficient way to produce a homogenous sample from the slags would be to reduce the particle size with a ceramic mortar and pestle. Small aliquots of sample were placed in the pestle and ground until all pieces of the sample passed the desired sieve size opening.

3.8 MINTEQA2 Modeling

Results from the pH-Dependent leaching tests were used with the geochemical speciation model MINTEQA2 to identify the solid phases controlling the leachate composition at each leachate pH. The leaching test results (detections only) were imported into the modeling program using the Multi-problem generator import option. Under Default Settings the option to not allow precipitation of oversaturated solids. The program was then run and the resulting mineral saturation indices (SIs) of the solids controlling constituent leaching were exported into Excel. The SI is the logarithmic ratio of the ion activity products (IAP) with the corresponding formation constant (K). Negative SIs indicate undersaturated minerals and positive SIs indicate oversaturated minerals (Allison et al., 1991). For each pH, minerals with SIs within +/- 2 units of zero were selected for further modeling. Each mineral within this range was modeled separately using the sweep component in

the program. For instance, all the minerals within this range containing aluminum were identified and total dissolved Al^{+3} was chosen for the pH sweep. For each pH, the first of the identified minerals containing aluminum was specified as an infinite solid which prevents it from completely dissolving and allows it to control aqueous-phase activity in the presence of other solids (Eighmy et al., 1995). The program was then run and the selected sweep results for Al^{+3} were exported to Excel and graphed. This was performed separately for each mineral after which the exported sweep results were graphed against the actual leaching data to identify which minerals best matched the data and therefore identified which solid (or solids) controlled the aluminum solubility. It should be noted that the NO_3^- concentrations imported into the model were truly representative of the constituents released from the material during pH-dependent leaching. Because the test involved the addition of HNO_3 (nitric acid) to reach target pHs, the NO_3^- leachate concentrations were elevated. They were included in the modeling, however, since they were representative of the leachate and could have helped control the leaching of certain constituents.

An issue was encountered with the SSFF and SSFW slag when running the initial modeling step to identify the SIs. Multiple errors were encountered and several minerals precipitated from the solution despite the checked option to not allow precipitation to occur. It is unclear why this occurred only with these materials and not with the BOF, SAW, and BF slags. An attempt to contact the MINTEQA2 model programmer regarding this issue was

unsuccessful. As a result, the SSFF and SSFW leachates were not modeled and are not included in the MINTEQA2 results section.

3.9 IWEM Modeling

If slag producers, regulators, and end-users move away from traditional characterization tests such as the TCLP and begin implementing tests such as those identified in Kosson et al. (2002), one important issue is how to interpret the leaching results. Unlike the TCLP test which has list of Toxicity Characteristic regulatory levels for comparison, it is unclear what regulatory levels to use for these tests or whether it is even appropriate to compare the results directly to such a list. In this research, leaching results were compared to EPA MCL drinking water standards which are discussed in Section 3.10. This approach however is considered extremely conservative for the beneficial use of slag in highway construction unless drinking water wells are located directly adjacent to the material. When fate and transport in the soil and groundwater is considered, reactions such as adsorption, dilution, and degradation can reduce constituent concentrations during transport from source to receptor. The use of fate and transport models can identify the effects of these processes on leachate concentrations. The EPA's Industrial Waste Management Model (IWEM) was used in this research to apply leachate concentrations to a hypothetical management scenario.

IWEM is based on the more complex Composite Model for Leachate Migration with Transportation Products (EPACMTP) but utilizes a simple interface making it ideal for users without modeling experience. The program is designed to determine the most appropriate waste management unit (WMU) design for a particular material by evaluating different types of liners and applying site-specific hydrogeologic conditions (IWEM Technical Background Document). The WMUs include a landfill, a waste pile, a surface impoundment, and a land application unit. Although not designed for use in a highway application, waste pile was chosen to use for the slag because of its description as a temporary source after which it is removed; similar to a layer of recycled material being removed after its lifespan is over. The input values required for the waste pile scenario include infiltration rates, groundwater pH, hydrogeologic conditions, distance to the receptor, partition coefficients, and leachate concentrations. To simplify the modeling process, a pre-set scenario taken from research by Jason Fopiano of the UNH RMRC was used. The scenario was created to model leaching from recycled materials used in a road in Wisconsin. The geologic and meteorological inputs are therefore similar to what is encountered in that geographic area. The following inputs were used in the model:

Input	Value
Waste pile area	200 ² m
Depth to water table	5 m
Soil Type	Silt/loam
Infiltration rate	0.095 m/year
Recharge Rate	0.0912

Groundwater pH	6.5
----------------	-----

The option exists to input a site-specific partitioning coefficient, K_d , which describes the partitioning of a constituent between the solid and aqueous phases. However, IWEM is also capable of calculating a K_d value for constituents of concern, although it is unclear from the model output what K_d values were actually used. Both the K_d value specified by IWEM and a value taken from the literature were used in this research.

The model was used with the some of the leaching results to determine the time-varying concentrations of a constituent in a groundwater monitoring well located 20 m from a highway source. This was achieved by setting the concentration and well distance as constant and then changing the operational time between 1 and 100 years. The concentrations in the well were then plotted against the operational time to identify whether the appropriate EPA MCL drinking water standard was exceeded and if so, at what point in time this occurred.

3.10 Laboratory Analysis

3.10.1 UNH Laboratory Analysis

The majority of the analytical testing of the leachate in this research was conducted on a Varian Vista Axial Inductively Coupled Plasma Atomic Emission Spectroscopy (ICP-AES) analyzer located at the RMRC (Figure 3.13). The ICP results were handled with the Vista v1.3 software. The

samples were analyzed for a list of inorganic elements that changed slightly between the first and second testing rounds. In some of the first round of testing, samples were analyzed for aluminum (Al), arsenic (As), barium (Ba), beryllium (Be), calcium (Ca), cadmium (Cd), chromium (Cr), copper (Cu), iron (Fe), potassium (K), magnesium (Mg), manganese (Mn), molybdenum (Mo), sodium (Na), nickel (Ni), lead (Pb), antimony (Sb), selenium (Se), thallium (Tl), vanadium (V), and zinc (Zn). During the first round of testing a new ICP multi-standard was used which also included silver (Ag), cobalt (Co), strontium (Sr), and titanium (Ti). Mercury (Hg) was not included in the calibration standards because it was not found in slag materials in any research identified in the literature search. There were occasionally ICP analyses where one or more elements were not analyzed because they were not in the calibration standards or a calibration error occurred during the analysis. The calibration range was below 10 mg/L for the first round of testing but was increased to 1000 mg/L during the second round of testing for elements with high concentrations in the leachates (Al, Fe, Ca, Mg, Mn). In the ICP method, a minimum of 3 replicate measurements was taken for each sample and averaged. Results were exported from Vista v1.3 and evaluated in Excel for calibration errors. Calibration outliers were removed to improve the calibration curve and more closely bound the sample concentration range for each element. All analytical results were exported from Vista in mg/l (ppm) and converted to µg/l (ppb) for better presentation of low results.

During the second round of testing, samples were sent to the Water Quality Analysis Laboratory at UNH's Water Resource Research Center in Durham, NH for anion analysis for nitrates (NO_3), chlorides (Cl), and sulfates (SO_4). The samples were collected simultaneously with the ICP samples but were preserved by freezing them in 60 ml poly bottles rather than with NH_4 . Samples were analyzed by ion chromatography. Nitrate concentrations for the pH-dependent leaching tests could not be accurately determined because of the high amount of nitrogen (as NH_4) added to some of the samples to reach target pHs. To ensure quality analytical data was being reported, a test was conducted to determine the Varian ICP instrument detection limits (IDL) for each constituent. A method was identified in the Varian help file that involved analyzing 10 replicates of blank ultra-pure water. Once the analysis was complete, the standard deviation of the detection signals for the 10 replicates for each constituent was calculated. These values were then multiplied by three to determine the IDL for each constituent. This method was performed twice and the average calculated IDLs are shown in Table 3.3. For the purpose of this research, the IDLs are considered a limit below which concentrations are regarded as estimates.

3.10.2 Additional Laboratory Analysis

Samples were sent to a commercial lab for verification of the UNH ICP analyses. Select SAW slag leachate samples from availability and pH-dependent leaching tests were sent to Eastern Analytical, Inc. (EAI) in Concord, NH for ICP-Mass Spectrometry (ICP-MS) analysis. According to

EAI, ICP-MS is capable of achieving lower detection limits than ICP-AES. Split samples were analyzed by ICP-AES at UNH. A reference sample was sent to EAI consisting of a NIST ICP standard (SRM 1643e) diluted to 50% to check the analysis accuracy.

Table 3.1. Sample weights of slags supplied to the RMRC by SMC, Inc.

Table 1
Samples Supplied by SMC, Inc.

Sample Name	Bags Received	Total Sample Weight (lbs)
Weathered Steel Slag Fines	2	21.22
Fresh Steel Slag Fines	2	20.42
Blast Furnace Slag	3	34.82
BOF Slag	3	41.92

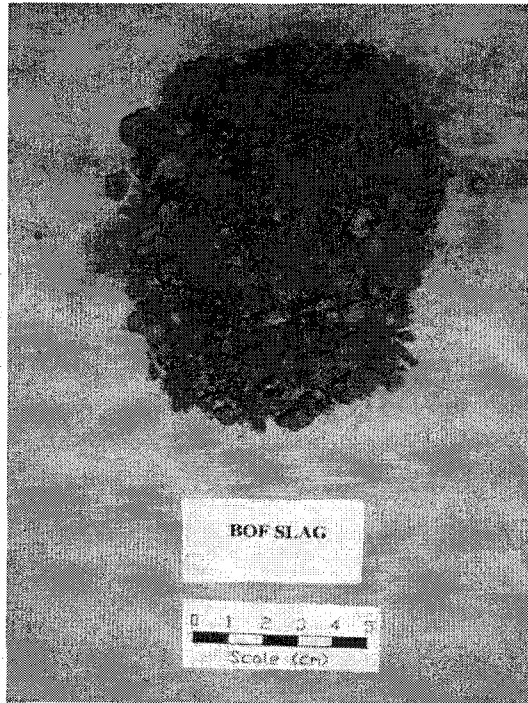


Figure 3.1. BOF slag received from SMC, Inc.

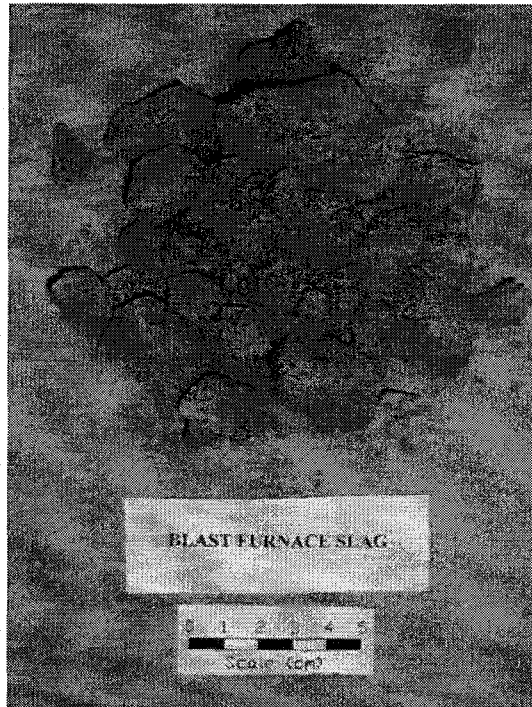


Figure 3.2. BF slag received from SMC, Inc.

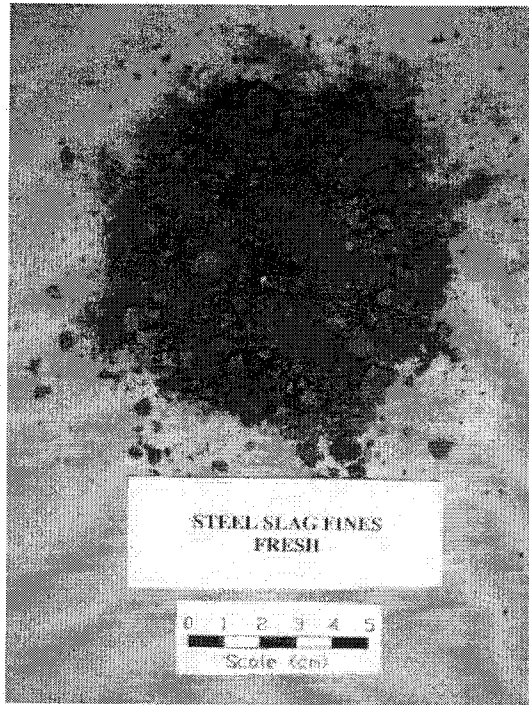


Figure 3.3. SSFF slag received from SMC, Inc.



Figure 3.4. SSFW slag received from SMC, Inc.

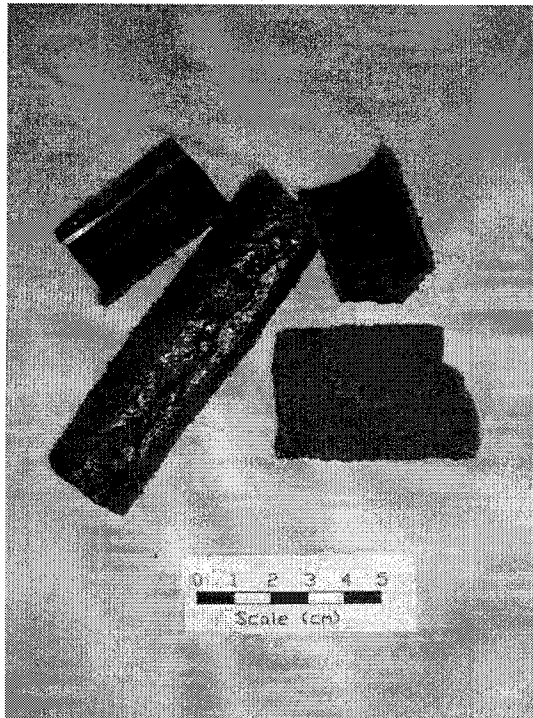


Figure 3.5. SAW slag received from Lincoln Electric.

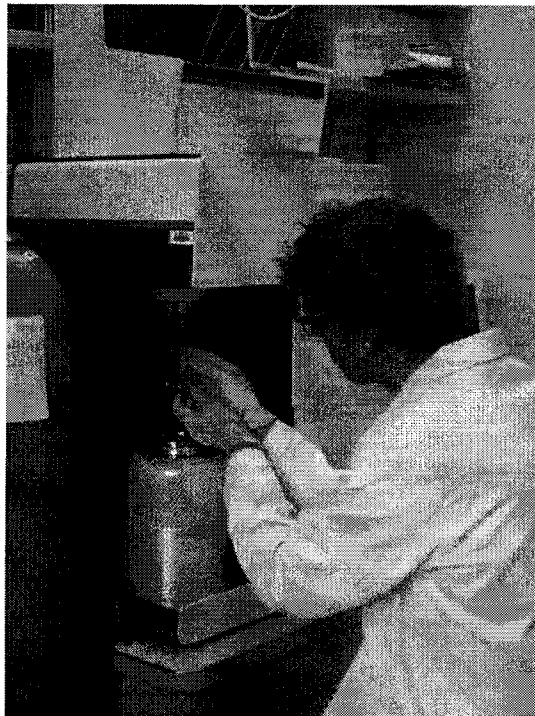


Figure 3.6. Tristar 3000 BET analyzer.

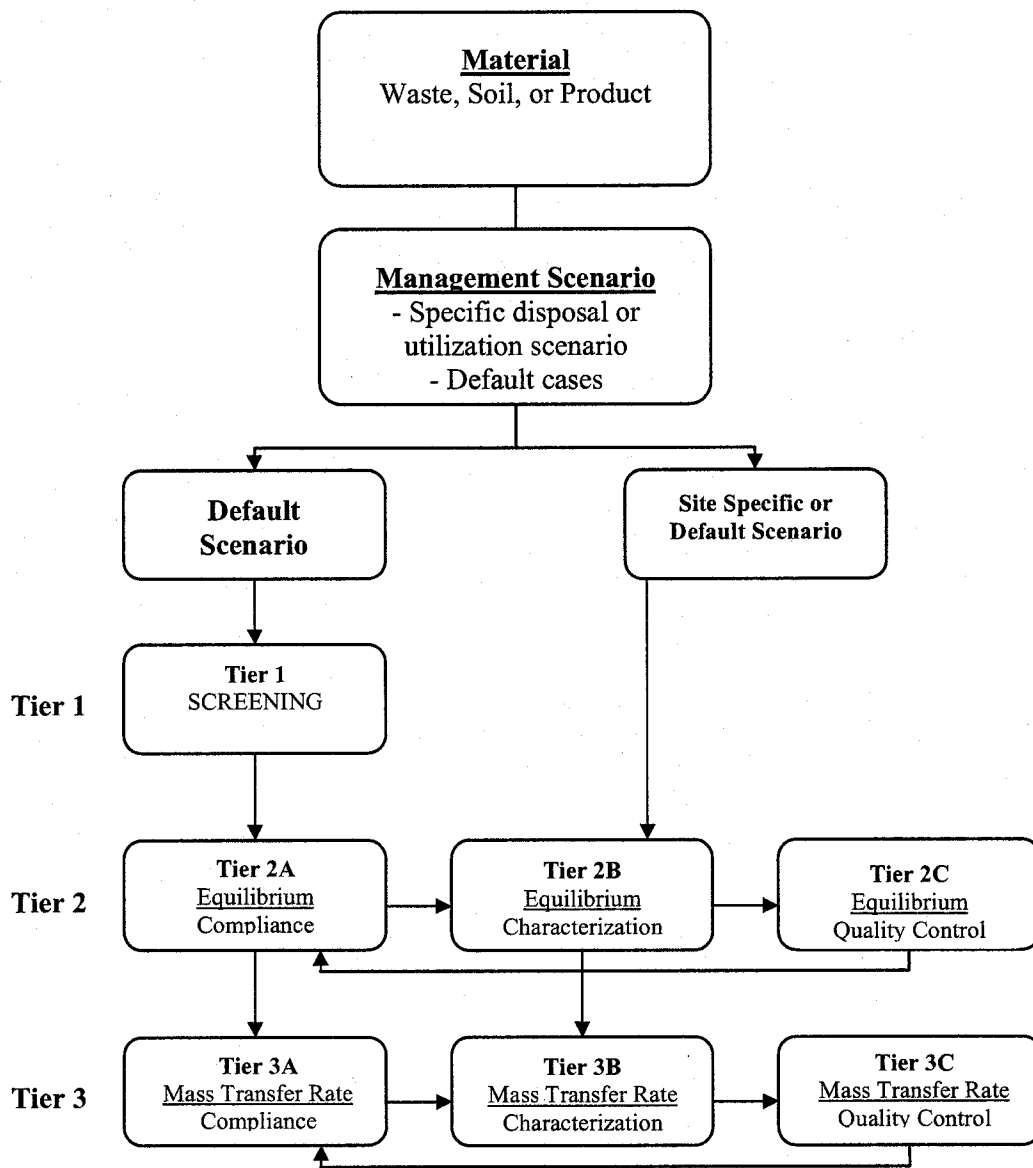


Figure 3.7. Leaching framework presented by Kosson, et al. (2002).

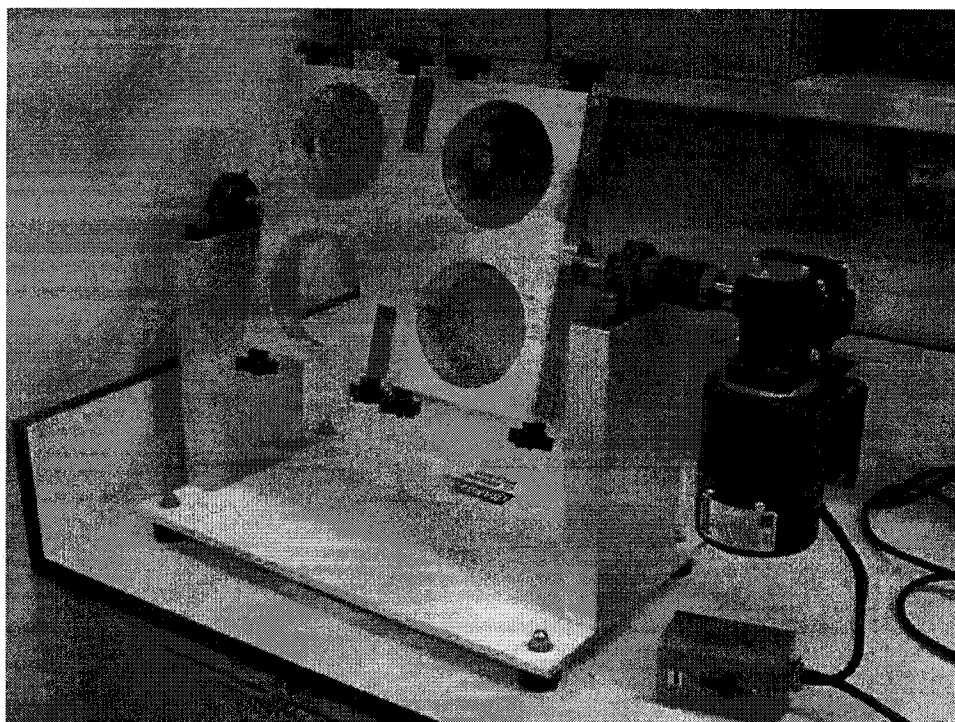


Figure 3.8. Continuous sample tumbler used for equilibrium leaching tests.

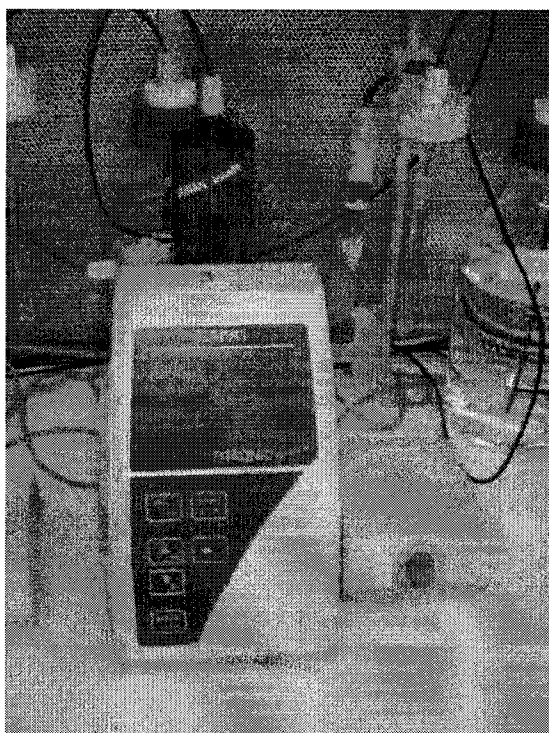


Figure 3.9. Schott Autotitrator used for tests requiring acid/base addition.

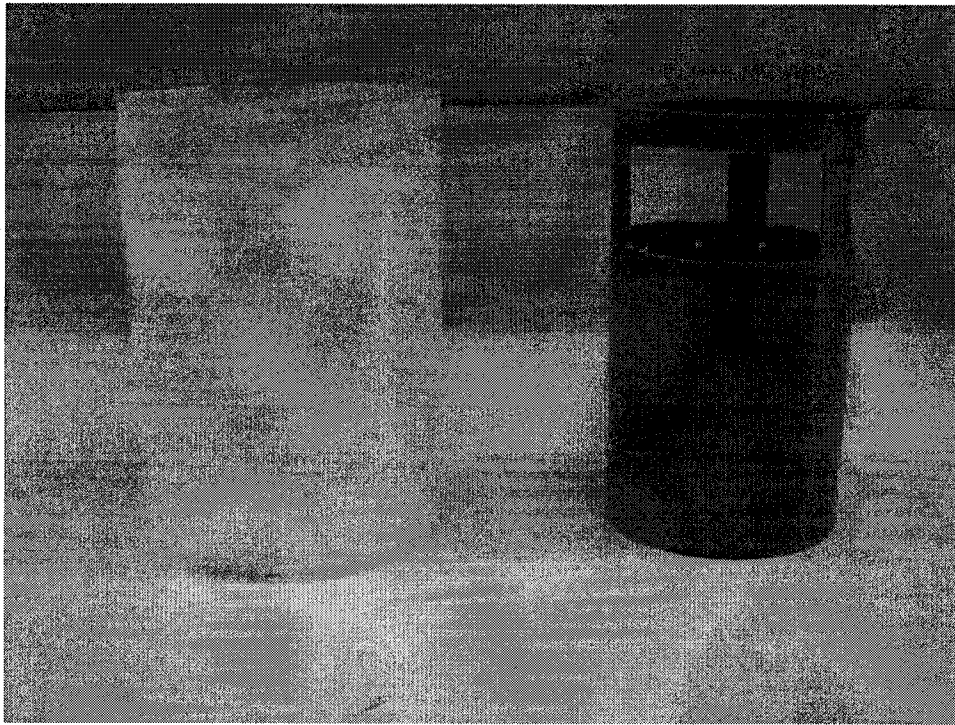


Figure 3.10. Compacted Granular Leaching Test mold (right) and leaching container (left).

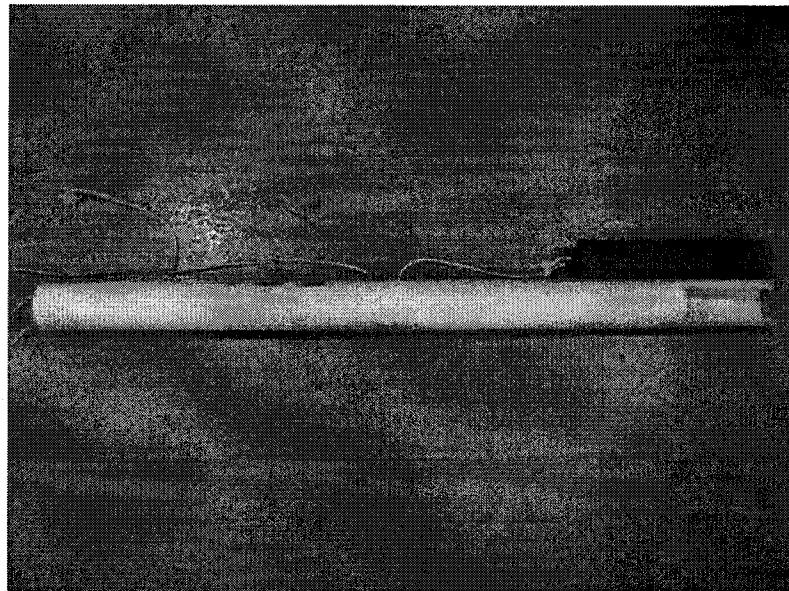


Figure 3.11. Ceramic hammer used for CGLT mold compaction.

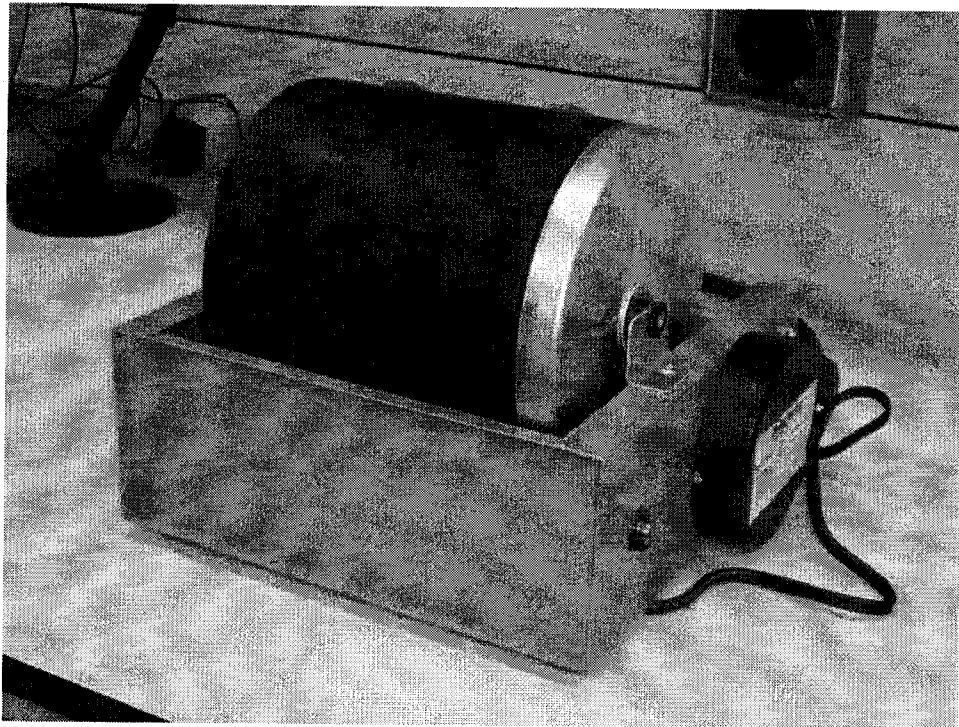


Figure 3.12. United Nuclear 12 lb ball mill with neoprene bladder.

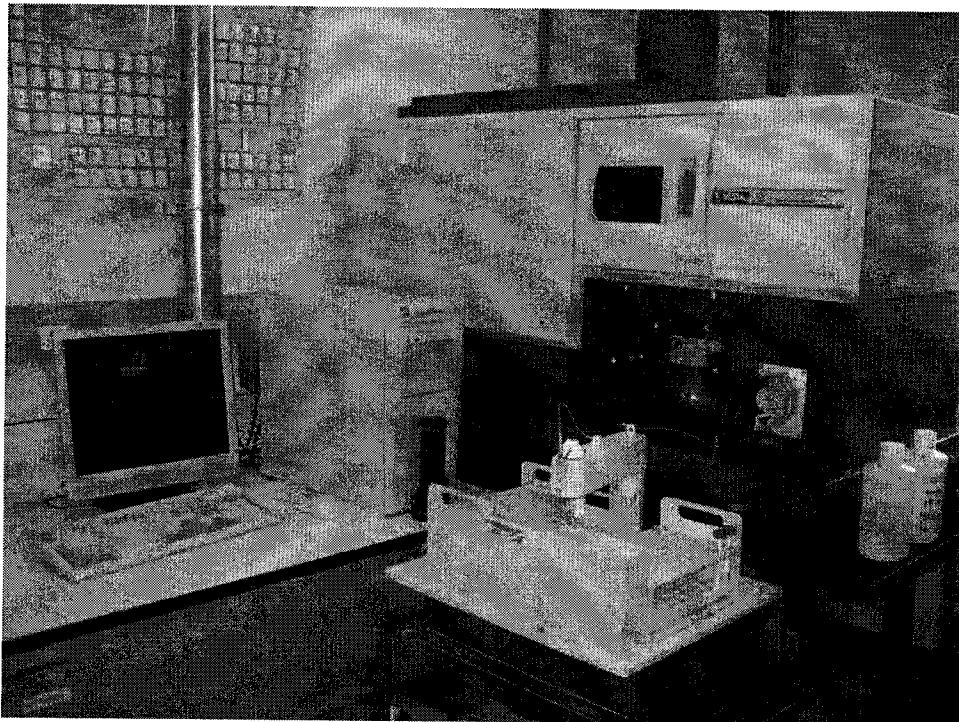


Figure 3.13. Varian ICP-AES used for inorganic analysis of leachates .

Table 3.2. EPA MCL Primary Drinking Water Standards.

Constituent	MCL (ug/l)
Antimony	6
Arsenic	10
Barium	2000
Beryllium	4
Cadmium	5
Chromium	100
Copper	1300
Lead	15
Selenium	50
Thallium	2

Table 3.3. Average IDL concentrations calculated for the ICP-AES.

Constituent	Average IDL (ppb)
Silver	1.04
Aluminum	6.70
Arsenic	9.61
Barium	0.06
Beryllium	0.03
Calcium	1.25
Cadmium	0.25
Cobalt	1.19
Chromium	0.51
Copper	1.01
Iron	1.53
Potassium	2.33
Magnesium	4.62
Manganese	0.12
Molybdenum	2.03
Sodium	5.95
Nickel	1.54
Lead	4.96
Antimony	8.33
Selenium	18.15
Tin	4.46
Strontium	0.03
Titanium	0.13
Thallium	9.83
Vanadium	0.90
Zinc	0.41

Chapter 4

RESULTS AND DISCUSSION

Chapter 4 presents the results from this research and discusses the implications for slag characterization. Where applicable, comparisons are made between the slag materials as well as the different test methods to identify trends in the data. The complete analytical results for each test are presented in the Appendix tables and a select group of constituents, mostly the EPA regulated inorganics, are presented in graphical format in this chapter.

4.1 Physical Characteristics

4.1.1 Grain Size Distribution

Grain size analysis was carried out on the two steel slag fines samples and the BOF slag. The SAW slag grain size analysis was not performed due to the elongated particle sizes (lack of grains) found in the sample. Figure 4.1 shows the grain size distributions for the three materials. The sieve analysis identified approximately 50% of the particles sizes for all three materials as under 2 mm with BOF slag showing 50% of the particles under 1 mm. Research by Proctor et al. (2000) showed a similar grain size distribution for BOF and EAF slags with 50% of the particle sizes below 3 mm. The significance of having an increased amount of fines in a sample relates to the mechanisms involved with constituent release. For materials with small

particle sizes the reaction and release of constituents is faster than materials with larger particle sizes in which release is more limited by diffusion (van der Sloot and Dijkstra, 2004). As was mentioned in Section 3.7, for materials with a large variation in particle size it is possible that the different size particles show different compositions. This is important when considering gradation requirements during beneficial use.

4.1.2 Moisture Content

Moisture content was determined during the sample preparation in the Surface Area analysis. Prior to BET analysis, the samples were dried using a heated degasser. Moisture content in percent was determined using equation 3.1 and the results are shown in Table 4.1. The SSFW slag contained the most moisture with more than 5 times the moisture content of the fresh sample. This was expected as the weathered sample is assumed to have been stockpiled during weathering and was most likely subject to precipitation or mechanical hydration. The SAW slag showed the lowest moisture content, most likely due to its glassy matrix and possibly a lack of contact with moisture (no stockpiling). Moisture in the form of humidity has been shown to affect the carbonation extent and leaching behavior of Portland cement-based materials and should be considered when comparing the leaching behavior of the different slag materials in this research (Sanchez et al., 2002). Although not measured, the higher moisture content of the SSFW slag most likely increased the humidity level during storage which could have affected material carbonation. However,

the optimum moisture content for slag carbonation was not identified in this research so the effect this had on the SSFW sample is unclear.

4.1.3 Surface Area

Samples were analyzed with a Micromeritics Tristar 3000 Surface Area Analyzer and the BET results in m^2/g are shown in Table 4.2. Three replicates of particle sizes under 125 microns (used for the availability and TC tests) and under 2 mm (used in LS and pH-D tests) were analyzed. One approximately 8 mm particle was also analyzed for the steel and iron slags. The SAW slag showed the lowest surface area with results two orders of magnitude lower than the steel and iron slags. The SSFW samples were lower than the weathered samples as well as the BOF and BF slags. The BOF and SSFW samples were most similar across the particle sizes. For the steel slags it appears that the <2 mm samples have a higher surface area than the <125 micron samples indicating the larger particles have a higher internal pore structure. This trend is not seen in the SAW slag or in the BF slag, which showed similar surface areas for all three particle sizes. The SSFF slag results compare well with the surface area results from Tossavainen et al. (2005) (see Table 2.4) for BOF and EAF slags. Overall the results are mostly lower than the surface area results reported by Gupta et al. (1994) (see Table 2.3) with comparable results only for one Open Hearth slag and one BOF slag sample.

Greater surface areas were expected with the samples containing smaller particle sizes, as is seen in comparing an amount of clay with the same amount of sand, for example. The opposite relationship was seen with the SSFW and BOF slag samples. It is assumed that both materials are weathered and from SEM analysis reported in a following section it was confirmed that both materials have complex surface structure on a microscopic level that could lead to higher surface areas. It is possible that with the finer particle sizes this surface structure is lost due to dissolution and/or mechanical breakdown which could lead to a decrease in particle size.

4.1.4 SEM Analysis

The SEM photos are shown in Figures 4.2 through 4.16. Each material is shown in approximately 17x to 30x, 1000x, and 10000x magnification. Additional photos with varying magnifications are also shown of other structures of interest. A bar scale is shown at the bottom of each photo. In comparing the fresh and weathered steel slag fines samples, the amorphous particles look similar in the lower magnification except finer particles under 300 microns appear to be attached to the surface of the SSFW. The presence of finer particles would most likely lead to a higher surface area for the SSFW slag than the SSFF slag, which is confirmed in the surface area analysis. This difference is further confirmed at 1000x magnification with the SSFW particle surface showing an extensive crystal lattice not observed on the SSFF surface. This crystalline structure most

likely is a result of the cyclic hydration and evaporation/precipitation of minerals to the surface. Huijgen et al. (2005) identified a porous coating on carbonated steel slag not present on fresh samples that was identified as CaCO_3 by SEM/EDX. The surface of the SSFF slag also shows some crystalline structures as seen with 10000x magnification, however these structures are different in shape. The BOF slag at low resolution shows a much more complex surface with some smooth surfaces (lower left) and jagged surfaces (lower center). Based on this particle it could be assumed that the BOF slag has a higher surface area than the steel slag fines samples, however due to the variety in BOF slag particle morphology this assumption is not valid. Additional BOF slag photos show the variety of particles found in the sample including spherical particles (Figure 4.17) and flat plates (Figure 4.18). The high resolution BOF photo shows a similar crystalline structure as the SSFW high resolution photo. The BF slag photos show a similar surface as the SSFW slag with finer particles possibly attached through surface cementation. BF slag is known for its hydraulic binding properties (Makela and Hoynala, 2000; Makikyro, 2004; van Oss, 2002). The low magnification SAW slag photo shows coarse particles fused into a flat surface. The grainy particles are the granular flux used in the SAW process. Further magnification of the flat area shows a pockmarked surface with depressions under 1 micron. Figure 4.19 shows a higher magnification photo of the flux particles fused into the flat surface.

The SEM photos reveal the differences in surface structure between the slag materials. Some materials such as the SSFW slag show a higher amount of surface crystallization than a material such as the SAW slag. One implication of this difference is possibly the higher amount of material available for immediate dissolution into the aqueous phase which could result in higher concentrations of soluble constituents during surface washoff.

4.1.5 XRPD

XRPD was used to identify the crystalline phases in the slag materials. Samples were taken from the sample batches used for the availability testing with particle sizes under 125 microns. The results from the three XRPD replicates are shown in Tables 4.3 through 4.7. The tables only contain minerals with more than one replicate identification and are sorted with high identification frequency (maximum of three) at the top of the list. Minerals identified as a major phase in at least one of the replicates are shown in bold. All other minerals were identified as minor phases. Interestingly, *Ca* is not listed in any of the steel slag XRPD results, with the exception of *Ca₂BrP* (SSFF slag), despite high concentrations of *Ca* identified in the leachates from multiple tests. Minerals containing *Ca* such as *CaO*, *CaFeO₂*, and *CaSe* were identified in the SSFF and SSFW samples but only in one replicate. For the SAW slag, only one replicate was identified containing *Ca* (*CaAgF₄*). Many *Ca*-containing minerals were identified in the raw data but the majority had high FOMs indicating a lack of

identification confidence. Possibly, the large amount of calcium in the leachate is contained in many minerals within the sample with concentrations too low for confident identification. Also likely is the presence of *Ca* in amorphous phases within the slags. Drizo et al. (2006) notes research by Bernier (2001) in which an EAF slag contained a large amount of amorphous material not detectable by XRD. Overall, the minerals in the steel slags with the highest confidence level contained the elements *Mg*, *Fe*, *Mn*, and *Al* which compares well to the leachate samples containing high concentrations of these same elements. Additionally, minerals containing *Se*, *Sb*, *Cu*, and *Cr* were identified in the steel slags with high confidence. Several minerals including Copper Iron Manganese Oxide, Zinc Vanadium Oxide, and Magnetite (syn) were identified in all three steel slags. In comparison, the BF slag (Table 4.6) did not contain any minerals found in the steel slags. The most notable difference was the presence of *Pb* and the lack of minerals containing *Fe*, with only two minerals identified. The lack of *Fe* was expected in the BF slag since the literature reports lower total *Fe* content compared to steel slags (Proctor et al., 2000). This *Fe* difference was not seen in the pH-dependent leaching results, however, since *Fe* leaching was similar between the steel and iron slags. The SAW slag XRPD results showed the largest amount of major mineral phases which contained a relative abundance of *Al* and *Co* with the additional presence of *Cu*, *Cr*, and *Ba*.

4.2 Total Leachable Composition

Total composition analysis is used to determine the total amount of a constituent present in a material in mg or μg of constituent per kg of sample. A modified EPA Method 3051 was used to digest (partially) the samples in preparation for ICP analysis. Because the slag samples could not be fully digested in this research, the total composition results are referred to as Total Leachable Concentration (TLC). Results for the TLC analysis are shown in Appendix Table 1 and in Figures 4.20 through 4.23 for the BOF, SSFF, SSFW, and SAW slags. The BF slag was not digested for TLC. Due to the aggressive nature of the test, large quantities of some constituents leached out of the samples. Several constituents were not detected in the TLC leachates including *As* in the SSFF, SSFW, and SAW samples and *Se* in the SSF, SSFW, and BOF samples. It is important to look for similar trends for these constituents in the other leaching tests to identify the effectiveness of this method as a screening tool and to determine the factors that affect their release, or immobilization in this case. For the steel slags, the highest release was for *Cr*, followed by *Ba* and *Cu*. *Sb* was also detected in high concentrations in the steel slags. In comparison, the highest detection in the SAW slag was for *Ba*, followed by *Cu*, *Cr*, *Ti*, and *Se*.

It is important to differentiate between Total Composition, or TLC in this research, and the amount of constituent that can leach out of a material in a realistic scenario. The presence of a large constituent concentration in a

material does not imply that all of that concentration is capable of leaching out. This is further validated when comparing the TLC results to results from the other leaching tests. Because the conditions involved in this particular test (strong acids and high heat) are not likely to be found in any beneficial use application, it is not recommended for making beneficial use determinations and is possibly only useful in identifying the presence or non-presence of a constituent in the material. One possible conclusion from this test is for when the release of a constituent is below the EPA MCL, such as for *Ba* in the steel slags. In this case, it could be concluded that even in the unlikely event that the material released all of this *Ba* at once, the MCL still would still not be exceeded.

4.3 Availability Testing

Method EA NEN 7371:2004 titled “The Maximum Availability Leaching Test”, was used to determine the maximum available fraction of constituent potentially available for release under extreme conditions without consideration of a timeframe. The ICP analysis results reported were converted from ug/l to ug/kg based on the amount of liquid and solid used in the test and are presented in Appendix Table 2. Graphs for select constituents are shown in Figures 4.24 through 4.28. It is important to note that the LS ratio used in the test was slightly higher than the one used to convert the MCL to ug/kg. Since acid was added to the sample in each round to lower the pH to the desired value the LS ratio was higher than the starting 50 ml/g. This acid amount varied between rounds as well so rather

than show a different MCL for each round the MCL shown uses an LS ratio of 100. An LS of 100 was used because the total liquid to solid ratio of the test is 1500 ml per 15 grams of when both rounds are considered.

4.3.1 SSFF Slag

The SSFF slag availability results for the ten EPA MCL regulated inorganics are shown in Figure 4.24 plotted against the MCLs. Results for *Sb* (R2) and *Tl* (R1,R2) were detected above the MCL. All of the constituents except *Pb* and *Be* were detected in the slag in at least one of the rounds. It is possible that the mobility of *Pb* is slow enough that 6 hours (total) of leaching time is not enough to allow for release under these conditions. *Ba*, *Cr*, *Se*, and *Tl* showed good correlation between R1 and R2, while concentrations for *As*, *Cd*, *Cu*, and *Sb* were only detected in one round.

4.3.2 SSFW Slag

The SSFW slag availability results for the ten EPA MCL regulated inorganics are shown in Figure 4.25 plotted against the MCLs. Overall the results were very similar to the SSFF availability data. Results for *Sb* and *Tl* were detected in both rounds above the MCL. Similar to the SSFF results, *Pb* and *Be* were detected in the slag in at least one of the rounds. *As* was not detected in either round compared to a detection (below the IDL) in R1 for the SSFF sample. Besides *As*, the only other difference between the fresh and weathered slag results was the detection of *Sb* in the SSFW R1

sample. *Ba*, *Cr*, *Sb*, *Se*, and *Tl* showed good correlation between R1 and R2, while concentrations for *Cd* and *Cu*, were only detected in one round.

4.3.3 BOF Slag

The BOF slag availability results for the ten EPA MCL regulated inorganics are shown in Figure 4.26 plotted against the MCLs. The results were similar to the other steel slags for *Ba*, *Be*, *Cr*, *Cu*, *Sb*, *Se*, and *Tl*. Result for *Cd* were noticeably higher in the BOF sample and *Pb* was detected just above the IDL but was not in the SSFF and SSFW results. Similar to the other steel slags, *Sb* and *Tl* were detected above the MCLs. Besides *Be* which was not detected, all of the constituents except *As* showed detections in both rounds, although some detections were below the IDL. Interestingly, *Pb* and *Se* were detected in the availability test (only one round above IDLs) and were not detected above the IDLs in the LS ratio leaching test.

4.3.4 SAW Slag

The SAW slag availability results for the ten EPA MCL regulated inorganics are shown in Figure 4.27 plotted against the MCLs. The results were noticeably different than the steel slag results with only *Ba* and *Be* concentrations detected above the IDLs. The only MCL exceedance was for *Tl*, although the concentrations were below the IDL. Both rounds of testing for *Cu* were non-detect.

4.3.5 BF Slag

The BF slag availability results for the ten EPA MCL regulated inorganics are shown in Figure 4.28 plotted against the MCLs. The results were noticeably different than the steel slag results with both *Be* and *Pb* detected above the IDLs and the MCLs and non-detect results for *Cr* and *Cd*. Both *Be* and *Pb* were non-detect and *Cr* and *Cd* were detected above the IDLs (R2 only) for the weathered and fresh steel slag fines samples. Similar to the steel slags, *Sb* and *Tl* were detected above the MCLs. *As* and *Se* concentrations were detected but were below the IDLs. It is important to note that since only one sampling round was conducted for the BF slag, direct comparisons to the other materials are not as accurate. Since a second round of sampling may have produced different results than the first round. *Ba* was detected at a concentration almost one order of magnitude higher than the steel slag results.

4.4 TCLP/SPLP Test

The TCLP is an EPA test designed to determine the mobility of organic and inorganic constituents in liquid, solid, and multiphase wastes. Although it was originally created to characterize waste headed for disposal in a municipal solid waste landfill, this test has been used to characterize materials proposed for beneficial use applications such as slag. The SPLP is an EPA test designed to determine the leaching potential of a material exposed to acidic precipitation in the form of acid rain. The extent of the SPLP testing on beneficial use materials is not known but since it was

identified as a basic EPA leaching characteristic test it was included in this research. Additionally, this test uses an extraction solution of nitric and sulfuric acids, which is more similar to other solutions used in this research than the acetic acid solution used in the TCLP test.

Table 4.8 shows the TCLP and SPLP results from samples sent to RL in Portsmouth, NH. In the TCLP results, *Cd*, *Cr*, *Ag*, and *Se* were detected in the slags but not above the TC regulatory levels. According to the TCLP criteria, all four slags are considered safe to commingle with MSW from a leaching standpoint. *Ag* was detected in three of the samples, but since it is not an MCL regulated constituent it was not included in the graphical presentation of the other leaching tests in this research. *Ag* results from the other leaching tests are presented in the Appendix data tables. Interestingly, there were no *Cd* or *Cr* detections for the BOF and SSFW slags despite there being equal, if not greater, available concentrations (TLC test) of these constituents in the materials compared to the SSFF slag, which showed detections in the TCLP test. Another inconsistency between the two tests is seen in the SAW slag where *Cd* and *Se* were detected above the TCLP detections limits but were below the detection limits in the availability test.

The SPLP results show detections for *Cr*, *Se*, and *Ag* but only one detection (BF *Ag*) overlaps with the TCLP results. The SAW slag results were all non-detect compared to three detections in the TCLP test. There were no

apparent SPLP exceedances, although the MCL drinking water standards for *As*, *Cd*, and *Pb* were below the laboratory detection limits, so exceedances could exist. A comparison of the SPLP results to the TCLP results suggests that pH and the leaching fluid (acetic or nitric/sulfuric) can affect the leaching properties of these materials. The LS ratio for both tests is 20 so this factor is removed.

It should be noted that the TCLP and SPLP results are shown in mg/l rather than the ug/kg units used in this research. It should also be noted that the detection limits reported by the lab are higher than the detection limits reported in this research. This does not reduce the effectiveness of the TCLP test since the detection limits are all well below the regulatory levels. It does, however, make comparisons to some of the leaching data from this research difficult since some leachate concentrations are below the RL detection limits.

4.5 Natural pH

Two tests were used to characterize the natural pH of the material under open and closed atmospheres and over a range of LS ratios. The first test identified the change in pH in an open atmosphere for 24 hours using an LS ratio of 20 (Figure 4.29). The SSFF slag test was cut short after 15 hours due to equipment failure. Between the materials, the SSFF slag showed the most alkaline pHs throughout the test with a high pH of 12.5 and the SAW slag showed the least alkaline pHs with a high pH of 9.3. The SSFW and

BOF slags showed similar pHs around 12. A trend seen in most of the slags is the decrease in pH over time, most likely due to atmospheric contact. This trend is most apparent in the BF and SAW slag samples. The second pH test identified the natural pH of the materials in a closed container over a range of LS ratios from 1 to 500. The general trend seen in Figure 4.30 is a decrease in pH as LS increases. This is most likely due to the depletion of the buffering capacity as more water comes in contact with the material. The drop in pH is approximately 0.95 to 1.2 for the steel slags, 0.4 for BF slag, and 0.7 for the SAW slag. The two tests in comparison show similar pHs for the steel slags and lower pHs in the open test for the BF and SAW slags indicating a relationship between atmosphere and pH for the latter materials. One deduction from the decreasing pHs in the LS ratio test is that the minerals that account for the buffering capacity in the steel slags are more soluble than those in the iron and SAW slags.

The significance of a material's natural pH relates both to constituent leaching and regulation. As previously mentioned, pH is known to control the solubility of many inorganic species (Lehmann et al., 2000; Kosson et al., 2002; SAIC, 2003), so understanding the pore-water pH within sample at a given time is important. pH can also be used as a regulatory tool depending on the type of material and the location. As mentioned in the Introduction, ODOT regulations require the pH of blast furnace slag, and possibly other slags as well, to be between 6.5 and 9 prior to beneficial use. InDOT specifications require a pH between 6.5 and 10.5. The two tests

used in this research identify the difficulty in characterizing the pH of a material considering the affect different factors have on pH. The BF slag in this research, for example, would fall within the InDOT pH range only in an open environment or in a closed environment at high LS ratios.

4.6 LS Ratio Leaching Test

The LS ratio leaching test identifies the solid-liquid partitioning of constituents over a range of LS ratios. Low LS ratios represent initial pore-water conditions within a layer of granular material while high LS ratios represent longer-term release scenarios (Kosson et al., 2002). If local infiltration rates and material volumes are estimated, LS ratios can be related to time providing an estimation of constituent release over the projected lifespan of a material. Calculations relating the ratios used in this research to time are presented later in this section. LS ratios of 0.5, 1, 2, 5, 10, and 100 ml of DI water per gram of material were used in this research for all samples except the first round of BOF slag in which an LS 100 sample was not run. ICP analysis results for both rounds of testing of the LS ratio leachate samples are presented in Appendix Tables 3-7 and select constituents are presented in Figures 4.31 through 4.92. As previously mentioned, only one round of testing was completed for the BF slag. Where applicable, EPA MCLs were graphed with the leaching results as a comparison. The MCLs were converted to ug/kg to match the LS ratio leaching results units of ug/kg. The majority of the constituents showed an increase in solubility as the LS ratio increased. In addition to this trend,

some constituents increased at a consistent rate while others appeared to level off at the higher ratios. As previously mentioned, high LS ratios allow more soluble constituents to release and possibly reach their maximum leachable content at the material's natural pH. Constituents that show consistent increase in release over the LS ratio range have not approached this maximum amount while release curves that decrease in slope at higher LS ratios are approaching this amount. A constant increase in slope indicates solubility controlled release (van der Sloot and Dijkstra, 2004). As the LS ratio increases more water comes in contact with the material and more constituent can be released before saturation is reached.

Results from the two sampling rounds did not always correlate, possibly indicating heterogeneity within the samples used for both rounds. The final pHs of the samples just prior to sampling are shown in Table 4.9. These alkaline pHs correlate well with results from the natural pH test conducted over a range of LS ratios previously mentioned in the results section. The solubility increase in some constituents compared to others in this test may be a result of these alkaline pHs and the amphoteric solubility release curves identified in the pH-dependent leaching test (presented in a later section). The pH figures indicate that the final pHs of the samples were lower for R2 testing than R1 with the exception of the SAW slag. Since pH is known to affect the solubility of inorganics, this difference may explain variations that exist between the two testing rounds. One explanation for the lower pHs in the second round could be a result of sample aging. Even

though the samples were stored in sealed containers they were exposed to the atmosphere occasionally when more material was required. The time span between sampling varied for each material but was as much as 17 months (BOF slag). Tossavainen (2005) attributed differences in duplicate tests with BF slags to reactions with CO₂ during storage. A recommendation for future work is to complete the two rounds of sampling for each material in a shorter amount of time to avoid aging differences. Although different than the normal aging process for steel and iron slags (intermittent wetting and drying/atmospheric contact), enough contact with carbon dioxide could have occurred to carbonate the material which has been shown to lower the pH of some materials. Differences between R1 and R2 pHs were the least with the SAW slag possibly indicating a lesser effect of carbonation in that material.

4.6.1 BOF Slag

Figures 4.31 through 4.42 show BOF slag leaching results for *Al, Ba, As, Ca, Cr, Cd, Cu, Mg, Pb, Sb, Se, and Tl*. This analyte list contains nine elements regulated under the EPA MCLs and three elements (*Al, Ca, Mg*) with high concentrations in steel slags. Some or all of the results for *As, Cd, Pb, Sb, Se, and Tl* were detected below the ICP IDLs as identified in the graphs indicating an estimation of constituent concentration for these results. In the case of *As, Sb, and Tl*, the IDLs are above the EPA MCLs making it difficult to accurately identify exceedances for these constituents. For the BOF slag figures, all of the graphs show a general increase in

constituent release with increasing LS ratio. Only *Ba* and *Ca* show a decrease in slope at a high LS ratio (or increased time) indicating a decrease in release and an approach to the maximum leachable amount at that pH. The remaining graphs do not give indication of a decrease in constituent release with time. An alternative explanation is that the solubility curves of these two constituents (*Ba* and *Ca*) are amphoteric and therefore a decrease in pH as LS increases leads to a slight decrease in solubility. At least one MCL exceedance occurred for *As*, *Sb*, and *Tl*, although the *Tl* exceedances occurred below the IDL and the *As* exceedance was only 2 ug/kg above the MCL. The *Sb* concentration for LS 1 was twice the MCL of 8 ug/kg. *Al*, *Ba*, and *Cr* show consistency between the first and second sampling rounds indicating that these constituents are possibly more consistently found in BOF slag particles or that they are more consistently found in soluble species within the particles. The differences between sampling rounds for *As*, *Cd*, *Pb*, *Sb*, *Se*, and *Tl* are possibly a result of some or all of the concentrations being detected below the IDLs. For *Cd*, ICP results were non-detect for all of the R2 samples compared to concentrations at or just above the IDL for R1. An additional explanation for the differences is the variation in pH between the two rounds. The R2 pHs were more than 1 unit lower than the R1 values for most LS ratios. Depending on the pH-dependent solubility curve, this pH variation could explain the variation in constituent concentrations. However, the R2 pH measurements taken most likely were a measurement error. A previously mentioned test was conducted one month before the R2 LS leaching test to

compare BOF slag pH to LS ratio and the pH results were more similar to the R1 pH results. Interestingly, Cd, Cr, and Cu were detected above the IDL in at least several LS ratios but were not detected above the IDLs in the availability test.

4.6.2 SSFF Slag

Figures 4.43 through 4.55 show SSFF slag leaching results for *Al, Ba, Be, As, Ca, Cr, Cd, Cu, Mg, Pb, Sb, Se, and Tl*. Some or all of the results for *As, Cd, Cu, Pb, Sb, Se, and Tl* were detected below the ICP IDLs as identified in the graphs indicating an estimation of constituent concentration for these results. The majority of the solubility curves for the constituents increase at a constant slope. Compared to the BOF slag solubility curves, results from the two rounds of testing for the SSFF slag did not agree. Results for *As, Be, Cd, Cu, Mg, Sb, and Tl* showed a greater variation between R1 and R2, indicated by differences in the slopes (*As* R2 results) or complete non-detect results (negative) for some LS ratios (*Be* R2 results were all non-detect). One explanation for the slope variations is that they mostly occur in results detected below the ICP IDLs and are therefore only estimations of the actual concentrations. Detection differences between rounds are most evident for *Be* and *Mg*, with a difference of over 1000 ug/l for LS 100. The leaching pHs of R1 and R2 differed by less than 0.53 units so pH most likely does not account for the differences in constituent concentrations. *Be* was not detected in the availability test for this material. Only *Sb* and *Tl* were detected at concentrations above EPA MCLs, similar to the availability test

results, but only for samples with high LS ratios. Since these ratios represent leaching over a long period of time, the likelihood of this material leaching these constituents above the MCLs at the material's natural pH is low in its lifespan. The *Tl* exceedance occurred in the R1 sample for LS 100 at a concentration over 3000 times the MCL. Since this concentration was so high compared to the MCL and the R1 result, a third sample was run for this LS ratio which resulted in a non-detect concentration. The *Sb* exceedances occurred in LS ratios 10 and 100 and were detected just above the IDL. Of the graphed constituents, only *Ba* and possibly *Ca* showed a decrease in solubility curve slope at high LS ratios indicating the constituents were reaching the maximum leachable amount at the natural pH of the material. The results for *Al* and *Ca* were similar to the other steel slag samples but differed for *Fe* and *Mg* with non-detects in R1 and R2 respectively.

4.6.3 SSFW Slag

Figures 4.56 through 4.67 show SSFW slag leaching results for *Al*, *As*, *Ba*, *Ca*, *Cr*, *Cu*, *Fe*, *Mg*, *Pb*, *Sb*, *Se*, and *Tl*. Concentrations of *Be* and *Cd* were non-detect for both rounds of sampling at all LS ratios. In comparison, the SSFF results for these constituents showed concentrations above the IDLs (R1 only). This may indicate that the soluble component of these constituents is more likely to release during the slag aging process when water and atmosphere are introduced to the material. *Be* was not detected in the BOF slag tests (possibly considered an aged sample) and *Cd* was detected only in the R1 samples. Some or all of the results for *As*, *Cu*, *Pb*,

Sb, *Se*, and *Tl* were detected below the ICP IDLs as identified in the graphs indicating an estimation of constituent concentration for these results. Similar to the SSFF slag, *Se* was detected above the IDL in the availability test but was below the IDL in this test. With the exception of *Cd*, the leachate concentrations for the graphed constituents with MCLs were similar to the previously reported results for BOF slag. The constituent concentrations for some LS ratios were often greater than the SSFF concentrations (*As*, *Ba*, *Cr*, *Sb*, *Se*, *Tl*) indicating the possible ineffectiveness of slag aging to decrease the likelihood of release for these constituents. This was not observed for *Be*, *Cd*, and *Pb* in which the SSFF concentrations were consistently greater than the SSFW results. MCL exceedances were observed for *Sb* (LS 5 and 100) and *Tl* (LS 10), however the *Tl* exceedance was detected below the IDL so it is considered an estimation of the actual concentration. This is consistent with the availability test results which showed MCL exceedances for *Sb* and *Tl*. The results for *Al*, *Ca*, *Fe*, and *Mg* were most similar to the BOF results.

4.6.4 BF Slag

Figures 4.68 through 4.77 show BF slag leaching results for *Al*, *As*, *Ba*, *Ca*, *Cr*, *Cu*, *Fe*, *Mg*, *Mn*, *Se*, and *Tl*. *Be*, *Pb*, and *Sb* were not detected in the samples. Interestingly, all three of these constituents were detected in the availability test. Since the test was only conducted once for this material it is not possible to compare rounds of sampling as in the previous samples. Overall, with the exception of *Se*, the MCL regulated constituent

concentrations were lower in the BF samples than in the steel slags. The most evident difference was for *Ba* and *Cr*, both of which were similar between the three other materials. Only the LS 100 sample was higher in the BF slag for *Ba* as shown in Figure 4.70. The decrease in the solubility curve slope seen in the steel slag *Ba* graphs was not evident for the BF slag possibly indicating solubility controlled release of this constituent. No MCL exceedances were detected in the samples, although *Tl* exceedances are possible since the MCL is below the IDL. *Mn* was detected in the BF slag but not in the steel slags. *Al* and *Mg* were detected at higher concentrations than the previous samples while *Ca* showed similar concentrations. Some or all of the results for *As*, *Cr*, *Cu*, *Se*, and *Tl* were detected below the ICP IDLs as identified in the graphs indicating an estimation of constituent concentration for these results. Interestingly, *Tl* was detected above the IDL in the availability test but below the IDL in this test, whereas the opposite relationship was seen with *Se*. Of the MCL constituents, only *Cr* appears to be approaching its available leaching concentration under these conditions. This trend for *Cr* was not seen in the steel slags results. Interestingly, when the leaching tests were complete after the required leaching time, a sulfur odor was detected once the containers were opened.

4.6.5 SAW Slag

Figures 4.78 through 4.92 show SAW slag leaching results for *Al*, *As*, *Ba*, *Ca*, *Cd*, *Cr*, *Cu*, *Fe*, *Mg*, *Mn*, *Se*, *Sb*, *Tl*. *Be* and *Pb* were not detected in the samples. MCL exceedances were measured in *Sb* and *Tl*, however the *Tl*

exceedences were all below the IDL so the concentrations are considered estimations. This is similar to the availability test where *Tl* also exceeded the MCL but was below the IDL. *Sb* did not show an exceedance for this material in the availability test. The *Sb* exceedances occurring at LS 0.5 and 1 indicates this constituent was easily released from the slag, possibly due to a washoff effect. Similar to the steel slags, some or all of the results for *As*, *Cu*, *Pb*, *Sb*, *Se*, and *Tl* were detected below the ICP IDLs as identified in the graphs indicating an estimation of constituent concentration for these results. The leaching results for *As*, *Cd*, *Cu*, *Sb*, *Se*, and *Tl* are similar to the steel slag results for at least three LS ratios. This is unexpected considering SAW slag is produced through a completely different process than the steel slags. The *Al* solubility curve differed from the other slags in that the concentrations were higher and they do not increase until LS 2. The *Ca* curve shows the opposite effect with a sharp concentration increase at low LS ratios and a decrease for the higher LS ratios, similar to the steel and iron slags. Due to the erratic data points and lack of correlation between sampling rounds in the *Fe* and *Mn* graphs it is difficult to identify trends in solubility. *Mg* concentrations were higher than the steel slags but mostly lower than the BF slag results. Interestingly, *Ba*, *Cr*, *Cu*, and *Se* showed similar or decreasing concentrations in LS ratios 0.5 through 2 indicating that solubility is not controlled by the amount of liquid in contact with the material, at least for lower LS ratios. For *Cu*, the concentrations decreased slightly from LS 0.5 to LS 10 (R1 only). It should be noted that these trends are not consistent for both sampling rounds. Overall, consistency between

R1 and R2 was the lower than the other slag samples with the exception of *Al* and *Mg* which showed similar results for the two rounds. Based on the information acquired from LE, all of the SAW slag obtained was produced from the same flux material, so the material should be somewhat homogenous. However, the slag could have been produced from welding several different types of metal, which may affect the constituent concentrations of the slag. An additional explanation for the difference is that the material used in each round contained different amounts of fines. Depending on the constituent, equilibrium is more readily reached with finer particles than with larger particles where diffusion may control release (Kosson et al., 2002). The samples used in R1 and R2 most likely contained different amounts of fines since the only control on particle size was that the material passed a No. 10 sieve.

4.6.6 LS Ratio Calculations

How LS ratios relate to time with respect to materials use in highway construction is a function of site specific properties such as precipitation rate, the presence of impermeable layers, and extent of compaction. A material placed in an embankment will have a higher LS ratio after a year than a material placed beneath a layer of paved asphalt due to different amounts of precipitation contact. The LS ratio of the material beneath the asphalt can change over time however, as the surface ages and cracks form, allowing precipitation to seep into the road. A material used in an arid part of the country will have a lower LS ratio than material used similarly in

an area with higher precipitation rates. Additionally, a material that is heavily compacted may have a lower LS ratio than a loosely packed material if water does not flow through the layer as easily. These site-specific factors are important to consider when determining the best use for a particular recycled material. Three scenarios are presented in the research to identify variations in LS ratios. Figure 4.93 depicts a 1 cubic meter section of steel slag with known density. LS ratios are calculated by introducing precipitation at three different rates and calculating the LS ratio as volume (ml) of water in contact with mass (g) of material using Equation 2.10. Three annual average precipitation rates were obtained from www.worldclimate.com and were used to translate LS ratios to years. The first two scenarios are for an uncapped embankment in Pittsburgh, PA and Columbus, OH, two areas where steel slag is accessible from steel slag production. The third scenario is for the steel slag cube placed beneath a layer of paved asphalt which diminishes the contact with precipitation greatly. All three scenarios assume the material is not placed beneath the water table. Actual data for infiltration rates beneath paved highways was not identified in this research although standard practice is to use 10% of the total precipitation rate (Apul, 2005). Table 4.10 shows the corresponding years for the LS ratios used in the leaching test in addition to three other LS ratios. Using this conversion method, a material used in an embankment in Columbus, OH would reach an LS ratio of 10 after 29.6 years. If the material were placed beneath a layer of paved asphalt the LS ratio would be reached in 296.5 years. This conservative approach assumes that 100% of the precipitation is entering

the embankment and disregards the effects of evaporation and runoff. The extent of these variables would depend on the local climate and the embankment construction design.

4.7 pH-Dependent Leaching Test

The pH-Dependent Leaching test identifies a material's ANC or BNC and constituent partitioning at equilibrium between aqueous and solid phases as a function of solution pH (Kosson et al., 2002). The ANC is an important property that identifies the sensitivity of a material to external factors (acid rain, CO₂, etc.) and addresses its long term stability (van der Sloot and Woelders, 2000). For instance, the solubility of constituents is determined in the LS ratio leaching test under pH conditions controlled by the material's natural pH. The natural pH of the material may change over time however due to acid rain and CO₂ contact. Material carbonation can result in the loss of alkalinity and a lowering of the pH in the material pore-water (Sanchez et al., 2002). The first step of the pH-dependent leaching test is to identify the ANC and BNC of each material through acid/base titrations. The second step involves extrapolating acid neutralization data from the curves and leaching the materials over a range of pHs that could be expected in the field (usually 3-12). ICP analysis results for both rounds of testing of the pH-dependent leachate samples are presented in Appendix. Tables 8-12 and select constituents are presented in Figures 4.103 through 4.176. Some figures contain missing data points, often at higher pHs, indicating a non-detect ICP result.

4.7.1 Acid Neutralization Capacity (ANC)

Due to the strong alkaline behavior of the slags, only the SAW and BF slags required the addition of a base (NaOH) to reach the higher target pHs. Therefore the curves are referred to as ANC curves and the addition of base is shown with a negative acid value. As previously mentioned in the Methods and Materials, the titrations were difficult due to the strong neutralizing behavior of the slags. Figure 4.94 shows one attempt to characterize the ANC of the steel and iron slags using the Schott Autotitrators and constant acid addition. The SAW slag was not run with this method. It is important to note the smooth curves produced by continuously adding acid to the samples. Figure 4.95 shows the ANC curves for the steel slags and the SAW slag produced using the autotitrator with a 15 minute equilibrium time between acid additions. At each addition of acid the pH dropped and then slowly increased as the acid reacted with the buffering capacity. The graph does not identify the true ANC of each material but does show differences between the four materials. The SSFF slag showed the highest buffering capacity while the SAW slag showed the least. The BOF and SSFW slags behaved similarly, a relationship also seen in the initial curves in Figure 4.94. Figure 4.96 shows the results from the test used to characterize pH change throughout the 48 hour pH-dependent leaching test. The pH does not appear to change greatly between 24 and 48 hours indicating equilibrium was most likely reached. It was concluded from this test that 48 hours was sufficient enough time for the samples to reach

equilibrium. Two assumptions in this conclusion are that 48 hours is enough time for samples with lower target pHs than 5.5 to reach equilibrium and that constituent release slows or stops completely once pH equilibrium has been reached. The second assumption could be validated with a kinetic study similar to this test with constituent measurement in addition to pH measurement at each time interval; however such a test was not included in this research.

It was decided that the most accurate way of identifying the ANC of the materials was to estimate the amount of acid required to reach the target pHs from the previous curves and conduct a trial and error test to determine the ANC curves. After the first round of pH-dependent leaching tests the acid amounts added to each sample were plotted against the final sample pH and extrapolations were again performed to better reach the target pHs in the second testing round. The acid addition schedule calculated for the second round is shown in Table 4.12. Figures 4.97 to 4.101 show the final ANC curves from both rounds testing and Figure 4.102 shows the combined ANC curves for comparison. All of the slag plots show a similar shape with a sharp decrease in slope at the higher pHs followed by a shallower slope in the lower pH range. This indicates a smaller buffering capacity between the materials' natural pHs to neutral pHs (6-8) compared to a higher buffering capacity from neutral conditions to acidic conditions.

4.7.2 SSFF Slag

The pH-dependent leaching test curves for the two rounds of SSFF slag are shown in Figures 4.103 through 4.117 for *Al*, *As*, *Ba*, *Be*, *Ca*, *Cd*, *Cr*, *Cu*, *Fe*, *Mg*, *Mn*, *Pb*, *Sb*, *Se*, and *Tl*. In all of the graphs the highest constituent solubilities were seen at lower pH levels. Graphs for *Al*, *Ba*, *Cu*, and *Cr* show amphoteric leaching curves with the lowest concentrations detected at neutral to slightly alkaline pHs. Identifying this leaching characteristic is important for materials such as steel slag that have high buffering capacities that control the pore water pH conditions. For instance, leaching results from the TCLP, SPLP, and the availability test are designed to predict leaching under aggressive environmental conditions. These tests however may underestimate the leaching potential of constituents with strong amphoteric pH-dependent leaching curves where minimum solubility occurs at neutral to slightly acidic pHs. Graphs for *As*, *Cr*, *Cu*, *Fe*, *Pb*, *Sb*, *Se*, and *Tl* showed at least one concentration below the IDL which mostly occurred at higher pHs. Graphs for all constituents except *Ba*, *Ca*, and *Mg* showed at least one non-detect concentration. Concentrations for *As*, *Pb*, *Sb*, and *Se* did not show any consistency between sampling rounds and only showed a general trend of increasing concentrations with decreasing pH. Interestingly, *Pb* was detected in this test but was not detected in the availability test at similar pHs of 4 and 7. This may be because the 6 hour leaching time was not long enough for *Pb* to equilibrate in the availability test compared to the 48 hour leaching time in the pH-dependent test. *Be* showed an interesting trend with almost constant concentrations from pH 6 to 12 indicating that

solubility does not change from neutral to alkaline conditions. Similar to the *Pb*, *Be* was not detected in the availability test. *Ca* shows a similar trend for both rounds, however this is due to the maximum detection limits of the ICP setup used and therefore concentrations may be higher for some pHs. MCL exceedances occurred for all of the regulated constituents. But since these exceedances only occurred at lower pHs (with the exception of *As* and *Tl*), it is unrealistic that they would actually occur with highly buffering slags used in a highway application. A more realistic application for these lower pH exceedances would be the use of steel slag as a neutralizing agent in acid mines. As a comparison for the *As* and *Tl* exceedances, the SSFF LS leaching results which were performed under very alkaline pHs did show one *Tl* exceedance but did not show any *As* exceedances.

4.7.3 SSFW Slag

The pH-dependent leaching test curves for the two rounds of SSFW slag are shown in Figures 4.118 through 4.132 for *Al*, *As*, *Ba*, *Be*, *Ca*, *Cd*, *Cr*, *Cu*, *Fe*, *Mg*, *Mn*, *Pb*, *Sb*, *Se*, and *Tl*. In all of the graphs with the exception of *Se* and *Pb*, the highest constituent solubilities were seen at the lower pH levels. Graphs for *Se* and *Pb* show the highest concentrations around pH 6. Graphs for *Al*, *Ba*, and *Cr* show amphoteric leaching curves with the lowest concentrations detected at neutral to slightly alkaline pHs. Graphs for *As*, *Cd*, *Cr*, *Cu*, *Pb*, *Sb*, *Se*, and *Tl* show some concentrations below the IDL which mostly occurred at higher pHs. Graphs for all constituents except *Ca* showed at least one non-detect concentrations. As previously mentioned,

the SSFF results showed no non-detects for *Ba* and *Mg* and *Ca*. Concentrations for *As*, *Ca*, and *Se* did not show any consistency between sampling rounds and only showed a general trend of increasing concentrations with decreasing pH. *Be* showed a similar trend as the SSFF slag with almost constant concentrations from pH 6 to 12 indicating that solubility does not change from neutral to alkaline conditions. *Ca* does not show the same trend as the SSFF slag but does show inconsistency between sample rounds. MCL exceedances occurred for all of the regulated constituents except *Se*, but only at lower pHs. More relevant to highly buffering slags are those constituents showing amphoteric leaching behavior. *Tl* exceedances occurred at pHs as high as 8.5.

4.7.4 BOF Slag

The pH-dependent leaching test curves for the two rounds of BOF slag are shown in Figures 4.133 through 4.147 for *Al*, *As*, *Ba*, *Be*, *Ca*, *Cd*, *Cr*, *Cu*, *Fe*, *Mg*, *Mn*, *Pb*, *Sb*, *Se*, and *Tl*. The results were not as consistent with the other steel slags indicated by discrepancies between the two sampling rounds and a lack of continuous curves, as seen in *As*, *Se*, and *Tl*. Most of these inconsistencies were seen below the IDLs, which likely contributes to the problem. However, particle heterogeneity seen in the SEM results could also contribute to these inconsistencies identifying the difficulty of characterizing a large amount of material with one round of testing. The graphs show results consistent with the other steel slags for *Al*, *Sb*, *Ba*, *Mg*, *Cr*, *Fe*,

The graph for *Cu* is more similar to the SSFW slag with a lack of an amphoteric pattern seen in the SSFF slag. With the exception of three R1 data points between pH 9 and 12, the *Be* graph is similar to the other steel slags with little change in solubility above pH 6. The graph for *Cd* is similar to the SSFW slag below pH 6 but showed concentrations above the IDL (R2 only) whereas the SSFW graph showed mostly non-detects. The *Se* results are also similar to the SSFW slag. MCL occurrences were seen in all of the regulated constituents in the lower pH range with the exception of *Tl* and *Sb*. The *Tl* and *Sb* exceedances however occurred below the IDL and therefore are estimates.

4.7.5 BF Slag

The pH-dependent leaching test curves for the one round of BF slag are shown in Figures 4.148 through 4.161 for *Al*, *As*, *Ba*, *Be*, *Ca*, *Cd*, *Cr*, *Cu*, *Fe*, *Mg*, *Mn*, *Pb*, *Se*, and *Tl*. Similar to the LS ratio leaching results, *Sb* was not detected in the pH-Dependent leaching test. Graphs for *Al*, *Ba*, *Ca*, *Cr*, *Cu*, *Fe*, *Mg*, and *Mn* showed mostly continuous solubility leaching curves (no irregular data points), while *As*, *Be*, *Cd*, *Pb*, *Se*, and *Tl* showed discontinuous curves with some erratic data points. These gaps may have been filled in with a second round of testing so direct comparisons to the steel slag graphs are not accurate. *Al*, *Fe*, *Mn*, and possibly *Cr* showed amphoteric solubility curves. The amphoteric solubility behavior seen in the steel slags for *Ba* was not seen in the BF slag where concentrations were relatively constant between pH 8 and 12. Because the minimum solubility

data points for *Cr* were detected below the IDL it is difficult to identify whether the concentrations are similar to *Ba* or show more of an amphoteric behavior. MCL exceedances occurred for *As*, *Ba*, *Be*, *Cd*, and *Cr* at pHs below 4 compared to below 6 for most of the steel slag exceedances. *Tl* exceedances occurred at pHs below 7. A similar trend seen in the *Ba*, *Ca*, *Cu*, *Fe*, *Mg*, *Mn*, and *Tl* graphs is a plateau of similar concentrations at acidic pHs followed by a steep decline in concentrations at neutral pHs and another plateau at alkaline concentrations. This trend was not as common in the steel slags. Similar to the LS ratio leaching test, a sulfur odor was detected after the leaching containers were opened. The sulfur odor appeared stronger in those containers containing more aliquots of acid.

4.7.6 SAW Slag

The pH-dependent leaching test curves for the both rounds of SAW slag are shown in Figures 4.162 through 4.176 for *Al*, *As*, *Ba*, *Be*, *Ca*, *Cd*, *Cr*, *Cu*, *Fe*, *Mg*, *Mn*, *Pb*, *Se*, and *Tl*. *As* was not detected across the pH range, however, there is a gap between pH 8 and 10 where solubility data is missing. *As* was detected in the LS ratio test but below the IDL. Since those final pHs were mostly between pH 10.4 and 11.6 they cannot be used to fill in this pH gap.

Overall, the results were not as erratic as some of the steel and iron slag results with recognizable solubility trends for most constituents. Similar to the other slags, solubility increased with decreasing pH with the exception

of an amphoteric behavior seen in some constituents. *Al*, *Ba*, *Cu*, *Fe*, and *Mn* showed amphoteric solubility curves and possibly *Sb* as well, although most of the data points were below the IDL. The other constituents showed a general decrease in solubility with increasing pH. MCL exceedances occurred for all of the regulated inorganics but mostly below pH 6. *Se* and *Tl* showed some exceedances between pH 6 and 8 which is significant since the buffering capacity of the SAW slag is not as great as the steel and iron slags.

4.7.7 pH Calculations

A calculation was conducted using the ANC data to predict how many years of acid rain contact would be required to reach target pHs. Figures 4.177 through 4.181 show the ANC graphs with target pHs ranging from 5.5 to 9 and the corresponding time prediction. According to the calculations, the highly buffered SSFF slag would reach a pH of 9 in approximately 13,900 years. This is compared to the BF slag which would reach a pH of 7.6 in only 420 years. It should be noted that this is a simplified prediction that assumes 100% of the precipitation comes in contact with the material (no runoff, saturated flow) and does not take into effect other pH reducing factors such as carbonation.

4.8 Compacted Granular Leaching Test (CGLT)

This CGL test was used to determine the mass transfer properties of constituents in a sample. ICP analysis results of the CGLT leachates are

presented in Appendix Tables 13-16. The test was conducted for the SSFF, SSFW, BOF, and SAW slag samples and select results are shown in Tables 4.13 through 4.24. The SSFF, SSFW, and SAW slag leachates were sampled on the same interval schedule whereas the BOF slag schedule varied slightly. The majority of the tested constituents were not detected in high enough concentrations to use in the mass transfer calculations. Most likely the diffusion rates for these constituent were too slow for measurable amounts to diffuse into the leachant. For the steel slags, *Al*, *Ba*, *Ca*, *K*, and *Na* were detected in all three materials with *Sr*, *Cr*, *Fe*, *Mg*, and *V* inconsistently detected. *Al*, *Ca*, *K*, *Mg*, and *Na* were detected in the SAW sample. The only MCL-regulated constituents detected were *Ba* and *Cr* and were only found in the steel slags. The *Ba* and *V* detected in the BOF slag test were also detected by Comans et al. (1991) in a similar tank leaching test and were attributed to the reducing conditions produced by the material and the closed atmosphere conditions. The results for each measured constituent are shown in three tables. The first table shows the cumulative release of each constituent into the leachant in mg per m² of exposed surface area calculated using Equation 3.2. Figures 4.182 through 4.185 show the cumulative constituent curves for each material in mg of constituent released per m² of exposed surface area. The second table shows the interval slopes and identifies intervals with diffusional release (0.5+/-0.15), wash-off release (<0.35), and dissolution release (>0.65). It should be noted that de Groot and van der Sloot (1992) identified diffusional release as 0.5+/-0.1, however the prior range identified in Kosson et al.

(2002) and NEN 7375 was used in this research. Matching the slope data to the figures identifies changes in release mechanisms throughout the test. One trend explained in NEN 7375 and de Groot and van der Sloot (1992) is the concept of constituent depletion. If the interval slopes are below 0.35 in the beginning of the test, the release mechanism is related to surface wash-off. This low slope occurs when the cumulative concentration released does not increase greatly after washoff occurs causing only a gradual increase in slope. If the interval slopes are below 0.35 in the middle and/or end of the test the constituent concentration is considered approaching depletion, or maximum leachable concentration, similar to what was discussed in the LS ratio leaching section. This depletion trend was seen in the SAW slag Mg results (Table 4.23) where the first three interval slopes are within the diffusion range and the last 5 intervals are below 0.35. The third table shows the D_{obs} values in m^2/s calculated using Equation 3.3. These calculations used the availability test results (average of R1 and R2) as specified by Kosson et al. (2002) and NEN 7375. The average D_{obs} values (De) and the $-\log D_{obs}$ values (pDe) calculated using Equation 3.4 are shown for each constituent. For the BOF slag, Mg and V D_{obs} values were not calculated because the slope values were not within the diffusion range. A similar situation occurred for Ba and Sr in the SAW slag sample. It is assumed that constituents with a higher frequency of slopes within 0.5+/-0.15 are more diffusion-controlled than those with a lower frequency. Table 4.25 shows the compiled pDe values for each material as well as additional calculated values.

For all four materials, the constituents with the highest mobility (pDe values below 11) were *Na* and *K*. This is generally consistent with pDe values presented for other secondary materials by Kosson et al. (1996) and de Groot and van der Sloot (1992). This is not consistent with BOF slag tank leaching results by Comans et al. (1991) (Table 2.10) where *V* and *Ba* exhibited the lowest pDe values (highest mobility). In this research, *Ba* showed low mobility (in one sample) and *V* release was found to be washoff-controlled for the BOF slag sample. The only other constituent identified with high mobility was *Ca* in the SAW slag sample. Of the EPA regulated inorganics, *Ba* was identified with low mobility in the BOF slag and average mobility in the SSFF slag while *Cr* was identified with average mobility in the BOF slag. *Fe* showed the lowest mobility with a pDe of 17.2. pDe values from the literature in Table 4.26 show similar low mobilities for *Cd*, *Pb*, and *Zn*. Overall, the SAW slag showed the lowest pDe values compared to the steel slags. The tortuosity values calculated using Equation 3.6 were similar for the steel slags but 20 to 25 times lower for the SAW slag. The steel slag tortuosity values were higher than the values from the literature presented in Table 4.25 with the exception of Fly Ash in asphalt. Chemical Retention (*R*) values calculated from the D_{obs} and tortuosity values using Equation 3.7 are also shown in Table 4.25 and range from 1 to 506.7. The *R* values shown in Table 4.26 are from the literature and range from 0.8 for *Na* to over 1.8×10^6 for *Cd*. It should be noted that the *R* values were not presented in Kosson et al. (1996) and were instead calculated

from the D_{obs} and τ values reported in the results using equation 3.7. The SAW slag R values are lower than the steel slag values for the measured constituents (other than Na) indicating higher mobility. Retention factors for similar slags were not identified in the literature so it is unclear whether the values from this research are typical.

One important consideration in the CGLT is the definition of available leaching content pertaining to the C_0 value used to calculate D_{obs} . Kosson et al. (2002) defines C_0 as the availability or total content of a constituent. An availability method is not specified but it is assumed to be either the EDTA method or Dutch Availability Test which are also presented in the report. The availability values used for the D_{obs} calculations in Tables 4.13-4.24 were from the Dutch test NEN 7341 which leaches the sample at pHs 7 and 4. An alternate approach suggested in this research is to use availability concentrations from the low LS ratio leaching test. The conditions used in the LS ratio test are most similar to the conditions found in the CGLT with respect to LS ratio and pH. This is particularly important for a material with a high buffering capacity such as steel slag which will not encounter neutral or acidic pH conditions within a realistic timeframe. The CGLT LS ratio during each leaching interval is approximately 0.25 to 0.45 depending on the material. Therefore, the LS 0.5 leaching results in mg/kg could be used for C_0 in replace of the NEN 7341 values. Table 4.27 shows the LS ratio availability method concentrations as well as the recalculated pDe values. With the exception of K for the SAW slag, all of the recalculated pDe values

are lower than the original values indicating the mobilities are higher. This decrease is the result of the lower availability concentrations in the denominators of the D_{obs} equation which leads to larger D_{obs} values and smaller pDe values. The most significance difference between the availability methods is for *Al* in the steel slags, *Fe* in the BOF slag, and *Mg* in the SAW slag, all of which show pDe decreases greater than 6.9. The simplified explanation for these lower values is that in order to describe the diffusional release observed in the CGLTs the diffusion rates must be faster than those presented in Table 4.25 given the smaller concentrations available for leaching. Table 4.28 presents the re-calculated tortuosity and R values using the LS ratio availability concentrations.

4.8.2 CGLT Diffusion Modeling

As previously mentioned, De values can be used to predict diffusional constituent release over a given timeframe using the equation 3.5. Table 4.29 shows release calculations for Ba and Cr for the BOF slag and SSFF slag (Ba only). D_{obs} values could not be calculated for MCL regulated constituents in the SSFW and SAW slags. Release estimates were calculated for 1, 5, 40, and 100 years from a 100 m² section of a 0.5 m thick layer of compacted slag in a base layer of road. The volume of this layer (V) is 50 m³ and the exposed surface area (S) is 210 m² which includes the exposed top, bottom, and ends of the section (2 ends parallel to the road). The other two ends are not exposed since this section was cut from a road layer. Table 4.29 shows calculated release estimates for both availability

methods, however, the values are the same for the two methods. This is expected since changing the availability only adjusts the D_{obs} and does not affect the cumulative constituent release observed in the CGLT. After 100 years, approximately 24% of the available *Cr* and 0.08% of the available *Ba* has been released from the BOF slag using the NEN 7341 availability results. In comparison, *Cr* is mostly depleted after one year and *Ba* is depleted after 5 years of release using the LS ratio availability results. For the SSFF slag, after 100 years approximately 42% of the *Ba* has been released using the NEN 7341 method and using the LS ratio method, depletion of the 0.25 mg/kg available is depleted in less than one year. These differences highlight the need for better understanding of the actual leaching potential of a material, especially when all factors that affect leaching are considered. Depending on the material and the site specific conditions involved, either availability value, or a value somewhere in between, may be appropriate to use.

4.9 MINTEQ Modeling

Visual MINTEQ was used to model the pH-dependent leaching test results in order to identify the solid phases controlling solubility or portions of it. The BOF, SAW, and BF slags were successfully modeled while issues were encountered preventing the modeling of the SSFF and SSFW leachate results. The modeling results are presented in Appendix Figures 1-41 and are graphed by constituent. For each constituent, the pH-dependent leaching results are graphed (solid line) as well as the minerals identified by

MINTEQA2 as possibly controlling the solubility (points). It should be noted that some constituent concentrations were non-detect at certain pH. These gaps are not shown with the solid line. The controlling minerals very rarely matched the entire constituent pH-dependent leaching curve and more often matched a portion of the curve within a pH range. Tables 4.30-4.32 show the controlling minerals and the pH ranges in which they match the constituent solubility curves. Matches were not listed unless more than one data point overlapped with the curve.

Considering the alkaline behavior of the slags in this research, significant solids are those that control constituent leaching. Within these natural pH ranges the model predicted some similarities between the three materials. *Ba* solubility is controlled by $\text{BaHAsO}_4 \cdot \text{H}_2\text{O}$ in the BOF and BF slags. Barite also controls *Ba* solubility at the lower pH range (9.5) of the BF slag. Tenorite (c) controls *Cu* solubility in the BF slag. $\text{Pb}(\text{OH})_2$ was identified as controlling *Pb* solubility in both the BOF slag and the SAW slag in similar pH ranges. Also of significance is the large amount of minerals controlling SO_4 solubility in the BF slag. The high presence of SO_4 in slag leachate is consistent with the literature and was confirmed with the anion analysis and the presence of sulfur odors in the leaching test leachates. Only one mineral, Spinel (MgAl_2O_4), was identified in both the MINTEQA2 model and the XRPD analysis for SAW slag.

4.10 IWEM Modeling

Fate and transport modeling was performed with the EPA's IWEM model to interpret the some of the leaching results from this research. Directly comparing leachate concentrations to EPA drinking water standards (MCLs), as has been done in the previous sections, could be considered overly conservative unless ad drinking water well is located directly beneath or adjacent to the slag. Based on the leaching data, the LS ratio leaching results for *Sb* were chosen as inputs into the model. *Sb* was identified as a constituent of concern in the SSFF, SSFW, BOF, and SAW slags given that MCL exceedances occurred in all four samples. With the exception of SSFF, the exceedances occurred in low LS ratios which are representative of initial pore-water conditions and initial leachate compositions within a layer of material (Kosson et al., 2002). These concentrations are more applicable for modeling than higher LS ratio concentrations that can represent leaching over hundreds of years. The *Sb* concentrations that exceeded the MCL and the corresponding LS ratios are shown below.

Material	Sb Concentration (mg/l)	LS ratio
BOF slag	0.016	1
SSFW	0.008	1
SSFF	0.011	10
SAW	0.036	1

These values were used as inputs in the program and the resulting concentrations in a monitoring well located 20 m downgradient were modeled over 100 years.

Figure 4.186 shows the predicted concentrations graphed against time for the four materials. Both the SAW and BOF slags were found to exceed the 0.006 mg/l MCL during the 100 year time frame. The SAW slag exceeded the MCL in approximately 14 years while the BOF slag exceedance occurred after 75 years. As previously mentioned, IWEM is capable of calculating a Kd value for constituents if values are not known, as was the case in this simulation. Allison and Allison (2005) identified average soil-water partitioning coefficients found in the literature for a range of constituents. An average Kd value for Sb of 251 l/g was reported and was entered into IWEM with the same inputs that were previously used. The model output reported a concentration of 0.0 mg/l in the monitoring well for all four materials after 100 years using this Kd value. The timeframe was then extended for the highest concentration (SAW slag-0.016 mg/l) to the maximum allowed time of 200 years. With this timeframe, the Sb concentration in the monitoring well was 4.27×10^{-8} mg/l. This modeling example identifies how conservative IWEM's fate and transport predictions can be when a Kd value is not specified.

An obvious possibility is that IWEM predictions are less conservative when more site specific information is input into the model, although this assumption would require more model testing. As was previously mentioned, leaching results combined with fate and transport modeling provides the most realistic approach to identifying potentially hazardous management scenarios. The leaching tests and the IWEM modeling in this

research have shown that there are varying levels of conservativeness involved with these methods. Using conservative leaching results (availability test) with conservative IWEM modeling (K_d value not specified) will obviously lead to a conservative hazard estimate. By increasing the amount of leach testing and the amount of data inputs, a more realistic estimation of environmental impact is possible.

4.11 Laboratory Validation

Split samples were sent to EA, Inc. for analysis with an ICP-MS to validate the results obtained from the RMRC ICP-AES. Samples were analyzed for *Be*, *Cd*, *Sb*, and *Tl* which all have low EPA MCLs are of concern. Table 4.33 shows the EA and RMRC results for the four SAW slag samples, a blank sample, and a NIST standard. The greatest discrepancy between results was for the *Se* analysis in which the RMRC value was over two hundred times the value reported by EA for one sample. The RMRC results for three of the SAW samples were higher than the EA results but the NIST results compared well. This would suggest that the discrepancy could be a result of matrix interference since the NIST standard contained low concentrations of other constituents compared to the high concentrations of some constituents (*Ca*, *Al*, *Fe*, etc.) found in the pH-dependent leaching and availability leachates. This discrepancy should be taken into consideration since *Se* concentrations were often detected in the slags. A recommendation for future work is to identify matrix interferences and take the proper laboratory steps to control them. For the other constituents in the

validation test, the RMRC result for *Sb* was slightly higher than the EA result and *Cd* and *Be* were similar.

Figure 4.1. Grain size distribution from sieve analysis.

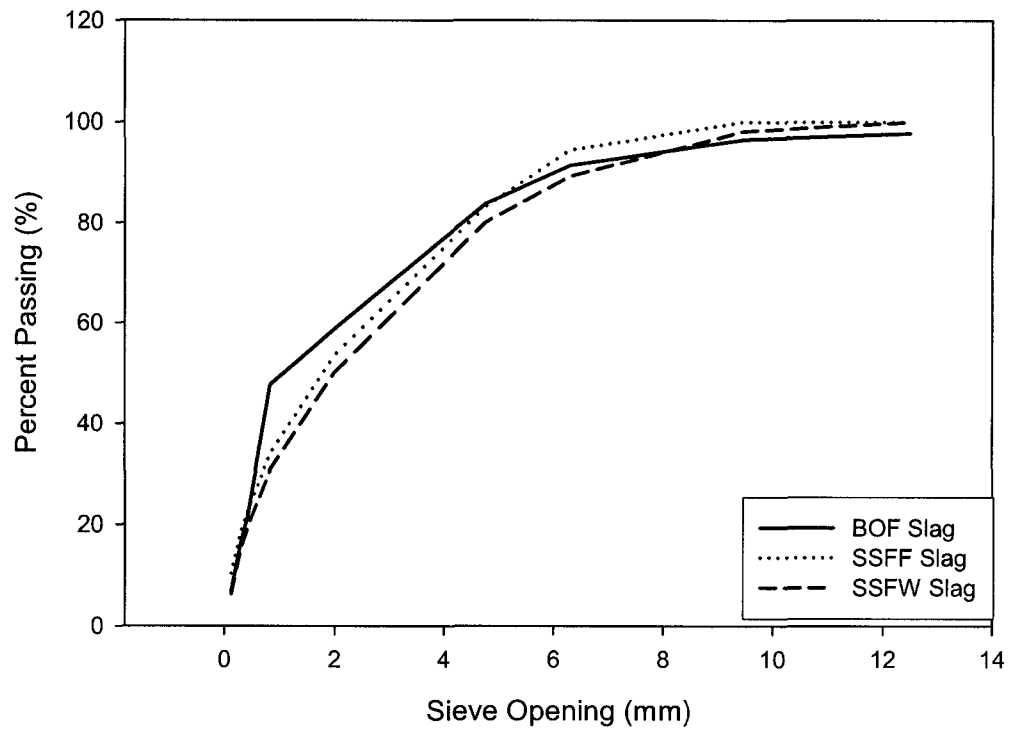


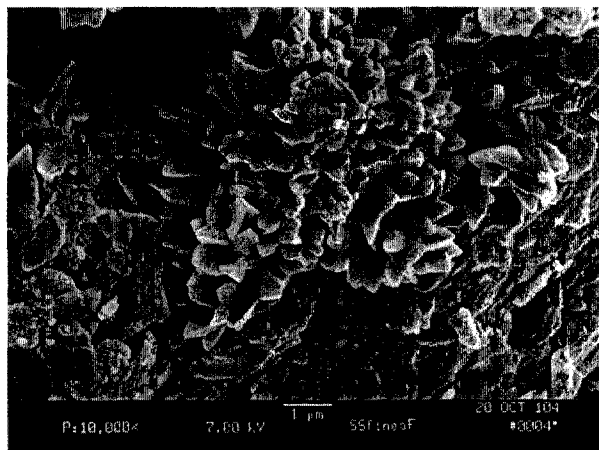
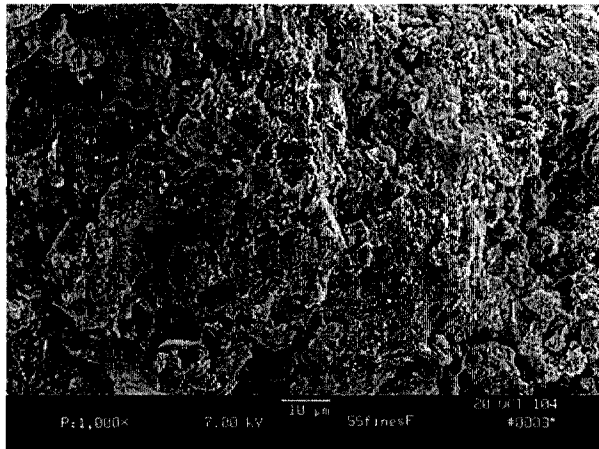
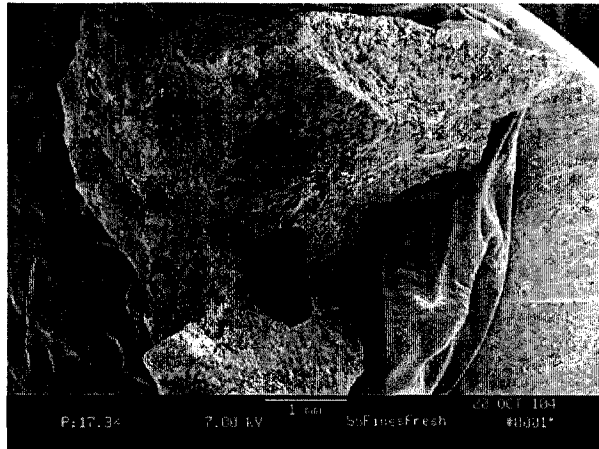
Table 4.1. Percent moisture content of received slags.

Material	Moisture Content %
SSFF Slag	0.060
SSFW Slag	0.331
BOF Slag	0.120
BF Slag	0.163
SAW Slag	0.011

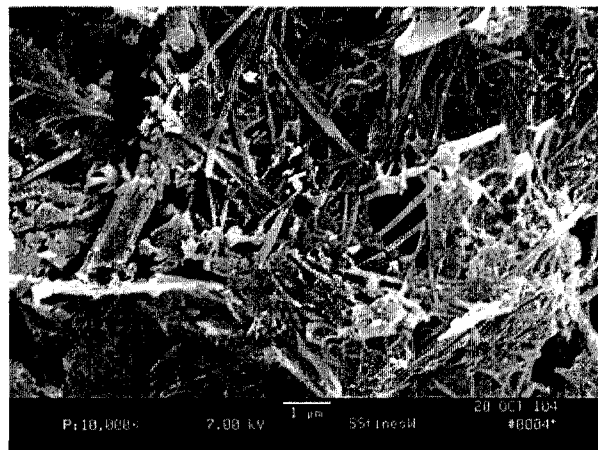
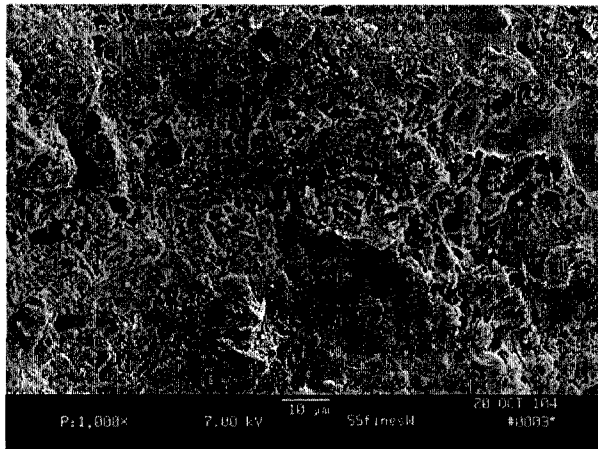
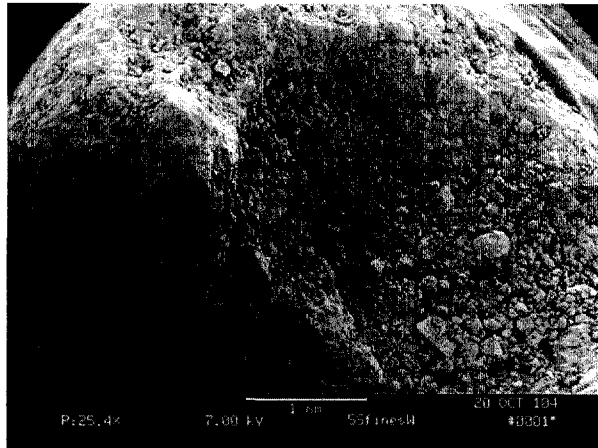
Table 4.2. Surface Area of different particle sized slags.

Material	Particle Size		
	<125um	<2mm	~8 mm
SSFF Slag	1.93	2.01	0.91
SSFW Slag	3.48	6.85	3.51
SAW Slag	0.09	0.08	NA
BOF Slag	3.02	5.58	3.59
BF Slag	3.04	3.02	3.18

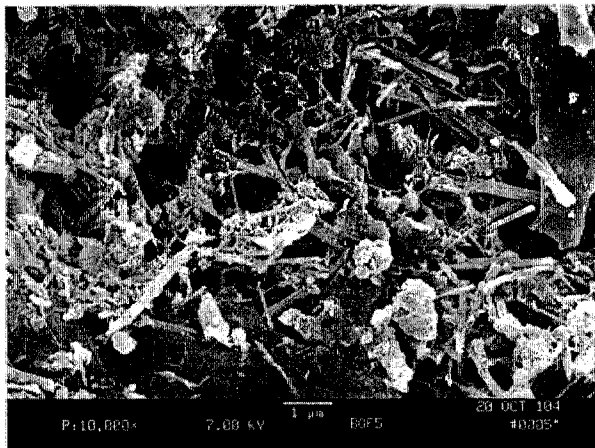
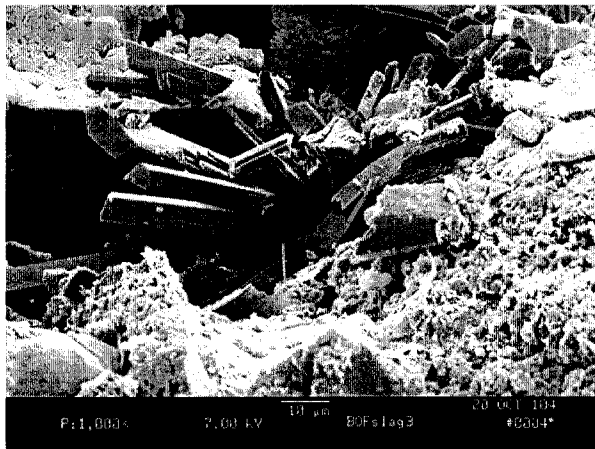
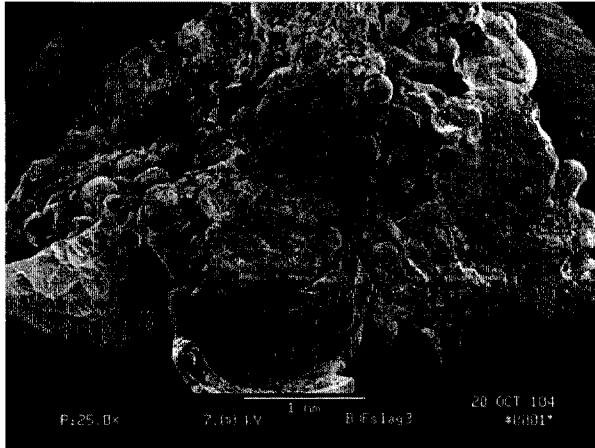
Notes:
All results in m²/g



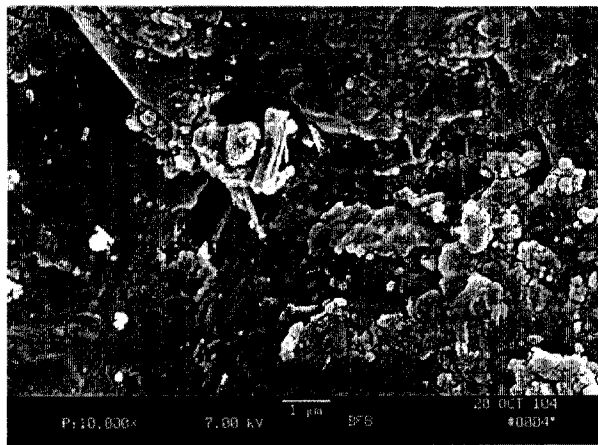
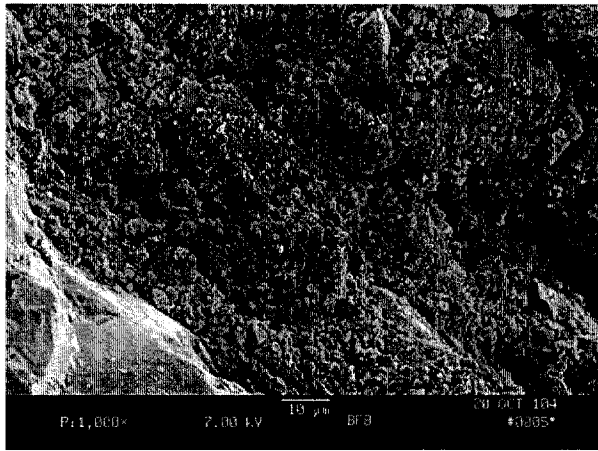
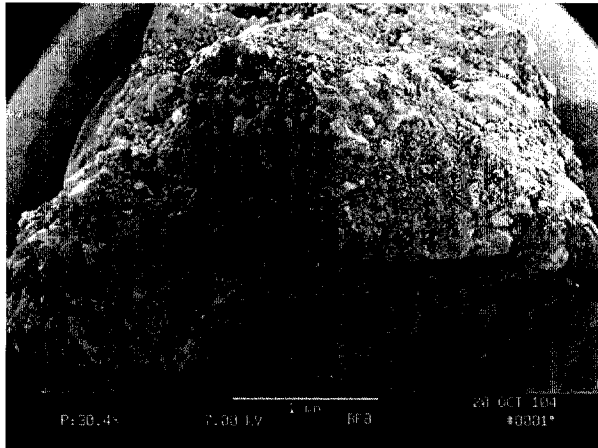
Figures 4.2-4.4: SEM images of SSFF slag in 17.3x, 1,000x, and 10,000x resolution



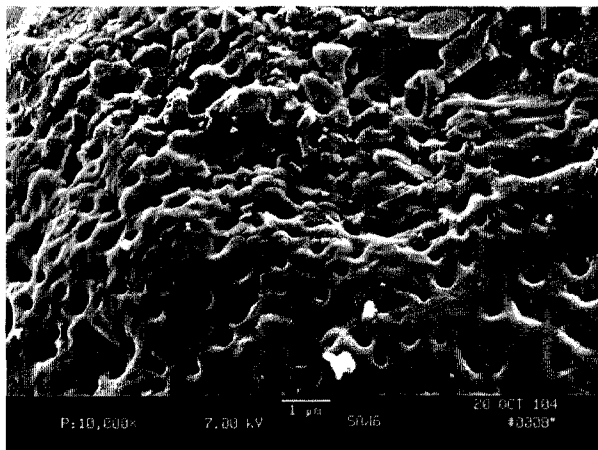
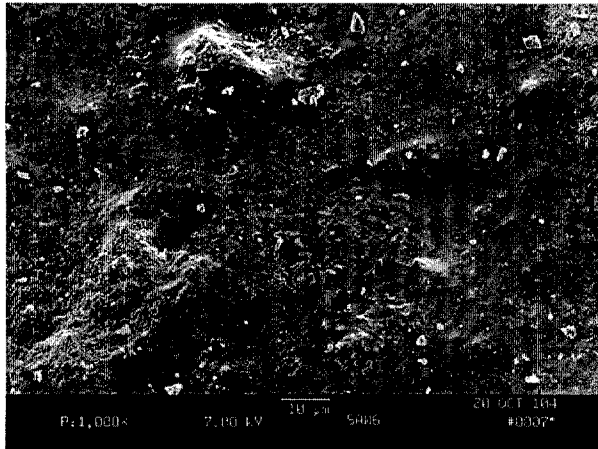
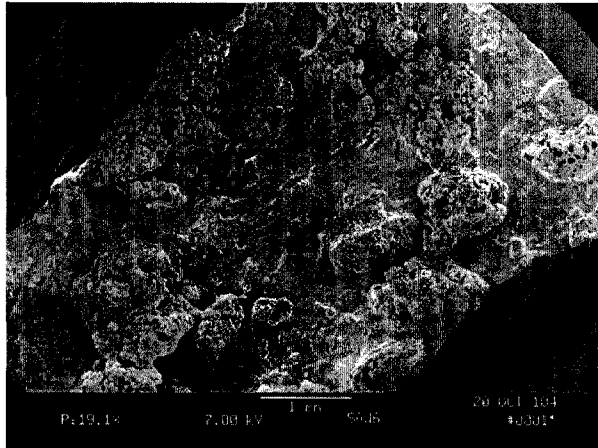
Figures 4.5-4.7: SEM images of SSFW slag in 25.4x, 1,000x, and 10,000x resolution



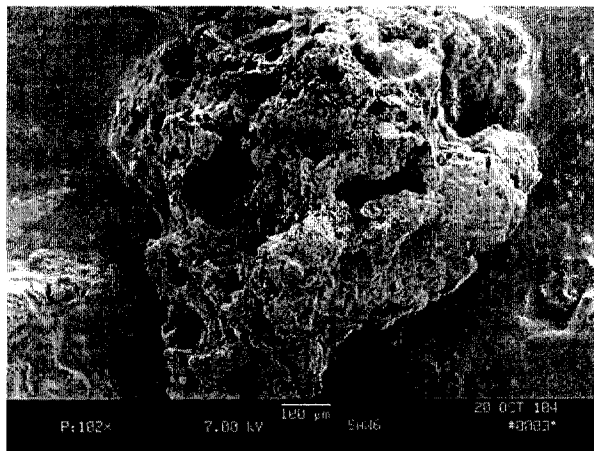
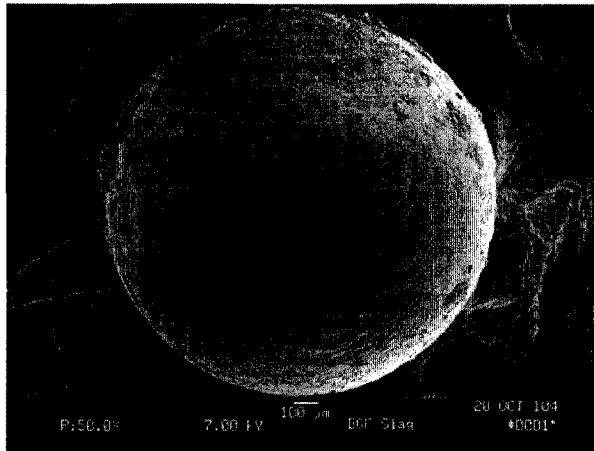
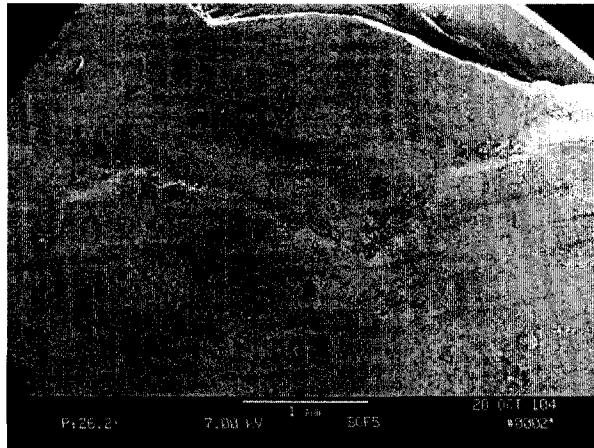
Figures 4.8-4.10: SEM images of BOF slag in 25x, 1,000x, and 10,000x resolution



Figures 4.11-4.13: SEM images of BF slag in 30.4x, 1,000x, and 10,000x resolution



Figures 4.14-4.16: SEM images of SAW slag in 19.1x, 1,000x, and 10,000x resolution



Figures 4.17-4.19: SEM images of flat and spherical BOF slag particles and SAW flux fused in the slag surface

Table 4.3. BOF Slag XRPD mineral list with FOMs.

Mineral	Chemical Formula	1st FOM	2nd FOM	3rd FOM
Magnesioferrite, ordered, syn	MgFe ₂ O ₄	4.9	6.7	5.5
Chromium Oxide	Cr-O	3.3	8.2	6
Lithium Cobalt Iron Oxide	Li _{0.3} CoFe ₂ O ₄	6.1	6.4	7.6
Iron Gallium Indium Oxide	InGaFe ₂ O ₄	7.2	7.2	6.2
Magnetite, syn	FeFe ₂ O ₄	7.9	7.5	5.3
Brunogeierite, syn	Fe ₂ GeO ₄	6.2	8.2	8.4
Lithium Manganese Titanium Oxide	LiMnTiO ₄	9.1	9.1	7.9
Zinc Iron Germanium Oxide	Zn _{0.5} Ge _{0.5} Fe ₂ O ₄	4.1		7.6
Manganese Aluminum Oxide	Mn ₂ AlO ₄	6.4		6.2
Zinc Chromium Iron Oxide	ZnFeCrO ₄	4.4		8.4
Copper Iron Manganese Oxide	CuFeMnO ₄	6		6.9
Lithium Cobalt Titanium Oxide	Li ₂ CoTi ₃ O ₈	4.8		8.2
Lithium Cobalt Iron Oxide	Li _{0.3} CoFe ₂ O ₄		6.4	7.3
Zinc Titanium Oxide	Zn ₂ TiO ₄	5.4		8.4
Manganese Rhodium Thallium	Rh ₂ MnTl		6.7	7.2
Iron Nickel Zinc Neodymium Oxide	Ni _{0.40} Zn _{0.60} Fe _{1.998} Nd _{0.002} O _{4+x}	6	8.5	
Manganese Chromium Antimony Oxide	Mn _{1.20} Cr _{1.70} Sb _{0.10} O ₄	6.1		8.9
Zinc Vanadium Oxide	Zn ₃ V ₃ O ₈	8		7.1
Copper Manganese Oxide	CuMn ₂ O ₄	6.3	9.1	
Aluminum Iridium	AlIr	9.3		6.3
Magnesiocoulsonite	Mg(V,Cr) ₂ O ₄	7		8.9
Qandilite, syn	Mg ₂ TiO ₄	6.1		10
Cobalt Titanium Oxide	Co ₂ TiO ₄	8.2		8.4
Cuprospinel	CuFe ₂ O ₄	6.8		9.8
Donathite	(Fe,Mg)(Cr,Fe) ₂ O ₄	8.3	8.9	

Notes:

Bold indicates Major Phase. All others are Minor Phases

Table 4.4. SSFF Slag XRPD mineral list with FOMs.

Mineral	Chemical Formula	1st FOM	2nd FOM	3rd FOM
Lithium Cobalt Iron Oxide	Li _{0.3} CoFe ₂ O ₄	5.4	5.3	8.2
Sodium Antimony Selenide	NaSbSe ₂	5	7.8	6.8
Copper Iron Manganese Oxide	CuFeMnO ₄	5.9	7.2	6.8
Zinc Vanadium Oxide	Zn ₃ V ₃ O ₈	5.7	7.1	7.2
Brunogeierite, syn	Fe ₂ GeO ₄	5.9	8	6.4
Manganese Oxide	Mn ₃ O ₄	6.3	8.9	6
Zinc Iron Germanium Oxide	Zn _{0.5} Ge _{0.5} Fe ₂ O ₄	5.9	7.6	8.2
Magnetite, syn	FeFe ₂ O ₄	7.2	8.4	8
Chromite, syn	FeCr ₂ O ₄	7.8	8.4	7.6
Donathite	(Fe,Mg)(Cr,Fe) ₂ O ₄	8.7	6.7	9.2
Cobalt Titanium Oxide	Co ₂ TiO ₄	9.1	8.5	8.3
Zinc Gallium Iron Oxide	ZnFeGaO ₄	9.1	8.6	8.4
Manganese Aluminum Oxide	Mn ₂ AlO ₄	7.8	9.8	9.3
Aluminum Vanadium Oxide	AlVO ₃	8.8	8.7	9.5
Lithium Copper Iron Oxide	LiCuFe ₂ O ₄	5.7		4.8
Chromium Oxide	Cr-O	7.5	6.8	
Lithium Iron Oxide	LiFeO ₂		9.3	5.3
Calcium Bromide Phosphide	Ca ₂ BrP	5.8	9.1	
Magnesioferrite, ordered, syn	MgFe ₂ O ₄	5.7	9.6	
Iron Gallium Indium Oxide	InGaFe+ ₂ O ₄	8.1		7.5
Romarchite, syn	SnO	9.4		6.9
Iron Titanium Hydride	H _{0.06} FeTi		9.3	7.1
Barium Cadmium	BaCd	7.1		9.7
Lithium Cobalt Titanium Oxide	LiCoTiO ₄	7.8		9.5
Zinc Titanium Oxide	Zn ₂ TiO ₄	9.6		7.7
Lithium Titanium Oxide	Li ₂ Ti ₂ O ₄	9.1	8.3	
Indium Nickel	InNi ₂	8.8	8.7	
Cobalt Iron Oxide	CoFe ₂ O ₄	8.9		8.8
Lithium Titanium Oxide	LiTi ₂ O ₄	9.3	8.5	
Strontium Manganese Oxide	SrMnO _{2.694}	8.6	9.5	
Barium Zirconium Oxide	Ba ₃ Zr ₂ O ₇	9.8	9.1	
Franklinite, syn	ZnFe ₂ O ₄	9.5		9.9

Notes:

Bold indicates Major Phase. All others are Minor Phases

Table 4.5. SSFW Slag XRPD mineral list with FOMs.

Mineral	Chemical Formula	1st FOM	2nd FOM	3rd FOM
Aluminum Vanadium Oxide	AlVO ₃	8.2	8.8	9.3
Lithium Titanium Oxide	LiTi ₂ O ₄	9.2	10	9.3
Lithium Cobalt Iron Oxide	Li _{0.3} CoFe ₂ O ₄	4.3	5.3	
Zinc Vanadium Oxide	Zn ₃ V ₃ O ₈	6.2	5.6	
Brunogeierite, syn	Fe ₂ GeO ₄	7.8	5.3	
Lithium Copper Iron Oxide	LiCuFe ₂ O ₄	9.2	5	
Potassium Iron Oxide	K ₆ Fe ₂ O ₅	8.2	7.2	
Zinc Iron Germanium Oxide	Zn _{0.5} Ge _{0.5} Fe ₂ O ₄	5.9	9.6	
Copper Iron Manganese Oxide	CuFeMnO ₄	6	9.7	
Magnesioferrite, ordered, syn	MgFe ₂ O ₄	6.6	9.8	
Zinc Titanium Oxide	Zn ₂ TiO ₄	8.1	8.5	
Magnetite, syn	Fe ₃ O ₄	8.2	8.9	
Cobalt Titanium Oxide	Co ₂ TiO ₄	9.5	8.5	
Manganese Oxide	Mn ₃ O ₄	8.2	9.9	
Copper Manganese Oxide	CuMn ₂ O ₄	9.2	9.5	
Lithium Titanium Oxide	Li _{0.8} Ti _{2.2} O ₄	9.6		9.3
Zinc Iron Manganese Chromium Oxide	Zn[Fe _{0.5} Mn _{0.5} Cr]O ₄	9.9	9	
Iron Gallium Indium Oxide	InGaFe ₂ O ₄	9.7	9.4	
Lithium Titanium Oxide	Li ₂ Ti ₂ O ₄	9.8		10
Magnesium Manganese Oxide	Mg ₆ MnO ₈		10	9.8

Notes:

Bold indicates Major Phase. All others are Minor Phases

Table 4.6. BF Slag XRPD mineral list with FOMs.

Mineral	Chemical Formula	1st FOM	2nd FOM	3rd FOM
Sodium Strontium Niobium Oxide	Na0.98Sr0.02NbO3	7.1	8.2	5.8
Macedonite, syn	PbTiO3	7	9.4	6.5
Akermanite, syn	Ca2MgSi2O7	9	7.8	6.4
Lead Antimony Oxide Chloride	PbSbO2Cl	7.3	8.1	9.3
Hardystonite, syn	Ca2ZnSi2O7	9.3	8.9	7.4
Aluminum Titanium	Al11Ti5	7.2	9.3	9.2
Boron Manganese	MnB	9.8	7.1	9.8
Germanium Hydrogen Phosphate	Ge(HPO4)2	4.9	5.2	
Sodium Aluminum Arsenate Hydroxide Hydrate	Na1.5Al2(OH)4.5(AsO4)37H2O		6.3	6.8
Magnesium Chloride Hydroxide Hydrate	Mg3(OH)5Cl4H2O	7.7	5.6	
Silver Manganese Oxide	Ag2MnO4		7	6.6
Zirconium Nitride Amide	ZrN(NH2)	8	5.6	
Barium Hydrogen Phosphite	Ba(H2PO2)2	7.8	6.9	
Copper Germanium Sulfide	Cu3GeS4	7		8
Ammonium Germanium Hydrogen Oxide	NH4H3Ge2O6	7.5	7.6	
Green Rust	Fe3.6Fe0.9(O,OH,SO4)9	8	8.2	
Copper Strontium Oxide	Cu2SrO2	8	8.4	
Silver Iodide	AgI	7.9		8.6
Iron Vanadium Oxide	FeVO4		8.8	8.4
Sodium Strontium Niobium Oxide	Na0.93Sr0.07NbO3	8.5		8.8
Boron Manganese	MnB	8.8		8.6
Lead Antimony Oxide Chloride	PbSbO2Cl		8.8	8.7
Calcium Cobalt Silicate	Ca2CoSi2O7		7.8	9.8
Cobalt Molybdenum Oxide	Co2Mo3O8		8.3	9.3
Tantalum Oxide Sulfate Hydrate	Ta2O3(SO4)24H2O		8.1	9.6
Copper Strontium Oxide	SrCu2O2	8.3	9.4	
Tin Phosphide	SnP	8.9		9.2
Sodium Chlorite	NaClO2	9.4		9
Sodium Copper Oxide	NaCuO2	8.8		9.8
Magnesium Hydride	MgH2	9.9		9.1
Tin Zirconium	Zr5Sn3		9.5	9.7
Bismuth Selenide Oxide	Bi2SeO2	9.8		9.6
Hauerite, syn	MnS2		10	9.4
Millerite	NiS	9.6	10	
Germanium Manganese	Ge4Mn		9.9	9.8

Notes:

Bold indicates Major Phase. All others are Minor Phases

Table 4.7. SAW Slag XRPD mineral list with FOMs.

Mineral	Chemical Formula	1st FOM	2nd FOM	3rd FOM
Ringwoodite, ferroan	(Mg,Fe) ₂ SiO ₄	7.8	6.8	1.7
Copper Cobalt Oxide	Cu _{0.92} Co _{2.08} O ₄	8.8	4.7	5.8
Lithium Aluminum Chromium Oxide	LiAl ₃ Cr ₂ O ₈	7.2	4.9	7.4
Spinel, syn	MgAl ₂ O ₄	9.1	4.2	6.7
Copper Aluminum Oxide	CuAl ₂ O ₄	8.8	6.3	5.4
Copper Cobalt Oxide	Cu _{0.76} Co _{2.24} O ₄	9	6.9	7
Cobalt Silicate	Co ₂ SiO ₄	7.2	7.8	8.8
Cobalt Aluminum Oxide	CoAl ₂ O ₄		5.3	7.3
Magnesium Aluminum Chromium Oxide	Mg(Al _{1.5} Cr _{0.5})O ₄	7.4	6.4	
Cobalt Nickel Oxide	Co ₂ NiO ₄		5.3	9.5
Gahnite, syn	ZnAl ₂ O ₄		5.9	8.9
Hercynite, syn	FeAl ₂ O ₄		6.8	9.8
Cobalt Oxide	Co ₃ O ₄		8.7	8.9
Zinc Cobalt Oxide	ZnCo ₂ O ₄		8.9	9.2
Aluminum Cobalt	AlCo		9.1	9.3
Barium Zinc Tungsten Oxide	Ba ₂ ZnWO ₆		9.8	8.8

Notes:

Bold indicates Major Phase. All others are Minor Phases

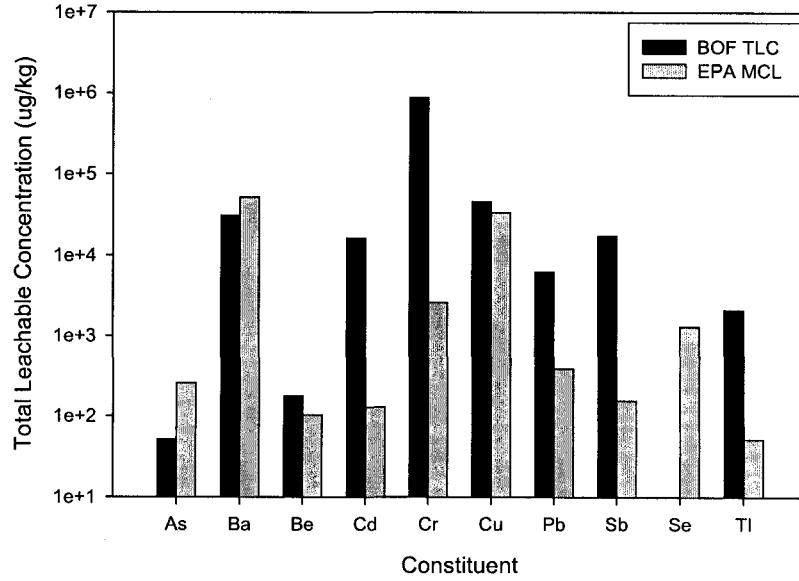


Figure 4.20. BOF slag total leachable composition results graphed with the corresponding EPA MCLs.

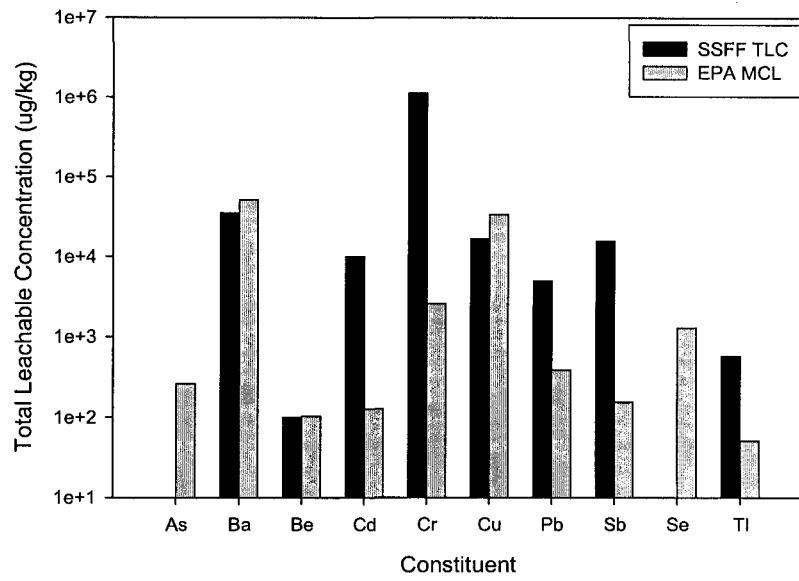


Figure 4.21. SSFF slag total leachable composition results graphed with the corresponding EPA MCLs.

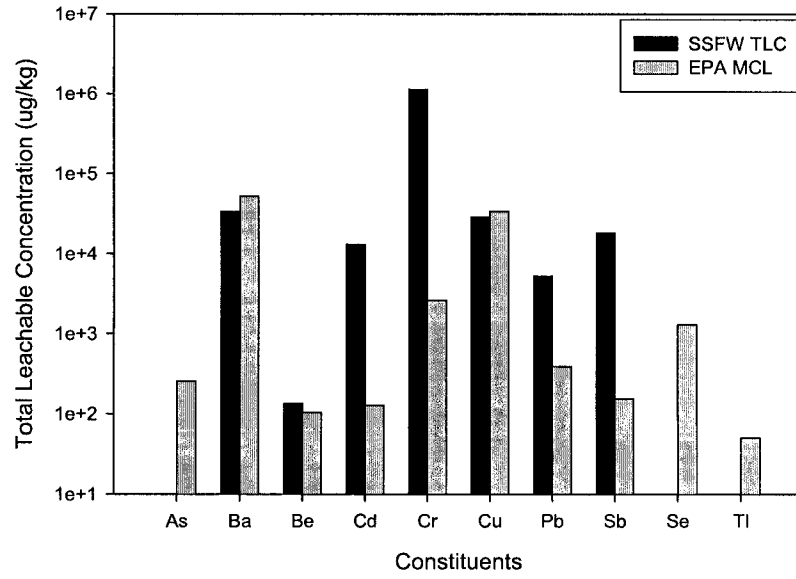


Figure 4.22. SSFW slag total leachable composition results graphed with the corresponding EPA MCLs.

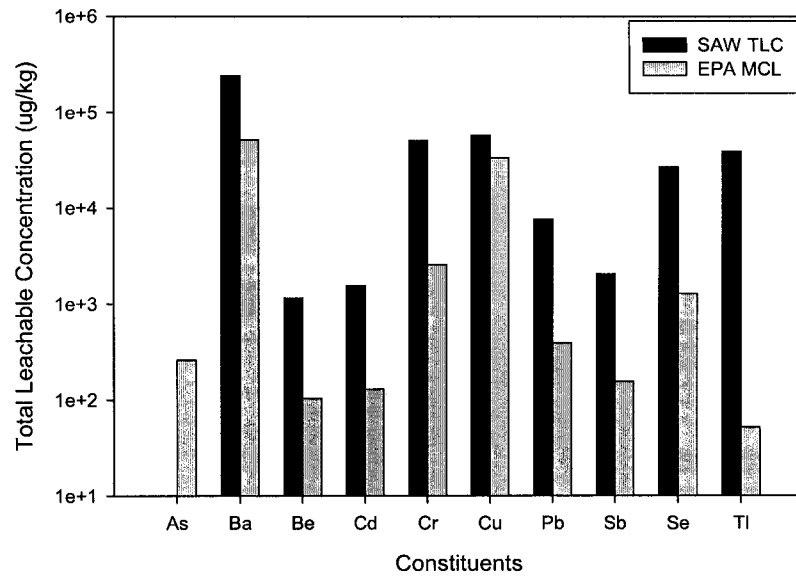


Figure 4.23. SAW slag total leachable composition results graphed with the corresponding EPA MCLs.

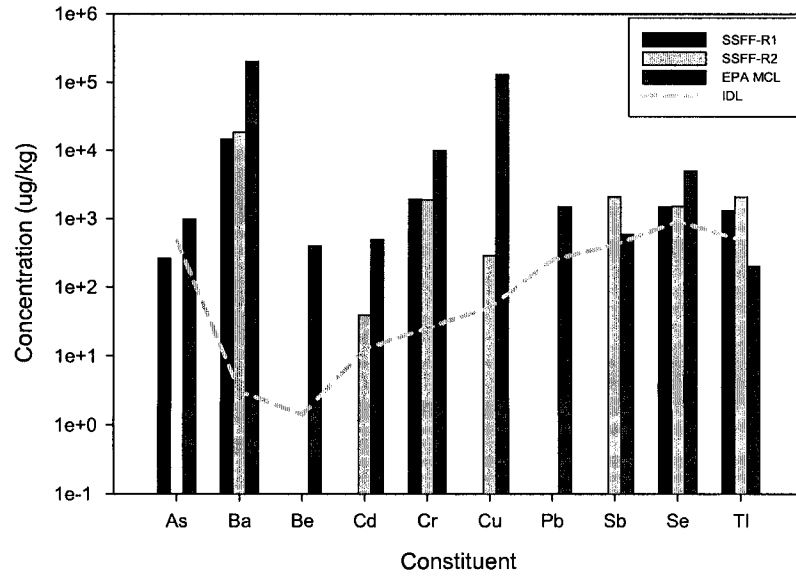


Figure 4.24. SSFF slag availability test results graphed with the corresponding EPA MCLs and IDLs.

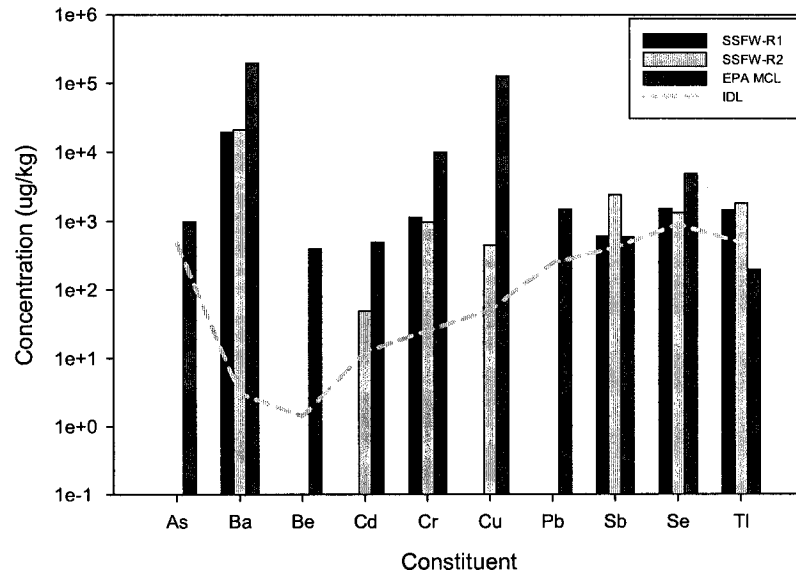


Figure 4.25. SSFW slag availability test results graphed with the corresponding EPA MCLs and IDLs.

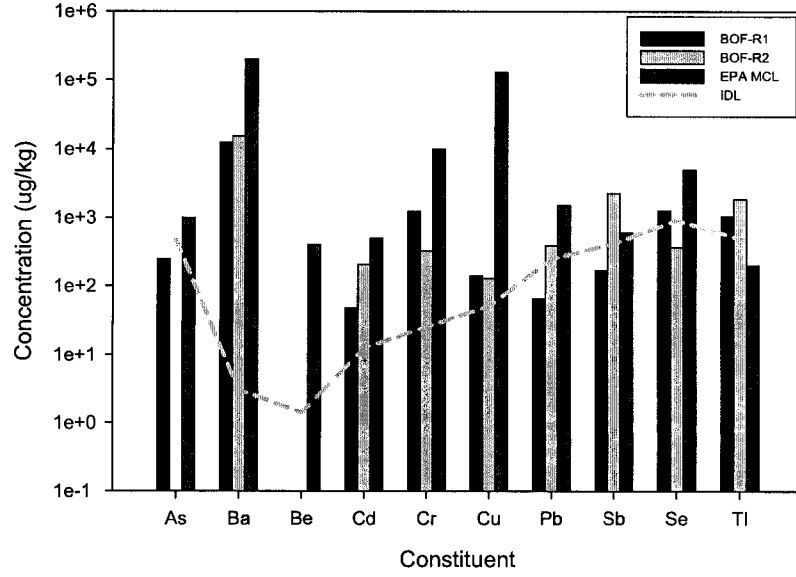


Figure 4.26. BOF slag availability test results graphed with the corresponding EPA MCLs and IDLs.

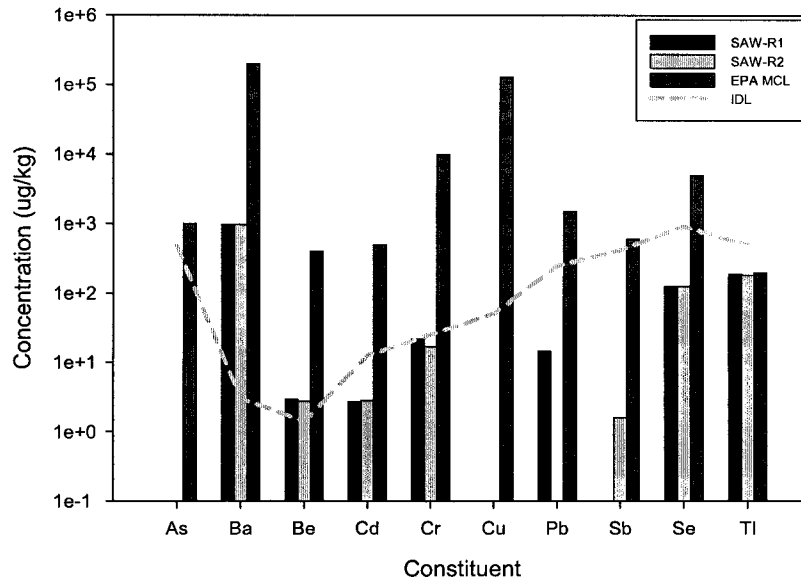


Figure 4.27. SAW slag availability test results graphed with the corresponding EPA MCLs and IDLs.

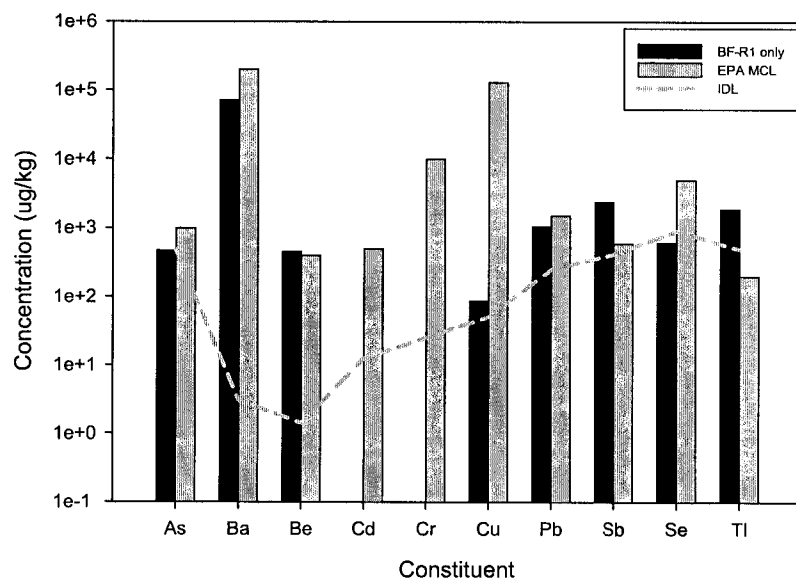


Figure 4.28. BF slag availability test results graphed with the corresponding EPA MCLs and IDLs.

Table 4.8. TCLP and SPLP analytical results from Resource Laboratories.

	SSFF Slag	SSFW Slag	BOF Slag	BF Slag	SAW Slag	Regulatory Level*
	mg/L	mg/L	mg/L	mg/L	mg/L	mg/L
As-TCLP	<0.02	<0.02	<0.02	<0.02	<0.02	5
Ba-TCLP	<0.9	<0.9	<0.9	<0.9	<0.9	100
Cd-TCLP	0.01	<0.01	<0.01	<0.01	0.05	1
Cr-TCLP	0.03	<0.02	<0.02	<0.02	<0.02	5
Pb-TCLP	<0.03	<0.03	<0.03	<0.03	<0.03	5
Hg-TCLP	<0.004	<0.004	<0.004	<0.004	<0.004	0.2
Se-TCLP	<0.08	<0.08	<0.08	<0.08	0.16	1
Ag-TCLP	<0.03	0.03	<0.03	0.06	0.03	5
As-SPLP	<0.02	<0.02	<0.02	<0.02	<0.02	0.01
Ba-SPLP	<0.9	<0.9	<0.9	<0.9	<0.9	2
Cd-SPLP	<0.01	<0.01	<0.01	<0.01	<0.01	0.005
Cr-SPLP	<0.02	0.02	0.02	<0.02	<0.02	0.1
Pb-SPLP	<0.03	<0.03	<0.03	<0.03	<0.03	0.015
Hg-SPLP	<0.004	<0.004	<0.004	<0.004	<0.004	0.002
Se-SPLP	<0.08	<0.08	<0.08	0.09	<0.09	0.1
Ag-SPLP	0.03	<0.03	0.06	0.04	<0.03	na

Notes:

Shaded indicates detection above detection limit

* = TC List levels applied to TCLP and EPA MCL drinking water standards applied to SPLPL

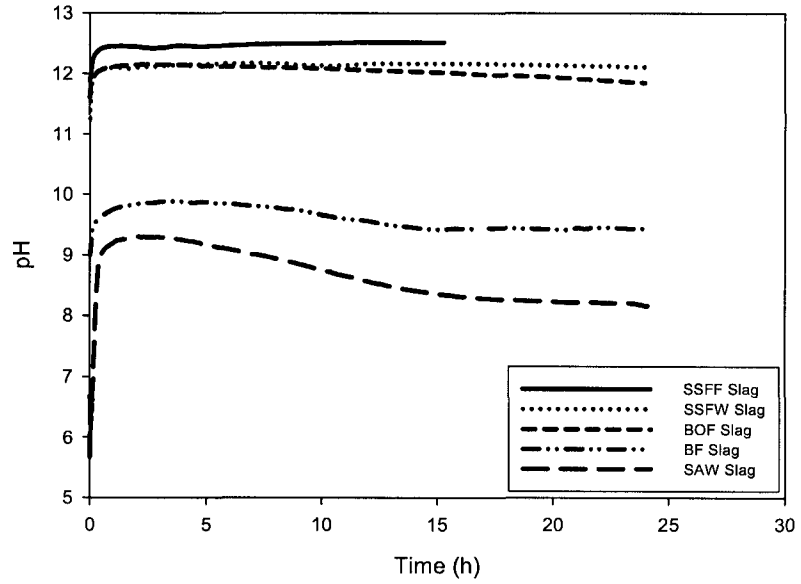


Figure 4.29. Slag natural pH over 24 hours in open containers.

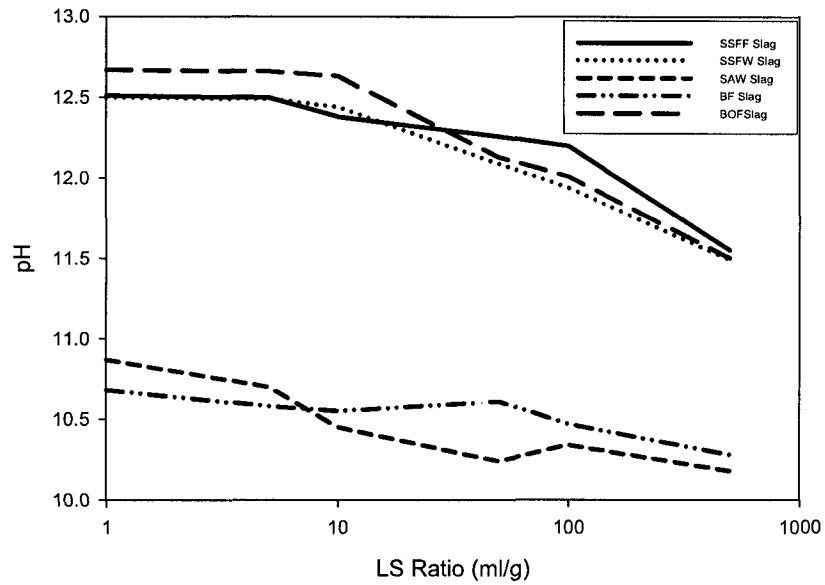
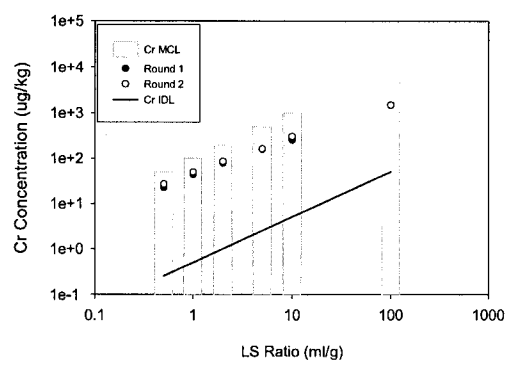
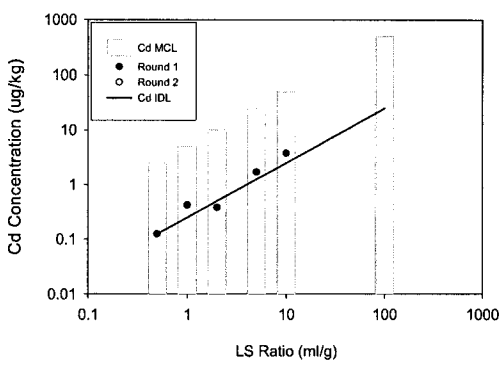
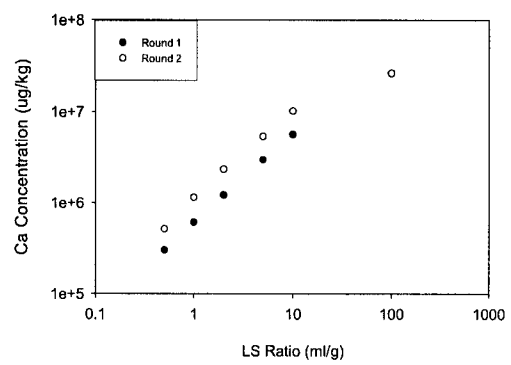
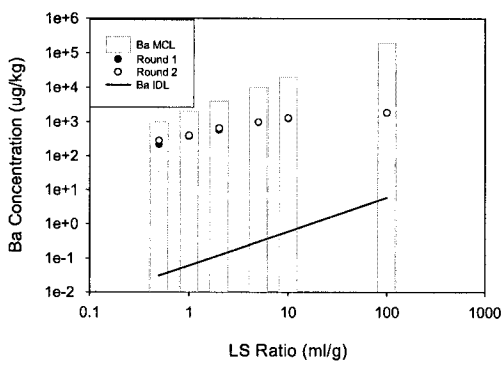
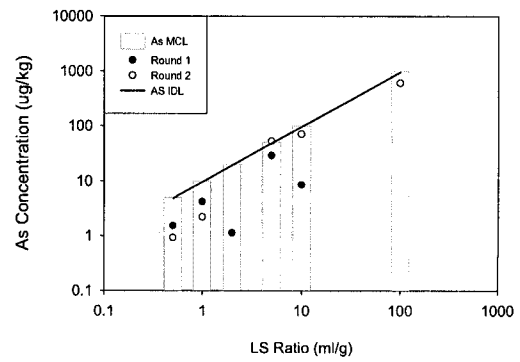
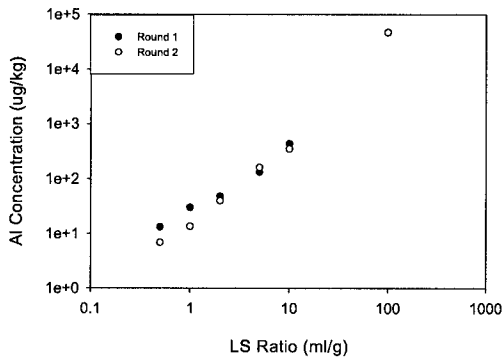
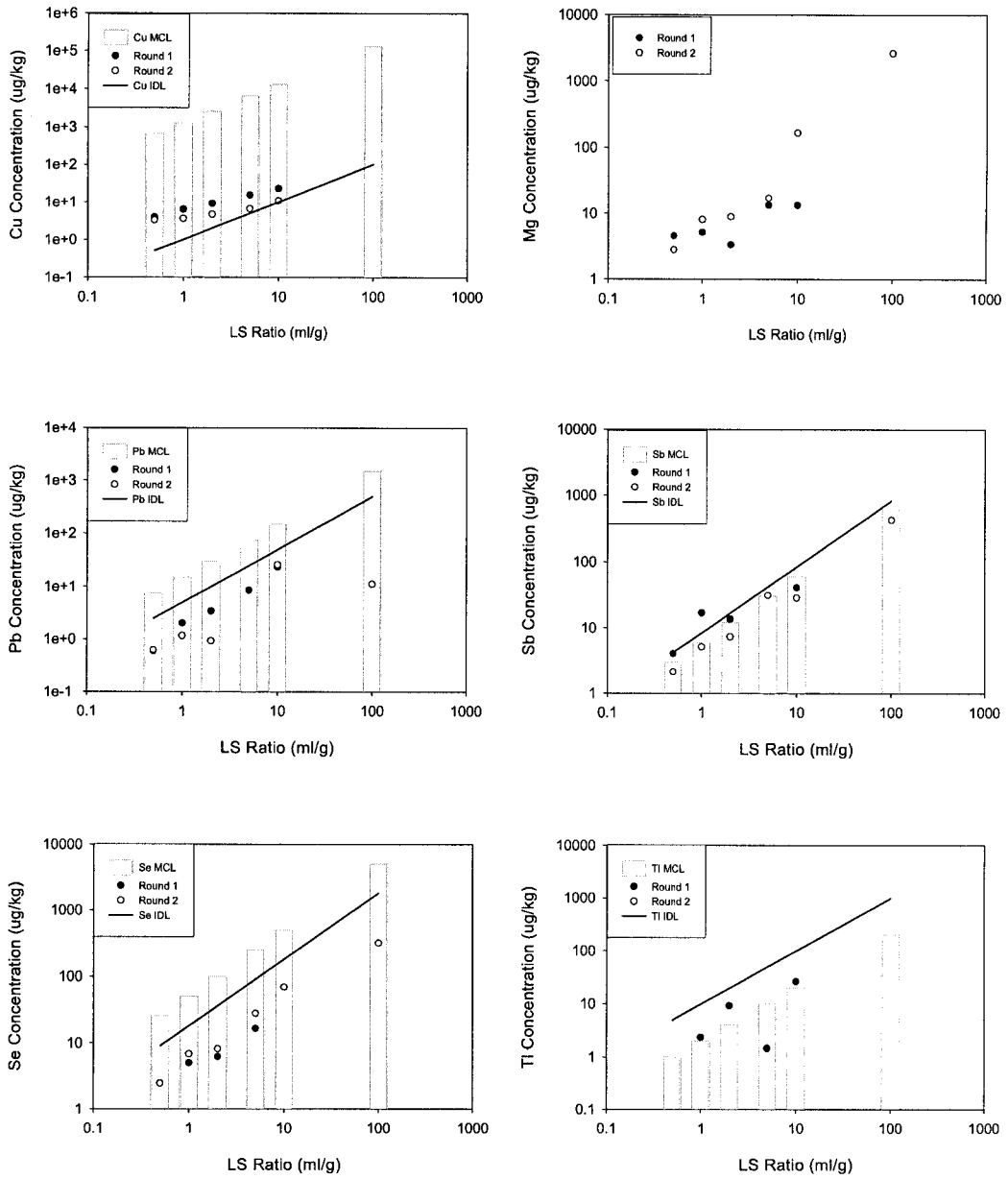


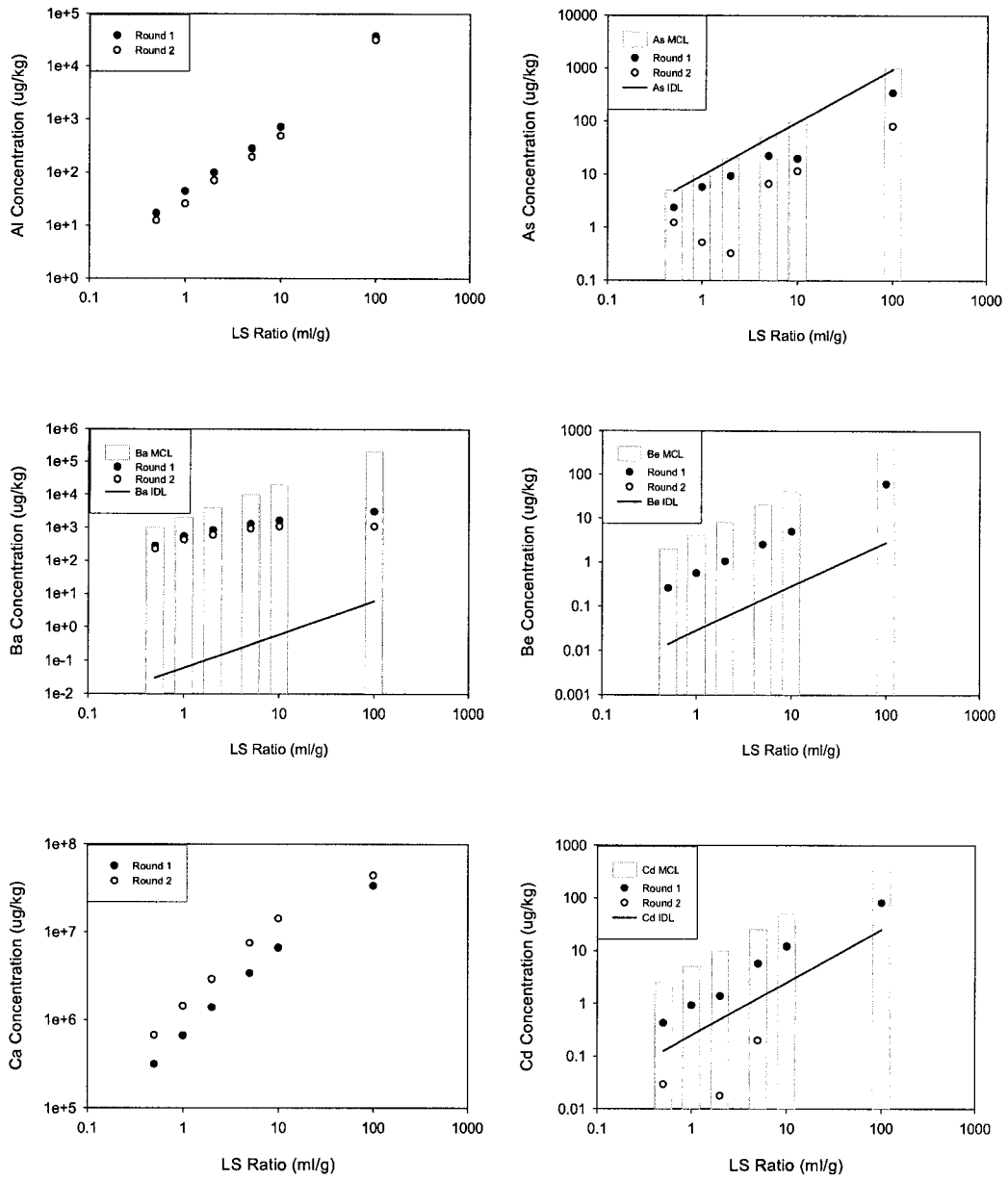
Figure 4.30. Slag natural pH over range of LS ratios in closed containers.



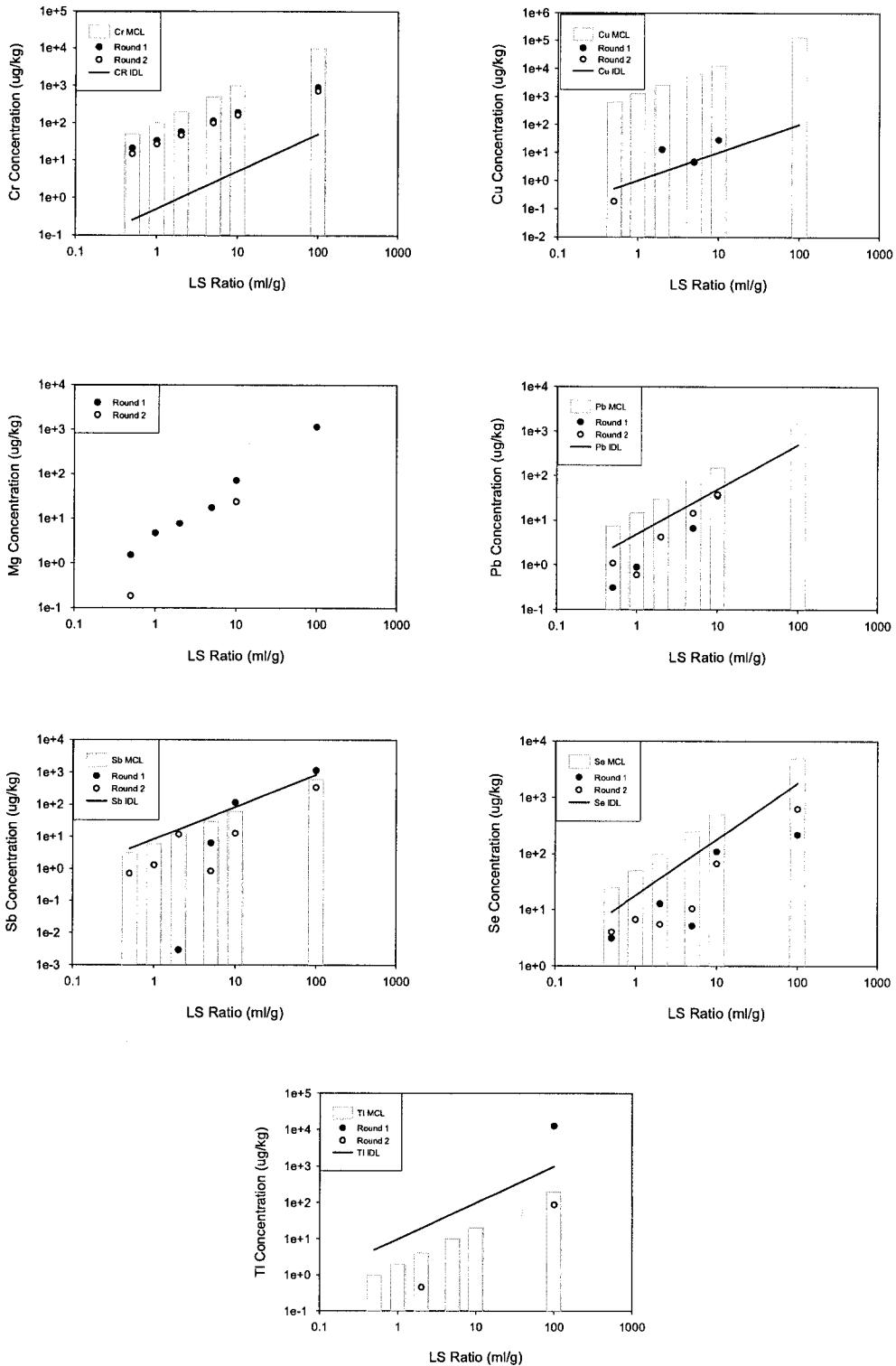
Figures 4.31-4.36. BOF slag *Al*, *As*, *Ba*, *Ca*, *Cd*, and *Cr* LS ratio leaching test results plotted with corresponding EPA MCLs and IDLs.



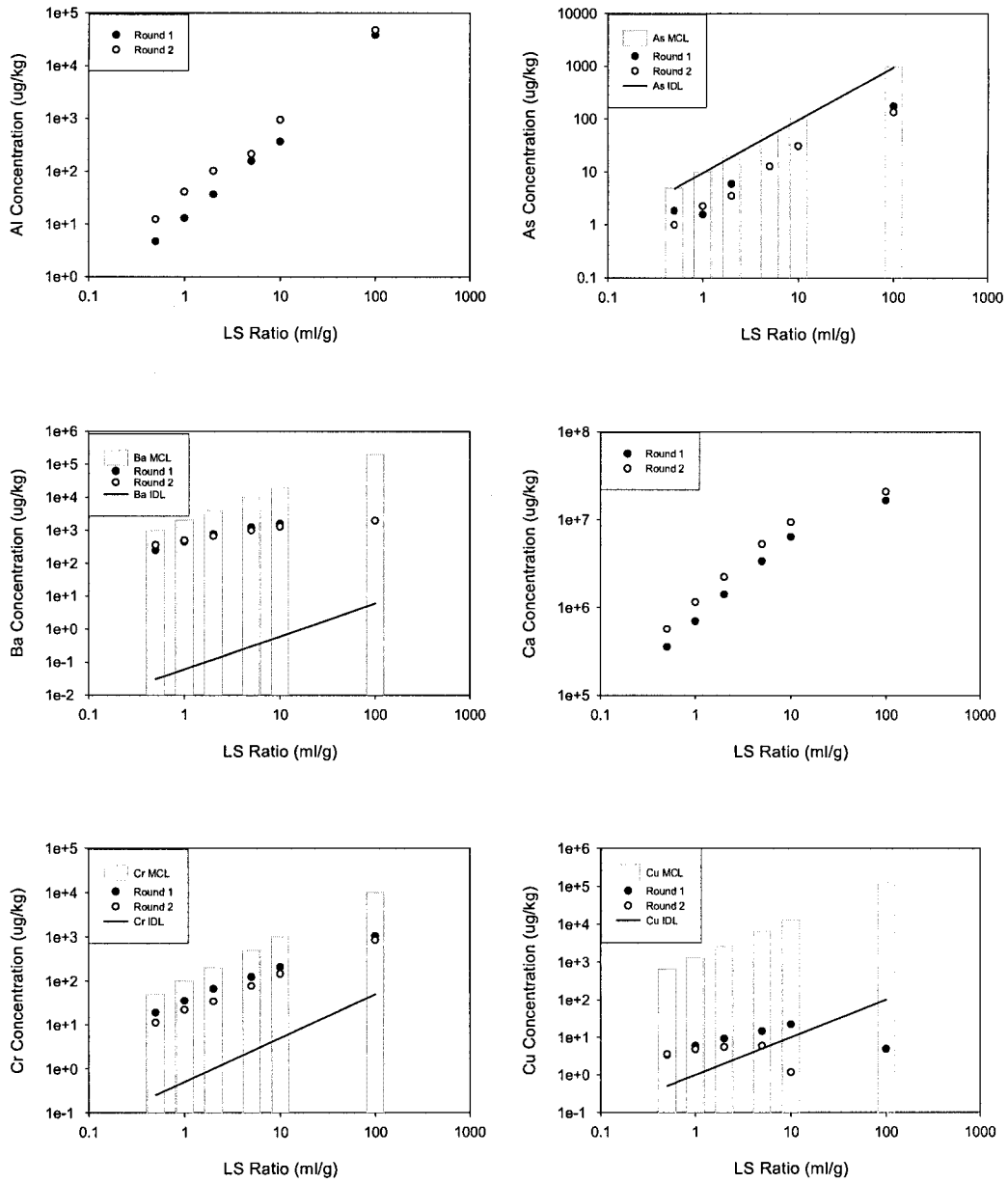
Figures 4.37-4.42. BOF slag *Cu*, *Mg*, *Pb*, *Sb*, *Se*, and *Ti* LS ratio leaching test results plotted with corresponding EPA MCLs and IDLs.



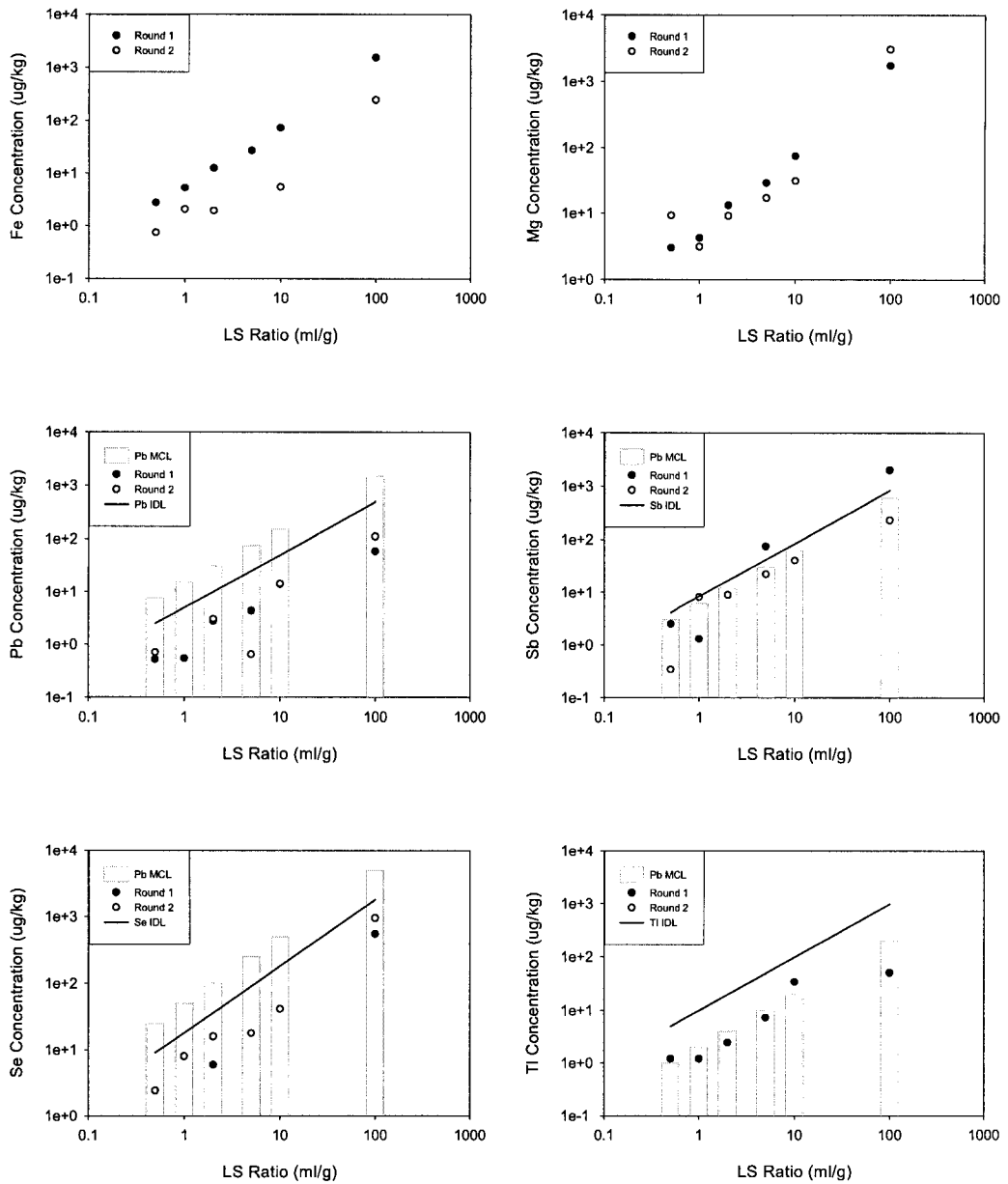
Figures 4.43-4.48. SSFF slag *Al*, *As*, *Ba*, *Be*, *Ca*, and *Cd* LS ratio leaching test results plotted with corresponding EPA MCLs and IDLs.



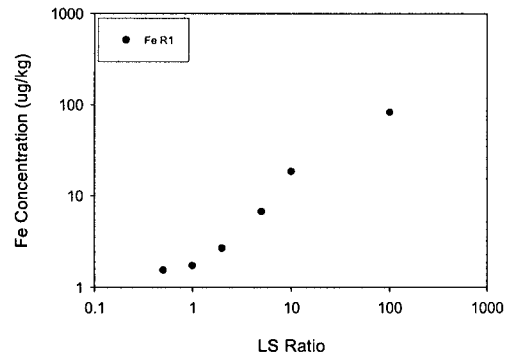
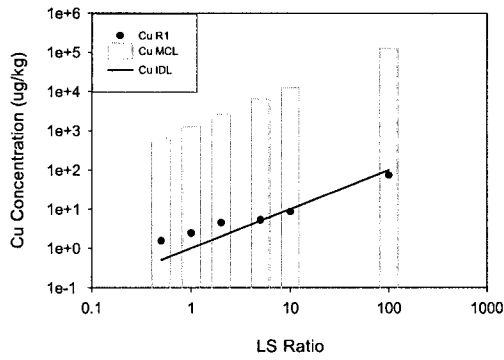
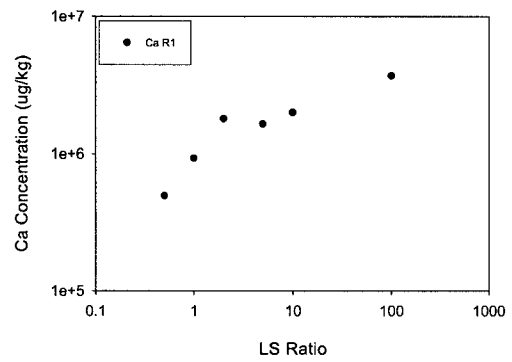
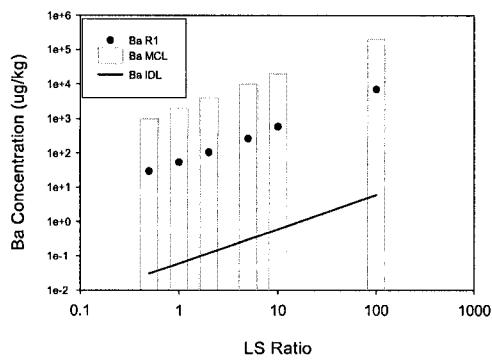
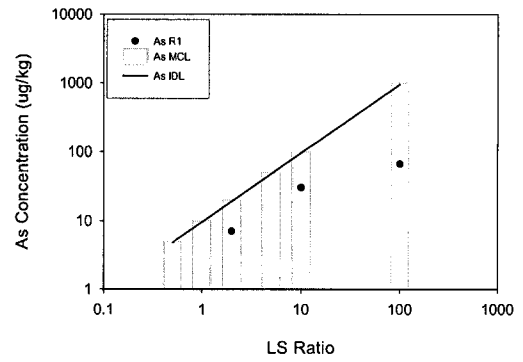
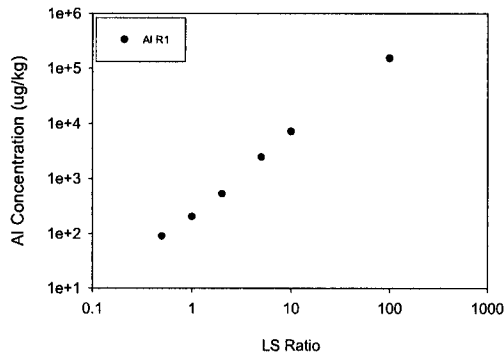
Figures 4.49-4.55. SSFF slag *Cr*, *Cu*, *Mg*, *Pb*, *Sb*, *Se*, and *Tl* LS ratio leaching test results plotted with corresponding EPA MCLs and IDLs.



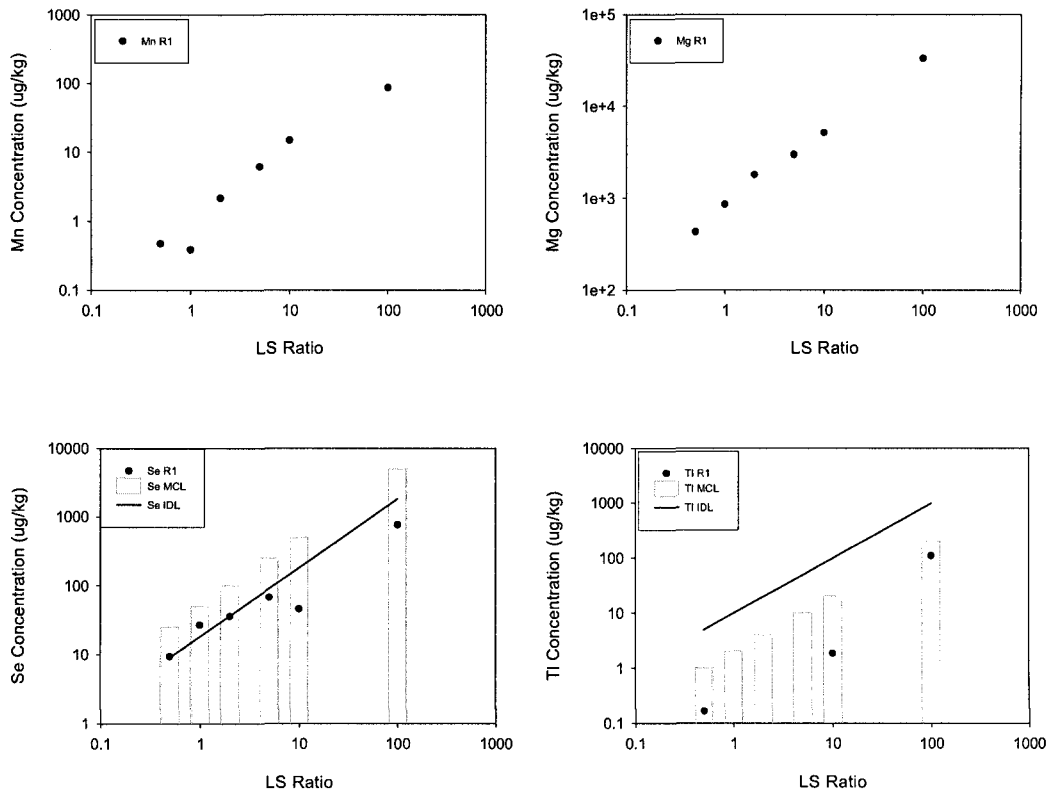
Figures 4.56-4.61. SSFW slag *Al*, *As*, *Ba*, *Ca*, *Cr*, and *Cu* LS ratio leaching test results plotted with corresponding EPA MCLs and IDLs.



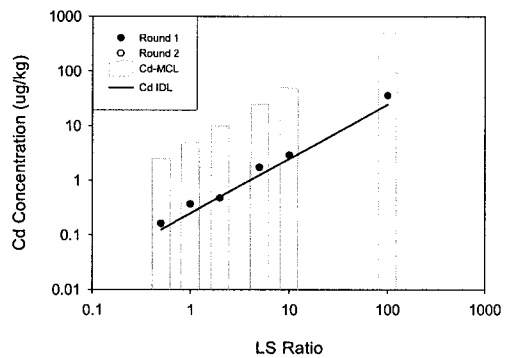
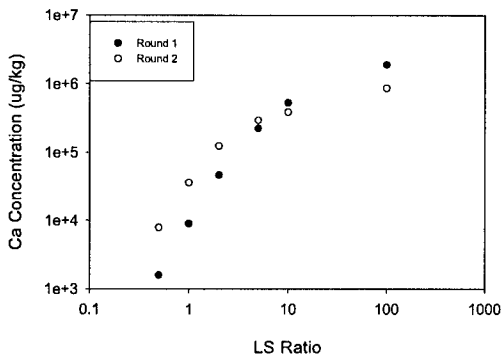
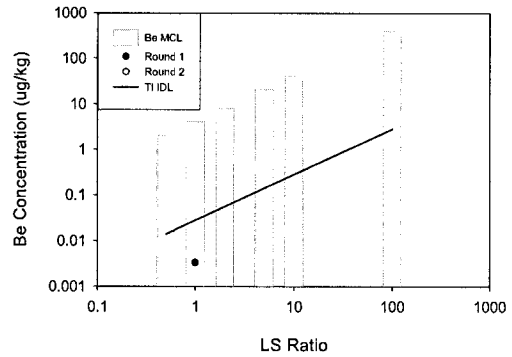
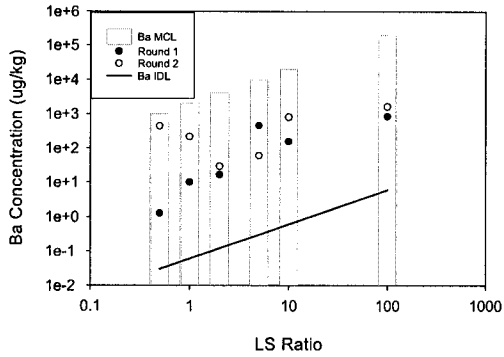
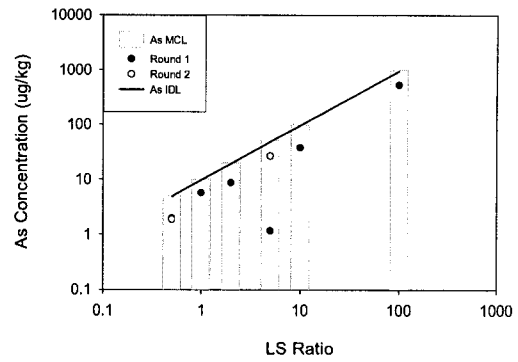
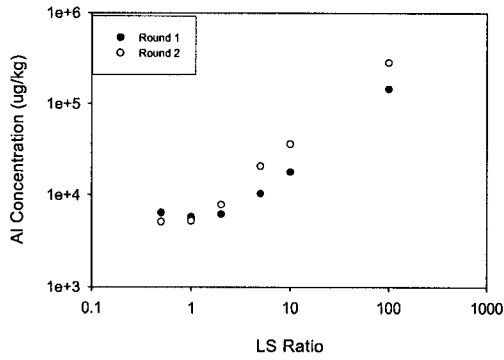
Figures 4.62-4.67. SSFW slag *Fe*, *Mg*, *Pb*, *Sb*, *Se*, and *Tl* LS ratio leaching test results plotted with corresponding EPA MCLs and IDLs.



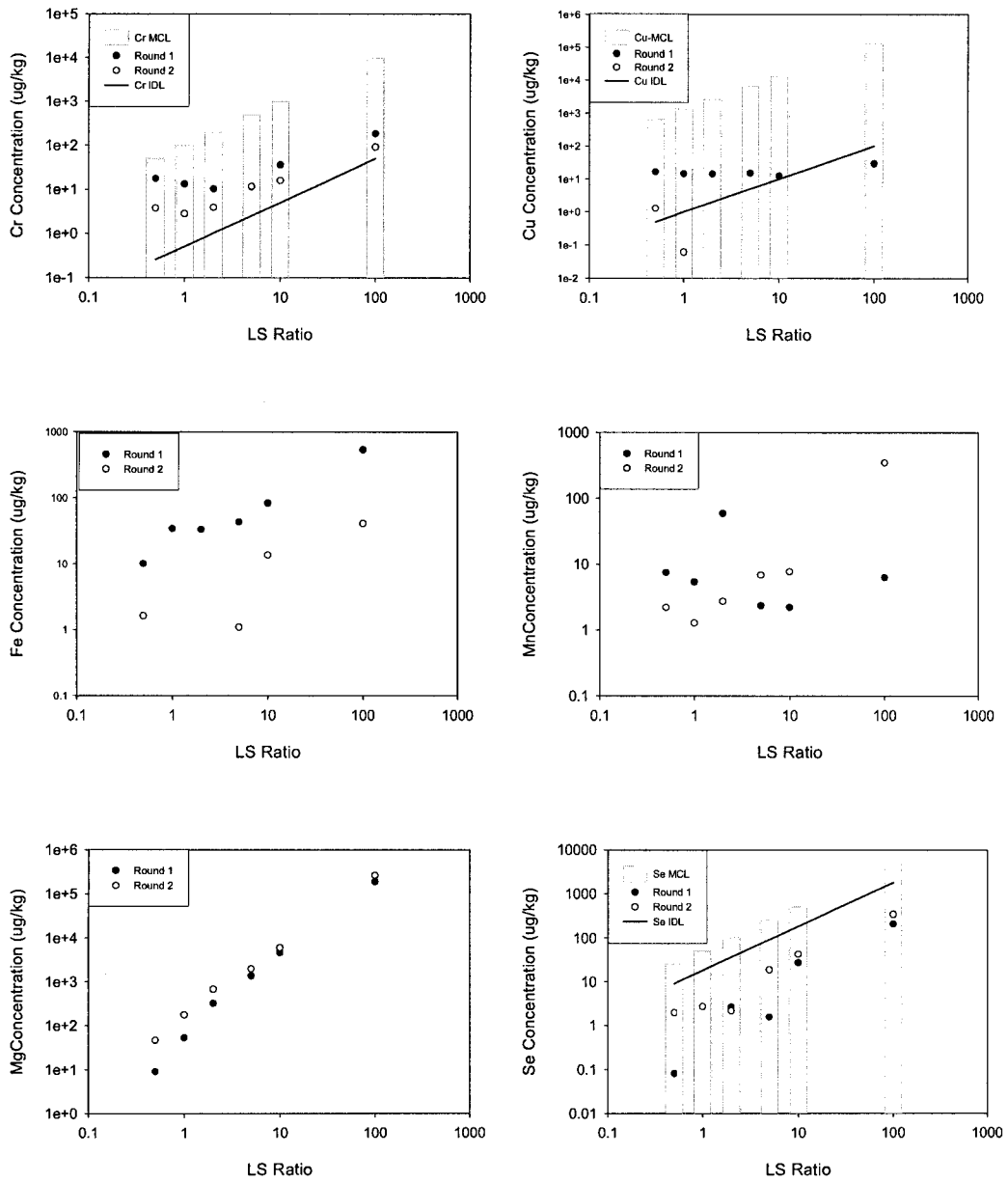
Figures 4.68-4.73. BF slag Al, As, Ba, Ca, Cu, and Fe LS ratio leaching test results plotted with corresponding EPA MCLs and IDLs.



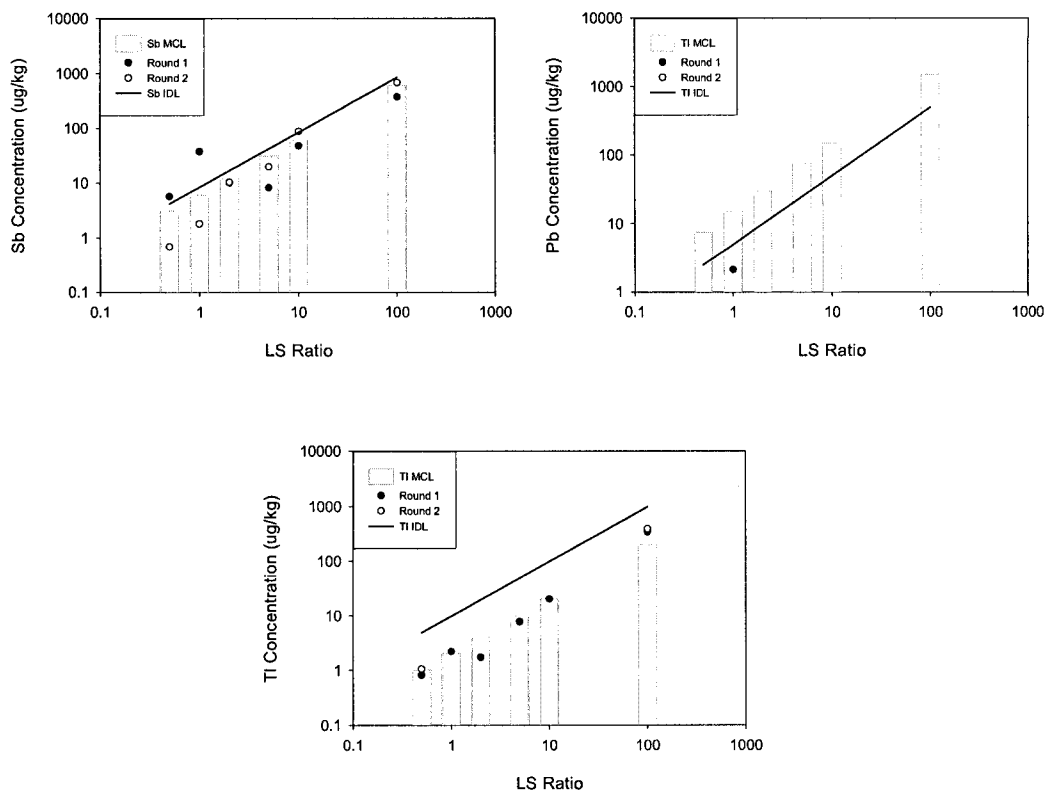
Figures 4.74-4.77. BF slag *Mn*, *Mg*, *Se*, and *Ti*/LS ratio leaching test results plotted with corresponding EPA MCLs and IDLs.



Figures 4.78-4.83. SAW slag Al, As, Ba, Be, Ca, and Cd LS ratio leaching test results plotted with corresponding EPA MCLs and IDLs.



Figures 4.84-4.89. SAW slag *Cr*, *Cu*, *Fe*, *Mn*, *Mg*, and *Se* LS ratio leaching test results plotted with corresponding EPA MCLs and IDLs.

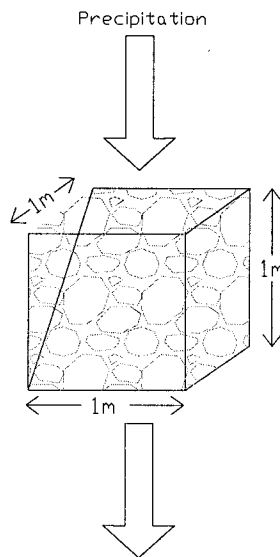


Figures 4.90-4.92. SAW slag *Sb*, *Pb*, and *Tl* LS ratio leaching test results plotted with corresponding EPA MCLs and IDLs.

Table 4.9. Final pHs of LS ratio leachates prior to sampling.

LS ratio (ml/g)	BOF Slag pHs		SSFF Slag pHs		SSFW Slag pHs		SAW Slag pHs		BF Slag pHs
	R1 (9/7/04)	R2 (8/31/05)	R1 (11/12/04)	R2 (8/9/05)	R1 (12/5/04)	R2 (9/21/05)	R1 (10/22/04)	R2 (9/9/05)	R1 (1/25/06)
0.5	12.46	11.42	12.44	12.28	12.82	12.51	11.6	11	10.63
1	12.43	11.5	12.7	12.2	12.85	12.5	11.35	10.81	10.85
2	12.49	11.46	12.77	12.24	12.84	12.47	11.06	10.7	10.87
5	12.44	11.15	12.77	12.29	12.83	12.44	10.83	10.59	10.59
10	12.47	11.42	12.76	12.34	12.82	12.46	10.52	10.39	11.15
100	12.48	11.48	12.46	12.1	12.3	11.97	9.85	9.93	10.58

Steel Slag Base Layer



Volume= 1m³
 Slag Density= 2600 kg/m³
 Slag Weight= 2600 kg

Figure 4.93. Steel slag LS ratio example with 1 cubic meter section of slag.

Table 4.10. LS ratio conversion to time for three hypothetical scenarios.

Location	Years to Reach LS Ratio		
	Columbus, OH	Indianapolis, IN	Columbus, OH-capped
LS Ratio (ml/g)	Annual Precipitation 877,000 ml	Annual Precipitation 1,020,000 ml	Annual Precipitation 87,700 ml
0.5	1.5	1.3	14.8
1	3.0	2.5	29.6
2	5.9	5.1	59.3
5	14.8	12.7	148.2
10	29.6	25.5	296.5
50	148.2	127.5	1482.3
100	296.5	254.9	2964.7
1000	2964.7	2549.0	29646.5

Table 4.11. Two different hypothetical scenarios showing an *As* MCL exceedance.

First Scenario							
Parameter	1st Storm	2nd Storm	3rd Storm	4th Storm	5th Storm	6th Storm	Totals
LS Ratio (l/kg)	0.33	0.33	0.33	0.33	0.33	0.33	2
Effluent Concentration (mg/l)	50	7	5	2	1	0.1	---
Effluent Concentration (mg/kg)	16.5	2.31	1.65	0.66	0.33	0.033	21.5
MCL (mg/l)	10	10	10	10	10	10	---
MCL (mg/kg)	3.33	3.33	3.33	3.33	3.33	3.33	20

2nd Scenario							
Parameter	1st Storm	2nd Storm	3rd Storm	4th Storm	5th Storm	6th Storm	Totals
LS Ratio (l/kg)	0.33	0.33	0.33	0.33	0.33	0.33	2
Effluent Concentration (mg/l)	14	12	11	10	9	9	---
Effluent Concentration (mg/kg)	4.62	3.96	3.63	3.3	2.97	2.97	21.5
MCL (mg/l)	10	10	10	10	10	10	---
MCL (mg/kg)	3.33	3.33	3.33	3.33	3.33	3.33	20

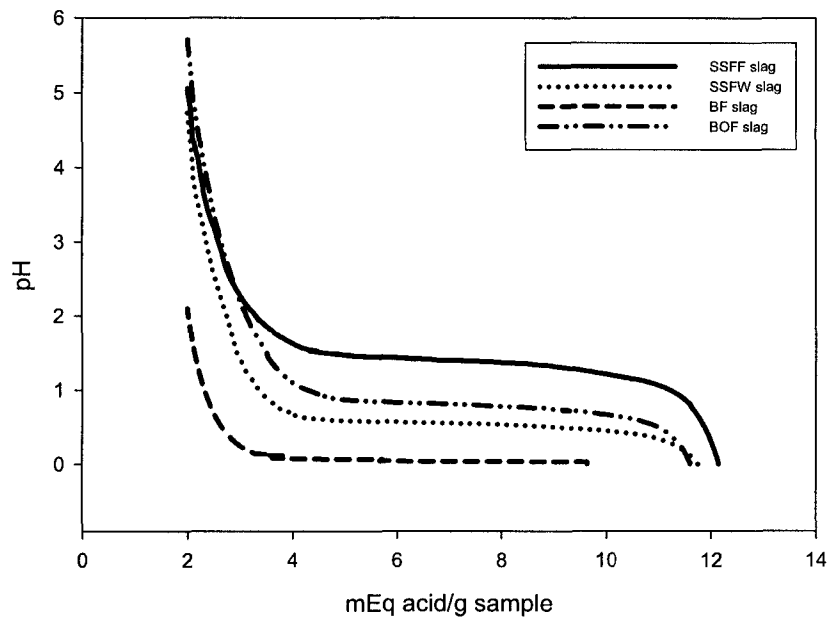


Figure 4.94. Initial ANC curves using continuous acid addition. These curves do not show the actual ANC since pH equalization is not reached.

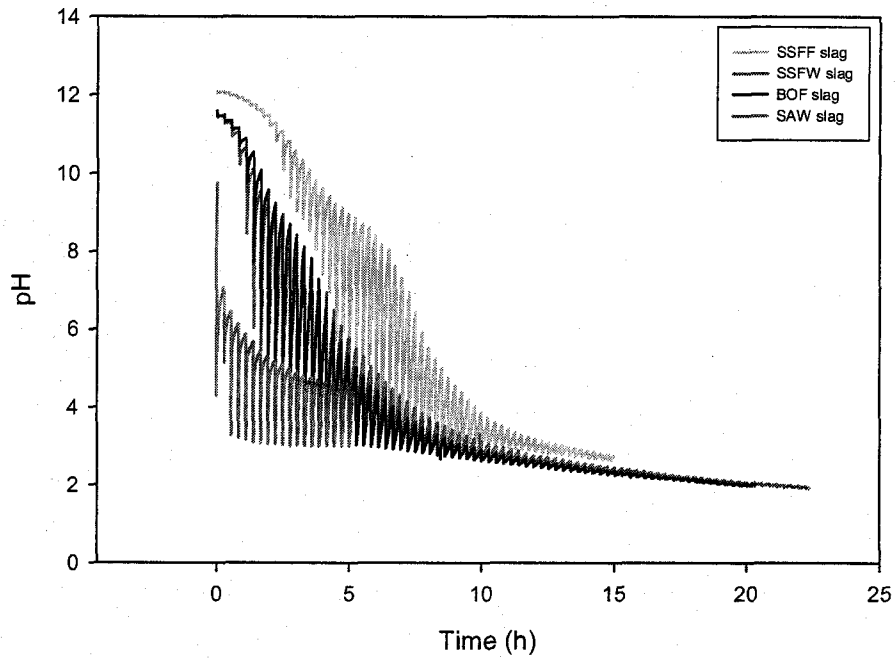


Figure 4.95. ANC curves using 15 minute equalization time between acid additions. These curves do not show the actual ANC since pH equalization is not reached.

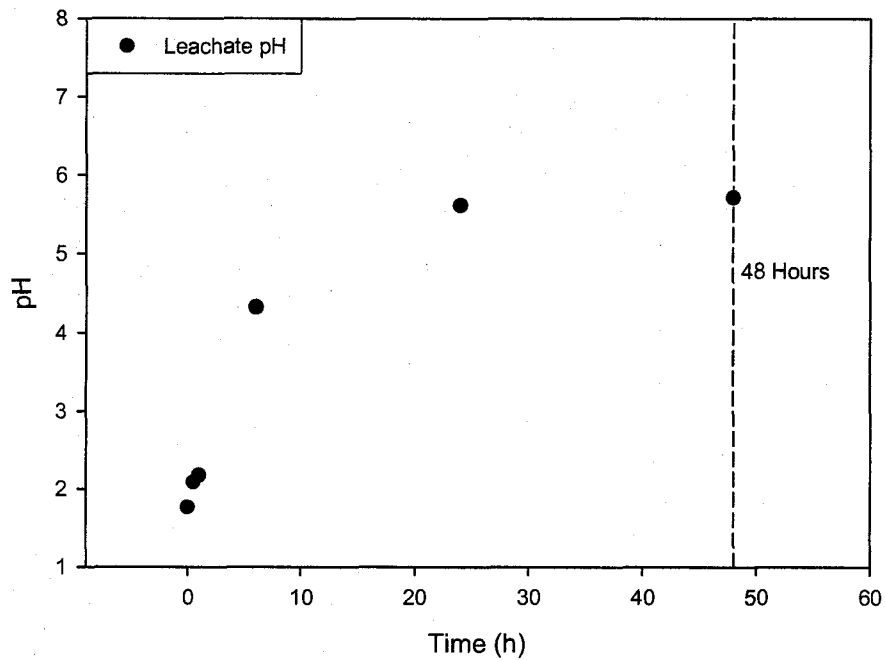


Figure 4.96. Test used to determine the change in pH over 48 hours during the LS ratio leaching test.

Table 4.12. R2 pH dependent leaching acid addition schedule.

Target pH	SSFF Slag		SSFW Slag		BOF Slag		SAW Slag		BF Slag	
	Equivalents of Acid/Base Added (meq/g)	Final pH	Equivalents of Acid/Base Added (meq/g)	Final pH	Equivalents of Acid/Base Added (meq/g)	Final pH	Equivalents of Acid/Base Added (meq/g)	Final pH	Equivalents of Acid/Base Added (meq/g)	Final pH
3	13.8	3.18	13.9	NA	13.03	2.20	16.66	<1	16.00	3.27
4	12.6	4.85	11.9	2.49	12.47	4.75	11.30	4.05	12.37	3.75
5	7.3	5.73	8.3	5.40	7.58	5.60	5.95	4.89	8.75	5.68
6	6.9	5.94	4.6	6.12	4.28	6.13	0.83	5.91	5.12	6.60
7	6.1	6.94	2.9	6.68	3.73	6.51	0.64	6.10	4.00	6.78
8	5.4	8.14	2.6	9.45	3.17	6.56	0.45	6.00	0.39	7.38
9	4.6	8.97	2.3	9.02	2.62	7.58	0.26	6.53	0.14	7.66
10	3.8	9.73	1.9	9.52	2.06	8.47	---1	10.48	0.07	9.46
11	3.1	10.65	1.6	9.88	1.51	9.87	-0.11	11.66	0.00	10.80
12	2.3	11.2	1.3	10.85	0.95	11.9	no sample		-0.05	11.66

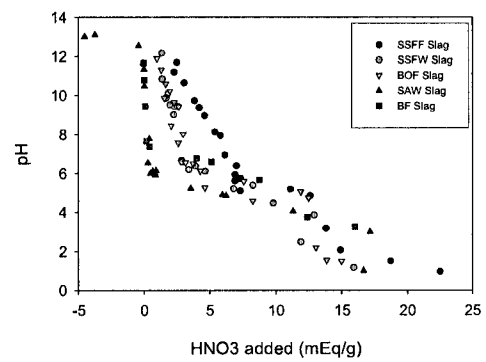
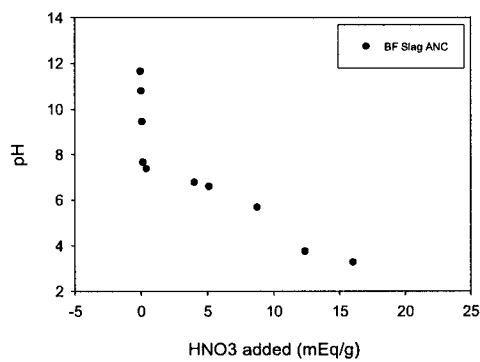
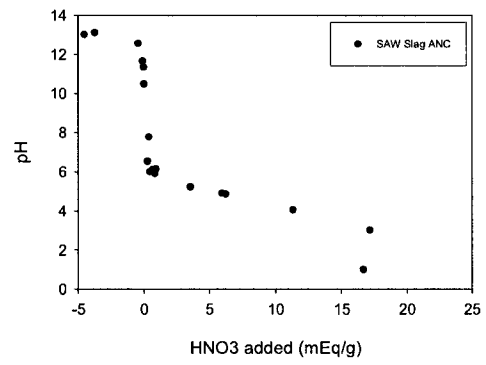
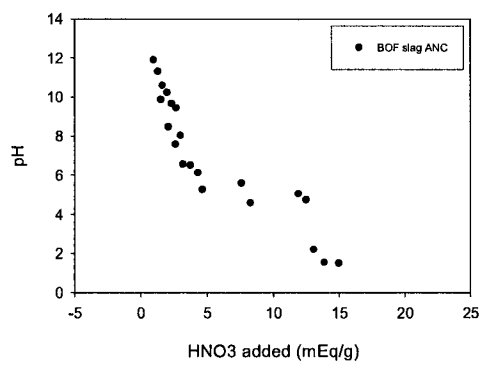
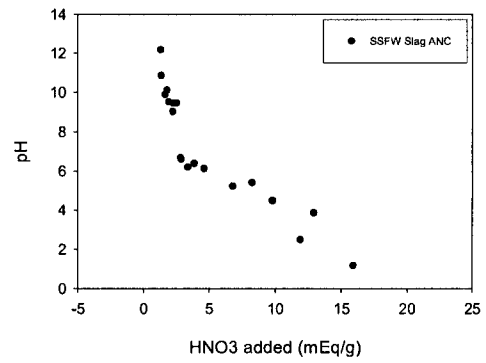
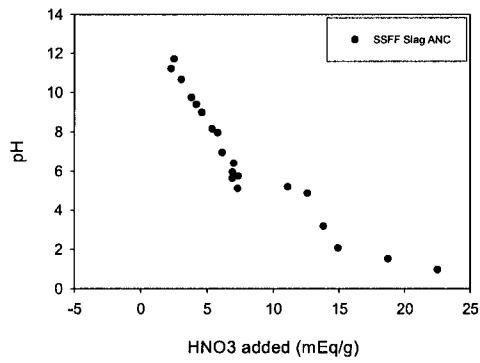
Notes

:

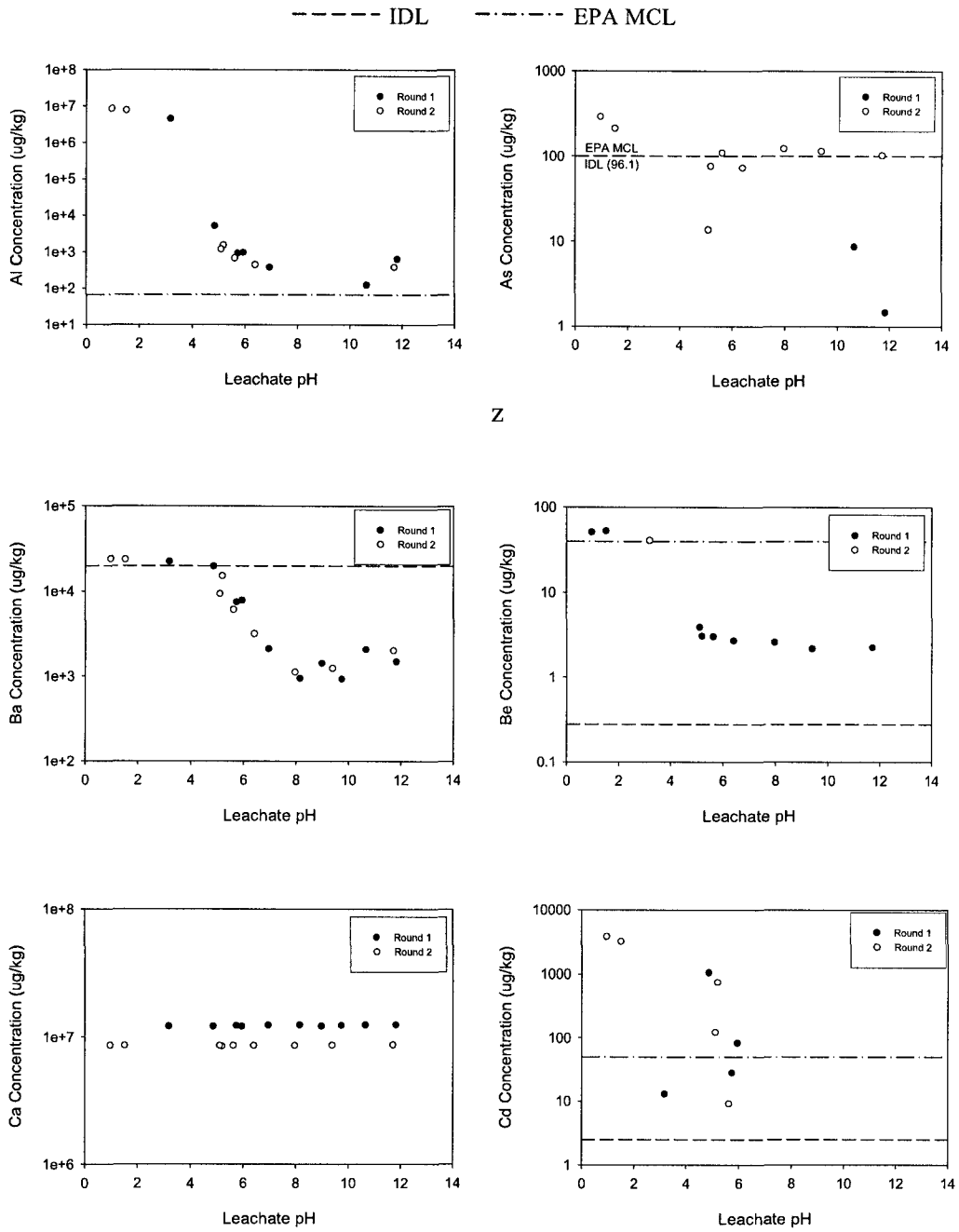
Negative mEq/g value indicates base added.

--- = no acid/base added

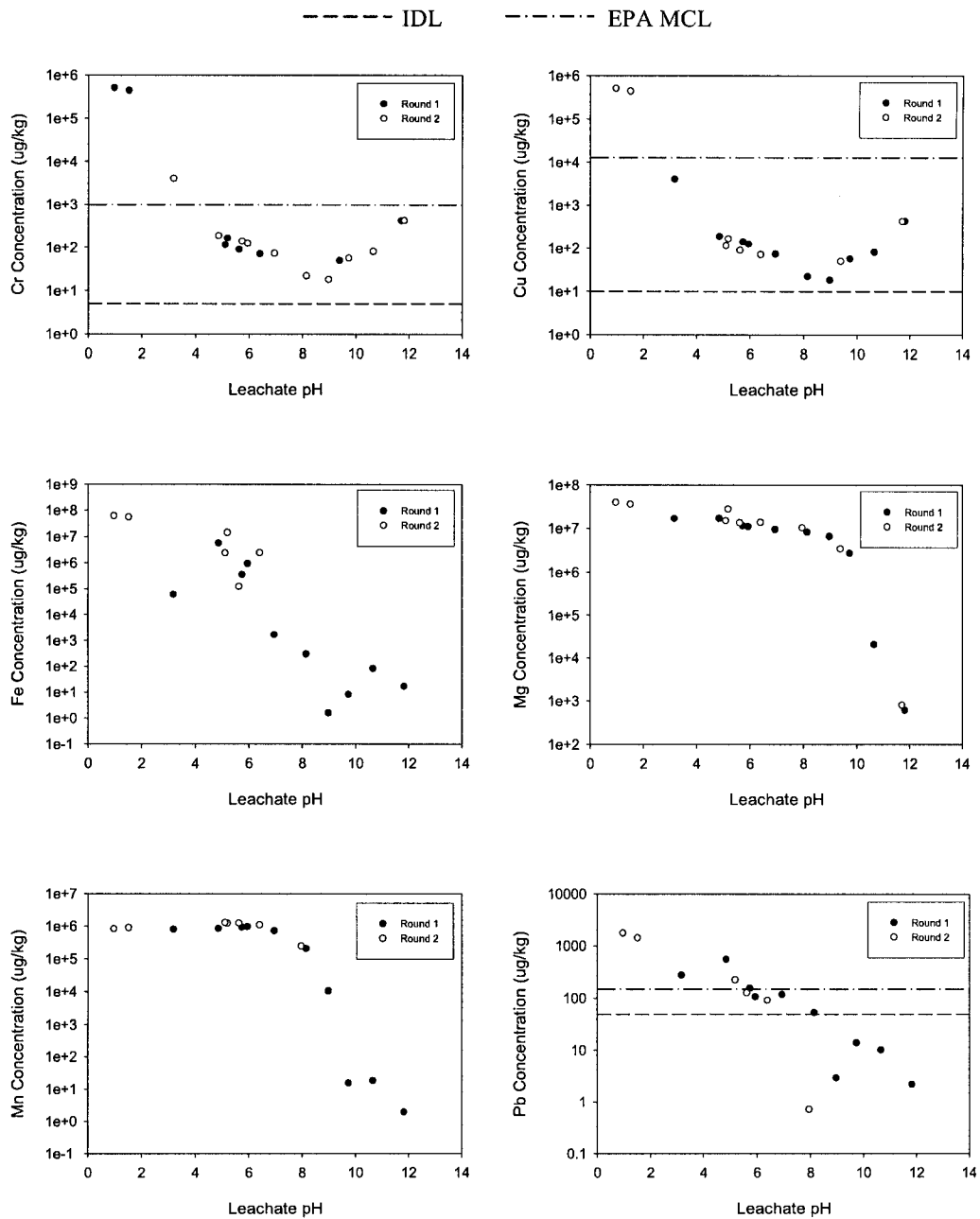
NA = pH measurement not possible due to colloidal sample



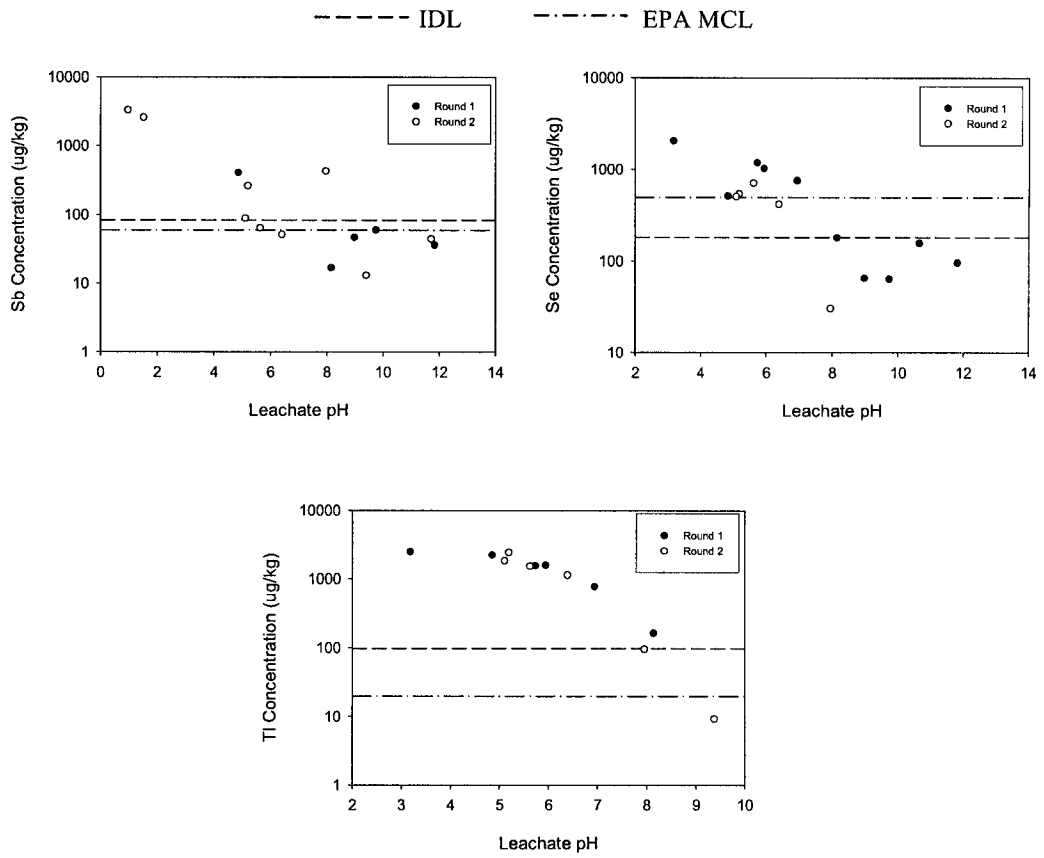
Figures 4.97-4.102. Individual pH dependent leaching final pH measurements (ANC) and combined values for comparison.



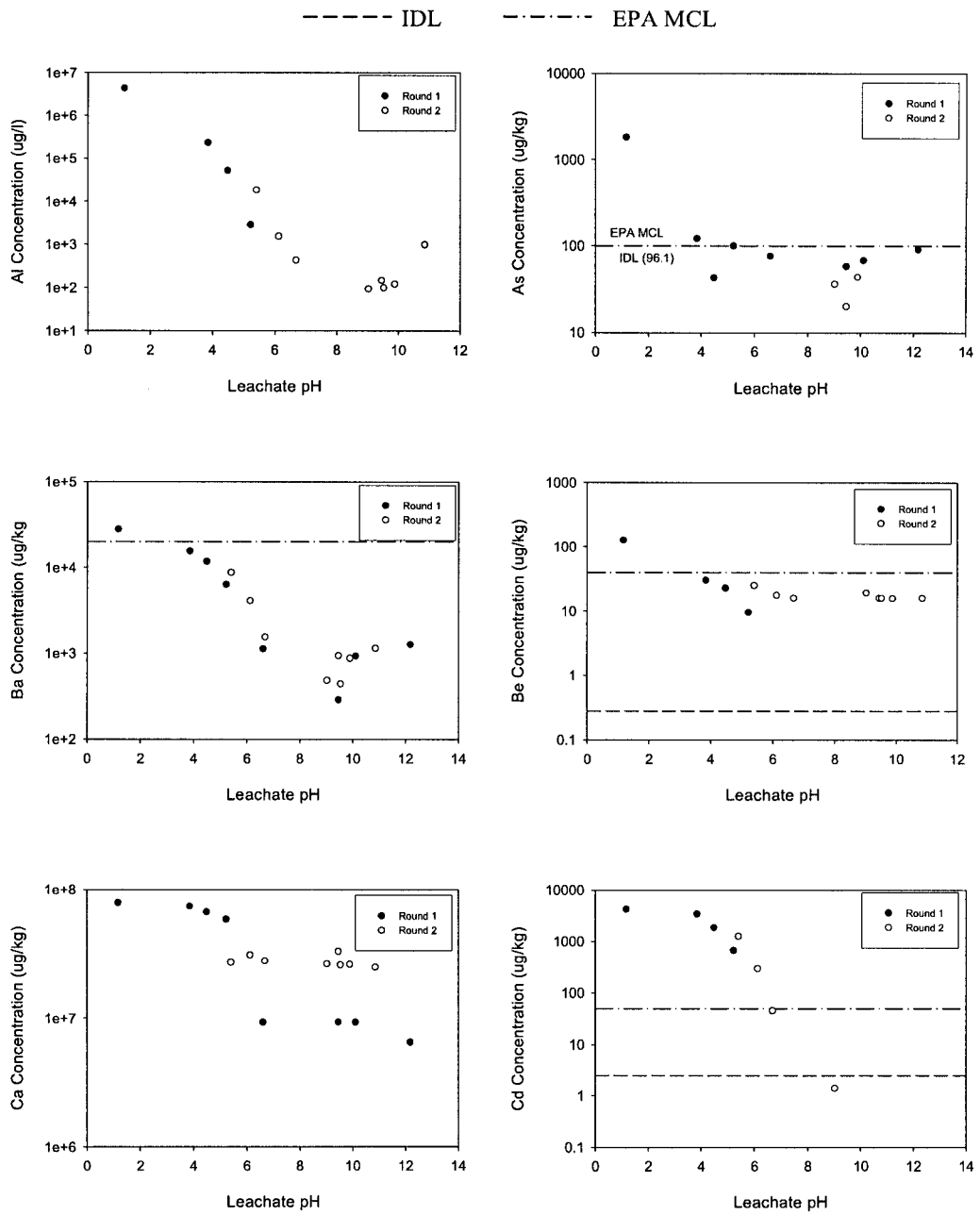
Figures 4.103-4.108. SSFF Al, As, Ba, Be, Ca, and Cd pH dependent leaching curves.



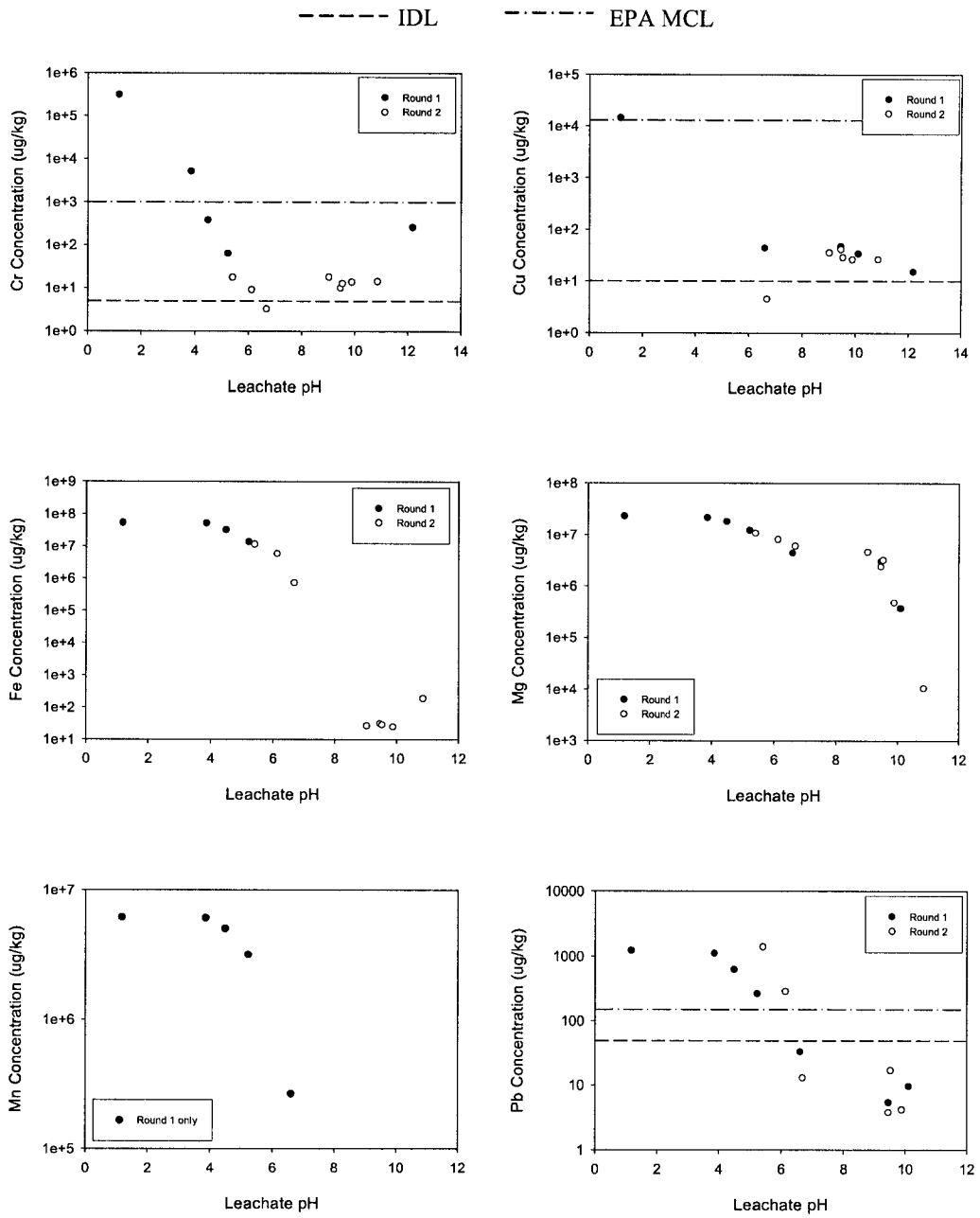
Figures 4.109-4.114. SSFF *Cr*, *Cu*, *Fe*, *Mg*, *Mn*, and *Pb* pH dependent leaching curves.



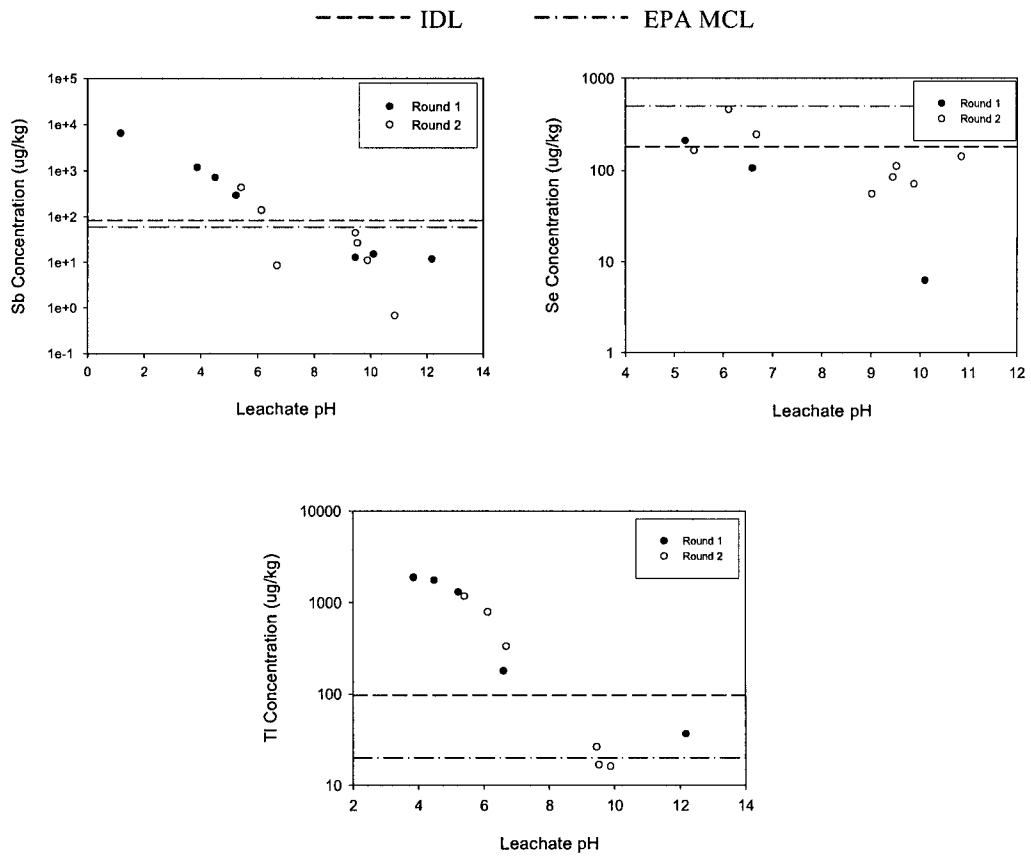
Figures 4.115-4.117. SSFF Sb, Se, and Tl pH dependent leaching curves.



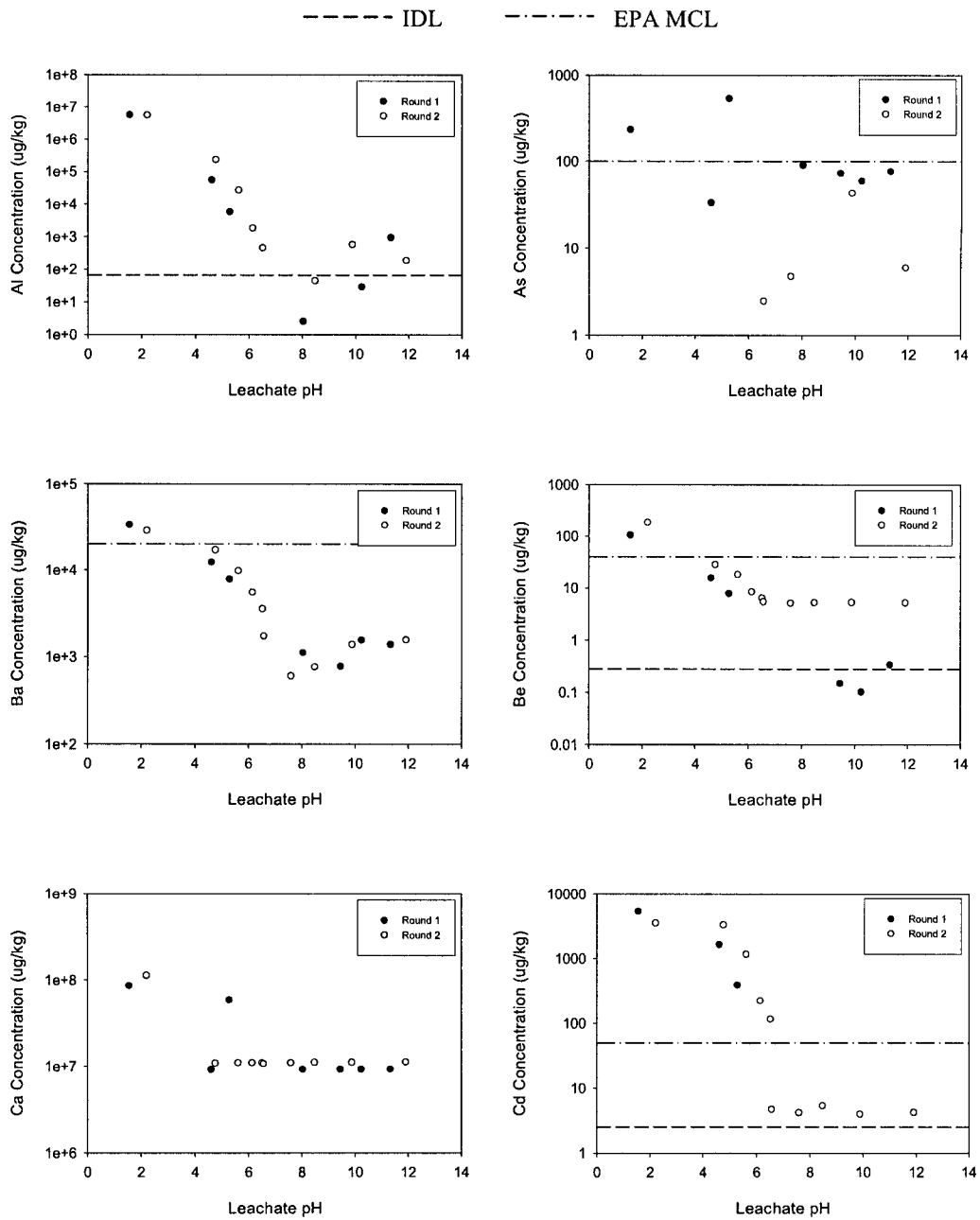
Figures 4.118-4.123. SSFW Al, As, Ba, Be, Ca, and Cd pH dependent leaching curves.



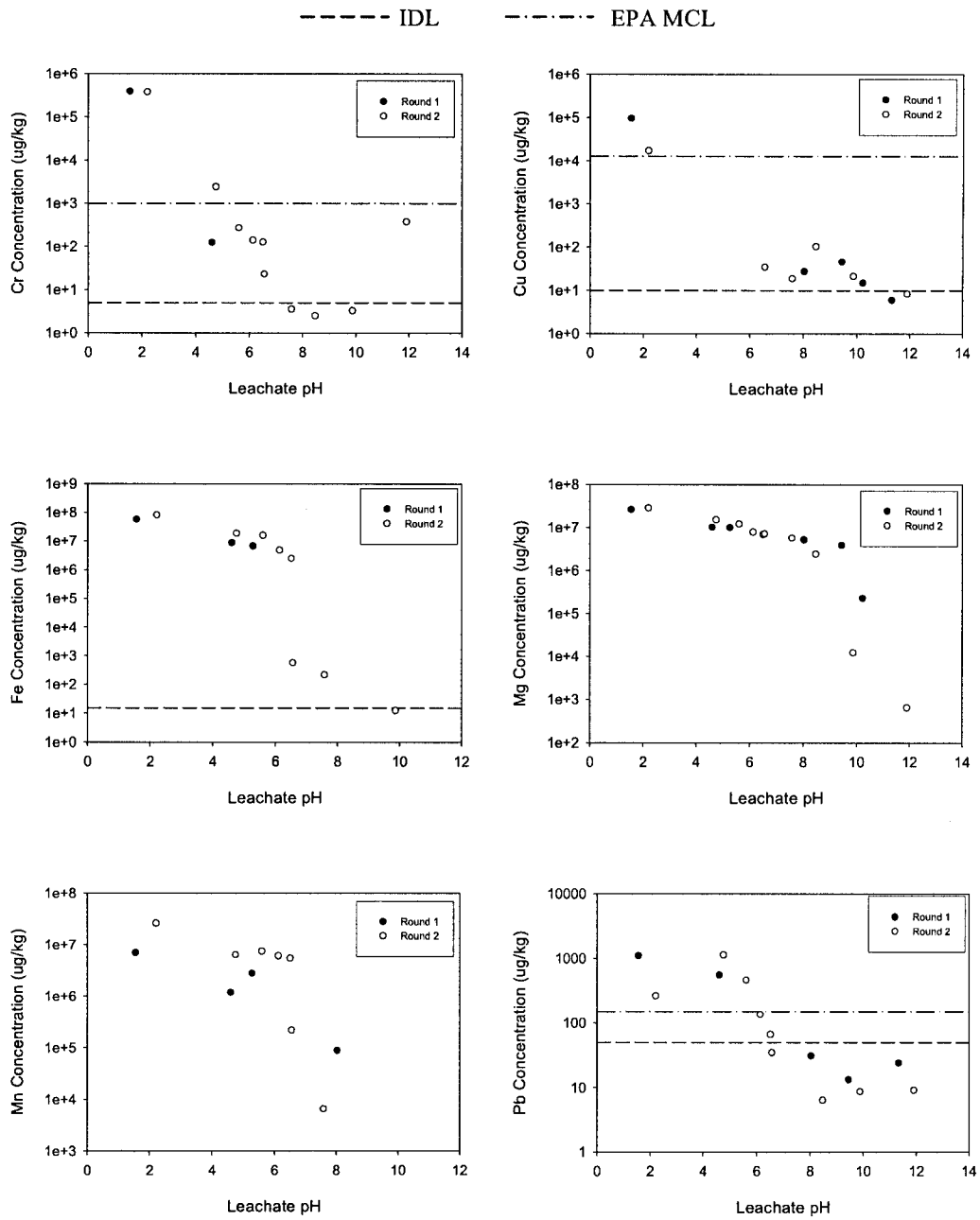
Figures 4.124-4.129. SSFW Cr, Cu, Fe, Mg, Mn, and Pb pH dependent leaching curves.



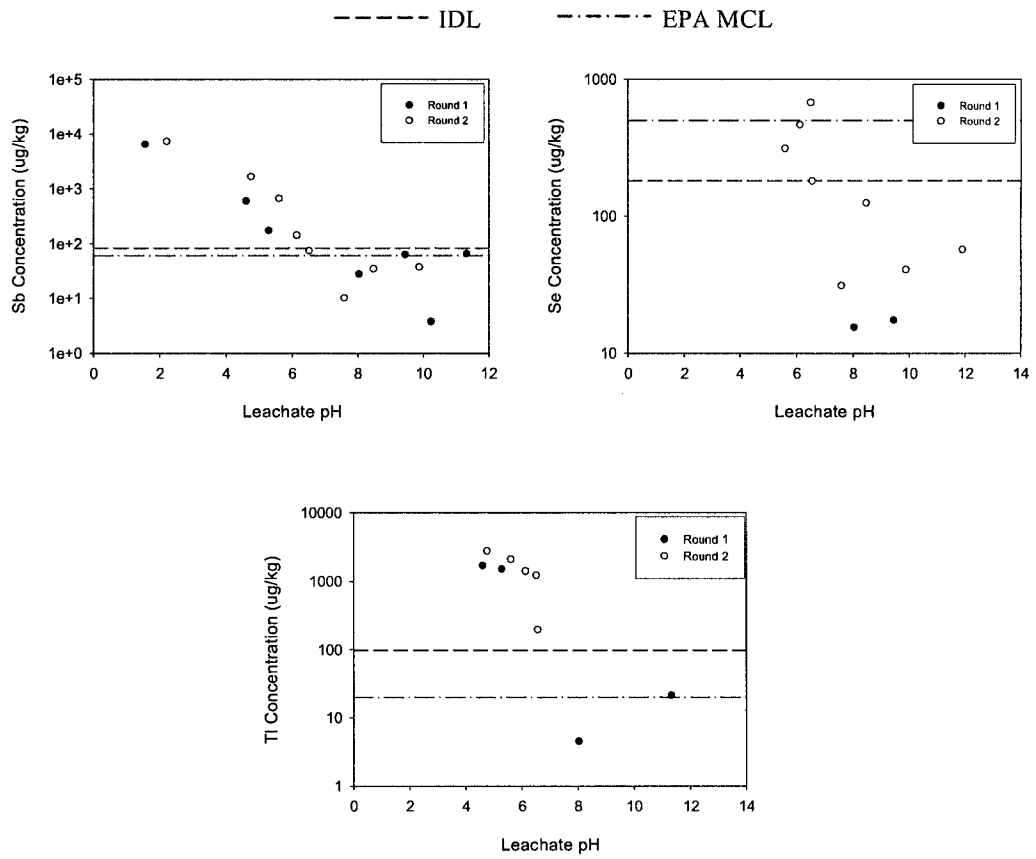
Figures 4.130-4.132. SSFW Sb, Se, and Tl pH dependent leaching curves.



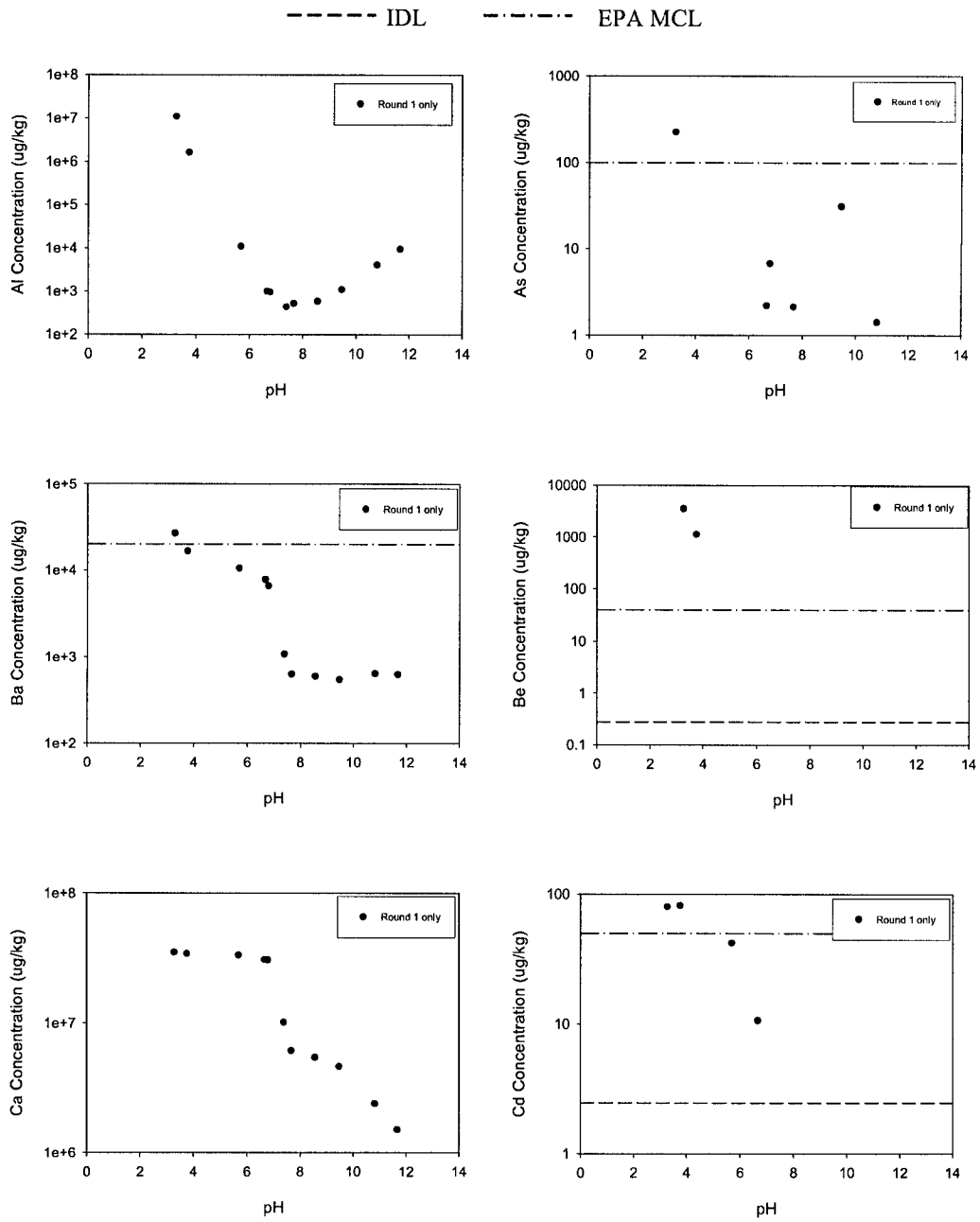
Figures 4.133-4.138. BOF Al, As, Ba, Be, Ca, and Cd pH dependent leaching curves.



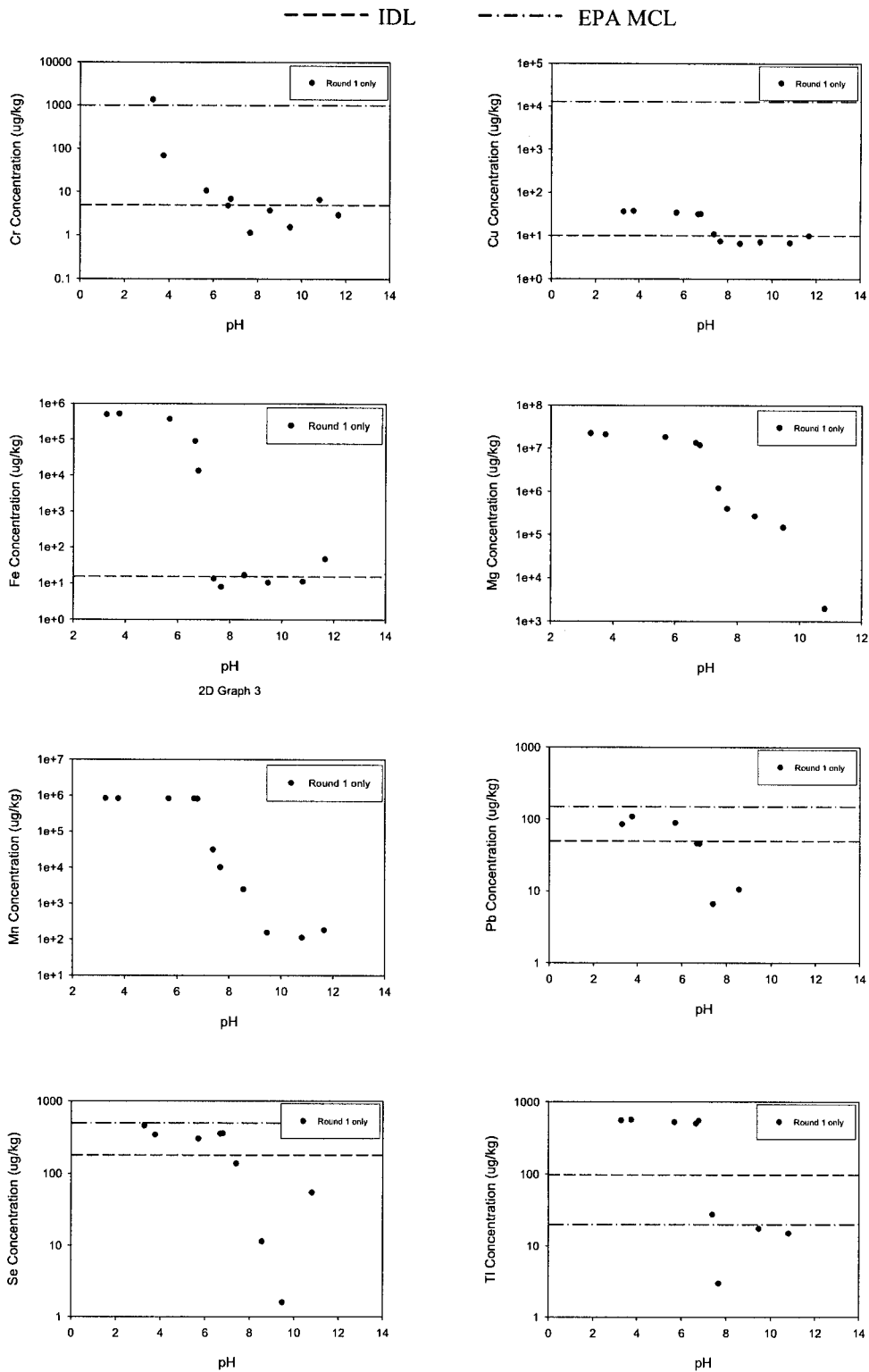
Figures 4.139-4.144. BOF *Cr*, *Cu*, *Fe*, *Mg*, *Mn*, and *Pb* pH dependent leaching curves.



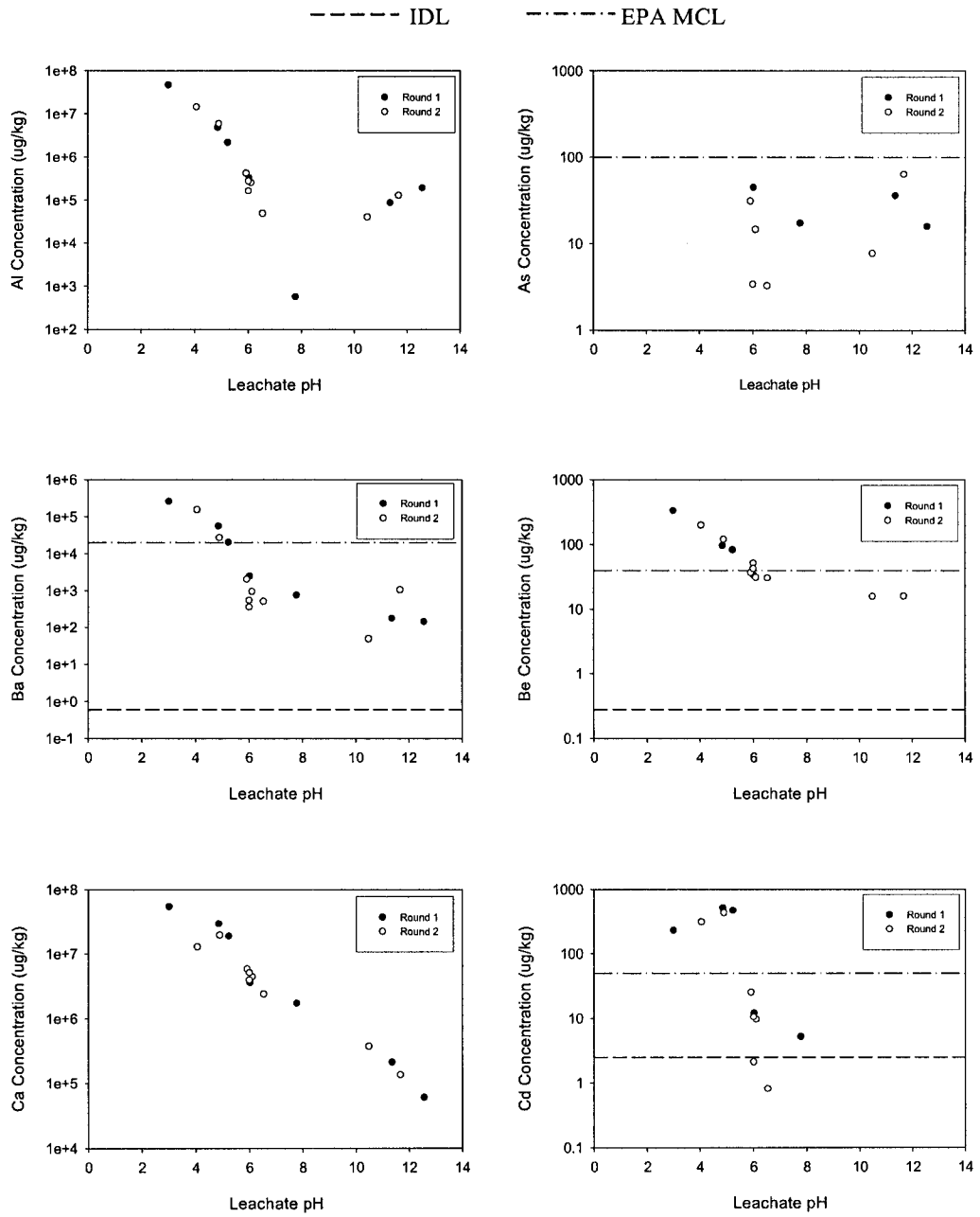
Figures 4.145-4.147. BOF *Sb*, *Se*, and *Tl* pH dependent leaching curves.



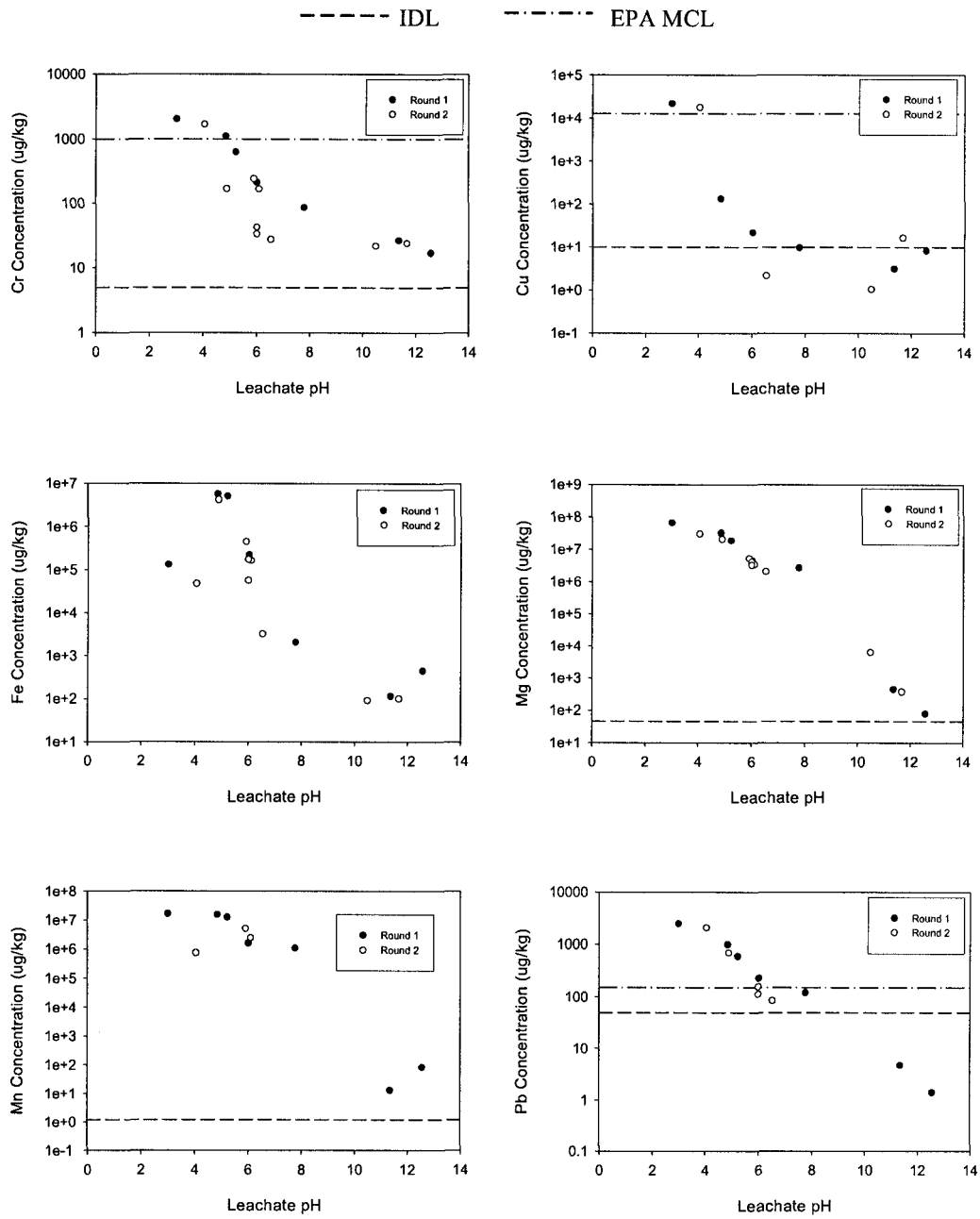
Figures 4.148-4.153. BF Al, As, Ba, Be, Ca, and Cd pH dependent leaching curves.



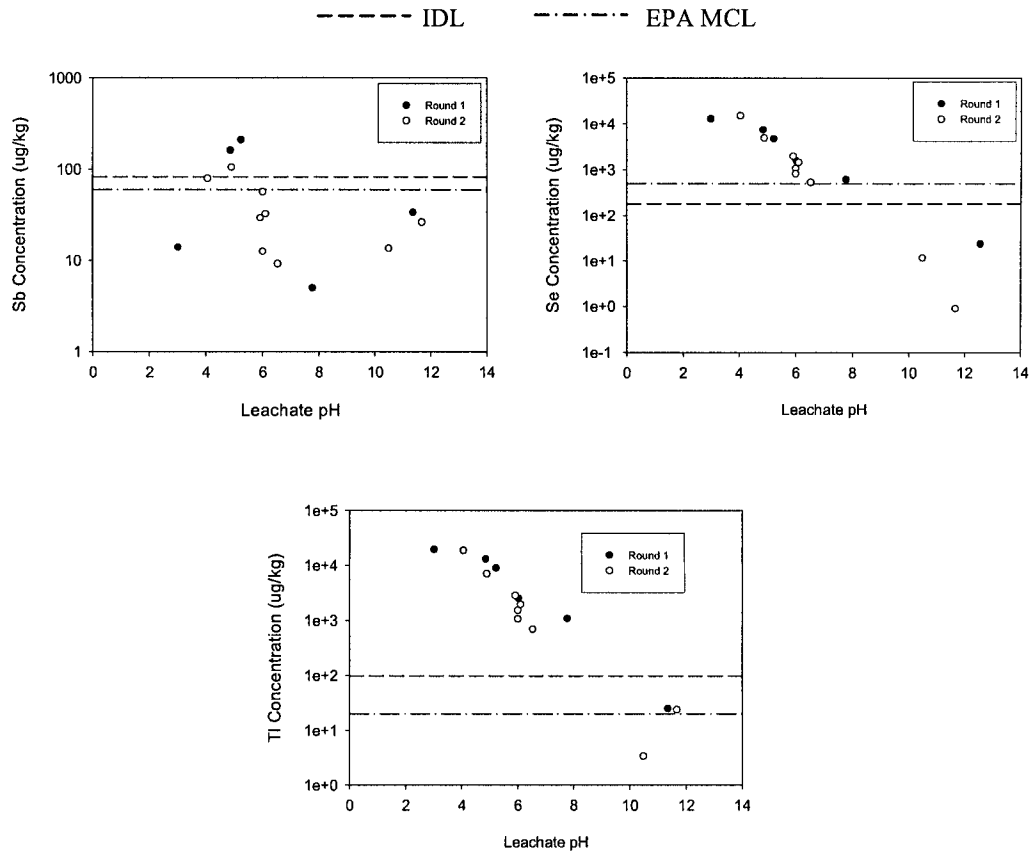
Figures 4.154-4.161. BF Cr, Cu, Fe, Mg, Mn, Pb, Se, and Tl pH dependent leaching curves.



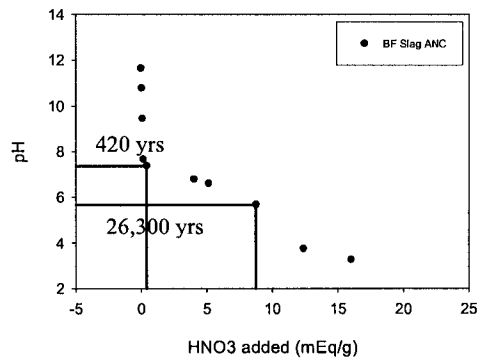
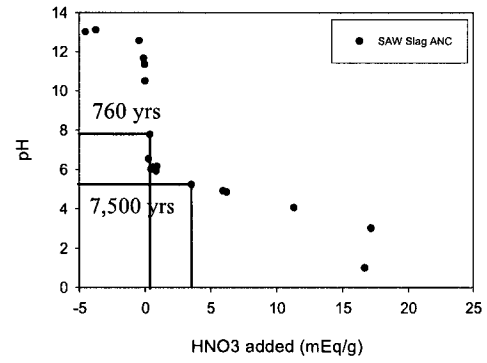
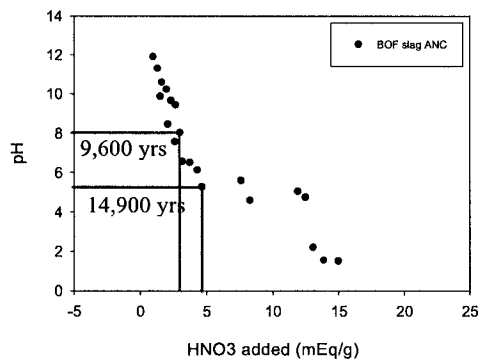
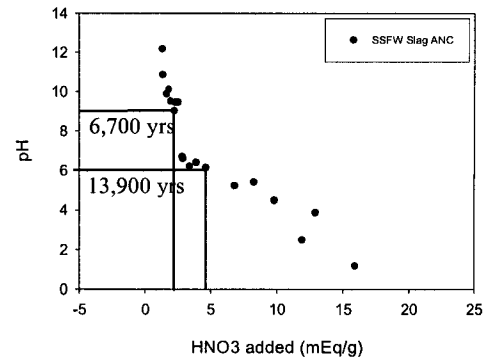
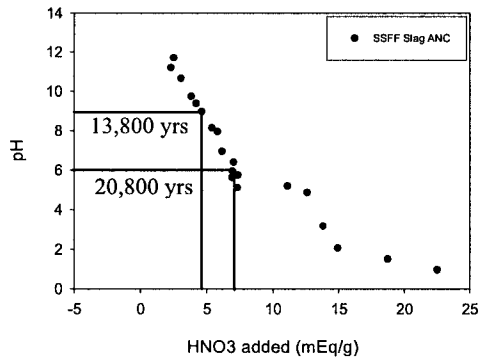
Figures 4.162-4.167. SAW Al, As, Ba, Be, Ca, and Cd pH dependent leaching curves.



Figures 4.168-4.173. SAW Cr, Cu, Fe, Mg, Mn, and Pb pH dependent leaching curves.



Figures 4.174-4.176. SAW Sb, Se, and Tl pH dependent leaching curves.



Figures 4.177-4.181. ANC curves with acid rain neutralization time predictions.

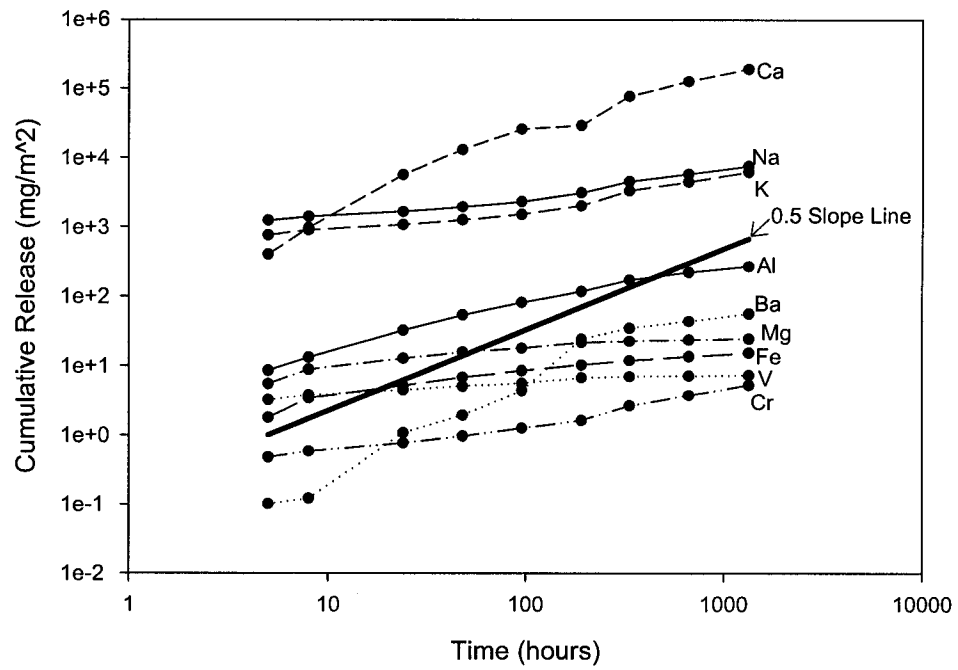


Figure 4.182. BOF slag CGLT cumulative release plot.

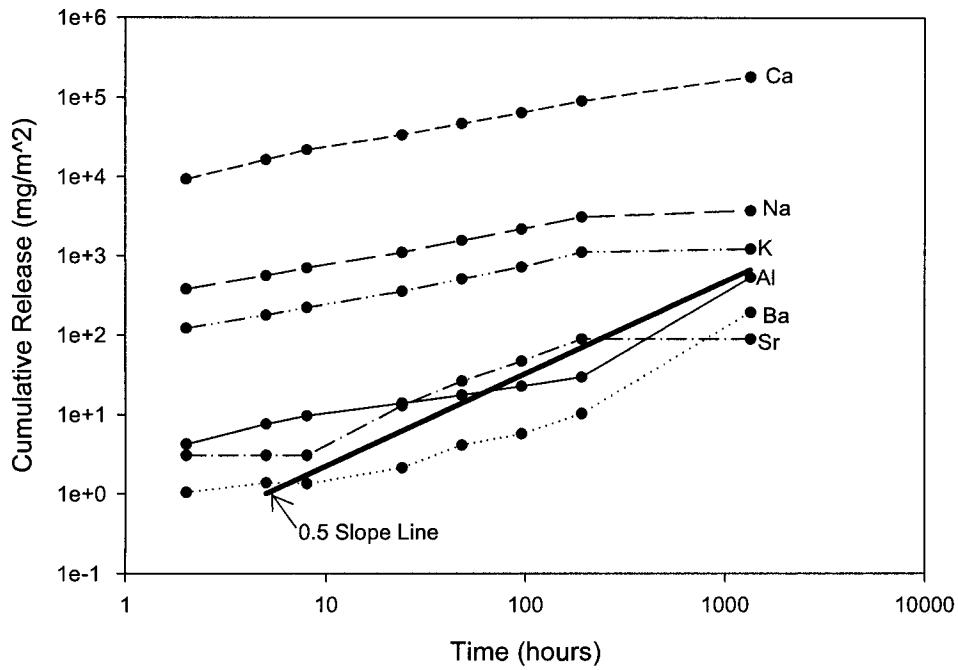


Figure 4.183. SSFF slag CGLT cumulative release plot.

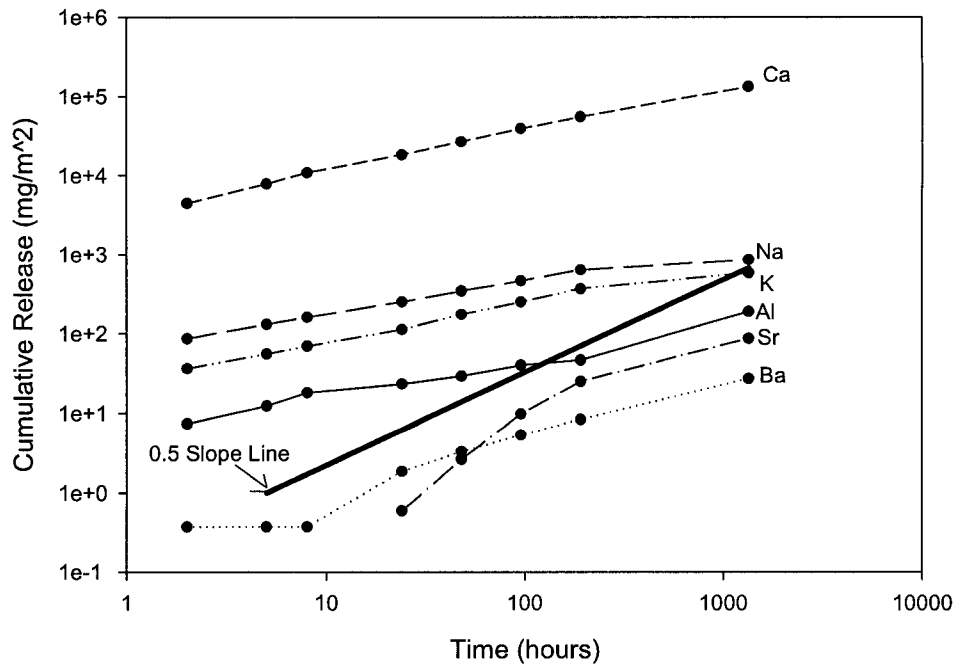


Figure 4.184. SSFW slag CGLT cumulative release plot.

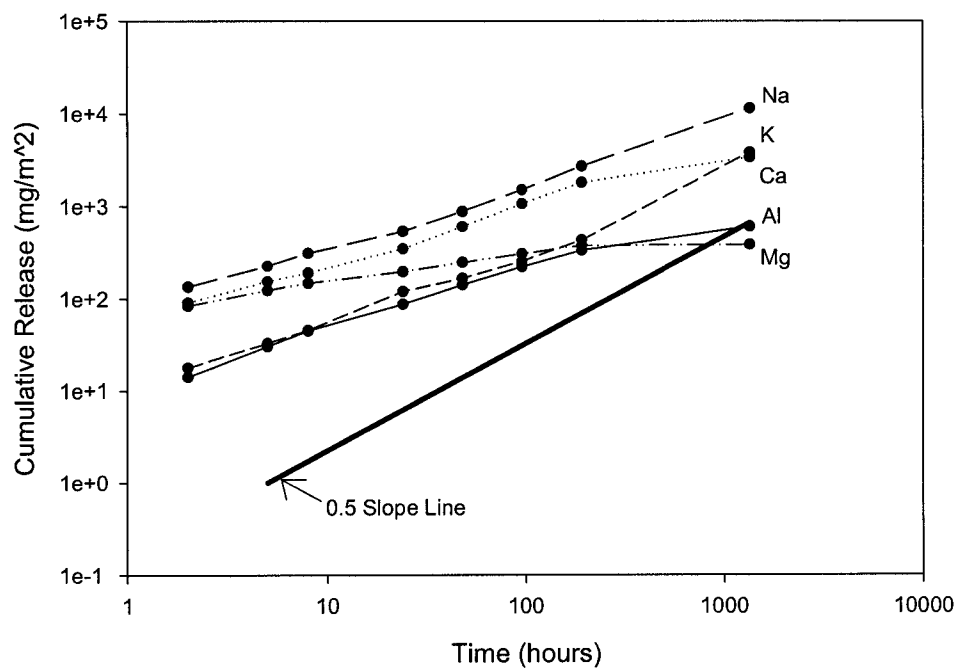


Figure 4.185. SAW slag CGLT cumulative release plot.

Table 4.13. BOF Slag CGLT results for the cumulative constituent release in mg/m2.

Constituent	Sampling Interval Time (hours)									Total Availability mg/kg
	5	8	24	48	96	192	336	672	1344	
Aluminum	8.60	13.16	32.41	53.86	81.05	116.53	170.95	220.88	267.88	126
Barium	0.10	0.12	1.08	1.93	4.40	24.19	34.90	43.60	56.29	14
Calcium	400.60	964.92	5631.24	12976.51	25847.49	29002.29	76490.84	125693.12	187843.67	121412
Chromium	0.48	0.59	0.77	0.97	1.27	1.63	2.67	3.77	5.28	1
Iron	1.79	3.43	5.19	6.85	8.52	10.34	11.93	13.66	15.38	1728
Magnesium	5.49	8.86	12.81	15.69	17.89	21.71	22.65	23.67	24.57	6428
Potassium	758.08	889.09	1073.54	1251.89	1506.20	2009.57	3309.35	4440.72	6106.47	230
Sodium	1233.74	1399.69	1652.21	1930.56	2314.77	3079.92	4511.58	5780.67	7491.04	176
Vanadium	3.22	3.78	4.50	5.09	5.62	6.73	7.02	7.20	7.37	11

Notes:

Sampling times are from the start of the test

Table 4.14. BOF Slag CGLT graphed interval slopes identifying intervals with diffusional release.

Constituent	Sampling Interval Time (hours)								
	5	8	24	48	96	192	336	672	1344
Aluminum	0.220	0.905	0.821	0.733	0.590	0.524	0.685	0.370	0.278
Barium	-0.234	0.392	1.990	0.837	1.184	2.460	0.655	0.321	0.368
Calcium	0.612	1.870	1.606	1.204	0.994	0.166	1.733	0.717	0.580
Chromium	-0.074	0.418	0.247	0.337	0.381	0.365	0.880	0.498	0.488
Iron	0.059	1.385	0.377	0.400	0.314	0.280	0.255	0.195	0.171
Magnesium	0.174	1.017	0.336	0.292	0.190	0.279	0.076	0.064	0.054
Potassium	0.677	0.339	0.172	0.222	0.267	0.416	0.891	0.424	0.460
Sodium	0.726	0.269	0.151	0.225	0.262	0.412	0.682	0.358	0.374
Vanadium	0.119	0.339	0.161	0.176	0.143	0.260	0.076	0.036	0.033

Notes:

Sampling times are from the start of the test

Shaded results are diffusion controlled (0.5+/-0.15)

Table 4.15. BOF Slag CGLT observed diffusivity (Dobs) and pDe calculations for intervals with diffusional release.

Constituent	Sampling Interval Time (hours)									Dobs Average (m ² /s)	pDe
	5	8	24	48	96	192	336	672	1344		
Aluminum	---	---	---	---	1.55E-13	1.32E-13	---	7.46E-14	---	1.20E-13	12.91
Barium	---	1.67E-16	---	---	---	---	---	---	1.942E-13	9.72E-14	13.01
Calcium	5.92E-17	---	---	---	---	---	---	---	6.184E-14	3.09E-14	13.50
Chromium	---	1.39E-12	---	---	4.67E-13	3.6E-13	---	9.37E-13	8.88E-13	8.09E-13	12.09
Iron	---	---	6.59E-18	6.1E-18	---	---	---	---	---	6.34E-18	17.19
Magnesium	---	---	---	---	---	---	---	---	---	NA	NA
Potassium	---	---	---	---	---	7.92E-12	---	1.14E-11	1.24E-11	1.05E-11	10.97
Sodium	---	---	---	---	---	3.13E-11	---	2.46E-11	2.236E-11	2.61E-11	10.58
Vanadium	---	---	---	---	---	---	---	---	---	NA	NA

Notes:

Sampling times are from the start of the test

--- = Dobs not calculated

Table 4.16. SSFF Slag CGLT results for the cumulative constituent release in mg/m².

Constituent	Sampling Interval Time (hours)								Total Availability mg/kg
	2	5	8	24	48	96	192	1344	
Aluminum	4.21	7.59	9.62	13.82	17.42	22.57	29.48	535.36	42
Barium	1.04	1.37	1.33	2.13	4.09	5.69	10.27	193.66	17
Calcium	9237.98	16237.30	21721.29	33446.24	46710.92	63748.06	90190.22	180770.74	153853
Potassium	121.84	178.02	222.22	355.32	510.94	721.25	1108.51	1219.00	254
Sodium	380.78	561.32	704.23	1102.16	1557.02	2154.20	3084.06	3712.91	259
Strontium	3.04	3.04	3.04	12.90	26.18	47.00	88.96	88.96	72

Notes:

Sampling times are from the start of the test

Table 4.17. SSFF Slag CGLT graphed interval slopes identifying intervals with diffusional release.

Constituent	Sampling Interval Time (hours)							
	2	5	8	24	48	96	192	1344
Aluminum	0.162	0.642	0.506	0.329	0.334	0.373	0.386	1.490
Barium	0.004	0.305	-0.062	0.425	0.946	0.476	0.851	1.509
Calcium	1.028	0.616	0.619	0.393	0.482	0.449	0.501	0.357
Potassium	0.541	0.414	0.472	0.427	0.524	0.497	0.620	0.049
Sodium	0.669	0.424	0.483	0.408	0.498	0.468	0.518	0.095
Strontium	0.125	0.000	0.000	1.316	1.021	0.844	0.921	0.000

Notes:

Sampling times are from the start of the test

Shaded results are diffusion controlled (0.5+/-0.15)

Table 4.18. SSFF Slag CGLT observed diffusivity (Dobs) and pDe calculations for intervals with diffusional release.

Constituent	Sampling Interval Time (hours)								Dobs Average (m2/s)	pDe
	2			24	48	96	192	1344		
Aluminum	---	3.0E-13	2.1E-13	---	---	5.7E-14	5.1E-14	---	1.5E-13	12.81
barium	---	---	---	1.7E-14	---	3.5E-14	---	7.3E-12	2.5E-12	11.61
Calcium	---	9.6E-14	1.1E-13	4.2E-14	5.6E-14	4.6E-14	5.6E-14	2.1E-14	6.1E-14	13.21
Potassium	2.1E-10	2.3E-12	2.7E-12	2.0E-12	2.8E-12	2.6E-12	4.4E-12	1.1E-14	2.9E-11	10.54
Sodium	---	2.3E-11	2.7E-11	1.7E-11	2.3E-11	2.0E-11	2.4E-11	3.5E-13	1.9E-11	10.71
Strontium	---	---	---	---	---	---	---	---	NA	NA

Notes:

Sampling times are from the start of the test

--- = Dobs not calculated

Table 4.19. SSFW Slag CGLT results for the cumulative constituent release in mg/m².

Constituent	Sampling Interval Time (hours)								Total Availability mg/kg
	2	5	8	24	48	96	192	1344	
Aluminum	7.379	12.349	18.059	23.290	29.323	40.059	46.357	188.354	190
Barium	0.373	0.373	0.373	1.867	3.301	5.345	8.371	27.191	20
Calcium	4431.53	7810.12	10800.0	18228.019	26769.753	39200.501	55271.933	133421.937	125180
Potassium	36.460	55.323	69.377	111.837	173.166	249.167	366.868	583.336	264
Sodium	85.916	130.530	159.662	249.855	342.630	459.541	635.211	856.297	227
Strontium	0.000	0.000	0.000	0.593	2.650	9.801	25.006	86.959	61

Notes:

Sampling times are from the start of the test

Table 4.20. SSFW Slag CGLT graphed interval slopes identifying intervals with diffusional release.

Constituent	Sampling Interval Time (hours)							
	2	5	8	24	48	96	192	1344
Aluminum	0.225	0.562	0.809	0.232	0.332	0.450	0.211	0.720
Barium	-0.111	0.000	0.000	1.465	0.822	0.695	0.647	0.605
Calcium	0.945	0.618	0.690	0.476	0.554	0.550	0.496	0.453
Potassium	0.405	0.455	0.482	0.435	0.631	0.525	0.558	0.238
Sodium	0.501	0.456	0.429	0.408	0.456	0.424	0.467	0.153
Strontium	---	---	---	---	2.161	1.887	1.351	0.640

Notes:

Sampling times are from the start of the test

Shaded results are diffusion controlled (0.5+/-0.15)

Table 4.21. SSFW Slag CGLT observed diffusivity (Dobs) and pDe calculations for intervals with diffusional release.

Constituent	Sampling Interval Time (hours)								Dobs Average (m2/s)	pDe
	2	5	8	24	48	96	192	1344		
Aluminum	---	3.1E-14	---	---	---	1.2E-14	---	---	2.1E-14	13.67
Barium	---	---	---	---	---	---	---	---	na	na
Calcium	---	3.3E-14	---	2.5E-14	3.5E-14	3.7E-14	3.1E-14	2.3E-14	3.1E-14	13.52
Potassium	5.8E-11	2.3E-13	2.5E-13	1.8E-13	4.0E-13	3.1E-13	3.7E-13	---	8.5E-12	11.07
Sodium	1.8E-10	1.8E-12	1.4E-12	1.1E-12	1.2E-12	9.9E-13	1.1E-12	5.6E-14	2.4E-11	10.62
Strontium	---	---	---	---	---	---	---	---	NA	NA

Notes:

Sampling times are from the start of the test

--- = Dobs not calculated

Table 4.22. SAW Slag CGLT results for the cumulative constituent release in mg/m2.

Constituent	Sampling Interval Time (hours)								Total Availability mg/kg
	2	5	8	24	48	96	192	1344	
Aluminum	14.08	30.43	44.74	87.66	141.65	220.49	335.79	608.28	152
Calcium	91.02	154.02	189.76	348.68	605.84	1071.56	1820.61	3372.72	314
Potassium	17.83	32.75	45.43	120.04	165.77	252.93	434.28	3829.44	13
Magnesium	83.62	123.79	147.42	196.01	247.34	305.69	377.28	384.93	289
Sodium	135.24	225.82	311.22	541.44	882.63	1519.49	2701.52	11478.64	70

Notes:

Sampling times are from the start of the test

Table 4.23. SAW Slag CGLT graphed interval slopes identifying intervals with diffusional release.

Constituent	Sampling Interval Time (hours)							
	2	5	8	24	48	96	192	1344
Aluminum	0.298	0.841	0.820	0.612	0.692	0.638	0.607	0.305
Calcium	0.508	0.574	0.444	0.554	0.797	0.823	0.765	0.317
Potassium	0.324	0.663	0.696	0.885	0.466	0.610	0.780	1.119
Magnesium	0.498	0.428	0.372	0.259	0.336	0.306	0.304	0.010
Sodium	0.552	0.559	0.683	0.504	0.705	0.784	0.830	0.743

Notes:

Sampling times are from the start of the test

Shaded results are diffusion controlled (0.5+/-0.15)

Table 4.24. SAW Slag CGLT observed diffusivity (Dobs) and pDe calculations for intervals with diffusional release.

Constituent	Sampling Interval Time (hours)*								Dobs Average (m2/s)	pDe
	2	5	8	24	48	96	192	1344		
Aluminum	--	--	--	4.0E-12	--	7.1E-12	7.6E-12	--	6.2E-12	11.21
Calcium	9.2E-12	1.3E-11	8.0E-12	1.3E-11	--	--	--	--	1.1E-11	10.97
Potassium	--	--	--	--	7.1E-10	1.3E-09	--	--	1.0E-09	9.00
Magnesium	9.2E-12	6.3E-12	4.2E-12	--	--	--	--	--	6.5E-12	11.19
Sodium	4.1E-10	5.4E-10	--	5.5E-10	--	--	--	--	5.0E-10	9.30

Notes:

Sampling times are from the start of the test

-- = Dobs not calculated

Table 4.25. Compiled CGLT pDe, Tortuosity, and Retention Factor values.

Constituent	pDe Values				Retention Factor (R) in Material				Diffusion Coefficient in Water ²
	BOF	SSFF	SSFW	SAW	BOF	SSFF	SSFW	SAW	
Tortuosity	47.13	63.61	51.34	2.47	na	na	na	na	na
Aluminum	12.92	12.81	13.67	11.21	na	na	na	na	na
Barium	13.01	11.61	---	nd	43.55	1.27	---	nd	9.7
Calcium	13.51	13.21	13.52	10.97	544.55	203.11	506.70	29.76	9.1
Chromium	12.09	nd	nd	nd	15.44	nd	nd	nd	9.23
Iron	17.20	nd	nd	nd	na	nd	nd	nd	na
Magnesium	---	nd	nd	11.19	---	nd	nd	56.57	9.04
Potassium	10.98	10.54	11.07	9.00	3.91	1.07	4.48	0.79	8.71
Sodium	10.58	10.71	10.62	9.30	1.00	1.00	1.00	1.00	8.91
Strontium	nd	13.00	---	nd	nd	na	---	nd	na
Vanadium	---	nd	nd	nd	---	nd	nd	nd	na

Notes:

- nd = indicates constituent not detected above IDL in sample
- = indicates no interval slopes within diffusion range
- na= not available

Table 4.26. Compiled CGLT pDe and Tortuosity values from the literature.

Constituent	Kosson, van der Sloot, Eighmy, (1996) ¹				de Groot and van der Sloot (1992)	Diffusion Coefficient in Water ²
	Bottom Ash	APC Residue	FA in Asphalt	BA in Concrete	Stabilized Coal Ash	---
Tortuosity	23	10	8000	36	19	---
Antimony	---	---	---	---	100	9.12
Arsenic	---	---	---	---	1.7	8.99
Barium	17.3	---	4,347.8	---	---	9.7
Cadmium	---	1,819,700.9	571.4	---	---	9.14
Calcium	173.1	10.0	157.4	2,777.8	---	9.1
Copper	---	97,723.7	24.4	858.4	450	9.11
Lead	658,070.1	758,577.6	2,381.8	666,342.5	---	9.02
Magnesium	---	---	---	---	---	9.04
Molybdenum	---	---	---	---	90	9
Potassium	1.1	1.0	1.0	1.4	---	8.71
Sodium	0.9	0.8	1.0	0.9	1	8.91
Zinc	169,150.1	776,247.1	306.8	271,454.8	---	9.11

Note:

--- = data not available

¹ = R values were not presented in report so they were calculated from pDe and τ

² = Compiled/calculated from Kosson et al. (1996) and de Groot and van der Sloot (1992)

Table 4.27. LS ratio availability results and re-calculated pDe values.

Constituent	BOF		SSFF		SSFW		SAW	
	Availability LS ratio (mg/kg)	pDE	Availability LS ratio (mg/kg)	pDE	Availability LS ratio (mg/kg)	pDE	Availability LS ratio (mg/kg)	pDE
Aluminum	0.01	4.72	0.01	5.91	0.01	4.96	5.74	8.36
Barium	0.25	9.51	0.25	7.97	0.30	---	nd	nd
Calcium	410.88	8.57	495.70	8.18	463.03	8.65	4.72	7.32
Chromium	0.02	9.08	nd	nd	nd	nd	nd	nd
Iron	0.002	5.51	nd	nd	nd	nd	nd	nd
Magnesium	0.004	---	nd	nd	nd	nd	0.03	3.15
Potassium	30.96	9.23	32.93	9.76	11.97	9.85	33.07	9.85
Sodium	34.95	9.18	42.26	9.07	15.16	9.56	39.62	8.81
Strontium	nd	nd	4.17	---	2.09	---	nd	nd
Vanadium	0.00	---	nd	nd	nd	nd	nd	nd

Notes:

nd = indicates constituent not detected above IDL in sample

--- = indicates no interval slopes within diffusion range

Table 4.28. Re-calculated tortuosity and R values using LS ratio availability results.

Constituent	pDe Values				Retention Factor (R) in Material				Diffusion Coefficient in Water ²
	BOF	SSFF	SSFW	SAW	BOF	SSFF	SSFW	SAW	
Tortuosity	1.86	1.46	4.43	0.79					
Aluminum	4.72	5.91	4.96	8.36	na	na	na	na	na
Barium	9.51	7.97	---	nd	0.343	0.0127	---	nd	9.7
Calcium	8.57	8.18	8.65	7.32	0.1576	0.0828	0.08	0.02	9.1
Chromium	9.08	nd	nd	nd	0.384	nd	nd	nd	9.23
Iron	5.51	nd	nd	nd	na	nd	nd	nd	na
Magnesium	---	nd	nd	3.15	---	nd	nd	1.63E-06	9.04
Potassium	9.23	9.76	9.85	9.85	1.79	7.71	3.11	17.32	8.71
Sodium	9.18	9.07	9.56	8.81	1.00	1.00	1.00	1.00	8.91
Strontium	nd	13.00	---	nd	nd	na	---	nd	na
Vanadium	---	nd	nd	nd	---	nd	nd	nd	na

Notes:

nd = indicates constituent not detected above IDL in sample

--- = indicates no interval slopes within diffusion range

na= not available

Table 4.29. Predicted long-term Ba and Cr diffusional release from BOF and SSFF slags

Availability Method	Constituent	1 year		5 year		40 year		100 year	
		BOF	SSFF	BOF	SSFF	BOF	SSFF	BOF	SSFF
NEN 7341	Barium	0.116	0.693	0.259	1.549	0.734	4.382	1.160	6.928
	Chromium	0.019	nd	0.042	nd	0.118	nd	0.187	nd
LS Ratio	Barium	0.116	0.693	0.259	1.549	0.734	4.382	1.160	6.928
	Chromium	0.019	nd	0.042	nd	0.118	nd	0.187	nd

Notes:

All results in mg/kg

nd = indicates constituent not detected above IDL in sample

Table 4.30. BOF slag MINTEQA2 modeling results showing minerals controlling constituent solubility over the indicated pH range..

Element	Minerals Controlling Solubility (pH range)		
	1st Mineral	2nd Mineral	3rd Mineral
Al	Al ₂ O ₃ (4.5-5.5)	Gibbsite (8.5-10)	Al(OH)SO ₄ (2-5)
As	none		
Ba	BaHAsO ₄ ·H ₂ O (4.5-12)	Barite (2-6.5)	
Ca	Gypsum (1.5-2, 5)		
Cd	CdMoO ₄ (4.5-5.5)		
Cl	Pb ₂ (OH) ₃ Cl (2-12)		
Cu	Atacamite (8.5-9.5)	Tenorite (am) (8.5-10)	
Mo	PbMoO ₄ (4.5-6)		
Pb	Pb(OH) ₂ (8-12)	PbMoO ₄ (4.5-6.5)	
Ni	Ni(OH) ₂ (c) (9.5-10.5)		
SO ₄	Al(OH)SO ₄ (4.5-5.5)	Barite (1.5-12)	Bronchantite (5.25-12)
Zn	none		

Notes:

Shaded minerals control solubility in the natural pH range of the material

Table 4.31. SAW slag MINTEQA2 modeling results showing minerals controlling constituent solubility over the indicated pH range.

Element	Minerals Controlling Solubility (pH range)	
	1st Mineral	2nd Mineral
Al	Al(OH) ₃ (soil) (10.5-11.5)	Alunite (3-6.5)
As	none	
Ba	BaHAsO ₄ ·H ₂ O (3-6)	
Be	none	
Ca	none	
Cr	none	
Fe	K-Jarosite (3-6)	Na-Jarosite (6)
Mg	Brucite (11-12.5)	Spinel (6.5-7.1)
Mo	PbMoO ₄ (6-6.5)	
Ni	Ni(OH) ₂ (c) (11.5-12.5)	
Pb	Pb(OH) ₂ (8-11)	PbMoO ₄ (3-6.5)
SO ₄	Alunite (6)	
V	none	
Zn	none	

Notes:

Shaded minerals control solubility in the natural pH range of the material

Table 4.32. BF slag MINTEQA2 modeling results showing minerals controlling constituent solubility over the indicated pH range.

Element	Minerals Controlling Solubility (pH range)					
	1st Mineral	2nd Mineral	3rd Mineral	4th Mineral	5th Mineral	6th Mineral
Ag	none					
Al	Al(OH) ₃ (5.5-7)	Al ₂ O ₃ (7.5-8.5)	AlOHSO ₄ (3-4)	Gibbsite (3-4, 9.5-10.5)		
As	none					
Ba	BaHAsO ₄ :H ₂ O (7-12)	Barite (3-9.5)				
Ca	none					
Cl	Cerargyrite (3-12)					
Cu	Tenorite (c) (8.5-11)					
Fe	H-Jarosite (3.5-5.5)	Na-Jarosite (3.5-6.5)				
Mg	Magnesioferrite (3-11)					
Ni	none					
Na	Na-Jarosite (3.5-11.5)					
Pb	none					
SO ₄	Al ₄ (OH) ₁₀ SO ₄ (5.5-9.5)	AlOHSO ₄ (3.5-5.5)	Alunite (5.5-8.5)	Barite (3.5-11)	Celestite (7.5-11)	Na-Jarosite (3.5-9.5)
Sr	none					
V	none					

Notes:

Shaded minerals control solubility in the natural pH range of the material

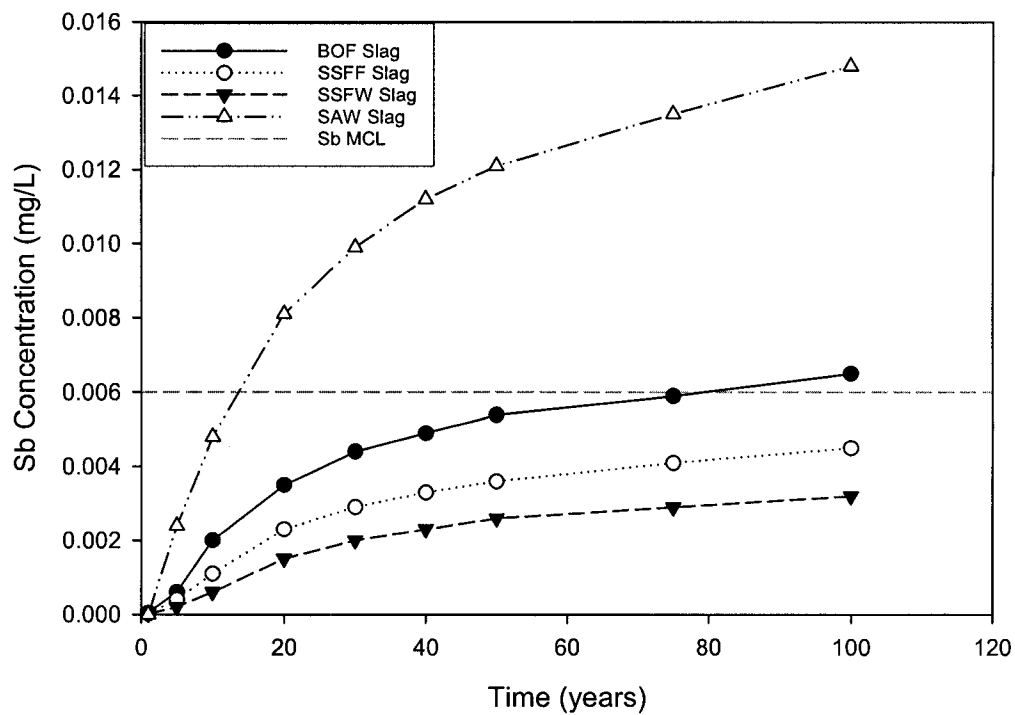


Figure 4.186. IWEM modeling for Sb concentrations in a monitoring well located 20 m from the source over 100 years.

Table 4.33. Laboratory validation split samples sent to EA, Inc.

Sample	Be		Cd		Sb		Ti	
	EA	RMRC	EA	RMRC	EA	RMRC	EA	RMRC
SAW-Availability test	0.003	0.002	0.002	0.002	<0.001	<0.006 (0.001)	<0.001	0.18
SAW pHD test (pH=5)	0.018	0.012	0.045	0.043	<0.001	0.01	0.003	0.704
SAW pHD test (pH=6.5)	0.002	0.003	<0.001	0.001	0.001	<0.006 (0.0009)	<0.001	0.069
SAW pHD test (pH=10.5)	<0.001	0.001	<0.001	0.001	<0.001	<0.006 (0.001)	<0.001	<0.009
DI Blank	<0.001	0.001	<0.001	0.001	<0.001	<0.006	<0.001	<0.009
NIST Standard	0.009	0.006	0.003	0.003	0.028	0.041	0.004	0.005

Notes:

All results in mg/l
 Detections below IDL shown in
 parentheses

CHAPTER 5

CONCLUSIONS

5.1 Laboratory Test Conclusions

In order to evaluate characterization techniques for industrial byproducts such as slag, five different types of slag were subjected to a set of simplified and complex tests designed to cover a wide range of conditions. Some of the leaching tests included in this set have been used historically for this type of material while others are currently being proposed for industrial byproduct characterization.

A total composition test was not successful due to incomplete sample digestion and therefore a TLC test was used. A possible use for this test is as a screening tool to identify the presence or non-presence of constituents in a material. This was slightly unsuccessful in the SSFF and SSFW slags in which arsenic and selenium were not detected in the TLC test but were detected in the LS ratio and pH-dependent leaching tests for these materials. Similar discrepancies were seen in the SAW and BOF slags as well. The availability test is described as a more realistic approach to determining total leachable content since neutral and slightly acidic

extraction solutions often found in field applications are used. For highly buffered materials such as steel slag though, even these pHs could be considered unrealistic. An additional problem encountered with the availability test was the lack of pH equilibration throughout the test which could lead to repeatability inconsistencies between tests depending on how fast neutralization reactions are occurring.

The natural pH test was used to identify the expected pH environment once the materials are placed in an application. Since pH has been shown to often control constituent solubilities, understand what the pH will be over a given timeframe is important. Numerous variables such as atmosphere and precipitation exposure can affect pH; therefore natural pH characterization should include the expected site-specific parameters if possible. The LS ratio and pH-dependent leaching tests can be used to characterize constituent leaching over a material's lifespan or over a range of pHs. The LS ratio test was identified as the most appropriate test for the slags since pH is controlled by the buffering capacities of the materials, similar to what would occur in actual field use. This test also provides a leaching timeframe if fill geometry and precipitation rate are estimated. Antimony was identified as a potential constituent of concern in the BOF, SSFF, and SSFW slags with EPA MCL exceedances mostly in the low LS ratios. Unlike the higher ratios which can represent hundreds to thousands of years of leaching depending on the management scenario, low LS ratios could be more realistically achieved in the materials' timeframe of use.

The pH-dependent leaching test was difficult to conduct due to the high buffering capacities of the materials. Information from this test identified the possibility for most of the constituents to leach from the materials in hazardous levels, though this generally occurred at neutral to acidic pHs. Solubility curves for some constituents such as barium and chromium showed an amphoteric shape with increasing concentrations at higher pHs compared to neutral pHs. Although no MCL exceedances were found at the high pHs, this trend is important to identify in the highly alkaline slags. Conservative calculations using the materials' acid neutralization capacities and precipitation rates from Ohio determined that the pHs below which the exceedances occurred would not be reached for thousands of years for the steel slags and hundreds of years for the blast furnace and SAW slags. Based on this knowledge, a shortened version of the pH-dependent leaching test is recommended which uses a more realistic pH range than 2 to 12 for these highly buffered materials.

The compacted granular leaching test was used to characterize the mass-transfer related release of constituents from the materials. This test is considered the least conservative test for a highway application such as a compacted layer of slag which may not have precipitation percolating through the material. The majority of the constituents tested were not detected in high enough concentrations to use in the mass-transfer calculations so a limited amount of information was gained from this test.

Using the sodium values, the material-specific property of tortuosity was calculated for the four materials tested. Only two EPA regulated constituents, barium and chromium, were detected in high enough concentrations to calculate diffusion coefficients. Although considered a less conservative test, the diffusion calculations involve using results from the availability or total composition tests which both have been identified in this research as unrealistic for the slags. Therefore a second set of mass transfer coefficients were calculated using availability concentrations from the LS ratio leaching test. The results from this alternate method were mostly lower amounts of constituents available for release and higher diffusion coefficients.

In order to interpret the leaching results, the EPA's IWEM program was used to determine the fate and transport effects on the data. Antimony was used in the modeling since it was identified in the LS ratio leaching test as a contaminant of concern. The model scenario involved monitoring the change in antimony concentrations (from LS ratio test) over 100 years in a ground water well located 20 meters downgradient from the source. The first modeling attempt used the program's default soil/water partitioning coefficient for antimony and identified MCL exceedances in the well for the SAW slag and BOF slag. The second attempt used a partitioning coefficient obtained from the literature and non-detect concentrations were predicted for all of the materials after 100 years. This modeling exercise identified the

variability in conservativeness when site-specific properties such as partitioning coefficients are used with the model.

According to the literature, steel slag has mechanical issues with volume stability due to expansion and must be stockpiled and aged prior to use in bound applications. Fresh and aged steel slag samples were subjected to the characterization techniques in this research, and from this the effects of slag weathering were identified from the results. The slags appeared physically similar on a macroscopic level but differed microscopically with surface crystallization and an increased surface seen in the weathered sample. Results from the availability test were similar but differed for the natural pH, LS ratio leaching, and pH dependent leaching tests. The weathered slag showed a lower, but still highly alkaline, pH than the fresh slag most likely as a result of increased water and atmospheric contact during the aging process. In the LS ratio test, cadmium was detected in the fresh sample but not in aged sample and copper was more consistently detected in the aged sample. This possibly indicates a decrease in cadmium solubility with weathering and an increase in copper solubility. This copper relationship was not confirmed in the pH-dependent test however, with an amphoteric curve and higher concentrations at high pHs seen in the fresh sample. Comparisons in the compacted granular leaching test showed slightly lower diffusion coefficients in the weathered sample than in the fresh sample indicating that slag aging may slow diffusional

constituent release. Barium was identified as showing diffusion-controlled release in the fresh sample but not in the weathered sample.

Based on the set of leaching tests used in this research there does not appear to be a single test capable of fully characterizing the slags. Subjecting the materials to the entire set of tests would be extremely expensive and time consuming however and is not recommended. Therefore, a shortened set of tests is suggested based on the properties of these materials. The LS ratio leaching test is recommended using a range of ratios expected in the field. An LS of 100 was used in this research but is considered unrealistic. The pH-dependent leaching test is also recommended but with a shortened range of pHs to match the pH range expected in the material's lifespan. This range would depend on the material's acid neutralization capacity and, using the slags in this research as an example, could be between 8 and 13 instead of 2 and 12. In both of these tests, understanding the pH of the material over a timeframe and under a range of conditions is key to characterizing leaching potential. With the other tests, the total composition test and availability test are considered overly conservative and do not realistically predict what constituents could leach from these materials. The compacted granular leaching test is regarded as too complex to perform considering the limited amount of data that was obtained for these materials.

5.2 Recommendations for Material Use

The overall goal of the set of leaching tests included in this research is to identify whether a material is safe to use in a particular application or whether it could harmfully affect the environment. An important concept in the beneficial use of recycled materials is that a material may be appropriate for one type of use but not for another depending on the material's properties and the environmental conditions associated with the application. Based on the leaching results the following recommendations can be made for the materials tested. It is important to note that these recommendations are based on the environmental properties and not the physical properties, which were not fully studied in this research.

Because the steel slags showed the lowest release of EPA-regulated constituents in the mass transfer based compacted granular leaching test (only *Ba* and *Cr* detected in measurable amounts), it could be concluded that a reduction of permeability within the material application through compaction could reduce the possibility of contaminant release. Therefore, loosely compacted applications are not recommended for the materials if extended periods of water contact are expected. If a loosely packed application is used, proper drainage below the material could reduce long-term water contact within the layer. It should be noted that the level of compaction achieved in the laboratory may not be possible in a field

application considering the large amount of fines included in the samples. Therefore, diffusion controlled release in a field application may differ from the results obtained in the laboratory due to this difference in compaction extent. Other ways to decrease water contact is to use the materials in applications located in arid climates or applications located beneath impermeable layers. The fresh steel slag material should technically not be used in applications since state regulations identified in this research require aging for all steel slags to reduce volume instability. One issue clearly identified by the leaching tests is the highly alkaline leachate produced from the steel slags. This issue is problematic due to the formation of clogging calcium carbonate deposits along the exterior of a highway as well as the damaging affects the runoff could have on surrounding vegetation and wildlife. The previous recommendation of water contact reduction through permeability reduction and application location could help reduce the production of highly alkaline leachate from the steel slag. Weathering did not appear to reduce the pH greatly as seen in the fresh and weathered steel slag natural pH tests.

Although not tested with the entire suite of leaching tests, the fewer MCL exceedances in the blast furnace slag results indicate that the material is possibly more suitable for high water contact applications than the steel slags. One possible issue with the blast furnace slag is the elevated sulfur content of the leachate. As was previously mentioned, sulfur odors were detected after the LS ratio and pH-dependent leaching test containers were

opened. This issue was possibly the cause of the Cleveland Airport environmental contamination and should be considered when determining the appropriate use for the material. Especially if reducing conditions, which are known to affect the release of sulfur compounds, are expected.

Unlike the steel and iron slags, specifics on the production volumes and stockpile locations are unclear for the SAW slag since it is new to the beneficial use market. If the physical properties of the slag were suitable for unbound applications and the production volumes were adequate for highway applications, a similar recommendation as the steel slags of reducing water contact is suggested. The SAW slag showed a higher release of constituents in the equilibrium-based tests where water contact was maximized. Applications that mimic this environment such as using the slag as a road sanding amendment or replacement is not recommended since water contact in this application is high. Due to the shape of the slag and the glassy nature, a possible use for SAW slag that reduces water contact is an aggregate replacement in concrete, similar to glasscrete in which crushed glass is used. This application might be more suitable for the lower volumes possibly associated with SAW slag production. In the LS ratio leaching test, plateauing concentrations in the lower LS ratios for some constituents indicated a washoff effect as a release mechanism. Therefore, it is recommended that the slag first go through a hydration stage, similar to steel slag, prior to beneficial use to reduce the possibility of constituent release.

CHAPTER 6

RECOMMENDATIONS FOR FUTURE RESEARCH

Future research efforts should continue to study the leaching characteristics of slags but with an emphasis on parameters not included in this work such as redox and intermittent wetting and drying. Achieving a better understanding of the environmental conditions that exist within a particular beneficial use application can help tailor an appropriate set of laboratory leaching tests that best simulate that application.

If similar future work is to be performed with an ICP-AES, identifying matrix interferences is recommended given the complex chemistry observed in the slag leachates. The laboratory validation study identified a possible false positive detection of *Tl* in several samples. It is not known whether additional interference issues existed for the constituents not included in the validation.

Another area for future research is studying the repeatability of these leaching tests on slags from the same source. An ideal characterization scenario would be if a large amount of slag from the same source could be

classified with a partial set of leaching tests. Kosson et al. (2002) suggests this approach in the presented framework with subsequent batches from the same source requiring less testing after the initial batch is fully tested. Since the heterogeneity of different materials may differ greatly, this approach should be tested with multiple batches of slags. This was not possible in this research given the small sample amounts provided and the limited timeframe and resources.

In order to identify the true total composition of the slags, a future recommendation is to use a different such as x-ray fluorescence that does not require complete digestion of the sample. The slag samples in this research could not be fully digested due high silica content and therefore total composition results were not obtained.

LIST OF REFERENCES

Allison, J.D., Brown, D.S., Novo-Gradac, K.J. (1991). *MINTEQA2/PRODEFA2, A Geochemical Assessment Model for Environmental Systems: Version 3.0 User's Manual*. Environmental Research Laboratory, U.S. Environmental Protection Agency.

Allison, J.D., Allison, T.L. (2005). *Partition Coefficients for Metals in Surface Water, Soil, and Waste*. Report Number EPA/600/R-05/074. U.S. Environmental Protection Agency.

Angus, M.J., Glasser, F.P. (1986). *Chemical environment in cement matrices*. Materials Research Society Symposia Proceedings. Stockholm, Sweden. pp. 547-556.

Apul, D. (2005). Personal communication.

Arm, M., Johansson, H.G., Ydrevik, K. (2001). *Performance-Related Tests on Air-Cooled Blast-Furnace Slag and Crushed Concrete, VTI Activities in the European ALT-MAT Project*. Beneficial Use of Recycled Materials in Transportation Applications. Nov. 13-15. Arlington, Virginia. pp. 237-248.

ASTSWMO (2000). *Beneficial Use Survey*. Association of State and Territorial Solid Waste Management Officials.

Ball, J.E., Jenks, R., Aubourg, D. (1998). *An assessment of the availability of pollutant constituents on road surfaces*. The Science of the Total Environment. 209(2-3). pp. 243-254.

Boyer, B. (1994). *Alkaline leachate and calcareous tufa originating from slag in a highway embankment near Baltimore, Maryland*. Transportation Research Record 1434. pp. 3-7.

Cleveland.com (2002). *Cleveland agrees to pay for replacing slag in runway*.

<http://www.cleveland.com/indepth/airport/index.ssf?/indepth/airport/more/1027683012274590.html>.

Comans, R.N.J., van der Sloot, H.A., Hoede, D., Bonouvie, P.A. (1991). *Chemical processes at a redox/pH interface arising from the use of steel slag in the aquatic environment*. Studies in Environmental Science. 48. pp. 243.

Council, Rocky River Watershed (2002). *State of the Rocky River*. <http://www.noaca.org/RockyRiver.pdf>.

de Groot, G., van der Sloot, H.A. (1992). *Determination of leaching characteristics of waste materials leading to environmental product*

certification. ASTM Special Technical Publication 1123. pp. 149-170.

Dippenaar, R. (2005). *Industrial uses of slag (the use and re-use of iron and steelmaking slags)*. Ironmaking and Steelmaking. 32(1). pp. 35-46.

Drizo, A., Forget, C., Chapius, R.P., Comeau, Y. (2006). *Phosphorus removal by electric arc furnace steel slag and serpentinite*. Water Research. 40(8). pp. 1547-1554.

Eighmy, T.T., Eusden, J.D., Krzanowski, J.E., Domingo, D.S., Stampfli, D., Martin, J.R., Erickson, P.M. (1995). *Comprehensive approach toward understanding element speciation and leaching behavior in municipal solid waste incinerator electrostatic precipitator ash*. Environmental Science & Technology. 29(3). pp. 629-646.

EPA, U.S. (2006). *TCLP Frequently Asked Questions*.
http://www.epa.gov/sw-846/faqs_tclp.htm.

Fallman, A.-M., Hartlen, J. (1994). *Leaching of slags and ashes. Controlling factors in field experiments versus laboratory tests*. ASTM Special Technical Publication 1198. pp. 39.

Fallman, A.-M., Rosen, B. (2001). *Leaching from Slags and Ashes in Lysimeters*. In: Eighmy, T. T. (Ed.), *Beneficial Use of Recycled Materials in Transportation Applications*. pp. 13-15.

Feldmann, R. M., Biros, D.J., Middleton, D.L. (1982). *Tufa precipitation and its effect on drainage of interstate highways in northeastern Ohio*. Bulletin of the Association of Engineering Geologists. 19(4). pp. 347-370.

Gupta, J.D., Kneller, W.A., Tamirisa, R., Skrzypczak-Jankun, E. (1994). *Characterization of base and subbase iron and steel slag aggregates causing deposition of calcareous tufa in drains*. Transportation Research Record 1434. pp. 8-16.

Harberts (2006). Harbert's Products Inc. <http://www.recycleflux.com/>.

Huijgen, W.J.J., Witkamp, G-J., Comans, R.N.J. (2005). *Mineral CO2 sequestration by steel slag carbonation*. Environmental Science & Technology. 39(24). pp. 9676-9682.

Juckes, L.M. (2003). *The volume stability of modern steelmaking slags*. Transactions of the Institution of Mining and Metallurgy, Section C: Mineral Processing and Extractive Metallurgy. 112(3). pp. 177-197.

Kosson, D.S., van der Sloot, H.A., Eighmy, T.T. (1996). *Approach for estimation of contaminant release during utilization and disposal of*

municipal waste combustion residues. Journal of Hazardous Materials. 47(1-3). pp. 43-75.

Kosson, D.S., van der Sloot, H.A. (1997). *Integration of testing protocols for evaluation of contaminant release from monolithic and granular wastes*. Studies in Environmental Science. 71. pp. 201.

Kosson, D.S., van der Sloot, H.A., Sanchez, F., Garrabrants, A.C. (2002). *An integrated framework for evaluating leaching in waste management and utilization of secondary materials*. Environmental Engineering Science. 19(3). pp. 159-204.

Lehmann, N.K.J., Hansen, J.B., Wahlstrom, M., Fallman, A.-M., Hjelmar, O. (2000). *Influence of critical test conditions on the results of pH-dependent leaching tests*. Report Number-TR 466. Nordtest.

Lemass, B. (1992). *Slag solutions for heavy duty road pavements*. Pavement Performance and Materials. 16(2). pp. 105-118.

Makela, H., Hoynala, H. (2000). *By-products and Recycled Materials in Earth Structures*. Report Number 92/2000. Tekes-National Technology Agency.

Makikyro, M. (2004). *Converting raw materials into the products-road base materials stabilized with slag-based binders*. Academic Dissertation. Faculty of Technology. University of Oulu. pp. 1-156.

Mathur, S., Soni, S.K., Murty, A. (1999). *Utilization of industrial wastes in low-volume roads*. Transportation Research Record 1652. pp. 246-256.

Morishita, S., Kiode, H., Komai, K. (1997). *Development of the new aging process of steel-making slag*. SEASI Quarterly (South East Asia Iron and Steel Institute). 26(1). pp. 37-48.

Motz, H., Geiseler, J. (2001). *Products of steel slags an opportunity to save natural resources*. Waste Management. 21(3). pp. 285-293.

Nomura, T., Enokido, T. (1981). *Study on utilization of BOF slag as road base material*. Nippon Steel Technical Report. 17). pp. 22-23.

NSA (2006). National Slag Association. <http://www.nationalslagassoc.org>.

OEPA (1994). *DSW-0400.007. Beneficial Use of Nontoxic Bottom Ash, Fly Ash and Spent Foundry Sand, and Other Exempt Waste*. Ohio Environmental Protection Agency.

Ogunro, V.O., Inyang, H.I. (2003). *Relating batch and column diffusion coefficients for leachable contaminants in particulate waste materials*. Journal

of Environmental Engineering. 129(10). pp. 930-942.

Pils, J.R.V., Karathanasis, A.D., Mueller, T.G. (2004). *Concentration and distribution of six trace metals in northern Kentucky soils*. Soil and Sediment Contamination. 13(1). pp. 37-51.

Proctor, D. M., Fehling, K. A., Shay, E. C., Wittenborn, J. L., Green, J. J., Avent, C., Bigham, R. D., Connolly, M., Lee, B., Shepker, T.O., Zak, M. A. (2000). *Physical and chemical characteristics of blast furnace, basic oxygen furnace, and electric arc furnace steel industry slags*. Environmental Science & Technology. 34(8). pp. 1576-1582.

Rohde, L., Washington Peres, N., Jorge Augusto Pereira, C. (2003). *Electric arc furnace steel slag: base material for low-volume roads*. Transportation Research Record. 2(1819). pp. 201-207.

Routley, M. (2004). *Opportunities for utilising the slag resulting from submerged arc welding*. Report Number-15102/1/04. The Welding Institute.

SAB (1999). *Waste leachability: the need for review of current agency procedures*. Report Number-EPA-SAB-EEC-COM-99-002. Science Advisory Board Environmental Engineering Committee.

SAIC (2003). *An assessment of laboratory leaching tests for predicting the impacts of fill material on ground water and surface water*. Report Number-03-09-107. Science Applications International Corporation, Washington State Department of Ecology.

Sanchez, F., Gervais, C., Garrabrants, A.C., Barna, R., Kosson, D.S. (2002). *Leaching of inorganic contaminants from cement-based waste materials as a result of carbonation during intermittent wetting*. Waste Management. 22(2). pp. 249-260.

Sanchez, F., Kosson, D.S. (2005). *Probabilistic approach for estimating the release of contaminants under field management scenarios*. Waste Management. 25(5). pp. 463-472.

Schweisstechnik, Bavaria (2006). <http://www.subarcflux.com>.

Simmons, J., Ziemkiewicz, P. (2003). *An Alternative Alkaline Addition for Direct Treatment of Acid Mine Drainage*. The Mining and Environment Conference. Sudbury, Ontario. pp. 1-8.

Skousen, J., Sencindiver, J., Owens, K., Hoover, S. (1998). *Physical properties of minesoils in West Virginia and their influence on wastewater treatment*. Journal of Environmental Quality. 27(3). pp. 633-639.

Today, Recycling Runway Project Halted by Recycled Slag.

<http://www.recyclingtoday.com/news/news.asp?ID=1412&SubCatID=30&CatID=7>.

Tossavainen, M., Yang, Q., Engstrom, F., Menad, N. (2005). *Characteristics of modified steel slag for use in construction*. Submitted to Waste Management, May 2005. pp. 1-27.

Tossavainen, M., Lind, L. (2005). *Leaching results of reactive materials*. Submitted to Construction and Building Materials, September 2005. pp. 1-20.

Turer, D., Maynard, J.B., Sansalone, J.J. (2001). *Heavy metal contamination in soils of urban highways: comparison between runoff and soil concentrations at Cincinnati, Ohio*. Water, Air, and Soil Pollution. 132(3-4). pp. 293-314.

Ugunro, V.O., Inyang, H.I. (2003). *Relating batch and column diffusion coefficients for leachable contaminants in particulate waste materials*. Journal of Environmental Engineering. 129(10). pp. 930-942.

USGS (2006). United States Geological Survey Mineral Commodity Summary. <http://minerals.usgs.gov/minerals/pubs/mcs/>.

van der Sloot, H.A. (1991). *Systematic leaching behaviour of trace elements from construction materials and waste materials*. Proceedings of the International Conference on Environmental Implications of Construction with Waste Materials. Nov. 10-14. Maastricht, The Netherlands. pp. 19.

van der Sloot, H.A., Woelders, H. (2000). *Leaching behavior of essential bioreactor rest product at different stages of degradation in lab and pilot scale to assess potential utilization options*. International Landfill Research Symposium. Dec. 11-13. Lulea, Sweden. pp. 1-11.

van der Sloot, H.A. (2000). *Comparison of the characteristic leaching behavior of cements using standard (EN 196-1) cement mortar and an assessment of their long-term environmental behavior in construction products during service life and recycling*. Cement and Concrete Research. 30(7). pp. 1079-1096.

van der Sloot, H.A., Mulder, E. (2002). *Test methods to assess environmental properties of aggregates in different applications: the role of EN 1744-3*. Report Number-ECN-C--02-011. The Energy Research Center of the Netherlands.

van der Sloot, H.A., Comans, R.N.J., Meeussen, J.C.L., Dijkstra, J.J. (2003). *Annex 5 Compacted Granular Leach Test Horizontal Standard*. Horizontal-23.

van der Sloot, H.A., Dijkstra, J.J. (2004). *Development of horizontally standardized leaching tests for construction materials: a material based or release based approach?* Report Number ECN-C--04-060. The Energy Research Center of the Netherlands.

van Oss, H. (2002). *Iron and steel slag statistic information*. U.S. Geological Survey.

Viklund-White, C., Ye, G. (1999). *Utilization and treatment of steelmaking slags*. Global Symposium on Recycling, Waste Treatment and Clean Technology (REWAS 1999). San Sebastian, Spain. pp. 337-345.

Wang, G., Emery, J. (2004). *Technology of slag utilization in highway construction*. Environmental Benefits of In-situ Material Recycling and Strengthening Session. Quebec City, Quebec. pp. 1-10.

Yan, J., Baverman, C., Moreno, L., Neretnieks, I. (1998). *Evaluation of the time-dependent neutralising behaviours of MSWI bottom ash and steel slag*. Science of the Total Environment. 216(1-2). pp. 41-54.

Yan, J., Moreno, L., Neretnieks, I. (2000). *Long-term acid neutralizing capacity of steel slag*. Waste Management. 20(2). pp. 217-223.

Ziemkiewicz, P. (1998). *Steel slag: application for AMD control*. Proceedings of the 1998 Conference on Hazardous Waste Research. Snowbird, Utah.

Ziemkiewicz, P., Skousen, J.G., Simmons, J.S. (2002). *Long-Term Performance of Passive Acid Mine Drainage Treatment Systems*. <http://www.wvu.edu/~agexten/landrec/PTperform.pdf>.

APPENDIX

Table 1. Total leachable concentration results.

Constituent	BOF Slag	SSFF Slag	SSFW Slag	SAW Slag
Ag	1.294E+03	1.681E+03	1.684E+03	2.445E+04
Al	6.465E+06	8.106E+06	5.488E+06	6.745E+07
As	5.181E+01	0.000E+00	0.000E+00	3.315E+00
Ba	3.123E+04	3.530E+04	3.360E+04	2.434E+05
Be	1.770E+02	1.015E+02	1.362E+02	1.161E+03
Ca	1.876E+08	2.254E+08	2.052E+08	6.962E+07
Cd	1.641E+04	1.011E+04	1.296E+04	1.564E+03
Co	6.810E+03	4.603E+03	5.813E+03	1.533E+04
Cr	8.694E+05	1.124E+06	1.131E+06	5.111E+04
Cu	4.580E+04	1.671E+04	2.870E+04	5.799E+04
Fe	6.484E+08	3.354E+08	5.118E+08	2.307E+07
K	2.876E+05	2.612E+05	2.672E+05	2.537E+06
Mg	4.099E+07	7.397E+07	5.815E+07	8.367E+07
Mn	1.725E+07	2.203E+07	2.166E+07	6.366E+07
Mo	5.909E+03	2.921E+03	5.342E+03	2.560E+03
Na	1.799E+05	2.189E+05	1.398E+05	1.990E+07
Ni	2.228E+04	6.124E+03	1.418E+04	4.841E+04
Pb	6.253E+03	4.996E+03	5.253E+03	7.662E+03
Sb	1.744E+04	1.566E+04	1.833E+04	2.069E+03
Se	0.000E+00	0.000E+00	0.000E+00	2.695E+04
Sn	1.898E+03	1.242E+03	8.110E+03	2.571E+03
Sr	7.658E+04	1.033E+05	8.099E+04	5.310E+04
Ti	1.176E+06	1.350E+06	1.615E+06	1.572E+06
Tl	2.118E+03	5.868E+02	0.000E+00	3.976E+04
V	4.038E+05	5.662E+05	5.340E+05	5.526E+04
Zn	1.573E+05	1.574E+05	2.108E+05	4.389E+04

Notes:

All results in ug/kg

zero values are considered non-detect

Table 2. Availability test results.

Constituent	BOF Slag		SSFF Slag		SSFW Slag		BF Slag		SAW Slag	
	R1	R2	R1	R2	R1	R2	R1	R2	R1	R2
Ag	0.000	0.000	0.000	0.000	0.000	0.000	0.000		11.577	9.950
Al	135359.090	115771.778	47781.883	36248.298	145297.664	234966.893	556711.058		147261.856	157426.143
As	248.722	0.000	263.683	0.000	0.000	0.000	468.254		0.000	0.000
Ba	12446.310	15511.231	14604.130	18567.436	19341.035	21215.221	70923.734		961.864	971.211
Be	0.000	0.000	0.000	0.000	0.000	0.000	449.604		2.956	2.768
Ca	1.350E+08	1.078E+08	1.596E+08	1.481E+08	1.270E+08	1.234E+08	7.751E+07		2.601E+05	3.681E+05
Cd	47.449	205.500	0.000	39.359	0.000	50.055	0.000		2.726	2.836
Co	21.073	0.000	0.000	0.000	0.000	0.000	0.000		78.776	71.958
Cr	1233.113	328.255	1937.809	1902.856	1160.000	985.870	0.000		22.019	16.967
Cu	141.841	129.427	0.000	292.444	0.000	454.236	85.761		0.000	0.000
Fe	6.865E+05	2.769E+06	4.873E+05	4.900E+05	1.774E+06	8.574E+05	7.073E+04		3.060E+04	3.229E+04
K	1.385E+05	3.212E+05	1.465E+05	3.621E+05	2.228E+05	3.055E+05	1.542E+06		1.143E+04	1.358E+04
Mg	7.939E+06	4.918E+06	1.142E+07	7.692E+06	1.025E+07	6.848E+06	1.438E+07		2.436E+05	3.336E+05
Mn	1.428E+06	1.165E+06	1.930E+06	1.351E+06	1.957E+06	1.527E+06	1.132E+06		9.323E+04	2.716E+05
Mo	201.813	0.000	0.000	0.000	0.000	0.000	0.000		1.104	2.289
Na	1.560E+05	1.955E+05	2.135E+05	3.037E+05	2.270E+05	NR	8.564E+05		6.588E+04	7.430E+04
Ni	787.168	648.640	497.153	327.035	1273.307	894.864	195.678		102.621	94.653
Pb	65.680	391.425	0.000	0.000	0.000	0.000	1044.383		14.508	0.000
Sb	168.496	2252.223	0.000	2105.651	614.051	2448.990	2405.114		0.000	1.615
Se	1267.873	369.539	1510.381	1522.328	1529.300	1348.258	618.990		126.088	127.866
Sn	31.047	1076.034	0.000	1107.121	0.000	1115.945	956.363		0.740	0.000
Sr	43292.584	54322.324	65355.122	78880.094	63688.087	57750.749	90511.304		176.773	258.772
Ti	0.000	1954.605	0.000	1966.593	0.000	2279.881	2600.037		55.380	14.733
Tl	1046.531	1878.548	1307.642	2102.712	1466.651	1857.010	1888.331		192.094	182.610
V	7346.065	14401.876	15064.898	20918.117	13380.588	11128.090	1758.621		24.502	27.571
Zn	26135.844	20593.727	21245.942	13795.863	45897.144	38820.490	760.109		127.098	108.545

Notes:

All results in ug/kg

NR= error with ICP analysis

zero values are considered non-detect

Table 3. BOF slag LS ratio leaching results.

Constituent	LS 0.5		LS 1		LS 2	
	R1	R2	R1	R2	R1	R2
Ag	NA	2.53	NA	4.26	NA	4.52
Al	13.23	6.78	29.95	13.60	47.91	39.69
As	1.52	0.92	4.16	2.20	1.12	0.00
Ba	212.64	280.91	371.91	392.54	573.00	648.51
Be	0.00	0.00	0.00	0.00	0.00	0.00
Ca	3.04E+05	5.18E+05	6.10E+05	1.15E+06	1.22E+06	2.33E+06
Cd	0.12	0.00	0.42	0.00	0.38	0.00
Co	NA	0.00	NA	0.00	NA	0.00
Cr	22.35	26.60	43.30	49.37	78.63	85.68
Cu	4.01	3.29	6.37	3.60	9.10	4.66
Fe	4.43	0.55	24.40	3.94	12.09	2.68
K	2.72E+04	3.47E+04	2.79E+04	4.43E+04	2.68E+04	4.51E+04
Mg	4.54	2.78	5.17	8.00	3.33	8.86
Mn	0.00	0.00	0.00	0.00	0.00	0.00
Mo	2.44	3.14	18.50	6.57	0.00	14.54
Na	3.30E+04	3.69E+04	3.92E+04	5.09E+04	4.54E+04	5.98E+04
Ni	0.15	0.59	0.81	1.18	0.10	2.19
Pb	0.59	0.62	2.02	1.16	3.40	0.93
Sb	4.01	2.12	16.76	5.11	13.49	7.29
Se	0.00	2.45	4.99	6.85	6.20	8.17
Sn	NA	0.00	NA	0.31	NA	0.00
Sr	NA	2940.83	NA	3997.72	NA	5091.29
Ti	NA	0.00	NA	0.00	NA	0.00
Tl	0.00	0.00	2.34	0.00	9.12	0.00
V	0.07	0.00	0.47	0.00	0.00	0.00
Zn	5.02	8.18	4.00	4.27	7.92	16.11

Notes:

All results in ug/kg

NA= not analyzed

zero values are considered non-detect

Table 3 (continued). BOF slag LS ratio leaching results.

Constituent	LS 5		LS 10		LS100	
	R1	R2	R1	R2	R1	R2
Ag	NA	3.53	NA	3.20		0.00
Al	131.25	159.91	433.96	344.60		47238.74
As	28.57	52.54	8.55	69.97		607.89
Ba	968.85	972.94	1262.27	1298.68		1842.10
Be	0.00	0.00	0.00	0.00		0.00
Ca	2.98E+06	5.40E+06	5.66E+06	1.03E+07		2.66E+07
Cd	1.70	0.00	3.79	0.00		0.00
Co	NA	0.00	NA	0.00		0.00
Cr	157.93	160.71	251.40	299.16		1483.03
Cu	15.31	6.65	22.90	10.86		0.00
Fe	29.45	5.30	64.50	30.79		493.10
K	3.62E+04	3.41E+04	3.09E+04	5.49E+04		4.66E+04
Mg	13.28	17.12	13.31	166.66		2618.45
Mn	0.00	0.00	0.00	0.00		0.00
Mo	0.00	26.12	0.00	39.89		208.64
Na	5.52E+04	6.17E+04	5.38E+04	7.57E+04		1.00E+05
Ni	0.00	3.86	0.37	13.39		77.33
Pb	8.44	0.00	23.30	25.76		11.07
Sb	0.00	31.04	40.79	28.35		427.53
Se	16.40	27.81	0.00	68.93		320.00
Sn	NA	0.00	NA	0.00		0.00
Sr	NA	6155.44	NA	6973.40		8568.57
Ti	NA	0.00	NA	0.00		0.00
Tl	1.45	0.00	26.17	0.00		0.00
V	0.96	0.00	0.00	0.00		722.16
Zn	21.09	7.73	21.80	20.81		171.77

Notes:

All results in ug/kg

NA= not analyzed

zero values are considered non-detect

Table 4. SSFF slag LS ratio leaching results.

Constituent	LS 0.5		LS 1		LS 2	
	R1	R2	R1	R2	R1	R2
Ag	NA	2.86	NA	3.03	NA	1.98
Al	17.15	12.45	44.09	25.82	99.02	69.91
As	2.36	1.24	5.79	0.52	9.27	0.33
Ba	274.98	225.96	536.50	423.96	825.64	602.59
Be	0.25	0.00	0.55	0.00	1.03	0.00
Ca	3.16E+05	6.75E+05	6.67E+05	1.44E+06	1.39E+06	2.90E+06
Cd	0.42	0.03	0.92	0.00	1.37	0.02
Co	NA	0.00	NA	0.00	NA	0.00
Cr	20.74	14.74	33.46	26.64	57.93	46.66
Cu	0.00	0.18	0.00	0.00	12.82	0.00
Fe	0.00	9.23	0.00	5.05	0.00	10.37
K	3.55E+04	3.03E+04	3.58E+04	3.38E+04	3.23E+04	2.69E+04
Mg	1.52	0.18	4.76	0.00	7.76	0.00
Mn	0.00	0.00	0.00	0.00	0.00	0.00
Mo	1.96	0.92	3.64	1.71	6.58	3.77
Na	4.85E+04	3.60E+04	8.24E+04	6.25E+04	9.52E+04	6.90E+04
Ni	0.07	0.64	0.00	0.00	0.00	0.00
Pb	0.31	1.08	0.88	0.59	0.00	4.20
Sb	0.00	0.71	0.00	1.29	0.00	11.71
Se	3.10	3.98	0.00	6.67	12.73	5.49
Sn	NA	1.63	NA	0.06	NA	2.70
Sr	NA	4167.97	NA	5580.55	NA	6357.46
Ti	NA	0.00	NA	0.00	NA	0.00
Tl	0.00	0.00	0.00	0.00	0.00	0.46
V	0.00	0.00	0.00	0.00	0.00	0.00
Zn	0.00	2.31	0.00	3.23	4.92	6.78

Notes:

All results in ug/kg

NA= not analyzed

zero values are considered non-detect

Table 4 (continued). SSFF slag LS ratio leaching results.

Constituent	LS 5		LS 10		LS100	
	R1	R2	R1	R2	R1	R2
Ag	NA	0.00	NA	0.00	NA	0.00
Al	280.90	194.13	715.67	484.16	37326.14	31629.50
As	22.10	6.64	19.73	11.51	342.26	80.64
Ba	1282.97	928.39	1655.78	1089.29	3082.30	1097.06
Be	2.49	0.00	4.93	0.00	60.59	0.00
Ca	3.39E+06	7.45E+06	6.62E+06	1.43E+07	3.37E+07	4.44E+07
Cd	5.67	0.20	12.02	0.00	80.97	0.00
Co	NA	0.00	NA	0.00	NA	0.00
Cr	114.97	101.38	193.95	165.32	906.32	725.23
Cu	4.56	0.00	27.69	0.00	0.00	0.00
Fe	0.00	26.35	0.00	134.27	102.41	931.10
K	3.45E+04	3.12E+04	3.38E+04	3.62E+04	4.89E+04	1.59E+04
Mg	17.57	0.00	70.65	23.95	1134.48	0.00
Mn	0.00	0.00	0.00	0.00	0.00	0.00
Mo	22.47	6.86	127.62	29.84	1106.65	150.99
Na	1.11E+05	8.54E+04	1.21E+05	9.62E+04	1.46E+05	7.68E+04
Ni	0.40	0.00	0.00	0.00	51.05	0.00
Pb	6.60	14.40	34.98	37.76	0.00	0.00
Sb	6.35	0.85	114.51	12.69	1138.22	340.49
Se	5.13	10.36	108.56	66.82	219.19	628.92
Sn	NA	6.80	NA	1.13	NA	24.91
Sr	NA	7536.47	NA	7792.98	NA	782.87
Ti	NA	0.00	NA	0.00	NA	0.00
Tl	0.00	0.00	0.00	0.00	12734.70	86.91
V	0.00	0.00	0.00	0.00	185.80	55.01
Zn	20.36	28.50	69.37	47.74	306.86	22.27

Notes:

All results in ug/kg

NA= not analyzed

zero values are considered non-detect

Table 5. SSFW slag LS ratio leaching results.

Constituent	LS 0.5		LS 1		LS 2	
	R1	R2	R1	R2	R1	R2
Ag	NA	2.11	NA	3.14	NA	3.10
Al	4.63	12.22	12.77	40.70	36.53	101.11
As	1.81	0.99	1.56	2.26	5.87	3.51
Ba	244.18	350.67	446.64	493.11	755.82	663.98
Be	0.00	0.00	0.00	0.00	0.00	0.00
Ca	3.56E+05	5.70E+05	7.02E+05	1.15E+06	1.40E+06	2.23E+06
Cd	0.00	0.00	0.00	0.00	0.00	0.00
Co	NA	0.00	NA	0.00	NA	0.00
Cr	19.08	11.24	35.33	22.45	66.06	34.49
Cu	3.40	3.62	5.92	4.82	9.23	5.53
Fe	2.71	0.74	5.24	2.02	12.47	1.93
K	9.30E+03	1.46E+04	1.77E+03	1.63E+04	5.55E+03	1.49E+04
Mg	3.00	9.22	4.25	3.11	13.25	9.08
Mn	0.00	0.00	0.00	0.00	0.00	0.00
Mo	0.00	2.31	10.71	5.03	9.91	8.58
Na	1.32E+04	1.71E+04	1.01E+04	2.01E+04	1.44E+04	2.13E+04
Ni	0.21	0.87	0.32	1.21	0.55	2.27
Pb	0.52	0.71	0.54	0.00	2.70	3.00
Sb	2.48	0.34	1.30	8.08	0.00	8.87
Se	0.00	2.39	0.00	7.97	5.90	15.89
Sn	NA	0.79	NA	1.19	NA	0.00
Sr	NA	2085.62	NA	3035.89	NA	3738.85
Ti	NA	0.00	NA	0.00	NA	0.00
Tl	1.20	0.00	1.21	0.00	2.44	0.00
V	0.15	0.00	0.00	0.00	1.82	0.00
Zn	0.53	32.77	0.21	9.08	16.03	5.49

Notes:

All results in ug/kg

NA= not analyzed

zero values are considered non-detect

Table 5 (continued). SSFW slag LS ratio leaching results.

Constituent	LS 5		LS 10		LS100	
	R1	R2	R1	R2	R1	R2
Ag	NA	2.56	NA	0.85	NA	13.76
Al	155.15	211.56	360.71	936.83	37972.73	47413.41
As	0.00	12.76	0.00	30.82	174.45	133.77
Ba	1214.11	975.67	1568.72	1282.46	1949.28	1972.83
Be	0.00	0.00	0.00	0.00	0.00	0.00
Ca	3.36E+06	5.30E+06	6.36E+06	9.37E+06	1.66E+07	2.10E+07
Cd	0.00	0.00	0.00	0.00	0.00	0.00
Co	NA	0.00	NA	0.00	NA	0.00
Cr	123.53	76.99	207.20	146.19	1035.99	852.88
Cu	14.48	5.92	21.96	1.17	4.91	0.00
Fe	26.95	0.00	72.46	5.45	1550.08	243.11
K	2.40E+03	1.37E+04	7.16E+03	1.33E+04	1.83E+04	1.53E+04
Mg	29.10	17.20	74.39	31.32	1747.65	3057.67
Mn	0.00	0.00	0.17	0.00	11.16	0.00
Mo	79.92	26.73	44.71	40.03	1257.69	151.12
Na	1.01E+04	2.26E+04	1.42E+04	2.06E+04	2.12E+04	2.71E+04
Ni	1.12	0.52	3.66	3.02	0.00	97.42
Pb	4.32	0.64	13.79	14.02	58.11	111.03
Sb	73.99	22.11	0.00	40.15	2018.15	231.81
Se	0.00	17.79	0.00	41.37	544.65	947.82
Sn	NA	0.00	NA	1.40	NA	110.03
Sr	NA	4580.90	NA	4820.52	NA	4870.11
Ti	NA	0.00	NA	0.00	NA	0.00
Tl	7.24	0.00	33.79	0.00	50.04	0.00
V	3.20	0.00	6.68	0.00	1696.26	2072.54
Zn	14.61	0.00	51.11	9.72	86.12	0.00

Notes:

All results in ug/kg

NA= not analyzed

zero values are considered non-detect

Table 6. SAW slag LS ratio leaching results.

Constituent	LS 0.5		LS 1		LS 2	
	R1	R2	R1	R2	R1	R2
Ag	NA	0.00	NA	0.00	NA	0.00
Al	6.37E+03	5.11E+03	5.75E+03	5.23E+03	6.15E+03	7.88E+03
As	1.95	1.85	5.64	0.00	8.63	0.00
Ba	1.27	442.29	9.99	213.40	16.46	28.68
Be	0.00	0.00	0.00	0.00	0.00	0.00
Ca	1.59E+03	7.85E+03	8.89E+03	3.57E+04	4.59E+04	1.24E+05
Cd	0.16	0.00	0.37	0.00	0.47	0.00
Co	NA	0.00	NA	0.00	NA	0.00
Cr	17.68	3.73	13.29	2.78	10.33	3.88
Cu	16.62	1.28	14.53	0.06	14.36	0.00
Fe	10.02	1.62	34.31	0.00	33.28	0.00
K	5.36E+04	1.25E+04	7.47E+04	1.11E+04	8.46E+04	1.19E+04
Mg	9.02	46.46	52.96	175.89	321.62	680.86
Mn	7.45	2.22	5.34	1.29	59.53	2.73
Mo	60.57	23.03	80.98	18.08	37.68	22.76
Na	3.59E+04	4.34E+04	8.18E+04	8.11E+04	1.77E+05	1.24E+05
Ni	0.60	0.00	0.42	0.00	0.71	0.00
Pb	0.00	0.00	2.10	0.00	0.00	0.00
Sb	5.64	0.69	36.62	1.78	10.12	10.33
Se	0.08	1.94	0.00	2.68	2.63	2.16
Sn	NA	0.00	NA	2.00	NA	4.31
Sr	NA	12.93	NA	33.61	NA	77.87
Ti	NA	0.00	NA	0.97	NA	2.15
Tl	0.81	1.05	2.20	0.00	1.70	0.00
V	71.95	0.00	55.04	11.74	38.19	16.90
Zn	0.07	14.25	8.61	14.53	109.50	0.73

Notes:

All results in ug/kg

NA= not analyzed

zero values are considered non-detect

Table 6 (continued). SAW slag LS ratio leaching results.

Constituent	LS 5		LS 10		LS100	
	R1	R2	R1	R2	R1	R2
Ag	NA	0.00	NA	2.62	NA	0.00
Al	1.03E+04	2.08E+04	1.79E+04	3.61E+04	1.46E+05	2.84E+05
As	1.15	26.36	37.67	0.00	525.00	0.00
Ba	456.01	59.65	156.47	809.46	855.07	1639.07
Be	0.00	0.00	0.00	0.00	0.00	0.00
Ca	2.23E+05	2.94E+05	5.27E+05	3.85E+05	1.90E+06	8.64E+05
Cd	1.74	0.00	2.93	0.00	35.84	0.00
Co	NA	0.00	NA	0.00	NA	0.00
Cr	11.42	11.81	36.14	16.07	185.64	92.24
Cu	15.25	0.00	12.56	0.00	29.21	0.00
Fe	43.05	1.09	83.81	13.52	538.56	41.18
K	1.09E+05	1.69E+04	9.90E+04	1.39E+04	1.25E+05	2.80E+04
Mg	1356.55	1949.74	4.60E+03	5.91E+03	1.88E+05	2.60E+05
Mn	2.34	6.78	2.21	7.67	6.23	349.46
Mo	38.44	42.56	14.54	57.88	0.00	460.11
Na	4.30E+05	2.06E+05	5.20E+05	2.07E+05	7.80E+05	3.32E+05
Ni	0.00	0.00	2.23	2.97	0.00	11.23
Pb	0.00	0.00	0.00	0.00	0.00	0.00
Sb	8.09	19.49	46.90	86.21	364.53	669.96
Se	1.54	18.58	27.02	42.48	205.34	342.95
Sn	NA	8.14	NA	17.12	NA	140.06
Sr	NA	224.55	NA	300.56	NA	718.45
Ti	NA	6.32	NA	11.43	NA	102.59
Tl	7.65	0.00	19.99	0.00	338.59	389.75
V	57.74	56.92	108.99	102.01	720.88	612.65
Zn	31.50	30.06	55.54	61.73	0.00	106.46

Notes:

All results in ug/kg

NA= not analyzed

zero values are considered non-detect

Table 7. BF slag LS ratio leaching results.

Constituent	LS 0.5	LS 1	LS 2	LS 5	LS 10	LS 100
Ag	0.73	1.01	1.51	1.92	2.94	22.93
Al	89.63	203.43	528.02	2424.63	7179.08	151866.35
As	0.00	0.00	7.00	0.00	30.49	66.38
Ba	29.11	53.19	103.45	262.95	579.94	6927.49
Be	0.00	0.00	0.00	0.00	0.00	0.00
Ca	4.93E+05	9.26E+05	1.79E+06	1.65E+06	1.99E+06	3.68E+06
Cd	0.00	0.00	0.00	0.00	0.00	0.00
Co	0.00	0.00	0.00	0.00	0.00	0.00
Cr	0.44	1.27	2.55	4.41	6.12	19.32
Cu	1.56	2.47	4.50	5.31	8.58	74.28
Fe	1.54	1.73	2.68	6.75	18.66	83.02
K	9.94E+04	1.40E+05	1.95E+05	2.24E+05	2.36E+05	2.66E+05
Mg	432.50	859.56	1789.85	2947.58	5133.44	33094.20
Mn	0.48	0.39	2.17	6.17	14.79	85.93
Mo	0.00	0.00	0.00	0.00	0.00	0.00
Na	3.51E+04	4.48E+04	5.56E+04	5.95E+04	5.92E+04	2.66E+04
Ni	0.07	-0.05	0.17	0.00	4.57	-58.98
Pb	0.00	0.00	0.00	0.00	0.00	0.00
Sb	0.00	0.00	0.00	0.00	0.00	0.00
Se	9.37	26.60	35.48	66.85	45.43	761.74
Sn	12.63	11.44	0.00	0.00	0.00	0.00
Sr	750.52	1193.80	2043.53	2513.77	3016.63	4230.45
Ti	0.00	0.00	0.00	0.00	0.00	0.00
Tl	0.16	0.00	0.00	0.00	1.84	110.02
V	0.08	0.27	0.42	0.00	0.00	0.00
Zn	1.44	1.20	0.62	2.64	1.18	113.90

Notes:

All results in ug/kg

zero values are considered non-detect

Table 8. BOF slag pH dependent leaching results.

pH	1.55	2.2	4.6	4.75	5.28	5.6	6.13	6.51	6.56
Round	1	2	1	2	1	2	2	2	2
Ag	0.0	552.2	0.0	502.2	0.0	268.0	141.7	120.9	33.0
Al	5.66E+06	5.61E+06	5.48E+04	2.36E+05	5.79E+03	2.70E+04	1837.7	461.1	0.0
As	233.8	0.0	33.4	0.0	534.3	0.0	0.0	0.0	2.5
Ba	33407.8	28812.5	12314.1	17016.6	7804.9	9845.3	5556.3	3566.8	1736.8
Be	105.1	185.7	15.6	28.2	7.8	18.2	8.4	6.4	5.4
Ca	8.57E+07	1.13E+08	9.17E+06	1.09E+07	5.88E+07	1.10E+07	1.10E+07	1.09E+07	1.08E+07
Cd	5349.1	3563.5	1656.0	3325.4	390.3	1168.1	224.3	116.6	4.7
Co	0.0	377265.1	0.0	2412.1	0.0	267.8	140.5	127.4	23.4
Cr	389485.0	377265.1	123.9	2412.1	0.0	267.8	140.5	127.4	23.4
Cu	96358.4	17315.4	0.0	0.0	0.0	0.0	0.0	0.0	34.8
Fe	5.83E+07	8.14E+07	8.68E+06	1.88E+07	6.72E+06	1.60E+07	4.82E+06	2.50E+06	571.8
K	1.92E+05	1.65E+05	1.85E+05	1.75E+05	9.53E+04	1.22E+05	9.56E+04	8.38E+04	9.19E+04
Mg	2.56E+07	2.85E+07	1.01E+07	1.52E+07	1.00E+07	1.21E+07	7.80E+06	6.89E+06	7.21E+06
Mn	6.96E+06	2.64E+07	1.18E+06	6.38E+06	2.76E+06	7.46E+06	6.08E+06	5.47E+06	2.19E+05
Mo	1184.0	1641.4	0.0	0.0	0.0	0.0	0.0	18.2	151.5
Na	2.89E+05	1.40E+05	1.82E+05	9.08E+04	1.65E+05	7.67E+04	6.93E+04	6.10E+04	6.75E+04
Ni	8550.2	9515.4	2342.7	3160.6	1653.1	3522.9	1146.7	827.5	491.1
Pb	1098.6	261.3	552.2	1132.3	0.0	459.4	134.5	66.2	34.6
Sb	6464.3	7301.7	587.5	1661.7	173.5	659.4	142.2	74.2	0.0
Se	0.0	0.0	0.0	0.0	0.0	311.5	464.0	674.1	179.8
Sn	0.0	156.3	0.0	241.8	0.0	82.2	23.0	11.8	29.6
Sr	0.0	82304.2	0.0	46901.7	0.0	37991.5	30667.9	27520.4	25079.4
Ti	0.0	1766798.6	0.0	3.1	0.0	95.3	0.0	0.0	0.0
Tl	0.0	0.0	1704.6	2791.0	1510.1	2101.6	1416.4	1225.8	196.1
V	2.65E+05	2.45E+05	140.0	1472.1	0.0	0.0	3.5	0.0	31.6
Zn	94191.0	70059.2	53485.1	42798.6	23995.7	34298.8	9247.9	3809.3	160.8

Notes:

All results in ug/kg

zero values are considered non-detect

Table 8 (continued). BOF slag pH dependent leaching results.

pH	7.58	8.03	8.47	9.44	9.87	10.23	11.32	11.9
Round	2	1	2	1	2	1	1	2
Ag	9.0	0.0	5.5	0.0	1.0	0.0	0.0	2.2
Al	0.0	2.6	44.8	0.0	578.0	29.2	955.9	190.4
As	4.8	90.7	0.0	72.9	43.3	59.5	76.8	6.0
Ba	607.6	1116.4	771.8	781.8	1394.7	1565.4	1393.5	1575.8
Be	5.1	0.0	5.2	0.1	5.3	0.1	0.3	5.2
Ca	1.10E+07	9.23E+06	1.11E+07	9.24E+06	1.12E+07	9.25E+06	9.29E+06	1.12E+07
Cd	4.2	0.0	5.3	0.0	4.0	0.0	0.0	4.2
Co	3.6	0.0	2.5	0.0	3.3	0.0	0.0	375.2
Cr	3.6	0.0	2.5	0.0	3.3	0.0	0.0	375.2
Cu	18.9	27.6	103.8	45.9	21.5	14.9	6.0	8.3
Fe	217.0	0.0	0.0	0.0	12.6	0.0	0.0	0.0
K	7.68E+04	8.75E+04	7.88E+04	8.20E+04	6.78E+04	6.06E+04	5.67E+04	5.44E+04
Mg	5.73E+06	5.19E+06	2.41E+06	3.86E+06	1.22E+04	2.26E+05	0.0	644.5
Mn	6.54E+03	88039.0	0.0	0.0	0.0	0.0	0.0	0.0
Mo	174.6	143.0	150.7	136.1	148.8	137.3	139.7	104.8
Na	6.21E+04	1.14E+05	6.24E+04	1.11E+05	5.39E+04	9.49E+04	8.35E+04	5.16E+04
Ni	39.0	210.8	8.0	41.3	0.0	12.0	0.0	0.0
Pb	0.0	31.0	6.4	13.2	8.7	0.0	24.1	9.1
Sb	10.2	27.6	34.8	62.9	37.4	3.8	65.3	0.0
Se	31.2	15.4	124.3	17.4	40.7	0.0	0.0	57.1
Sn	9.9	0.0	0.0	0.0	7.1	0.0	0.0	18.3
Sr	21061.3	0.0	18192.2	0.0	15804.4	0.0	0.0	12283.9
Ti	14.5	0.0	0.0	0.0	0.0	0.0	0.0	0.0
Tl	0.0	4.5	0.0	0.0	0.0	0.0	21.4	0.0
V	653.3	163.2	574.1	1131.8	625.5	837.6	276.6	30.8
Zn	0.0	44.0	85.2	25.7	30.6	0.0	0.0	0.0

Notes:

All results in ug/kg

zero values are considered non-detect

Table 9. SSFF slag pH dependent leaching results.

pH	0.96	1.51	3.18	4.85	5.1	5.19	5.62	5.73	5.94	6.39
Round	1	1	2	2	1	1	1	2	2	1
Ag	0.00	0.00	386.32	324.62	0.00	0.00	0.00	174.50	171.44	0.00
Al	8.5E+06	7.7E+06	4.5E+06	5.1E+03	1194.93	1518.27	675.89	919.94	961.85	450.46
As	290.25	211.20	0.00	0.00	13.60	76.56	110.02	0.00	0.00	72.90
Ba	2.4E+04	2.4E+04	2.2E+04	2.0E+04	9.4E+03	1.5E+04	6.1E+03	7.5E+03	7.8E+03	3178.57
Be	51.10	52.62	40.74	0.00	3.89	3.07	3.03	0.00	0.00	2.70
Ca	8.6E+06	8.6E+06	1.2E+07	1.2E+07	8.6E+06	8.5E+06	8.6E+06	1.2E+07	1.2E+07	8.6E+06
Cd	3798.03	3221.96	12.96	1049.72	122.26	741.77	9.14	28.22	82.89	0.00
Co	0.00	0.00	495.26	790.96	0.00	0.00	0.00	226.53	250.22	0.00
Cr	5.1E+05	4.5E+05	4.1E+03	187.30	115.77	165.10	91.31	140.42	125.38	71.72
Cu	1.1E+04	9.4E+03	6.6E+03	0.00	5.55	0.00	57.73	36.75	26.76	87.87
Fe	6.2E+07	5.5E+07	6.0E+04	5.7E+06	2.4E+06	1.4E+07	1.2E+05	3.6E+05	9.4E+05	2.4E+06
K	2.3E+05	2.4E+05	2.8E+05	1.9E+05	1.1E+05	1.6E+05	9.5E+04	1.2E+05	1.1E+05	9.7E+04
Mg	4.0E+07	3.6E+07	1.7E+07	1.7E+07	1.5E+07	2.8E+07	1.4E+07	1.2E+07	1.1E+07	1.4E+07
Mn	8.2E+05	8.8E+05	7.9E+05	8.4E+05	1.3E+06	1.2E+06	1.2E+06	9.3E+05	9.6E+05	1.1E+06
Mo	856.67	594.31	0.39	0.00	0.00	0.00	80.92	30.73	20.18	85.65
Na	3.6E+05	3.8E+05	2.1E+05	2.0E+05	2.4E+05	3.0E+05	2.3E+05	1.8E+05	1.7E+05	2.5E+05
Ni	1.7E+03	1.4E+03	1.3E+03	2.0E+03	7.1E+02	1.5E+03	6.5E+02	6.9E+02	7.2E+02	5.6E+02
Pb	1754.20	1425.55	273.63	556.49	0.00	222.25	127.13	154.10	106.96	91.44
Sb	3306.36	2573.49	0.00	404.32	88.97	262.18	64.14	0.00	0.00	51.44
Se	0.00	0.00	2045.93	514.51	509.49	541.76	712.84	1182.44	1021.60	419.45
Sn	0.00	0.00	0.00	70.27	0.00	0.00	0.00	0.00	0.00	0.00
Sr	0.00	0.00	6.6E+04	6.1E+04	0.00	0.00	0.00	4.7E+04	4.5E+04	0.00
Ti	0.00	0.00	116.46	0.00	0.00	0.00	0.00	0.00	0.00	0.00
Tl	0.00	0.00	2493.03	2223.61	1842.79	2450.04	1538.66	1564.83	1590.53	1136.03
V	5.0E+05	4.0E+05	0.00	0.00	0.00	0.00	0.00	0.00	0.00	48.94
Zn	4.4E+04	4.2E+04	3.5E+04	3.7E+04	2.5E+04	2.3E+04	1.2E+01	2.2E+04	2.3E+04	520.57

Notes:

All results in ug/kg

zero values are considered non-detect

Table 9 (continued). SSFF slag pH dependent leaching results.

pH	6.94	7.95	8.14	8.97	9.38	9.73	10.65	11.7	11.82
Round	2	1	2	2	1	2	2	1	2
Ag	107.37	0.00	44.33	25.89	0.00	18.46	13.88	0.00	10.18
Al	383.99	0.00	0.00	0.00	0.00	0.00	124.96	391.07	640.29
As	0.00	122.47	0.00	0.00	114.50	0.00	8.62	101.84	1.46
Ba	2117.86	1120.41	945.73	1426.97	1248.64	930.71	2086.76	2030.02	1490.26
Be	0.00	2.60	0.00	0.00	2.17	0.00	0.00	2.26	0.00
Ca	1.2E+07	8.6E+06	1.2E+07	1.2E+07	8.6E+06	1.2E+07	1.3E+07	8.7E+06	1.3E+07
Cd	0.00	0.00	0.00	0.00	0.00	0.00	0.00	0.00	0.00
Co	0.00	0.00	0.00	0.00	0.00	0.00	0.00	0.00	0.00
Cr	74.16	0.00	22.14	18.22	50.49	57.04	81.24	421.01	427.21
Cu	78.30	51.17	38.27	44.31	44.78	44.82	35.94	43.33	24.71
Fe	1.7E+03	0.00	299.38	1.57	0.00	8.39	82.87	0.00	17.26
K	9.5E+04	7.8E+04	1.0E+05	9.2E+04	5.9E+04	8.5E+04	7.7E+04	4.7E+04	5.6E+04
Mg	9.6E+06	1.1E+07	8.3E+06	6.7E+06	3.4E+06	2.7E+06	2.1E+04	8.2E+02	6.2E+02
Mn	7.2E+05	2.5E+05	2.0E+05	1.0E+04	0.00	15.36	18.20	0.00	1.93
Mo	108.69	503.49	136.29	117.08	61.23	127.52	109.90	18.39	62.37
Na	1.6E+05	2.2E+05	1.5E+05	1.4E+05	1.9E+05	1.3E+05	1.2E+05	1.4E+05	1.1E+05
Ni	3.2E+02	71.24	87.47	25.39	13.21	15.33	12.44	0.00	8.84
Pb	116.83	0.72	53.26	2.93	0.00	13.98	10.08	0.00	2.20
Sb	0.00	428.47	16.94	46.82	13.07	59.93	0.00	44.05	36.02
Se	759.10	30.49	180.20	65.34	0.00	63.77	156.99	0.00	95.89
Sn	0.00	0.00	0.00	0.00	0.00	8.84	0.00	0.00	0.00
Sr	39876.13	0.00	3.5E+04	3.0E+04	0.00	2.6E+04	2.3E+04	0.00	16756.22
Ti	0.00	0.00	0.00	0.00	0.00	0.00	0.00	0.00	0.00
Tl	777.10	95.69	163.85	0.00	9.22	0.00	0.00	0.00	0.00
V	95.31	770.75	975.41	1523.36	1309.74	1446.66	976.98	13.19	0.18
Zn	181.87	0.00	0.00	57.84	0.00	0.00	2.04	0.00	0.38

Notes:

All results in ug/kg

zero values are considered non-detect

Table 10. SSFW slag pH dependent leaching results.

pH	1.17	3.85	4.48	5.22	5.4	6.12	6.6	6.68
Round	1	1	1	1	2	2	1	2
Ag	0.00	0.00	0.00	0.00	30.58	50.24	0.00	25.48
Al	4.32E+06	2.30E+05	5.18E+04	2827.89	1.82E+04	1528.22	0.00	430.66
As	1814.38	121.44	42.86	99.59	0.00	0.00	76.13	0.00
Ba	27760.07	15554.88	11755.64	6354.37	8761.47	4110.81	1124.79	1542.00
Be	126.09	30.23	22.75	9.51	25.07	17.57	0.00	16.01
Ca	7.89E+07	7.4E+07	6.7E+07	5.88E+07	2.72E+07	3.09E+07	9.27E+06	2.79E+07
Cd	4219.03	3386.82	1858.58	671.89	1261.02	295.93	0.00	45.15
Co	0.00	0.00	0.00	0.00	289.15	103.03	0.00	21.78
Cr	310086.30	5117.53	376.16	63.20	17.58	9.10	0.00	3.25
Cu	14339.64	0.00	0.00	0.00	0.00	0.00	43.84	4.48
Fe	5.28E+07	5.09E+07	3.22E+07	1.37E+07	1.15E+07	5.87E+06	0.00E+00	7.26E+05
K	1.38E+05	1.16E+05	8.87E+04	8.58E+04	2.53E+05	1.70E+05	3.33E+04	1.03E+05
Mg	2.29E+07	2.16E+07	1.81E+07	1.22E+07	1.07E+07	8.15E+06	4.45E+06	6.10E+06
Mn	6.17E+06	6.09E+06	5.03E+06	3.18E+06	0.00	0.00	2.64E+05	0.00
Mo	1155.57	0.00	0.00	13.86	0.00	0.00	127.53	0.00
Na	1.83E+05	1.63E+05	1.55E+05	1.39E+05	1.25E+05	9.40E+04	4.76E+04	6.52E+04
Ni	7326.47	3629.31	3513.59	1418.59	1156.84	431.58	593.26	50.13
Pb	1231.22	1118.80	622.10	264.32	1407.74	286.56	33.46	13.04
Sb	6417.29	1186.29	714.54	289.01	428.76	139.50	0.00	8.59
Se	0.00	0.00	0.00	209.99	164.98	457.67	105.76	243.74
Sn	0.00	0.00	0.00	0.00	209.46	82.29	0.00	26.95
Sr	0.00	0.00	0.00	0.00	28203.36	22722.20	0.00	16749.65
Ti	0.00	0.00	0.00	0.00	0.00	0.00	0.00	0.00
Tl	0.00	1878.95	1760.33	1303.54	1176.41	793.72	180.97	334.93
V	214899.74	6398.95	483.48	62.44	1918.70	356.69	5.29	0.00
Zn	82923.92	56936.82	50066.73	26016.51	35477.27	5399.87	132.53	120.05

Notes:

All results in ug/kg

zero values are considered non-detect

Table 10 (continued). SSFW slag pH dependent leaching results.

pH	9.02	9.45	9.45	9.52	9.88	10.1	10.85	12.17
Round	2	1	2	2	2	1	2	1
Ag	22.60	0.00	23.57	19.06	18.53	0.00	19.53	0.00
Al	93.01	0.00	147.00	98.83	120.33	0.00	979.91	0.00
As	36.38	58.24	20.05	0.00	43.93	67.86	0.00	90.64
Ba	487.34	286.97	939.99	439.98	876.32	933.43	1143.82	1263.98
Be	19.39	0.00	15.99	15.91	15.87	0.00	15.92	0.00
Ca	2.64E+07	9.29E+06	3.29E+07	2.59E+07	2.63E+07	9.28E+06	2.49E+07	6.52E+06
Cd	1.40	0.00	0.00	0.00	0.00	0.00	0.00	0.00
Co	8.33	0.00	5.90	2.54	3.88	0.00	4.21	0.00
Cr	17.93	0.00	9.95	12.75	13.77	0.00	14.25	260.46
Cu	35.66	47.49	41.16	28.60	26.29	34.36	26.38	15.25
Fe	26.68	0.00	31.36	28.77	24.59	0.00	189.99	0.00
K	7.49E+04	2.82E+04	9.68E+04	7.26E+04	5.78E+04	2.26E+04	4.91E+04	8281.89
Mg	4.65E+06	3.00E+06	2.40E+06	3.25E+06	4.81E+05	3.73E+05	1.05E+04	0.00
Mn	0.00	0.00	0.00	0.00	0.00	0.00	0.00	0.00
Mo	0.00	126.45	0.00	0.00	0.00	119.17	0.00	1.70
Na	5.51E+04	4.01E+04	5.99E+04	5.10E+04	4.39E+04	3.37E+04	4.13E+04	1.78E+04
Ni	23.26	18.46	16.33	18.19	8.18	8.23	11.28	0.00
Pb	0.00	5.41	3.81	17.14	4.17	9.60	0.00	0.00
Sb	0.00	12.90	44.70	26.69	11.23	15.25	0.68	11.83
Se	55.24	0.00	84.58	111.82	71.00	6.26	142.25	0.00
Sn	53.18	0.00	8.88	1.07	39.09	0.00	13.66	0.00
Sr	15165.31	0.00	17206.69	14223.04	13457.35	0.00	12227.13	0.00
Ti	0.00	0.00	0.00	0.00	0.00	0.00	0.00	0.00
Tl	0.00	0.00	26.35	16.80	16.16	0.00	0.00	36.55
V	970.18	1386.42	585.77	526.52	492.40	822.12	560.43	0.00
Zn	0.00	0.00	0.00	0.00	0.00	0.00	0.00	0.00

Notes:

All results in ug/kg

zero values are considered non-detect

Table 11. SAW slag pH dependent leaching results.

pH	3.01	4.05	4.85	4.89	5.23	5.91	6	6
Round	1	2	1	2	1	2	2	2
Ag	0.00	2007.81	0.00	490.26	0.00	185.22	61.85	55.08
Al	4.6E+07	1.4E+07	4.8E+06	5.9E+06	2.2E+06	4.1E+05	2.7E+05	1.6E+05
As	0.00	0.00	0.00	0.00	0.00	31.25	3.40	0.00
Ba	2.61E+05	1.55E+05	5.58E+04	2.73E+04	2.02E+04	2056.22	553.49	362.59
Be	332.08	198.77	96.14	120.77	82.49	36.92	51.62	42.55
Ca	5.5E+07	1.3E+07	3.0E+07	2.0E+07	1.9E+07	5.8E+06	5.1E+06	3.9E+06
Cd	231.40	314.94	518.72	436.57	471.39	25.27	10.57	2.12
Co	0.00	2.41E+04	0.00	10989.36	0.00	3342.39	2109.88	1514.55
Cr	2030.45	1687.53	1108.74	169.94	629.35	241.16	42.43	33.33
Cu	2.19E+04	1.78E+04	134.81	0.00	0.00	0.00	0.00	0.00
Fe	1.3E+05	4.7E+04	5.6E+06	4.2E+06	5.1E+06	4.6E+05	1.7E+05	5.7E+04
K	3.8E+06	2.4E+06	1.3E+06	1.9E+06	6.9E+05	1.9E+05	1.9E+05	1.4E+05
Mg	6.7E+07	3.1E+07	3.3E+07	2.1E+07	1.9E+07	5.3E+06	4.1E+06	3.3E+06
Mn	1.64E+07	7.44E+05	1.54E+07	0.00	1.25E+07	5.03E+06	0.00	0.00
Mo	10.03	55.68	50.04	551.67	133.51	92.14	171.89	141.97
Na	9.2E+06	6.1E+05	8.8E+06	8.4E+05	6.0E+06	8.8E+05	8.6E+05	7.5E+05
Ni	2.7E+04	2.4E+04	1.7E+04	1.4E+04	1.3E+04	2.8E+03	2.1E+03	1.5E+03
Pb	2475.58	2062.56	981.98	683.97	587.68	0.00	154.42	112.21
Sb	14.10	79.69	160.60	105.36	209.75	29.56	57.07	12.68
Se	1.28E+04	1.50E+04	7346.08	4873.97	4676.12	1972.96	1074.46	821.23
Sn	0.00	0.00	0.00	83.48	0.00	0.00	19.92	13.92
Sr	0.00	34563.39	0.00	23589.97	0.00	3001.58	1845.68	1322.10
Ti	0.00	13.15	0.00	90.97	0.00	0.00	20.17	19.42
Tl	2.0E+04	1.9E+04	1.3E+04	7047.56	8899.41	2835.18	1529.97	1068.21
V	0.00	0.00	0.00	80.44	0.00	12.56	5.97	16.67
Zn	2.5E+04	2.1E+04	1.5E+04	1.3E+04	1.2E+04	2454.86	1381.38	750.51

Notes:

All results in ug/kg

zero values are considered non-detect

Table 11 (continued). SAW slag pH dependent leaching results.

pH	6.02	6.1	6.53	7.77	10.48	11.35	11.66	12.56
Round	1	2	2	1	2	1	2	1
Ag	0.00	153.18	35.21	0.00	7.39	0.00	5.43	0.00
Al	3.3E+05	2.5E+05	4.9E+04	5.7E+02	4.0E+04	8.7E+04	1.3E+05	1.9E+05
As	44.77	14.60	3.27	17.33	7.72	35.85	63.41	15.79
Ba	2485.16	949.69	517.58	767.94	49.15	178.29	1071.27	144.74
Be	33.62	31.09	30.67	0.00	15.86	0.00	16.04	0.00
Ca	3.6E+06	4.4E+06	2.4E+06	1.7E+06	3.7E+05	2.1E+05	1.4E+05	6.0E+04
Cd	12.13	9.69	0.81	5.19	0.00	0.00	0.00	0.00
Co	0.00	2029.54	966.37	0.00	7.03	0.00	3.33	0.00
Cr	211.63	168.73	27.59	86.43	21.88	26.59	24.26	16.99
Cu	21.87	0.00	2.19	9.71	1.07	3.15	16.52	8.14
Fe	2.2E+05	1.6E+05	3249.40	2071.93	92.61	114.97	101.39	447.26
K	2.0E+05	3.7E+05	8.0E+04	8.7E+04	2.2E+04	2.7E+04	4.1E+04	4.3E+04
Mg	4.5E+06	3.4E+06	2.1E+06	2.7E+06	6.5E+03	4.6E+02	3.8E+02	8.0E+01
Mn	1.58E+06	2.41E+06	0.00	1.08E+06	0.00	12.86	0.00	81.86
Mo	33.71	78.99	135.27	29.23	78.61	8.22	78.31	9.23
Na	9.3E+05	8.8E+05	5.2E+05	7.1E+05	2.0E+05	7.9E+05	1.1E+06	7.3E+05
Ni	2.8E+03	1.6E+03	950.98	988.53	5.51	0.00	8.96	0.00
Pb	224.12	0.00	83.80	119.65	0.00	4.71	0.00	1.39
Sb	0.00	32.74	9.21	5.00	13.67	33.95	26.49	0.00
Se	1561.70	1433.14	530.19	611.10	11.73	0.00	0.90	23.85
Sn	0.00	0.00	14.53	0.00	13.07	0.00	13.43	0.00
Sr	0.00	3195.63	569.58	0.00	0.00	0.00	0.00	0.00
Ti	0.00	0.00	20.31	0.00	18.41	0.00	18.55	0.00
Tl	2528.51	1945.39	693.39	1082.55	3.40	25.13	24.06	0.00
V	0.00	14.20	41.36	11.57	101.28	333.05	237.93	412.12
Zn	2193.14	1142.17	229.34	0.00	0.00	0.00	94.82	0.00

Notes:

All results in ug/kg
zero values are considered non-detect

Table 12. BF slag pH dependent leaching results.

pH	3.27	3.75	5.68	6.66	6.78	7.38	7.66	8.55	9.46	10.8	11.66
Ag	71.33	68.56	80.01	63.04	57.44	6.58	3.63	3.14	2.80	2.93	2.39
Al	1.09E+07	1.62E+06	10887.20	1003.55	958.75	434.23	522.31	586.16	1113.44	4089.70	9562.15
As	224.18	0.00	0.00	2.20	6.76	0.00	2.13	0.00	31.06	1.40	0.00
Ba	2.68E+04	1.65E+04	10541.58	7776.57	6557.10	1085.99	636.08	601.87	550.76	648.62	630.15
Be	3556.47	1127.76	0.00	0.00	0.00	0.00	0.00	0.00	0.00	0.00	0.00
Ca	3.49E+07	3.40E+07	3.33E+07	3.05E+07	3.05E+07	1.01E+07	6.12E+06	5.44E+06	4.63E+06	2.41E+06	1.51E+06
Cd	79.76	81.51	41.96	10.67	0.00	0.00	0.00	0.00	0.00	0.00	0.00
Co	0.00	0.00	0.00	0.00	0.00	0.00	0.00	0.00	0.00	0.00	0.00
Cr	1336.15	68.29	10.57	4.83	6.88	0.00	1.13	3.70	1.53	6.59	2.93
Cu	36.07	37.27	34.13	31.43	31.97	10.75	7.31	6.49	7.07	6.73	9.83
Fe	4.88E+05	5.14E+05	3.69E+05	9.05E+04	1.35E+04	13.45	7.96	16.70	10.38	11.21	47.15
K	2.92E+06	2.47E+06	1.70E+06	1.35E+06	1.23E+06	4.30E+05	3.40E+05	3.24E+05	3.08E+05	3.01E+05	3.39E+05
Mg	2.25E+07	2.12E+07	1.83E+07	1.35E+07	1.19E+07	1.20E+06	4.01E+05	2.72E+05	1.47E+05	1970.71	0.00
Mn	8.42E+05	8.31E+05	8.24E+05	8.20E+05	8.01E+05	3.11E+04	1.00E+04	2471.19	155.49	111.43	181.93
Mo	0.00	0.00	0.00	0.00	0.00	0.00	0.00	0.00	0.00	0.00	0.00
Na	1.20E+06	1.18E+06	1.04E+06	7.75E+05	6.65E+05	1.41E+05	9.19E+04	8.38E+04	7.77E+04	6.82E+04	1.13E+06
Ni	26.52	46.64	38.59	25.34	28.57	13.67	3.23	7.78	2.48	0.00	0.00
Pb	84.54	108.10	89.10	45.80	45.49	6.62	0.00	10.49	0.00	0.00	0.00
Sb	39.95	0.00	0.00	0.00	0.00	0.00	0.00	0.00	0.00	0.00	0.00
Se	462.87	343.19	303.42	357.38	359.62	138.31	0.00	11.36	1.59	54.79	0.00
Sn	0.00	0.00	0.00	0.00	0.00	0.00	0.00	0.00	0.00	0.00	0.00
Sr	1.25E+05	1.14E+05	9.15E+04	6.61E+04	5.76E+04	1.10E+04	5.90E+03	5.25E+03	4278.44	2969.79	2086.30
Ti	203.41	0.00	0.00	0.00	0.00	0.00	0.00	0.00	0.00	0.00	0.00
Tl	556.36	564.58	529.26	505.64	550.32	27.52	2.97	0.00	17.52	14.95	0.00
V	3651.79	1158.31	0.00	0.00	0.00	0.00	0.00	15.52	149.07	361.15	11.61
Zn	282.23	136.09	91.41	52.58	13.41	1.55	0.87	0.00	0.00	0.00	16.77

Notes:

All results in ug/kg

zero values are considered non-detect

Table 13. BOF slag CGLT results.

Time	5hr	8hr	24hr	48hr	96hr	192hr	336hr	672hr	1344hr
Al	0.085992	0.045595	0.192558	0.214444	0.271948	0.354744	0.544195	0.499348	0.470005
As	0.0018	0.0049	0.0016	0.0000	0.0000	0.0034	0.0023	0.0063	0.0002
Ba	0.001013	0.000205	0.009615	0.008517	0.024619	0.197903	0.107116	0.087055	0.126825
Be	0.0000	0.0000	0.0000	0.0000	0.0000	0.0000	0.0000	0.0000	0.0000
Ca	4.0060	5.6433	46.6632	73.4527	128.7098	31.5480	474.8855	492.0228	621.5055
Cd	0.0005	0.0003	0.0001	0.0000	0.0001	0.0001	0.0001	0.0000	0.0001
Co	0.0010	0.0001	0.0002	0.0002	0.0003	0.0006	0.0001	0.0000	0.0004
Cr	0.0048	0.0010	0.0018	0.0020	0.0029	0.0036	0.0104	0.0110	0.0151
Cu	0.0018	0.0000	0.0000	0.0000	0.0000	0.0007	0.0027	0.0024	0.0042
Fe	0.0179	0.0164	0.0176	0.0166	0.0167	0.0182	0.0159	0.0172	0.0172
K	7.580785	1.310097	1.844497	1.783523	2.543119	5.033635	12.99785	11.31371	16.65747
Li	0.0010	0.0000	0.0004	0.0003	0.0021	0.0083	0.0172	0.0179	0.0263
Mg	0.0549	0.0337	0.0395	0.0288	0.0221	0.0381	0.0094	0.0103	0.0090
Mn	0.0000	0.0000	0.0000	0.0000	0.0000	0.0000	0.0000	0.0000	0.0000
Mo	0.0060	0.0022	0.0017	0.0017	0.0013	0.0020	0.0019	0.0022	0.0026
Na	12.33736	1.659507	2.525227	2.783477	3.842133	7.651507	14.31662	12.69086	17.10372
Ni	0.0000	0.0000	0.0000	0.0000	0.0000	0.0000	0.0000	0.0000	0.0000
Pb	0.0054	0.0023	0.0031	0.0021	0.0028	0.0030	0.0032	0.0037	0.0026
Sb	0.0031	0.0047	0.0030	0.0019	0.0026	0.0029	0.0015	0.0033	0.0017
Se	0.0030	0.0021	0.0021	0.0065	0.0000	0.0037	0.0049	0.0039	0.0025
Sr	0.0000	0.0043	0.0882	0.1349	0.2194	0.1388	0.8419	0.8329	1.1279
Ti	0.0058	0.0052	0.0049	0.0049	0.0048	0.0050	0.0047	0.0047	0.0047
Tl	0.0026	0.0000	0.0000	0.0000	0.0009	0.0013	0.0025	0.0008	0.0009
V	0.0322	0.0056	0.0073	0.0058	0.0053	0.0111	0.0029	0.0018	0.0017
Zn	0.0003	0.0000	0.0005	0.0001	0.0005	0.0207	0.0020	0.0074	0.0025

Notes:

All results in mg/l

zero values are considered non-detect

Table 14. SSFF slag CGLT results.

Constituent	2hr	5hr	8hr	24hr	48hr	96hr	192hr	1344hr
Ag	0.000	0.000	0.000	0.000	0.000	0.000	0.000	0.002
Al	0.042	0.034	0.020	0.042	0.036	0.051	0.069	0.134
As	0.001	0.002	0.005	0.004	0.006	0.000	0.006	0.003
Ba	0.010	0.003	0.000	0.008	0.020	0.016	0.046	0.180
Be	0.000	0.000	0.000	0.000	0.000	0.000	0.000	0.000
Ca	92.380	69.993	54.840	117.250	132.647	170.371	264.422	903.517
Cd	0.000	0.000	0.000	0.000	0.000	0.000	0.000	0.000
Co	0.000	0.000	0.000	0.000	0.000	0.000	0.000	0.000
Cr	0.002	0.001	0.001	0.002	0.002	0.003	0.004	0.022
Cu	0.000	0.000	0.000	0.000	0.000	0.000	0.000	0.001
Fe	0.000	0.000	0.000	0.000	0.000	0.000	0.000	0.001
K	1.218	0.562	0.442	1.331	1.556	2.103	3.873	26.892
Mg	0.016	0.002	0.000	0.000	0.000	0.000	0.000	0.010
Mn	0.000	0.000	0.000	0.000	0.000	0.000	0.000	0.000
Mo	0.000	0.000	0.000	0.007	0.002	0.001	0.001	0.003
Na	3.808	1.805	1.429	3.979	4.549	5.972	9.299	48.886
Ni	0.000	0.000	0.000	0.000	0.000	0.000	0.000	0.000
Pb	0.001	0.002	0.002	0.001	0.001	0.001	0.002	0.002
Sb	0.004	0.000	0.000	0.005	0.000	0.003	0.000	0.001
Se	0.007	0.005	0.007	0.007	0.010	0.007	0.003	0.018
Sn	0.000	0.000	0.000	0.000	0.000	0.000	0.000	0.000
Sr	0.030	0.000	0.000	0.099	0.133	0.208	0.420	2.176
Ti	0.000	0.000	0.000	0.000	0.000	0.000	0.000	0.000
Tl	0.000	0.000	0.001	0.003	0.001	0.002	0.000	0.000
V	0.006	0.006	0.004	0.004	0.002	0.002	0.000	0.000
Zn	0.001	0.003	0.000	0.000	0.000	0.002	0.002	0.002

Notes:
All results in mg/l

Table 15. SSFW slag CGLT results.

Constituent	2hr	5hr	8hr	24hr	48hr	96hr	192hr	1344hr
Ag	0.000	0.000	0.000	0.000	0.000	0.000	0.000	0.001
Al	0.074	0.050	0.057	0.052	0.060	0.107	0.063	0.106
As	0.001	0.002	0.002	0.000	0.000	0.002	0.002	0.000
Ba	0.004	0.000	0.000	0.015	0.014	0.020	0.030	0.212
Be	0.000	0.000	0.000	0.000	0.000	0.000	0.000	0.000
Ca	44.315	33.786	29.899	74.280	85.417	124.307	160.714	781.378
Cd	0.000	0.000	0.000	0.000	0.000	0.000	0.000	0.000
Co	0.000	0.000	0.000	0.000	0.000	0.000	0.000	0.000
Cr	0.001	0.001	0.001	0.001	0.002	0.003	0.003	0.021
Cu	0.000	0.000	0.000	0.000	0.000	0.000	0.000	0.002
Fe	0.000	0.000	0.000	0.000	0.000	0.000	0.000	0.001
K	0.365	0.189	0.141	0.425	0.613	0.760	1.177	13.450
Mg	0.002	0.001	0.001	0.000	0.000	0.000	0.000	0.005
Mn	0.000	0.000	0.000	0.000	0.000	0.000	0.000	0.000
Mo	0.009	0.001	0.000	0.000	0.000	0.000	0.001	0.003
Na	0.859	0.446	0.291	0.902	0.928	1.169	1.757	15.194
Ni	0.000	0.000	0.000	0.000	0.000	0.000	0.000	0.001
Pb	0.001	0.000	0.000	0.001	0.001	0.000	0.002	0.000
Sb	0.005	0.000	0.003	0.002	0.000	0.000	0.001	0.004
Se	0.007	0.000	0.001	0.005	0.003	0.008	0.000	0.008
Sn	0.001	0.000	0.000	0.000	0.000	0.001	0.000	0.000
Sr	0.000	0.000	0.000	0.006	0.021	0.072	0.152	1.332
Ti	0.000	0.000	0.000	0.000	0.000	0.000	0.000	0.000
Tl	0.000	0.000	0.003	0.001	0.001	0.003	0.000	0.000
V	0.004	0.003	0.004	0.003	0.003	0.004	0.000	0.000
Zn	0.000	0.004	0.003	0.001	0.000	0.001	0.001	0.001

Notes:

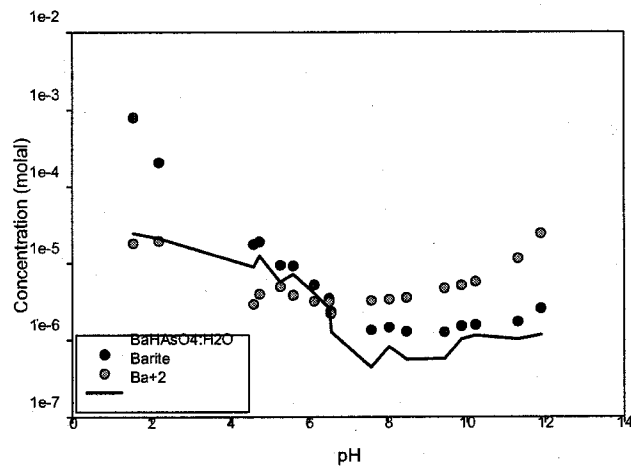
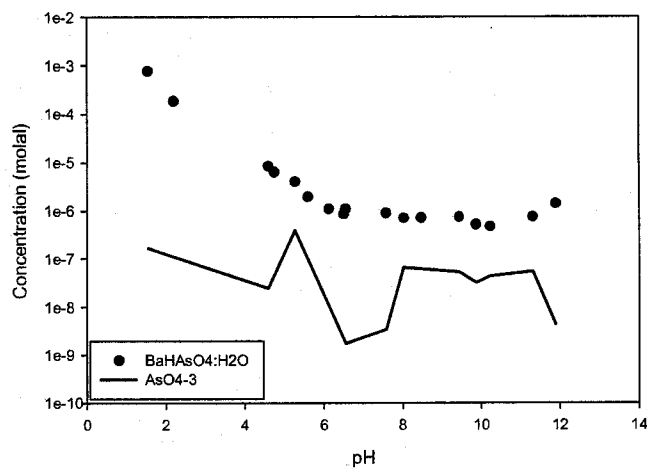
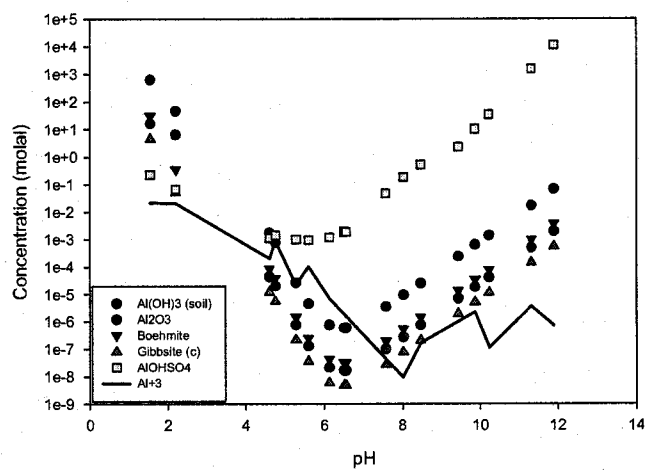
All results in mg/l

Table 16. SAW slag CGLT results.

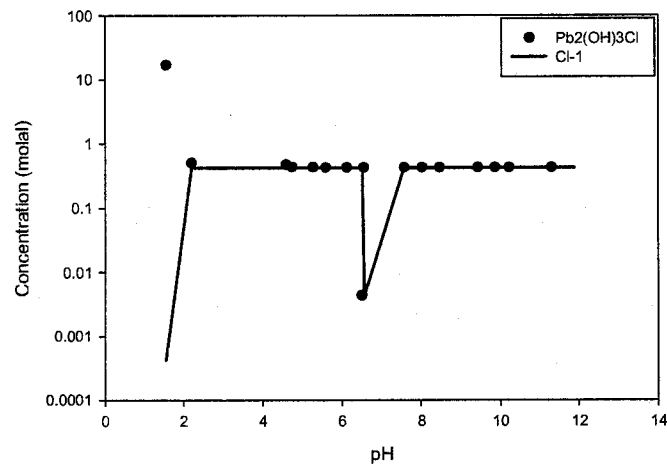
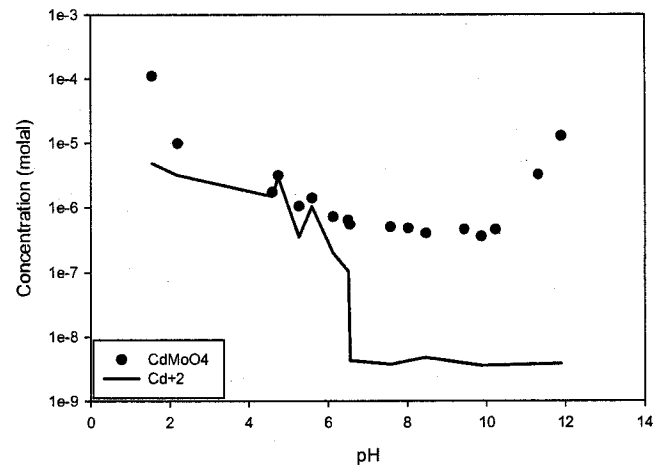
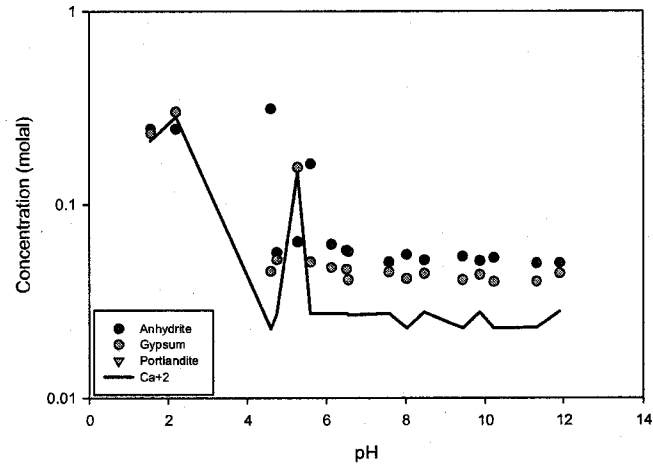
Constituent	2hr	5hr	8hr	24hr	48hr	96hr	192hr	1344hr
Ag	0.0000	0.0000	0.0000	0.0000	0.0000	0.0000	0.0000	0.000
Al	0.1408	0.1635	0.1431	0.4292	0.5399	0.7884	1.1530	4.394
As	0.0000	0.0030	0.0000	0.0000	0.0012	0.0000	0.0033	0.002
Ba	0.0000	0.0000	0.0000	0.0000	0.0000	0.0000	0.0000	0.007
Be	0.0000	0.0000	0.0000	0.0000	0.0000	0.0000	0.0000	0.000
Ca	0.910	0.630	0.357	1.589	2.572	4.657	7.491	16.528
Cd	0.0000	0.0000	0.0000	0.0000	0.0000	0.0000	0.0000	0.000
Co	0.0000	0.0000	0.0000	0.0000	0.0000	0.0000	0.0000	0.000
Cr	0.0001	0.0002	0.0000	0.0000	0.0001	0.0001	0.0001	0.002
Cu	0.0000	0.0000	0.0000	0.0000	0.0000	0.0000	0.0000	0.002
Fe	0.0000	0.0000	0.0000	0.0000	0.0000	0.0000	0.0000	0.000
K	0.1783	0.1492	0.1268	0.7462	0.4572	0.8716	1.8135	33.952
Mg	0.8362	0.4017	0.2363	0.4858	0.5134	0.5834	0.7159	0.063
Mn	0.0363	0.0320	0.0197	0.0111	0.0000	0.0000	0.0000	0.000
Mo	0.0009	0.0004	0.0006	0.0007	0.0008	0.0009	0.0009	0.024
Na	1.3524	0.9057	0.8541	2.3022	3.4119	6.3686	11.8203	88.048
Ni	0.0000	0.0000	0.0000	0.0000	0.0000	0.0000	0.0000	0.000
Pb	0.0000	0.0013	0.0001	0.0007	0.0004	0.0000	0.0002	0.001
Sb	0.0005	0.0000	0.0011	0.0010	0.0022	0.0009	0.0016	0.014
Se	0.0027	0.0054	0.0022	0.0074	0.0055	0.0005	0.0104	0.002
Sn	0.0009	0.0000	0.0000	0.0013	0.0000	0.0000	0.0000	0.003
Sr	0.0000	0.0000	0.0000	0.0000	0.0000	0.0000	0.0000	0.016
Ti	0.0000	0.0000	0.0000	0.0000	0.0000	0.0000	0.0000	0.002
Tl	0.0000	0.0000	0.0000	0.0000	0.0018	0.0011	0.0000	0.000
V	0.0004	0.0005	0.0000	0.0004	0.0005	0.0011	0.0026	0.031
Zn	0.0001	0.0020	0.0007	0.0000	0.0000	0.0004	0.0000	0.000

Notes:

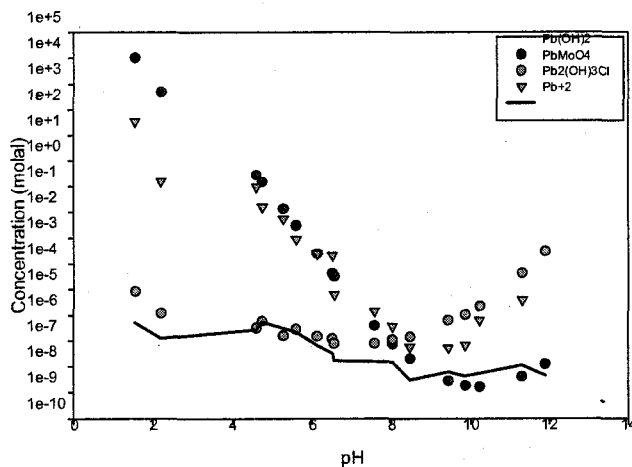
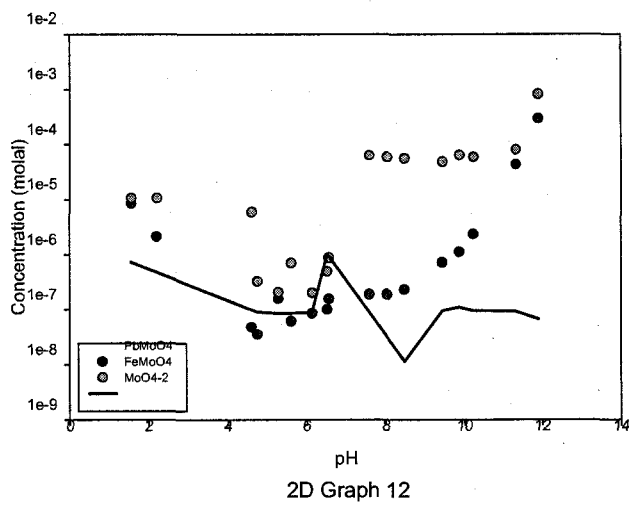
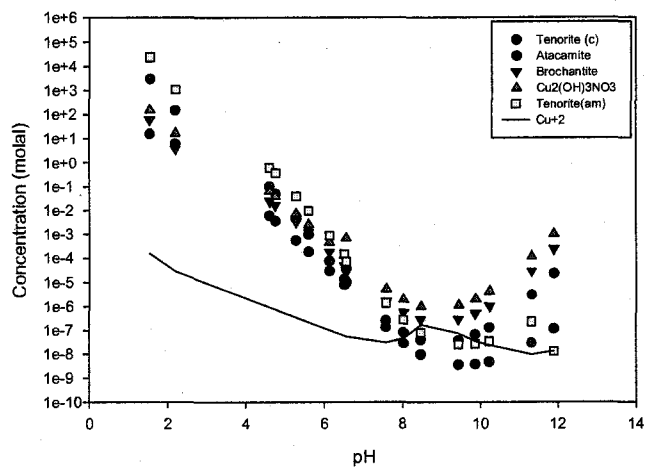
All results in mg/l
zero values are considered non-detect



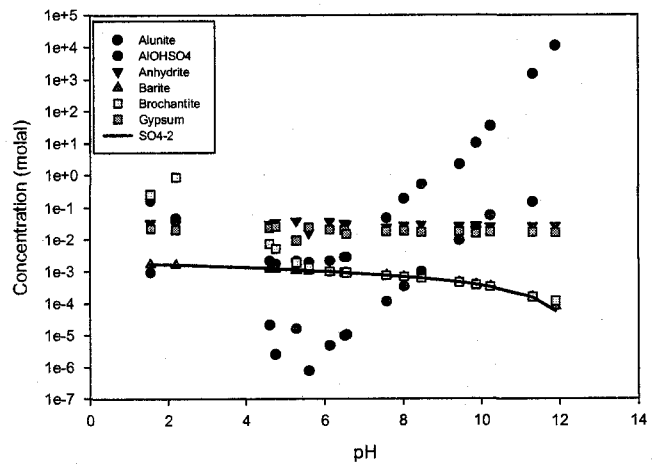
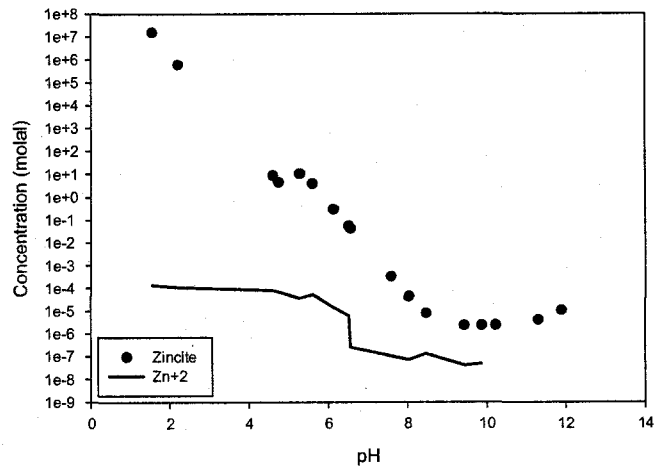
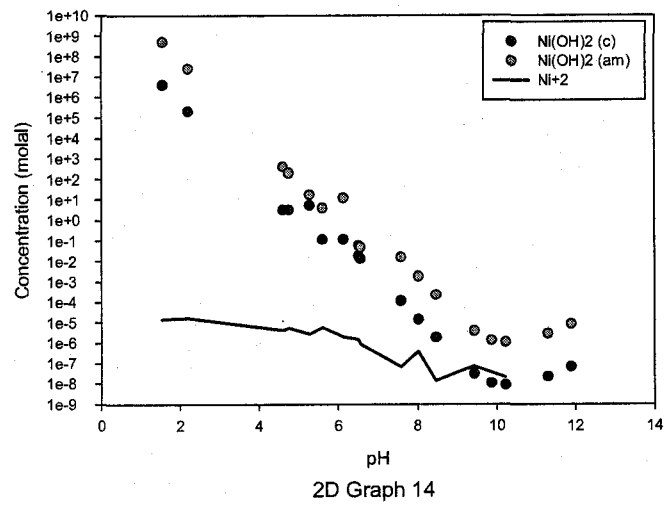
Figures 1-3. BOF Slag MINTeqA2 plots for Al, As, and Ba.



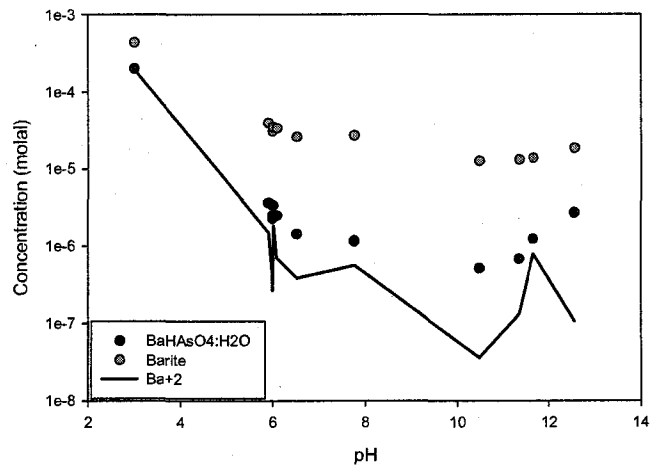
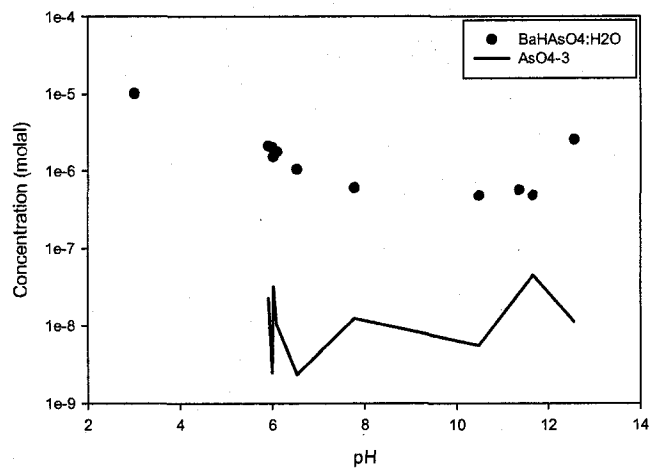
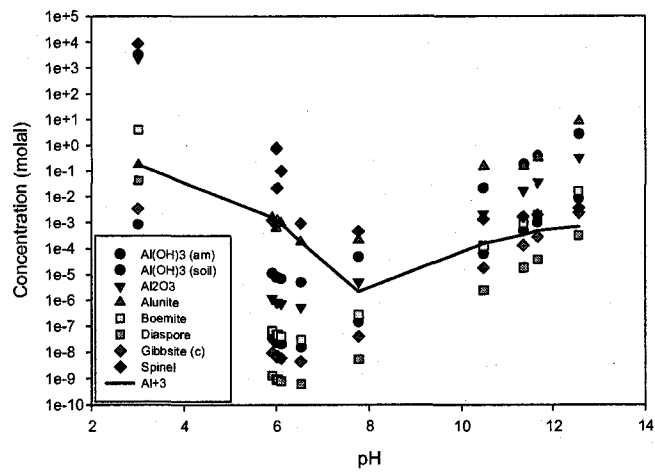
Figures 4-6. BOF Slag MINTeqQA2 plots for Ca, Cd, and Cl.



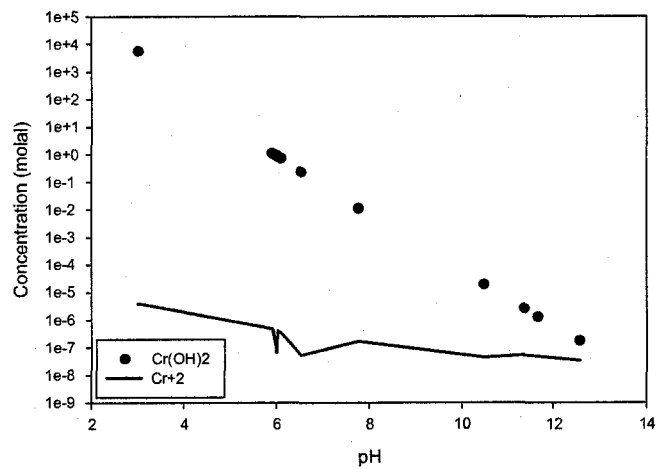
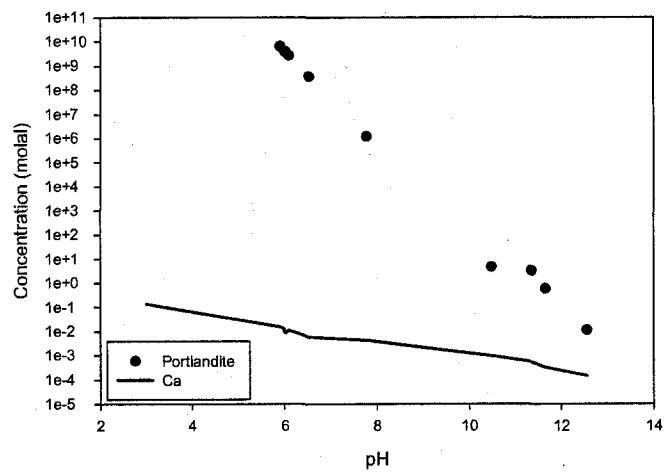
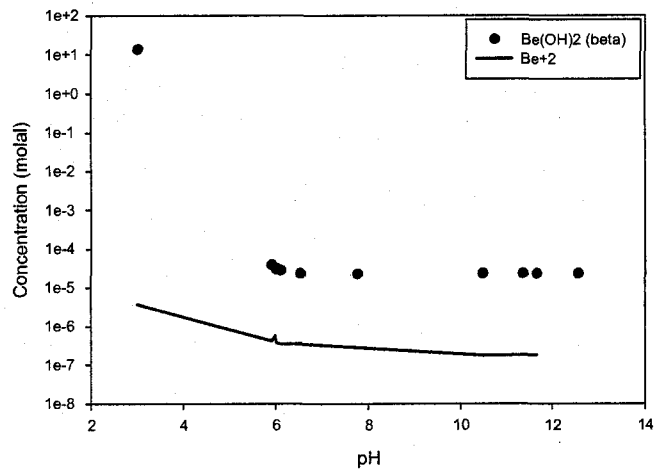
Figures 7-9. BOF Slag MINTQA2 plots for *Cu*, *Mo*, and *Pb*.



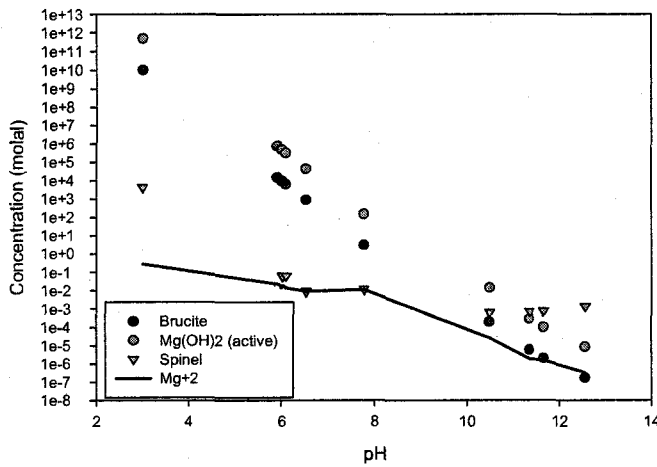
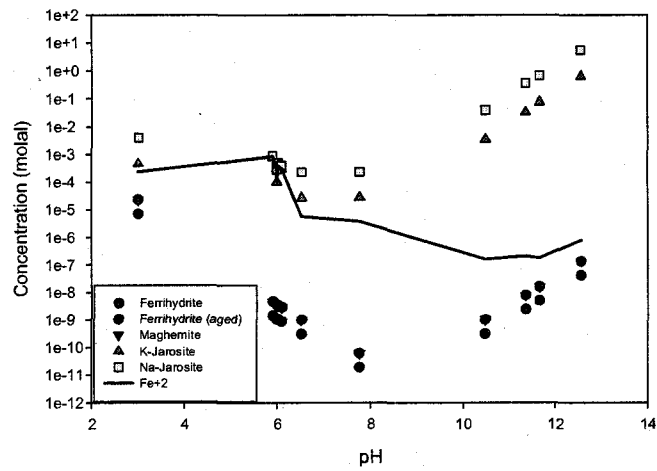
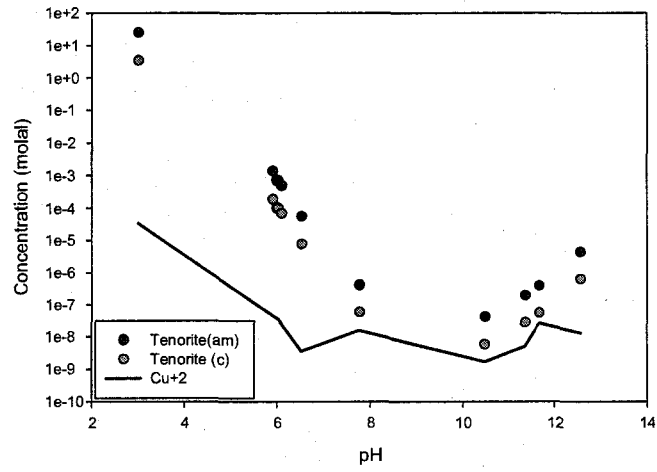
Figures 10-12. BOF Slag MINTQA2 plots for Ni, Zn, and SO₄.



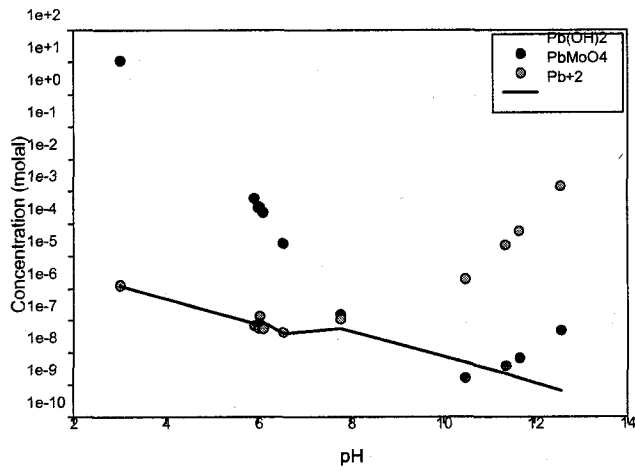
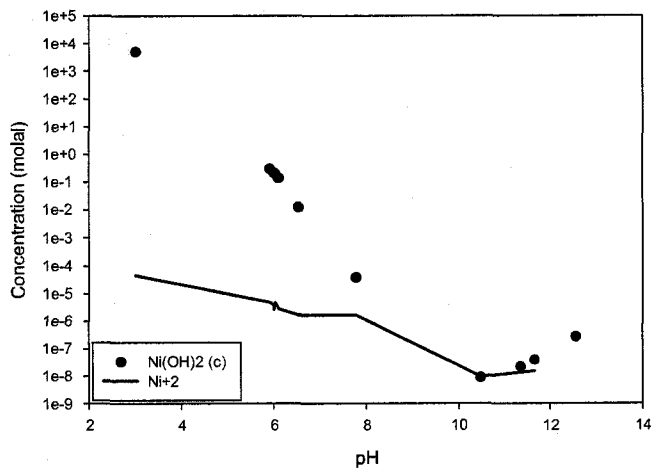
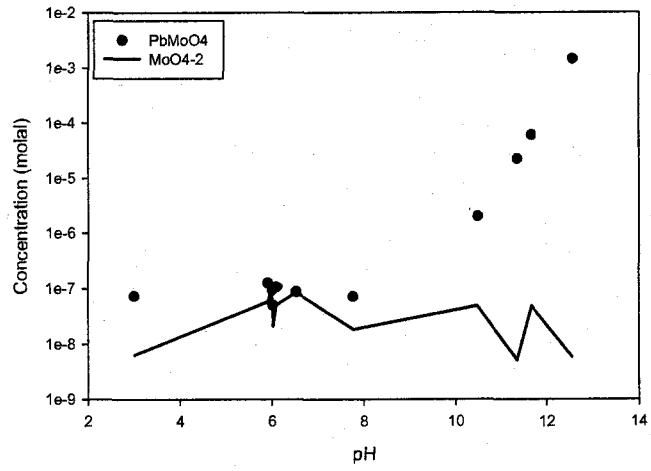
Figures 13-15. SAW Slag MINTQA2 plots for Al, As, and Ba.



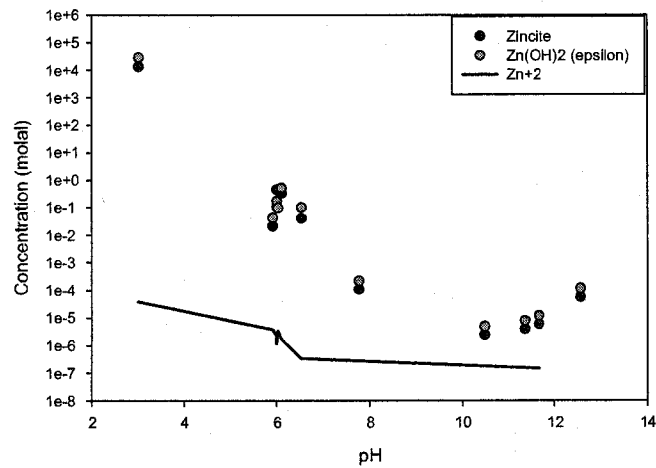
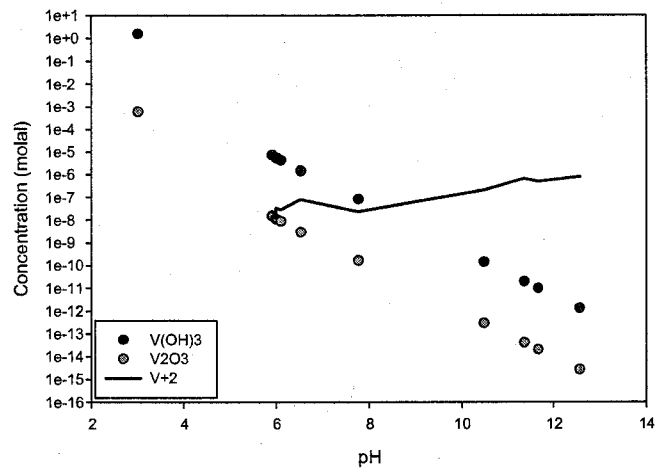
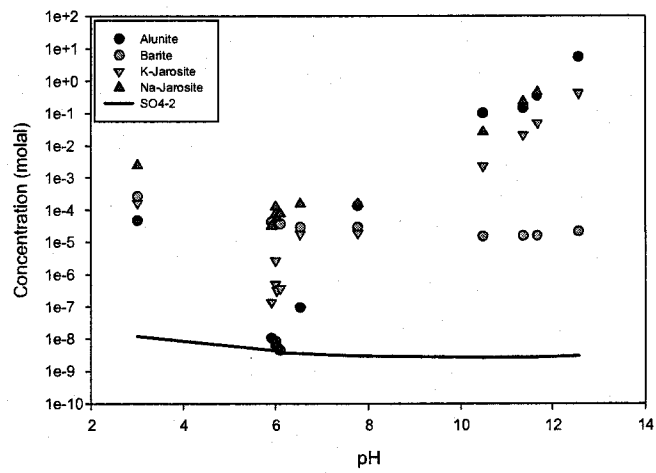
Figures 16-18. SAW Slag MINTQA2 plots for Be, Ca, and Cr.



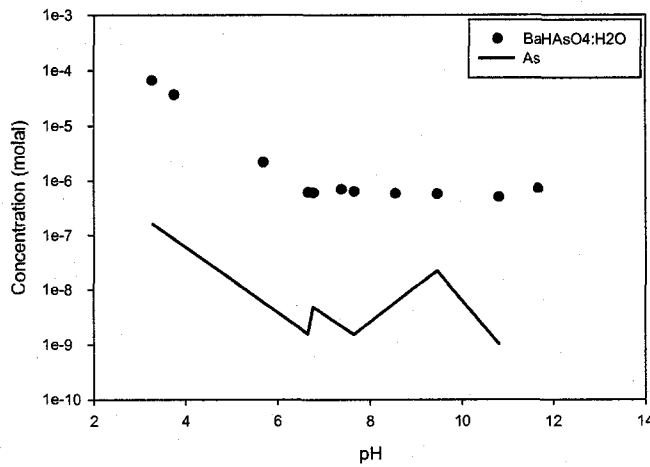
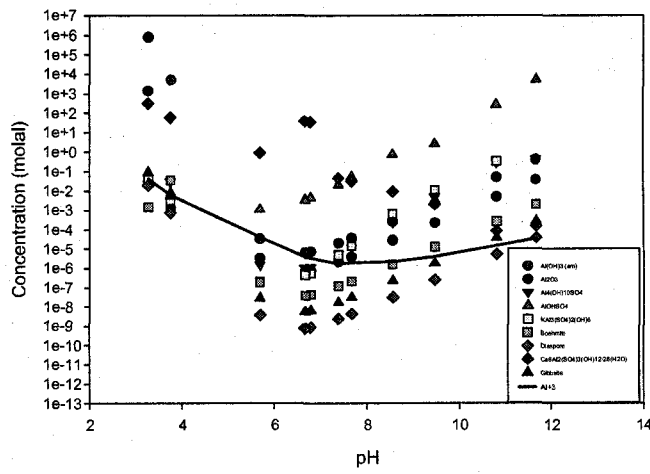
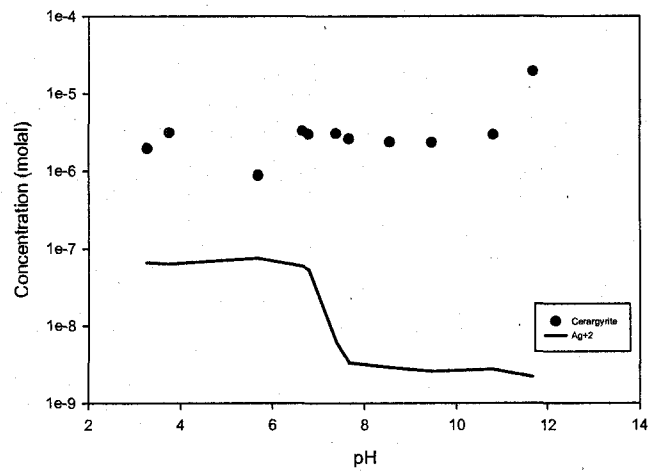
Figures 19-21. SAW Slag MINTEQA2 plots for Cu, Fe, and Mg.



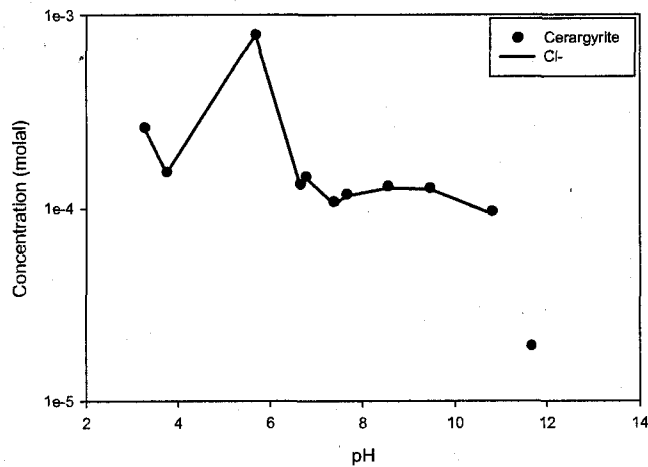
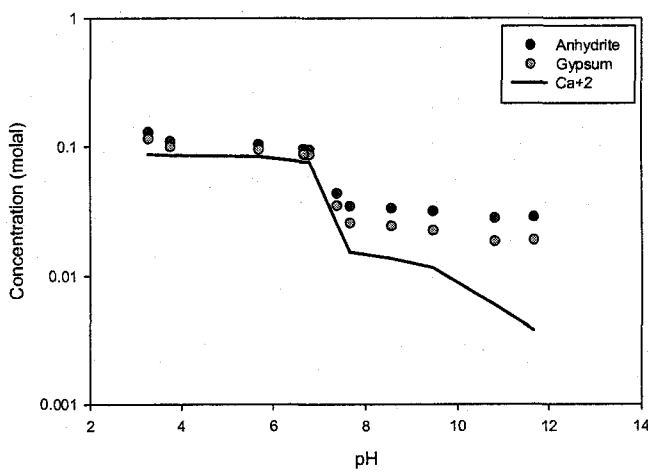
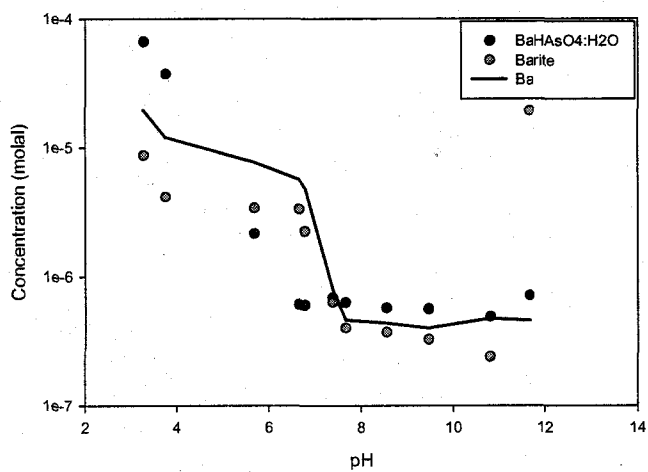
Figures 22-24. SAW Slag MINTEQA2 plots for *Mo*, *Ni* and *Pb*.



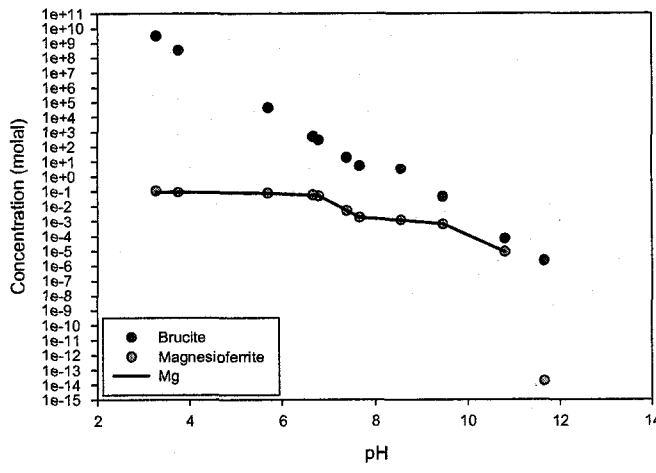
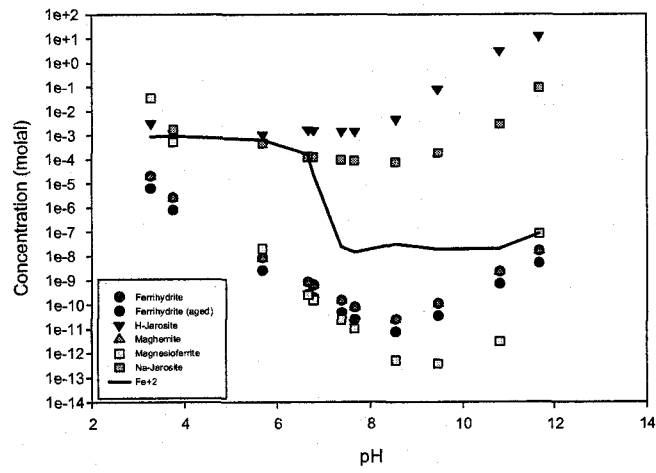
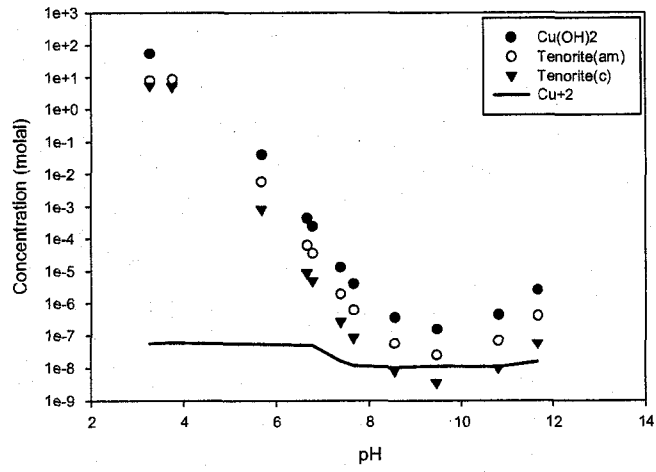
Figures 25-27. SAW Slag MINTQA2 plots for SO_4 , V, and Zn.



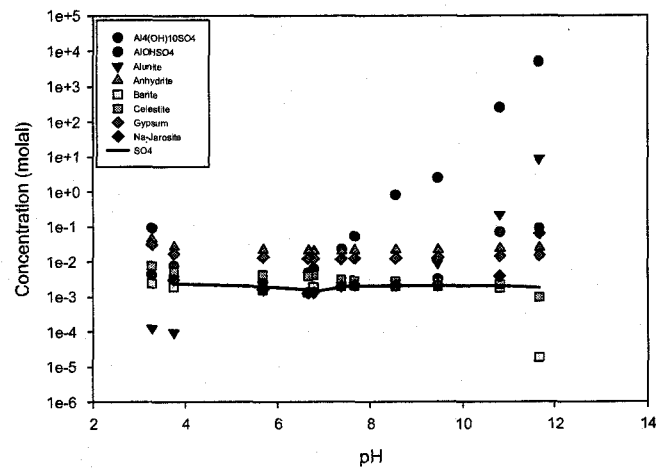
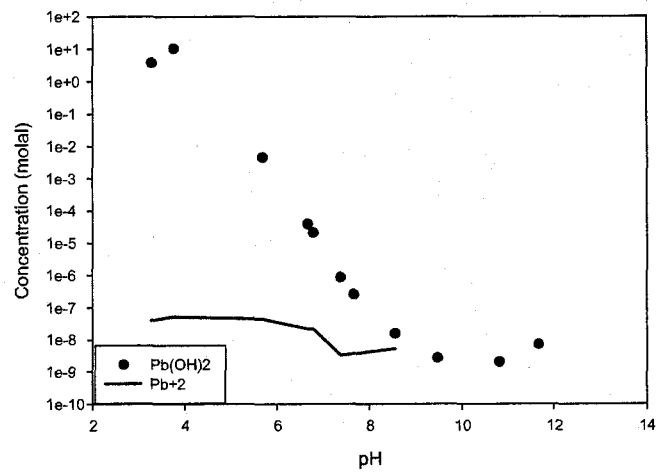
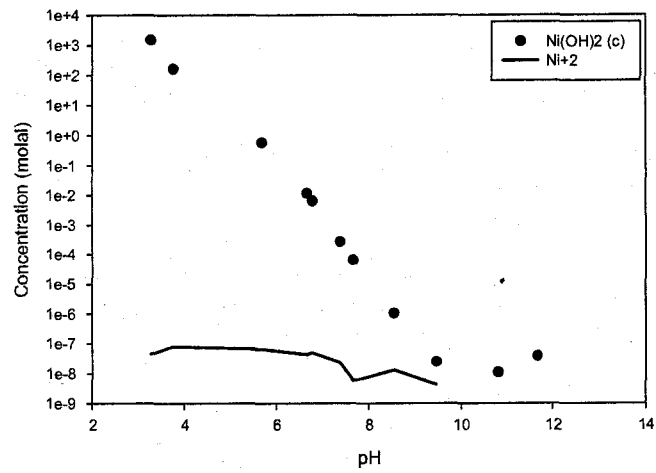
Figures 28-30. BF Slag MINTQA2 plots for *Ag*, *Al*, and *As*.



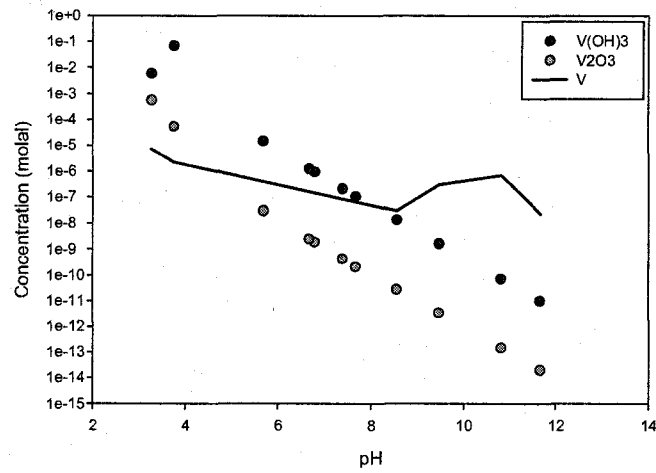
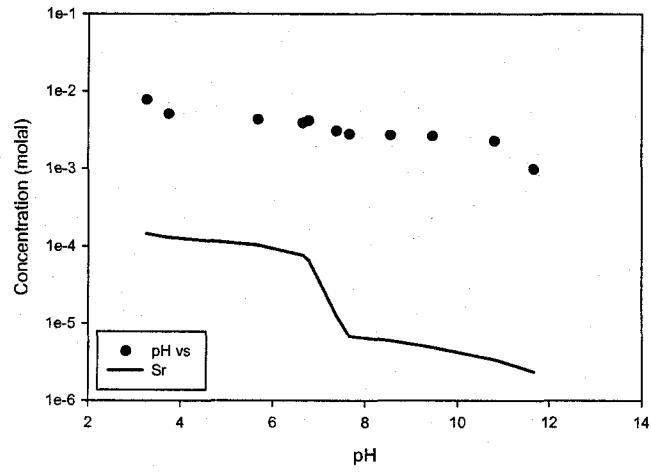
Figures 31-33. BF Slag MINTQA2 plots for Ba, Ca, and Cl.



Figures 34-36. BF Slag MINTEQA2 plots for Cu, Fe, and Mg.



Figures 37-39. BF Slag MINTeq plots for Ni, Pb, and SO_4 .



Figures 40-41. BF Slag MINTEQA2 plots for *Sr* and *V*.